

**A Prospective Study of Clinical and Laboratory
Parameters in Patients with Non- Small Cell Lung
Cancer Undergoing Immunotherapy
– Correlation with Clinical Outcome**



Konstantinos Rounis, MD
University of Crete, Medical School



**“Μελέτη Κλινικοεργαστηριακών παραμέτρων
σε ασθενείς με μη Μικροκυτταρικό Καρκίνο
Πνεύμονος που υποβάλλονται σε Ανοσοθεραπεία
– Συσχέτιση με Κλινική έκβαση”**

Κωνσταντίνος Ρούνης,
Πανεπιστήμιο Κρήτης, Ιατρική Σχολή

Cover image

Et in Arcadia ego (also known as *Les bergers d’Arcadie* or *The Arcadian Shepherds*),
1637–38 painting by **Nicolas Poussin** (1594–1665)

*This Phd Thesis serves as a tribute
to George Rounis enduring legacy, 1955- 2021*

I'll fly a starship
Across the Universe divide
And when I reach the other side
I'll find a place to rest my spirit if I can
Perhaps I may become a highwayman again
Or I may simply be a single drop of rain
But I will remain"

Jimmy Webb, *Highwayman* (1985)

Prologue

The quote of the Cretan author Nikos Kazantzakis “*Every perfect traveler always creates the country where he travels*” reflects ideally in hindsight my feelings spectrum upon the completion of my PhD Thesis. The emotional fluctuation that has accompanied the course of this journey could only be represented as the mathematical visualization of a sine function rather than a linear one.

Nevertheless, like all the important journeys, this one too has to end. Initially, I would like to thank the University of Crete for providing me with the opportunity and an optimal academic environment to take my first baby steps as a researcher.

I wish to extend my foremost gratitude to my esteemed professors and mentors, Dimitrios Mavroudis and Sofia Agelaki. My profound interactions with Professor Dimitrios Mavroudis, our dialogues concerning the optimization of individual patient treatment plans, and our exploration of research avenues in this burgeoning era of molecular medicine have indelibly shaped my identity as a young oncologist and researcher. Likewise, my ongoing exchanges with Professor Sofia Agelaki, characterized by her meticulous attention to detail—although initially leading to moments of frustration—have profoundly sculpted my thought processes as a researcher and a clinician. To both mentors, I am profoundly appreciative for the opportunities they have extended and the intellectual challenges they have graciously posed throughout these formative years. I am truly fortunate to have had mentors of your caliber and I could not have imagined better ones.

I also wish to express my deep appreciation to Professor Nikolaos Tzanakis of the University of Crete, as well as to my initial mentor, the ever-memorable Konstantinos Papanastasiou from St. Savvas Hospital in Athens. Additionally, I recognize with gratitude the guidance of my esteemed colleague, Dr. Ioannis Gioulbasanis, whose expertise and valuable counsel have been instrumental during the research process and the subsequent data analysis of my doctoral thesis. Furthermore, I extend my acknowledgments to Professor Alexandra Georgiou of Harokopio University of Athens for her insightful guidance throughout my research endeavor. My heartfelt thanks extend to Professor Ioannis Tsamardinos and his team for their sagacious guidance and invaluable counsel during the phase of data analysis. I am appreciative of the guidance and camaraderie of my mentors and colleagues at the Karolinska Comprehensive Cancer Center, including Luigi De Petris, Professor Simon Ekman and Giuseppe Stragliotto.

In conclusion, I express my profound gratitude to Chara Papadaki for her exceptional guidance, patience, and unwavering encouragement throughout the entirety of my doctoral research. It would be remiss not to offer a special acknowledgment to my fellow researcher and steadfast “brother-in-arms” Dimitrios Makrakis, whose unwavering dedication, intellect, and resolve were pivotal to the realization of our research endeavors. I am confident that he will continue to evoke pride with his trajectory as an oncologist in the “New World”.

However, paramount above all, I reserve my deepest gratitude for my parents, Dimitra Kolostoumpi-Rounis and my cherished father, George Rounis, who has since departed from this world. Their boundless love, unwavering dedication, enduring support and ethos have unequivocally defined parenthood for me.

Stockholm,

2023/08/12

Konstantinos Rounis

Abstract

Lung cancer constitutes the primary cause of mortality associated with malignancy on a global scale, with Non-Small Cell Lung Cancer (NSCLC) being its most prevalent histological subtype. Despite extensive research efforts spanning over three decades, the prognosis of patients with metastatic NSCLC remains poor. The introduction of immunotherapy into clinical practice has revolutionized oncology worldwide. Immunotherapy, delivered in the form of monoclonal antibodies targeting proteins that act as immune checkpoint inhibitors, offers the potential for prolonged remission in a small but significant subset of patients afflicted by a broad spectrum of neoplasms, including NSCLC.

However, following the initial enthusiasm, a plethora of research inquiries emerged as a result of the necessity to enhance the clinical outcomes for our patients. A minority, approximately one-third, of patients receiving immunotherapy for NSCLC will derive clinical benefit from it. Additionally, the mechanisms of primary and acquired resistance to these monoclonal antibodies remain incompletely understood, and there exists a lack of predictive and prognostic biomarkers. Until now, only the levels of PD-L1 protein expression on the surface of cancer cells or immune cells within the tumor microenvironment have been statistically correlated with clinical outcomes in the prospective clinical trials which led to the regulatory approval of these drugs. Considering these aforementioned factors alongside the escalating cost of administering these medications, which places increasing economic strain on national healthcare systems, the identification of essential biomarkers becomes imperative. This is necessary not only for optimizing patient selection for immunotherapy in NSCLC, but also for decoding the mechanisms underlying primary and acquired resistance.

A multitude of clinical, laboratory, and radiological parameters have been linked to the clinical outcome of patients with NSCLC undergoing cytotoxic chemotherapy. Furthermore, pharmaceutical agents such as antibiotics and steroids have been associated with diminished immune response and are frequently administered to patients with neoplasms undergoing immunotherapy. Moreover, factors associated with the pathogenesis of the cancer cachexia syndrome, diagnosed in approximately half of NSCLC patients, have been linked to reduced immune response and susceptibility to infections. Finally, the composition of adipose tissue in the human body has been indicated as a prognostic indicator in cancer patients and a significant regulator of the immune system, primarily in preclinical models.

The objective of this doctoral dissertation was to conduct a prospective observational registry study on patients with NSCLC who received therapy at the Oncology Clinic of the University Hospital of Heraklion. The aim was to explore potential associations between clinical and laboratory factors, as well as the presence of cancer cachexia syndrome and adipose tissue composition, with the clinical outcome of these patients. During the two-year period from November 15, 2017, to November 15, 2019, prospective clinical, laboratory, and radiological data were collected for 83 patients with NSCLC who received immunotherapy at the University Hospital of Heraklion.

The first publication resulting from this study analyzed the clinical and laboratory data of the 66 patients in our cohort who received immunotherapy as a second-line treatment.

Prolonged administration of antibiotics (cumulatively for more than 14 days) and the presence of secondary osteopathic lesions emerged as independent negative predictive factors for disease stabilization after immunotherapy administration. Furthermore, these factors were also identified as independent prognostic factors for reduced survival. Interestingly, administration of antibiotics did not impact patient outcomes; only prolonged administration had a significant effect. The data were further analyzed using the JADBio artificial intelligence platform, which identified prolonged antibiotic administration, body mass index (BMI), and the presence of hepatic and bone metastases as significant factors associated with an increased likelihood of disease progression, indicating a less favorable response to immunotherapy. The resulting algorithm demonstrated an ability to predict disease stabilization probability at approximately 80%. These findings highlighted the pivotal role of the microbiome in orchestrating an effective immune response, as well as the adverse impact of the presence of osteopathic secondary lesions on the clinical outcome of metastatic NSCLC patients receiving immunotherapy.

In the second scientific publication, the impact of cachexia syndrome presence on the clinical outcome of 83 patients with metastatic NSCLC receiving immunotherapy was investigated. Patient classification concerning the underlying cachexia syndrome was based on criteria previously established by the international consensus for this syndrome's study in 2011. These criteria included weight loss exceeding 5% during the last six months before immunotherapy initiation, or any degree of weight loss $> 2\%$ and BMI $< 20 \text{ kg/m}^2$, or skeletal muscle mass index at the level of the third lumbar vertebra (LSMI) $< 55 \text{ cm}^2/\text{m}^2$ for males and $< 39 \text{ cm}^2/\text{m}^2$ for females. LSMI was calculated using computed tomography images of the abdomen at immunotherapy initiation and every 3 months thereafter, employing the Slice-O-Matic Tomovision method. Half of the cohort patients under study were diagnosed with cachexia syndrome. Cachectic patients exhibited statistically significantly lower response rates to immunotherapy compared to non-cachectic patients. Furthermore, the presence of cancer cachexia syndrome independently predicted an increased likelihood of disease progression as the optimal treatment response. Lastly, cachexia syndrome presence independently predicted reduced survival in patients with NSCLC receiving immunotherapy. This study, the first prospective investigation into the effect of cachexia syndrome on the clinical outcome of immunotherapy-treated patients, revealed that the presence of cancer cachexia syndrome constitutes an independent negative predictive and prognostic factor in patients with NSCLC undergoing immune checkpoint inhibitor therapy. Further research at translational and molecular levels concerning the metabolic dysregulation associated with cachexia syndrome presents a promising avenue for deciphering the mechanisms underlying both primary and secondary resistance to immunotherapy.

In the third publication, prospective data from 52 patients in our cohort with sufficient or appropriate radiological data were analyzed. The objective of this study was to explore the impact of differential adipose tissue compartment composition and skeletal muscle tissue density on the therapeutic effectiveness of immunotherapy. Tissue composition was calculated by measuring the density of different types of adipose tissue (visceral, subcutaneous, and intramuscular fat) and muscle at the level of the third lumbar vertebra using computed tomography scans at immunotherapy initiation, applying the Slice-O-Matic Tomovision technique. Densities were converted into indices [Intramuscular Fat Index

(IMFI), Visceral Fat Index (VFI), Subcutaneous Fat Index (SFI), Lumbar Skeletal Muscle Index (LSMI)] by dividing these values by the patients' height squared. Patients were classified dichotomously based on their initial values of IMFI, VFI, and SFI, according to the median value for their gender. Muscle tissue classification was also dichotomous. The classification thresholds for LSMI were $55 \text{ cm}^2/\text{m}^2$ for males and $39 \text{ cm}^2/\text{m}^2$ for females, which were previously established by the international consensus for defining cachexia syndrome and serving as numerical thresholds for sarcopenia. Patients responding to immunotherapy had significantly higher SFI distributions compared to non-responders. The presence of sarcopenia and low subcutaneous fat density index were both significantly correlated with reduced survival in our cohort patients. An interesting finding was that in the univariate analysis exploring the correlation of IMFI, VFI, SFI, and LSMI as continuous variables with patient survival, the only variable that showed a statistically significant positive correlation was the subcutaneous fat density index. This study, the first prospective investigation into the effect of adipose tissue distribution on immunotherapy-treated NSCLC patients, highlighted the potential impact and significant role of subcutaneous adipose tissue density on immune response against malignancies at a clinical level.

In conclusion, the scientific publications resulting from this doctoral thesis emphasized the significance of concomitant medications, particularly antibiotic treatment, as well as secondary bone lesions in the efficacy of immunotherapy in NSCLC patients. Moreover, the two publications investigating the influence of cachexia syndrome and adipose tissue distribution represent a "proof of concept" at a clinical level for the predictive and prognostic importance of metabolic dysregulation as a phenomenon occurring due to neoplastic processes in patients receiving immune response-modulating therapy. The study examining cachexia syndrome underscored the central role of advanced cachexia syndrome as a negative prognostic and predictive biomarker in the current era of immunotherapy. The results of the third study, revealing the predictive and significant role of subcutaneous fat density, represent clinical evidence of an additional and underexplored role. Further research at translational and molecular levels regarding the specific characteristics of the tumor microenvironment in cachectic patients as well as those with adipose tissue metabolic deregulation could serve as a pivotal link in the chain for discovering new biomarkers and therapies aiming to optimize immunotherapy as a cornerstone in cancer management.

Περίληψη

Ο καρκίνος πνεύμονα αποτελεί την κύρια αιτία θνητότητας σχετιζόμενη με κακοήθεια σε διεθνές επίπεδο με τον Μη Μικροκυτταρικό Καρκίνο Πνεύμονα (ΜΜΚΠ) να αποτελεί τον πιο συχνό ιστολογικό του υπότυπο. Παρά τις εκτεταμένες ερευνητικές προσπάθειες για πάνω από τρεις δεκαετίες η πρόγνωση των ασθενών με μεταστατικό ΜΜΚΠ παραμένει πτωχή. Η είσοδος της ανοσοθεραπείας στην κλινική πράξη επέφερε μία επανάσταση στην κλινική άσκηση της ογκολογίας σε μία παγκόσμια κλίμακα. Η ανοσοθεραπεία, που χορηγείται με τη μορφή μονοκλωνικών αντισωμάτων έναντι πρωτεϊνών που δρουν ως αναστολείς σημείων ελέγχου του ανοσοποιητικού συστήματος, προσφέρει τη δυνατότητα μακροχρόνιας ύφεσης σε ένα μικρό αλλά σημαντικό ποσοστό ασθενών πασχόντων από ένα ευρύ φάσμα νεοπλασιών, μεταξύ αυτών και ο ΜΜΚΠ.

Εν τούτοις, ύστερα από την έλευση του αρχικού ενθουσιασμού μία πληθώρα ερευνητικών ερωτημάτων δημιουργήθηκε ως απόρροια ανάγκης βελτίωσης των κλινικών εκβάσεων των ασθενών. Ένα μικρό ποσοστό, περίπου το ένα τρίτο, των ασθενών που λαμβάνουν ανοσοθεραπεία για ΜΜΚΠ θα έχουν κλινικό όφελος από τη χορήγηση της. Επιπλέον, οι μηχανισμοί πρωτογενούς και δευτερογενούς αντίστασης σε αυτά τα μονοκλωνικά αντισώματα δεν έχουν κατανοηθεί και υπάρχει μία έλλειψη προγνωστικών και προβλεπτικών βιοδεικτών. Μέχρι σήμερα, μόνο τα επίπεδα έκφρασης της πρωτεΐνης PD-L1 στην επιφάνεια των καρκινικών κυττάρων ή στην επιφάνεια των κυττάρων του ανοσοποιητικού συστήματος που εδράζονται στο μικροπεριβάλλον του όγκου έχουν συσχετιστεί σε στατιστικά σημαντικό βαθμό με την κλινική έκβαση των ασθενών στις προοπτικές κλινικές μελέτες που οδήγησαν στην έγκριση αυτών των φαρμάκων από τους αρμόδιους ρυθμιστικούς οργανισμούς. Εάν κάποιος συλλογιστεί τα προαναφερθέντα δεδομένα συνάμα με το κόστος χορήγησης αυτών των φαρμάκων το οποίο θέτει ολόένα και αυξανόμενη οικονομική πίεση στα εθνικά συστήματα υγείας η εύρεση απαραίτητων βιοδεικτών καθίσταται απαραίτητη όχι μόνο για την βελτιστοποίηση της επιλογής ασθενών με ΜΜΚΠ που θα λάβουν ανοσοθεραπεία, αλλά και για την αποκωδικοποίηση των μηχανισμών πρωτογενούς και δευτερογενούς αντίστασης.

Μία πληθώρα κλινικών, εργαστηριακών και ακτινολογικών παραμέτρων έχουν συσχετιστεί με την κλινική έκβαση των ασθενών με ΜΜΚΠ που λαμβάνουν κυτταροτοξική χημειοθεραπεία. Επιπλέον φαρμακευτικά σκευάσματα όπως τα αντιβιοτικά και τα κορτικοστεροειδή έχουν σχετιστεί με μειωμένη ανοσολογική απάντηση και χορηγούνται συχνά σε ασθενείς με νεοπλασίες που λαμβάνουν ανοσοθεραπεία. Επιπροσθέτως, οι παράγοντες που έχουν συσχετιστεί με την παθογένεση του συνδρόμου καρκινικής καχεξίας, το οποίο διαγιγνώσκεται στους περίπου μισούς πάσχοντες από ΜΜΚΠ, έχει συσχετιστεί με μειωμένη ανοσολογική απάντηση και ευπάθεια σε λοιμώξεις. Τέλος, η σύνθεση του λιπώδους ιστού στο ανθρώπινο σώμα έχει αναφερθεί ως προγνωστικός δείκτης σε ασθενείς με κακοήθειες και ως σημαντικός ρυθμιστής του ανοσοποιητικού συστήματος σε προκλινικά ως επί το πλείστον μοντέλα.

Ο σκοπός αυτής της διδακτορικής διατριβής ήταν η διενέργεια μίας προοπτικής, καταγραφικής μελέτης παρατήρησης σε ασθενείς με ΜΜΚΠ που έλαβαν θεραπεία στην Ογκολογική Κλινική του Πανεπιστημιακού Νοσοκομείου Ηρακλείου με σκοπό τη διερεύνηση πιθανών συσχετίσεων κλινικών και εργαστηριακών παραγόντων καθώς και της

ύπαρξης συνδρόμου καρκινικής καχεξίας και της σύστασης του λιπώδους ιστού με την κλινική έκβαση των ασθενών αυτών. Κατά τη διετία λοιπόν από τις 15 Νοεμβρίου 2017 έως τις 15 Νοεμβρίου 2019 κατεγράφησαν προοπτικά κλινικά, εργαστηριακά και ακτινολογικά δεδομένα 83 ασθενών με ΜΜΚΠ που έλαβαν ανοσοθεραπεία στο Πανεπιστημιακό Νοσοκομείο Ηρακλείου.

Στην πρώτη δημοσίευση που προέκυψε αναλύθηκαν κλινικά και εργαστηριακά δεδομένα των 66 ασθενών της κοορτής μας που έλαβαν ανοσοθεραπεία ως δεύτερης γραμμής θεραπεία. Η παρατεταμένη χορήγηση αντιβιοτικών (αθροιστικά για πάνω από 14 ημέρες) και η παρουσία οστικών δευτεροπαθών εντοπίσεων αποτέλεσαν ανεξάρτητους αρνητικούς προβλεπτικούς παράγοντες για σταθεροποίηση νόσου ύστερα από χορήγηση ανοσοθεραπείας. Επιπλέον οι ίδιοι παράγοντες αποτέλεσαν ανεξάρτητους προγνωστικούς παράγοντες για μειωμένη επιβίωση. Ενδιαφέρον ήταν ότι η χορήγηση αντιβιοτικών δεν επηρέασε την έκβαση των ασθενών αλλά μόνο η παρατεταμένη χορήγηση αυτών. Τα δεδομένα αναλύθηκαν επιπλέον στην πλατφόρμα τεχνητής νοημοσύνης JADBio η οποία ύστερα ανέδειξε την παρατεταμένη χορήγηση αντιβιοτικών, τον δείκτη μάζας σώματος (BMI) καθώς και την παρουσία ηπατικών και οστικών μεταστάσεων ως τους σημαντικούς παράγοντες που σχετίζονται με αυξημένη πιθανότητα προόδου νόσου ως καλύτερη απάντηση στην ανοσοθεραπεία. Ο αλγόριθμος που προέκυψε είχε τη δυνατότητα να προβλέπει την πιθανότητα σταθεροποίησης νόσου κατά περίπου 80%. Τα αποτελέσματα αυτά ανέδειξαν τον κεντρικό ρόλο του μικροβιώματος για την ενορχήστρωση μία αποτελεσματικής ανοσολογικής απόκρισης καθώς και την αρνητική επίδραση της παρουσίας των οστικών δευτεροπαθών εντοπίσεων στην κλινική έκβαση των ασθενών με μεταστατικό ΜΜΚΠ που λαμβάνουν ανοσοθεραπεία.

Στην δεύτερη επιστημονική ανακοίνωση διερευνήθηκε η επίπτωση της παρουσίας συνδρόμου καρκινικής καχεξίας στην κλινική έκβαση των 83 ασθενών με μεταστατικό ΜΜΚΠ που λαμβάνουν ανοσοθεραπεία. Η κατάταξη των ασθενών όσον αφορά το αν έπασχαν από υποκείμενο σύνδρομο καρκινικής καχεξίας έγινε με βάση τα κριτήρια που είχαν τεθεί προηγουμένως από τη διεθνή συναίνεση για τη μελέτη αυτού του συνδρόμου το 2011. Αυτά αποτελούσαν την απώλεια βάρους μεγαλύτερη του 5% τους τελευταίους έξι μήνες πριν από την έναρξη της ανοσοθεραπείας ή οποιονδήποτε βαθμό απώλειας βάρους >2% και BMI <20 kg/m² ή δείκτη σκελετικής μυϊκής μάζας στο επίπεδο του τρίτου οσφυϊκής σπονδύλου (LSMI) <55 cm²/m² για άνδρες και <39 cm²/m² για γυναίκες. Ο LSMI υπολογίστηκε χρησιμοποιώντας απεικονίσεις υπολογιστικής τομογραφίας της κοιλιάς κατά την έναρξη της ανοσοθεραπείας και κάθε 3 μήνες έκτοτε με την χρήση της μεθόδου Slice-o-Matic- Tomovision. Οι μισοί ασθενείς της κοορτής που μελετήθηκε διαγνώστηκαν με σύνδρομο καρκινικής καχεξίας. Οι καχεκτικοί ασθενείς εμφάνισαν κατώτερα ποσοστά απόκρισης στην ανοσοθεραπεία σε στατιστικά σημαντικό βαθμό σε σχέση με τους μη καχεκτικούς. Επιπλέον, η παρουσία του ανωτέρου συνδρόμου αποτέλεσε ανεξάρτητο προβλεπτικό παράγοντα αυξημένης πιθανότητας για πρόοδο νόσου ως βέλτιστη απόκριση στη θεραπεία. Τέλος, η παρουσία καρκινικής καχεξίας αποτέλεσε ανεξάρτητο προγνωστικό παράγοντα για μειωμένη επιβίωση σε ασθενείς με ΜΜΚΠ που λάμβαναν ανοσοθεραπεία. Η μελέτη αυτή, η οποία αποτελεί την πρώτη προοπτική μελέτη διερεύνησης της επίδρασης της καρκινικής καχεξίας στην κλινική έκβαση των ασθενών που λαμβάνουν ανοσοθεραπεία, ανέδειξε ότι η παρουσία του ανωτέρου συνδρόμου αποτελεί ανεξάρτητο αρνητικό προβλεπτικό και προγνωστικό παράγοντα σε ασθενείς με ΜΜΚΠ που λαμβάνουν θεραπεία

με αναστολές σημείου ελέγχου του ανοσοποιητικού συστήματος. Περαιτέρω έρευνα σε μεταφραστικό και μοριακό επίπεδο πάνω στην επίδραση της μεταβολικής απορρύθμισης που αποτυπώνεται φαινοτυπικά με το σύνδρομο καρκινικής καχεξίας αποτελεί μία υποσχόμενη οδό για την αποκωδικοποίηση των μηχανισμών πρωτοπαθούς και δευτεροπαθούς αντίστασης στην ανοσοθεραπεία.

Στην τρίτη δημοσίευση αναλύσαμε προοπτικά δεδομένα από τους 52 ασθενείς της κοορτής μας για τους οποίους υπήρχαν επαρκή ή κατάλληλα ακτινολογικά δεδομένα. Ο σκοπός αυτής της μελέτης ήταν η διερεύνηση της επίδρασης της διαφορικής σύνθεσης των διαμερισμάτων του λιπώδους ιστού και της πυκνότητας του σκελετικού μυϊκού ιστού στην θεραπευτική αποτελεσματικότητα της ανοσοθεραπείας. Η σύνθεση των ιστών του σώματος υπολογίστηκε μετρώντας την πυκνότητα των διαφορετικών τύπων του λιπώδους ιστού (σπλαχνικό, υποδόριο και ενδομυϊκό λίπος) και των μυών στο επίπεδο του τρίτου οσφυϊκού σπονδύλου σε κάθε ασθενή με απεικονιστική τομογραφία υπολογιστή κατά την έναρξη της ανοσοθεραπείας, με την εφαρμογή της τεχνικής Slice-O-matic tomovision. Οι πυκνότητες μετατράπηκαν σε δείκτες [Δείκτης Ενδομυϊκού Λίπους (IMFI), Δείκτης Σπλαχνικού Λίπους (VFI), Δείκτης Υποδόριου Λίπους (SFI), Δείκτης Σκελετικής Μυϊκής Μάζας οσφυϊκής περιοχής (LSMI)] διαιρώντας αυτές με το ύψος των ασθενών στο τετράγωνο. Οι ασθενείς ταξινομήθηκαν βάσει των αρχικών τους τιμών IMFI, VFI και SFI με δυαδικό τρόπο, σύμφωνα με την διάμεση τιμή για το φύλο τους. Οι ασθενείς ταξινομήθηκαν όσον αφορά τον μυϊκό ιστό επίσης δυαδικά. Τα όρια ταξινόμησης για το LSMI ήταν $55 \text{ cm}^2/\text{m}^2$ για τους άνδρες και $39 \text{ cm}^2/\text{m}^2$ για τις γυναίκες, οι οποίες είχαν καθοριστεί προηγουμένως από τη διεθνή συναίνεση για τον ορισμό του συνδρόμου καρκινικής καχεξίας, ως τα αριθμητικά κατώφλια για τον ορισμό της σαρκοπενίας. Οι ασθενείς που ανταποκρίθηκαν στην ανοσοθεραπεία είχαν υψηλότερες κατανομές SFI σε στατιστικά σημαντικό βαθμό σε σύγκριση με τους μη ανταποκρινόμενους. Η ύπαρξη σαρκοπενίας καθώς και ο χαμηλός δείκτης πυκνότητας υποδόριου λιπώδους ιστού συσχετίστηκαν σε στατιστικά σημαντικό βαθμό με μειωμένη επιβίωση στους ασθενείς της κοορτής μας. Ενδιαφέρον εύρημα, ήταν ότι κατά την μονοπαραγοντική ανάλυση που ανέλυσε τη συσχέτιση των IMFI, VFI, SFI και LSMI ως συνεχείς μεταβλητές, η μόνη μεταβλητή που έδειξε θετική συσχέτιση σε στατιστικά σημαντικό βαθμό με την επιβίωση των ασθενών ήταν ο δείκτης πυκνότητας υποδόριου λίπους. Η μελέτη αυτή, η οποία αποτέλεσε την πρώτη προοπτική μελέτη που διερεύνησε την επίδραση της σωματικής κατανομής του λιπώδους ιστού σε ασθενείς με ΜΜΚΠ που λαμβάνουν ανοσοθεραπεία, ανέδειξε την πιθανή επίδραση και σημαντικό ρόλο του υποδόριου λιπώδους ιστού στην ανοσολογική απάντηση κατά των κακοηθειών.

Συμπερασματικά, οι επιστημονικές δημοσιεύσεις που προέκυψαν κατά την εκπόνηση αυτής της διδακτορικής διατριβής ανέδειξαν αρχικά τη σημασία των συγχորηγούμενων φαρμάκων και δη της αντιβιοτικής αγωγής καθώς και των δευτεροπαθών οστικών εντοπίσεων στην αποτελεσματικότητα της ανοσοθεραπείας σε ασθενείς με ΜΜΚΠ. Επιπλέον, οι δύο δημοσιεύσεις όπου μελετήθηκε η επίδραση της καρκινικής καχεξίας καθώς και η κατανομή του λιπώδους ιστού αποτελούν «απόδειξη αρχής» σε κλινικό επίπεδο της προβλεπτικής και προγνωστικής σημασίας της μεταβολικής απορρύθμισης που συμβαίνει ως επιφανόμενο των νεοπλασματικών διεργασιών σε ασθενείς με νεοπλασίες που λαμβάνουν θεραπεία με τροποποιητές της ανοσολογικής απάντησης. Η μελέτη που διερεύνησε την επίδραση του φαινομένου καρκινικής καχεξίας επισήμανε τον κεντρικό ρόλο του ανωτέρου συνδρόμου ως προγνωστικός και προβλεπτικός βιοδείκτης στη σημερινή εποχή της ανοσοθεραπείας.

Τα αποτελέσματα της τρίτης μελέτης που ανέδειξαν την προβλεπτική και σημασία της πυκνότητας του υποδόριου λίπους στην ανοσολογική απόκριση, ως απόδειξη σε κλινικό επίπεδο ενός επιπρόσθετου και ελλιπώς μελετημένου ρόλου του. Περαιτέρω έρευνα σε μεταφραστικό και μοριακό επίπεδο των ιδιαίτερων χαρακτηριστικών του μικροπεριβάλλοντος του όγκου σε καχεκτικούς ασθενείς αλλά και σε ασθενείς με διαταραχές του λιπώδους ιστού μπορεί να αποτελέσει ένα σημαντικό κρίκο στην αλυσίδα για την εύρεση νέων βιοδεικτών και νέων θεραπειών προς την βελτιστοποίηση της ανοσοθεραπείας ως ακρογωνιαίο λίθο στην αντιμετώπιση των κακοηθειών.

Tables, Figures & Diagrams

1. Tables:

Table 1: Baseline patient characteristics. (page 53-55)

Table 2: Effect of the studied parameters on disease stabilization rates (PR or SD). ATB=Antibiotics, b: PPis=Proton pump inhibitors, c: BMI=Body mass index, d: LN=Lymph nodes, e: Disease burden high=More than 2 organs affected with metastatic disease, f: LDH=Lactate dehydrogenase, g: UNL=Upper normal limit (247 units/liter), h: NLR=Neutrophil to lymphocyte ratio, i: PDL1=Programmed death ligand 1. (page 55-56)

Table 3: Log-rank test demonstrating the effect of the analyzed variables on progression-free survival (PFS) and overall survival (OS). a: BMI=Body mass index, b: High disease burden: >2 organs with metastatic disease, low disease burden: ≤2 organs with metastatic disease, c: LN=Lymph Nodes, d: LDH=Lactate dehydrogenase, e: NLR=neutrophil/lymphocyte ratio, f: Administration of >10 mg of prednisolone equivalent for ≥10 days, g: ATB=Antibiotics, h: PPis=Proton pump inhibitors. (page 59-60)

Table 4: Univariate and multivariate analysis utilizing Cox Regression Method. a: ATB = Antibiotics, b: NRL = Neutrophil to Lymphocyte ratio, c: UNL = Upper normal limit (247 Units/liter). (page 61)

Table 5: Baseline patient characteristics. (page 64)

Table 6: Effect of the analyzed parameters on objective response rates (ORR). CR: Complete response, PR: Partial response, SD: Stable disease, PD: Progressive disease. (page 66-67)

Table 7: Effect of the analyzed parameters on disease control rates (DCR). CR: Complete response, PR: Partial response, SD: Stable disease, PD: Progressive disease. (page 67-68)

Table 8: Univariate and multivariate logistic regression on the odds ratio (OR) of the analyzed parameters on the probability of developing disease progression (PD) as response to treatment with ICIs. OR: Odds Ratio, AUC: Area under the curve, PS: Performance status by ECOG. (page 69)

Table 9: Log-rank test on the effect of the studied variables on PFS and OS (n=83). *: high disease burden was defined as >2 organs with metastatic spread. ICI: Immune checkpoint inhibitor; LSMI: lumbar skeletal muscle index (at the level of 3rd lumbar vertebra); LNV, lower normal value that was set for males =55 cm²/m² and for females =39 cm²/m². (page 71-72)

Table 10: Univariate and multivariate analysis using Cox regression method in the whole patient population. *: high disease burden = metastatic dissemination in > 2 organs, PFS: Progression free survival; OS: Overall survival; HR: Hazard Ratio; ICI: Immune checkpoint inhibitor; PD-L1: Programmed death ligand-1. (page 73)

Table 11: Baseline patient characteristics. BMI = Body mass index, SD = Standard deviation, PD-L1 = Programmed death ligand-1, ICI = Immune checkpoint inhibitor, LSMI: Lumbar skeletal muscle index (At the level of 3rd lumbar vertebra), LNL: Lower normal limit, 55 cm²/m² for males and 39 cm²/m² for females, IMFI = Intramuscular Fat Index (At the level of 3rd lumbar

vertebra), VFI = Visceral Fat Index (At the level of 3rd lumbar vertebra), SFI = Subcutaneous Fat Index (At the level of 3rd lumbar vertebra). (page 75-76)

Table 12: Response, survival and follow-up results for the whole patient population. CR: Complete response, PR: Partial response, SD: Stable disease, PD: Progressive disease, irAEs = Immune-related Adverse Events. (Page 77-78)

Table 13: Effect of the studied variables on objective response rate (ORR). BMI=Body mass index; SD=Standard deviation; LSMI=Lumbar skeletal muscle index (At the level of 3rd lumbar vertebra), LNL: Lower normal limit, 55 cm²/m² for males and 39 cm²/m² for females; IMFI=Intramuscular Fat Index (At the level of 3rd lumbar vertebra); VFI=Visceral Fat Index (At the level of 3rd lumbar vertebra); SFI=Subcutaneous Fat Index (At the level of 3rd lumbar vertebra). (page 79-80)

Table 14: Log-rank test on the effect of the studied variables on PFS and OS. BMI=Body mass index, ICI=Immune checkpoint inhibitor, PD-L1=Programmed death ligand-1, LSMI=Lumbar skeletal muscle index (cm²/m²) (At the level of 3rd lumbar vertebra), LNL=Lower normal limits, 55 cm²/m² for males and 39 cm²/m² for females, IMFI=Intramuscular fat index (cm²/m²) (At the level of 3rd lumbar vertebra), Low: Below gender specific median value, VFI=Visceral fat index (cm²/m²) (At the level of 3rd lumbar vertebra), Low: Below gender specific median value, SFI=Subcutaneous fat index (cm²/m²) (At the level of 3rd lumbar vertebra), Low: Below gender specific median value. (page 82-83)

Table 15: Univariate analysis using Cox regression method investigating the hazard ratios of the BMI*, IMFI, VFI and SFI as continuous nominal variables (cm²/m²) on PFS and OS. Gender was used as a stratification factor. BMI: Body mass index (kg/m²), LSMI: Lumbar skeletal muscle index (cm²/m²), IMFI = Intramuscular fat index (cm²/m²), VFI = Visceral fat index (cm²/m²), SFI = Subcutaneous fat index (cm²/m²); * BMI, IMFI, VFI and SFI were calculated at the beginning of immunotherapy. (page 84)

Table 16: Univariate analysis using Cox regression method investigating the hazard ratios of the analyzed categorical covariates on PFS and OS. BMI=Body mass index, PD-L1=Programmed death ligand-1, LSMI=Lumbar skeletal muscle index (cm²/m²), LNL: 55 cm²/m² for males and 39 cm²/m² for females, IMFI=Intramuscular fat index (cm²/m²). Low: Below gender specific median value, VFI=Visceral fat index (cm²/m²). Low: Below gender specific median value, SFI=Subcutaneous fat index (cm²/m²). Low: Below gender specific median value. (page 86)

Table 17: Summary of the representative clinical studies that examine the effect of cachexia and body composition on treatment outcomes in cancer patients treated with immunotherapy. (page 94)

2. Figures:

Figure 1: Schematic representation of the potential antitumor mechanism of CTLA-4 or PD1/PDL1 [2] axis blockade. **A.** CTLA-4 inhibition allows the interaction of CD28 with B7-1 or B7-2 thus allowing for T cell activation upon the presentation from the APC of the cancer neoantigen to the T cell. **B.** Inhibition of the PD1/PDL1 [2] axis allows for the T cell upon activation from the cancer neoantigen presented by the tumor cell to effectively exert its anti-tumoral effects. (page 22)

Figure 2: The dual role of a wide range spectrum of cachexia pathogenetic mechanisms and their contribution both on the phenotypical changes of cancer cachexia syndrome such as muscle wasting and adipose tissue remodeling and the inhibition of a successful anti-tumor immune response. **MDSC:** Myeloid derived suppressor cell, **M1 & M2:** M1 and M2 macrophage subtypes, **N1 & N2:** N1 and N2 tumor infiltrating neutrophils subtypes, **CAF:** Cancer associated fibroblast, **DC:** Dendritic cell, **NK:** Natural killer cell, **EMT:** Epithelial-to- mesenchymal transition, **PPARα:** Peroxisome proliferator-activated receptor alpha, **ActRIIB:** Type IIβ activin receptor, **gp130:** Glycoprotein 130, **TGFβR1-3:** Transforming growth factor beta receptors 1-3, **TIM3:** T-cell immunoglobulin and mucin-domain containing-3, **TNFR1:** Tumor necrosis factor receptor 1, **CXCR1/2:** C-X-C motif chemokine receptor 1-2, **NLP3:** Nodule inception protein-like protein 3. (page 28)

Figure 3: Potential synergistic mechanism potentiating immunotherapy effect derived from the dual inhibition of PD-1/PD-L1 and P-Selectin/PSGL-1 interactions. **MDSC:** Myeloid derived suppressor cell, **PSGL-1:** P-selectin glycoprotein ligand 1, **PD-1:** Programmed cell death protein 1, **PD-L1:** Programmed cell death protein 1 ligand. (page 34)

Figure 4: Hypothetic Kaplan-Meier curve that depicts the observed phenomenon in phase 3 trials where patients in the immunotherapy arm experience worse survival than the patients in the chemotherapy arm in the first 3-6 months after treatment initiation. (page 37)

Figure 5: Tomovision analysis of the abdominal computed tomography scans of two individuals in our cohort **A.** A male patient with baseline LSMI = 55.02 cm²/m² without sarcopenia **B.** A male patient with baseline LSMI=39.45 cm²/m² consistent with sarcopenia. **LSMI:** Lumbar Skeletal Muscle Index (cm²/m²) (At the level of 3rd lumbar vertebra). (page 46)

Figure 6: SliceOmatic tomovision analysis of the computed tomography scan of a male patient distinguishing the different context of **Visceral Adipose Tissue (VAT)**, **Intramuscular Adipose Tissue (IMAT)**, **Subcutaneous Adipose Tissue (SAT)** and skeletal muscle according to their differential **Hounsfield Units (HU)** references. (page 48)

Figure 7: Illustration of the learning procedure undertaken by JADbio for the classification analysis of our dataset. JADbio explored 3017 configurations and conducted training for a total of 211190 models. (page 51)

Figure 8: Bar plots visualizing the effect of **(A)** antibiotic administration **(B)** prolonged antibiotic (More that 14 cumulative days of antibiotic usage 30 days before the initiation of immunotherapy and within the first 12 weeks of treatment) administration and **(C)** steroid administration >10 mg on disease stabilization rates (PR or SD; Chi- square test, 95%). (page 56)

Figure 9: Mann-Whitney U test examining the effect of the duration of ATB administration in days on **Disease Control Rates (DCR)**. On the left side are the days on ATB of the patients that experienced **progressive disease (PD)** and on the right side the days on ATB of those who had DCR (PR or SD) as response to immune checkpoint inhibitors administration. (page 57)

Figure 10: Forest plot depicting the odds ratios of the studied parameters for disease stabilization (PR or SD) in **(A)** univariate binary regression analysis and **(B)** multivariate binary regression analysis that included the variables that reached statistical significance (p<0.05) in the univariate analysis. (LB: Lower border, UB: Upper border). (page 57)

Figure 11: Survival Analysis Utilizing Kaplan-Meier Method and Cox Regression. **A.** Impact of **Extended Antibiotic (ATB)** Usage on **Progression-Free Survival (PFS)**. **B.** Influence of Extended ATB Usage on **Overall Survival (OS)**. **C.** Scatterplot Illustrating the Influence of ATB Duration in Days as a Continuous Variable on PFS. **D.** Scatterplot Demonstrating the Relationship Between ATB Duration in Days as a Continuous Variable. (page 60)

Figure 12: **A.** Distribution of the performance metric (AUC) of our model. The distribution is computed on out of sample predictions of the current model. **B.** Receiver Operating Characteristic (ROC) Curve for the best performing model (Support Vector Machines (SVM) of type C-SVC with Polynomial Kernel and hyper- parameters: cost = 0.01, gamma = 1.0, degree = 4). The classification threshold for the 95% confidence intervals has been set at the average F1/accuracy/Balance accuracy. (page 62)

Figure 13: **A.** Feature importance plot: This chart reports feature importance defined as the percentage drop in predictive performance when the feature is removed from the model. Grey lines indicate 95% confidence intervals. **B.** The Box-Plot contrasts the cross-validated predicted probability of belonging to a specific class against the actual class of the samples. Well-performing models are expected to provide predictions that are close to 1 for the actual class and close to 0 for all other class. Class 1 is the probability of achieving PR or SD as response to immunotherapy and class 2 is the probability of developing disease progression. (page 62)

Figure 14: The Kruskal-Wallis test was employed to assess potential distinctions in the distributions of baseline **Lean Skeletal Muscle Index (LSMI)** values between males with cachexia and those without, as well as between females with cachexia and those without. (page 65)

Figure 15: The Kruskal-Wallis test was employed to examine potential disparities in the distributions of **Lean Skeletal Muscle Index (LSMI)** change percentages during **Immune-Oncology (I-O)** treatment A) Between patients who achieved **Complete Response (CR)** or **Partial Response (PR)** and those who experienced **Stable Disease (SD)** or **Progressive Disease (PD)**. B) Between patients who achieved CR, PR, or PD and those who experienced PD. C) Between individuals who attained prolonged disease control for six months or more and those who did not. (page 68)

Figure 16: Forest plots illustrating the odds ratios of the analyzed variables concerning the likelihood of experiencing disease progression as the best response to **Immune Checkpoint Inhibitor (ICI)** treatment, delineated as follows: **(A)** Univariate analysis; and **(B)** Multivariate analysis. The variables include **ICI** (Immune Checkpoint Inhibitor), **BMI** (Body Mass Index), **PD-L1** (Programmed Death-Ligand 1), and **PS** (Performance Status). (page 68)

Figure 17: Kaplan-Meier survival curves illustrating the impact of baseline Cancer Cachexia Syndrome (CCS) on Progression-Free Survival (PFS) **(A)** and Overall Survival (OS) **(B)**, as well as the influence of baseline Lumbar Skeletal Muscle Index (LSMI) values on PFS **(C)** and OS **(D)**. **CCS**, cancer cachexia syndrome; **PFS**, progression free survival (months); **OS**, overall survival (months); **LSMI**, lumbar skeletal muscle index (cm^2/m^2) (at the level of 3rd lumbar vertebra); **LNL**, lower normal limit ($55 \text{ cm}^2/\text{m}^2$ for males and $<39 \text{ cm}^2/\text{m}^2$ for females). (page 70)

Figure 18: Log-rank test demonstrating the effect of LSMI reduction% >5 during I-O on PFS **(A)** and OS **(B)**. **LSMI**, lumbar skeletal muscle index (cm^2/m^2) (at the level of 3rd lumbar vertebra); **I-O**, immunotherapy; **PFS**, progression free survival; **OS**, overall survival. (page 70)

Figure 19: Log rank test demonstrating the effect of cancer cachexia syndrome on overall survival amongst the patients' subgroups that received PD-1/PD-L1 inhibitors as first line treatment (A) and second line treatment (B). OS, overall survival; PD-1, programmed death-1; PD-L1, programmed death ligand 1. (page 71)

Figure 20: Log-rank test demonstrating the effect of cancer cachexia syndrome on 6 months survival. (page 71)

Figure 21: Scatter-plots demonstrating the correlation between baseline BMI values and A. baseline VFI values, B. baseline SFI values C. baseline LSMI values D. baseline IMFI values. BMI=Body mass index, LSMI: Lumbar skeletal muscle index (At the level of 3rd lumbar vertebra), IMFI=Intramuscular Fat Index (At the level of 3rd lumbar vertebra), VFI=Visceral Fat Index (At the level of 3rd lumbar vertebra), SFI=Subcutaneous Fat Index (At the level of 3rd lumbar vertebra) (page 76)

Figure 22: Scatter-plots demonstrating the correlation between baseline LSMI values and A. baseline IMFI values, B. baseline VFI values C. baseline SFI values. LSMI: Lumbar skeletal muscle index (At the level of 3rd lumbar vertebra), IMFI=Intramuscular Fat Index (At the level of 3rd lumbar vertebra), VFI=Visceral Fat Index (At the level of 3rd lumbar vertebra), SFI=Subcutaneous Fat Index (At the level of 3rd lumbar vertebra) (page 77)

Figure 23: Box-plots demonstrating the differential distributions (Mann Whitney U test) of A. Baseline* BMI values between responders and non-responders B. IMFI values between responders and non-responders C. VFI values between responders and non-responders D. LSMI values between responders and non-responders E. IMFI values in patients who achieved disease control (CR or PR or SD) versus those who experienced PD F. LSMI values of individuals who achieved disease control versus those who had disease progression. BMI=Body mass index, LSMI: Lumbar skeletal muscle index (At the level of 3rd lumbar vertebra), IMFI=Intramuscular Fat Index (At the level of 3rd lumbar vertebra), VFI=Visceral Fat Index (At the level of 3rd lumbar vertebra), SFI=Subcutaneous Fat Index (At the level of 3rd lumbar vertebra), CR: Complete response, PR: Partial response, SD: Stable disease, PD: Progressive disease * Baseline: At the beginning of immunotherapy (page 78)

Figure 24: Box-plots depicting the baseline* differential distributions (Mann Whitney U test) of A. SFI (cm²/m²) between responders (CR or PR) and non-responders (SD or PD) to I-O B. SFI (cm²/m²) between patients who achieved disease control (CR or PR or SD) as result of I-O versus those who developed disease progression (PD). C. BMI (kg/m²) between patients who achieved disease control as result of I-O administration in comparison to those who developed disease progression and D. VFI (cm²/m²) between individuals who experienced disease control under I-O versus those who had disease progression. I-O = Immunotherapy; BMI = Body mass index; VFI = Visceral Fat Index (At the level of 3rd lumbar vertebra); SFI = Subcutaneous Fat Index (At the level of 3rd lumbar vertebra); CR = Complete response; PR = Partial response; SD = Stable disease, PD = Progressive disease. *Baseline = At the beginning of immunotherapy. (page 79)

Figure 25: Kaplan-Meier curves demonstrating the effect of A. Baseline*¹ LSMI*² values on PFS B. Baseline LSMI values on OS C. Baseline SFI*³ values on PFS D. Baseline SFI values on OS. LSMI = Lumbar skeletal muscle index (At the level of 3rd lumbar vertebra); SFI = Subcutaneous Fat Index (At the level of 3rd lumbar vertebra); OS = Overall survival; PFS = Progression free

survival. ^{*1} Baseline: At the beginning of immunotherapy with PD-1/PD-L1 inhibitors. ^{*2} LNL: Lower normal limit, 55 cm²/m² for males and 39 cm²/m² for females. ^{*3} High and low classification for SFI represents above and below gender specific median value, respectively. (page 81)

Figure 26: Log-rank test demonstrating the different survival outcomes of **A**. The patients in our cohort according to the combination of their baseline^{*1} SFI and LSMI values **B**. Between patients with high^{*2} SFI and LSMI \geq LNL^{*3} and patients with high SFI and LSMI $<$ LNL. LSMI=Lumbar skeletal muscle index (cm²/m²) (At the level of 3rd lumbar vertebra), SFI=Subcutaneous fat index (cm²/m²) (At the level of 3rd lumbar vertebra), OS=Overall survival. ^{*1} Baseline: At the beginning of immunotherapy; ^{*2} Low: Below gender specific median value; High: Above gender specific median value; ^{*3} LNL: Lower normal limit, 55 cm²/m² for males and 39 cm²/m² for females (page 83)

Figure 27: Scatter-plot demonstrating the overall survival values of the patients according to their baseline SFI. Univariate Cox Regression analysis for OS for SFI as continuous variable HR=0.983 (0.970-0.997), p=0.014. Gender was used as a stratification factor. (page 84)

Figure 28: Forest plots demonstrating the hazard ratios and their 95% confidence intervals of the analyzed parameters on **A**. Probability of disease progression **B**. Probability of death under treatment with ICIs. BMI = Body mass index; PD-L1 = Programmed death ligand-1, ICI = Immune checkpoint inhibitor; LSMI: Lumbar skeletal muscle index (At the level of 3rd lumbar vertebra); LNL: Lower normal limit, 55 cm²/m² for males and 39 cm²/m² for females; IMFI = Intramuscular Fat Index (At the level of 3rd lumbar vertebra); VFI = Visceral Fat Index (At the level of 3rd lumbar vertebra); SFI = Subcutaneous Fat Index (At the level of 3rd lumbar vertebra). ^{*1,2,3,4,5,6} SFI, VFI, IMFI, LSMI, PD-L1 and BMI values were calculated at the beginning of treatment with ICIs. ^{*1,2,3} Low for SFI, VFI and IMFI means below gender specific median value. (page 85)

3. Diagrams:

Diagram 1: Timeline of FDA approval of immune checkpoint inhibitors for the treatment of metastatic Non-Small Cell Lung Cancer (NSCLC). (page 25)

Diagram 2: Flow chart of our study. ^{*1}: Classification for cachexia was conducted according to the criteria by Fearon *et al.* [1]. ^{*2}: LSMI: Lumbar Skeletal Muscle Index. (page 47)

Table of Contents

1. Introduction	21
1.1 Immunotherapy as a novel treatment modality for metastatic Non-Small Cell Lung Cancer	21
1.2 Definition of Cancer Cachexia Syndrome and interrelated molecular pathways between Cancer Cachexia and immune response	26
1.3 The necessity for the discovery of immunotherapy biomarkers	36
2. Aims of the thesis	41
3. Methods	42
3.1 Study design	42
3.2 Definition of cachexia syndrome and adipose tissue indices in the study population	46
3.3 Statistical analysis and model design analysis	49
4. Study design	52
4.1 Clinical parameters as determinants of outcome in patients with Non-Small Cell Lung Cancer treated with PD-1/PD-L1 inhibitors	52
4.2 Cancer cachexia syndrome as a biomarker of immunotherapy outcomes in metastatic Non-Small Cell Lung Cancer	63
4.3 Adipose tissue composition as a prognostic and predictive biomarker of immunotherapy outcomes in metastatic Non-Small Cell Lung Cancer	74
5. Discussion	87
5.1 Disease characteristics and antibiotic usage as determinants of immunotherapy outcomes	87
5.2 Cancer cachexia as predictive and prognostic factor in the immunotherapy era	89
5.3 Subcutaneous adipose tissue density and sarcopenia as pivotal components in the orchestration of robust anti-tumor immune response	91
6. Conclusions and future perspectives	95
7. References	96
8. Abbreviations	107
9. Acknowledgements	108
10. Published scientific papers as result of this PhD Thesis	109

1. Introduction

1.1 Immunotherapy as a novel treatment modality for metastatic Non-Small Cell Lung Cancer

Primary Lung Cancer is the leading cause of cancer-related deaths in a global scale [2], thus representing a major public health issue. Despite the remarkable improvements in diagnostic modalities more than half of newly diagnosed patients with lung cancer are diagnosed with metastatic disease [3]. Although a plethora of chemotherapeutic agents has been investigated for the treatment of metastatic lung cancer, the aforementioned nosology had been the foster child of failed clinical trials with 5 year survival being well below 10% [3].

From a histological standpoint, lung cancer is divided into two broad histological subtypes, Small Cell Lung Cancer (SCLC) and Non-Small Cell Lung Cancer (NSCLC) with the latter being further subdivided to lung adenocarcinoma (LADC) and squamous cell lung carcinoma (sqLC) [4]. The discovery of driver mutations in a small subset of individuals with LADC and the subsequent development of small molecular tyrosine kinase inhibitors [5] offered improved clinical outcomes in the patients suffering from these specific molecular subtypes of LADC(6–8). However, the majority of malignancies in patients with NSCLC do not bear any targetable driver mutations thus leading to their systemic therapy to be based on a platinum doublet backbone with poor long term survival rates [3].

The modulation of immune system against cancer cells has not been a new concept, *ex nihilo nihil fit*. Since the middle ages there have been reports of spontaneous regression of tumors in individuals when they got transmitted febrile diseases like malaria [9]. In 1891, surgeon William Coley, later known as the father of immunotherapy, injected three patients suffering from soft tissue sarcomas with a specific streptococcal preparation (known as Coley's toxins) observing a prolonged antitumoral effect [10]. Almost a century after, Rosenberg et al [11] investigated the antitumoral effect of administration of in vitro expanded autologous tumor infiltrating lymphocytes (TILs) with concurrent high dose interleukin-2 (IL-2). Consequently, the modern era for cancer immunotherapy had begun. Accumulated knowledge during the years led to the acknowledgement of immunoediting as the process of immune evasion by the cancer cells through stepwise genomic evolution and modulation of the tumor environment during the course of disease trajectory [12]. Immune evasion now stands as one of the hallmarks of malignancy development and evolution [13].

The discovery and cloning of *Ctla-4* [14,15] and *PDCD1* [16] genes and the unraveling of the physiologic roles of their encoding proteins cytotoxic T-lymphocyte-associated protein 4 (CTLA-4) and programmed-cell death protein 1 (PD-1) respectively, as immune checkpoints led to a new age of immune system modulation against cancer [17]. In these initial scientific reports, the role of CTLA-4 and PD-1 as negative regulators of immune response was revealed by demonstrating that *Ctla-4^{-/-}* and *PDCD1^{-/-}* mice demonstrated serious, even fatal, autoimmune phenomena [14,15,18].

More specifically, the initial step for the activation of T cells against a specific antigen requires the interaction of the T-cell receptor (TCR) complex with the antigenic epitope which is bound to the major histocompatibility complex (MHC) proteins of the antigen presenting cell (APC) [19]. However, the previous condition is necessary but not sufficient for effective T cell activation. The additional interaction of the protein CD28 in

the cell membrane of T cells with the proteins CD80 (or B7-1) or CD86 (or B7-2) in the membrane of the APC is required for the proper activation of the T cells [19]. CTLA-4 shares homology with CD28 and if it is expressed in the surface of T cells binds with B7-1 or B7-2 with much higher affinity than CD28, thus preventing the co-activation signal and leading the T cell into anergy [20]. In addition, CTLA-4 is highly expressed in the T regulatory cells (Tregs) contributing to their immune suppressing function with two proposed suggested mechanisms, either through the limiting of the availability of CD80/86 ligands for the necessary co-stimulation mediated by CD28/B7-(1 or 2) interaction [21] or through APC-mediated trans-endocytosis of CD80/86 ligands [22]. On the other hand, the biological network involving PD-1 (or else CD273) and its ligands, programmed-cell death protein ligand 1 (PD-L1) and programmed-cell death ligand 2 (PD-L2) is a critical pathway for the achievement of equilibrium of peripheral tolerance under physiologic conditions [23]. PD-1 is expressed normally in a spectrum of immune cells such as activated natural killer (NK) T cells, B cells, immature Langerhans' cells and activated T cells [24]. Protein-protein interaction between PD-1 and its ligands PD-L1 and PD-L2 either in the level of APC-T cell interaction or in the level of cancer cell-T cell interaction leads to inhibition of further intracellular signaling from the activated TCR and the inhibition of the linker of activated T cells (LAT) protein causing the T cells to fall into anergy or apoptosis [25]. Expression of the PD-L1 is used by the cancer cells as one of the aspects of immunoediting for the successful evasion of host's immune system [25]. Preclinical data demonstrated that the inhibition of CTLA-4 [26,27] and PD-1 [27], respectively, led to tumor shrinking in various tumor models, thus identifying them as potential drug targets from a pharmacodynamic perspective. An overview of the underlying mechanism of the expected antitumoral effect derived from PD-1/PD-L1-2 pathway inhibition or CTLA-4 inhibition is demonstrated in figure 1.

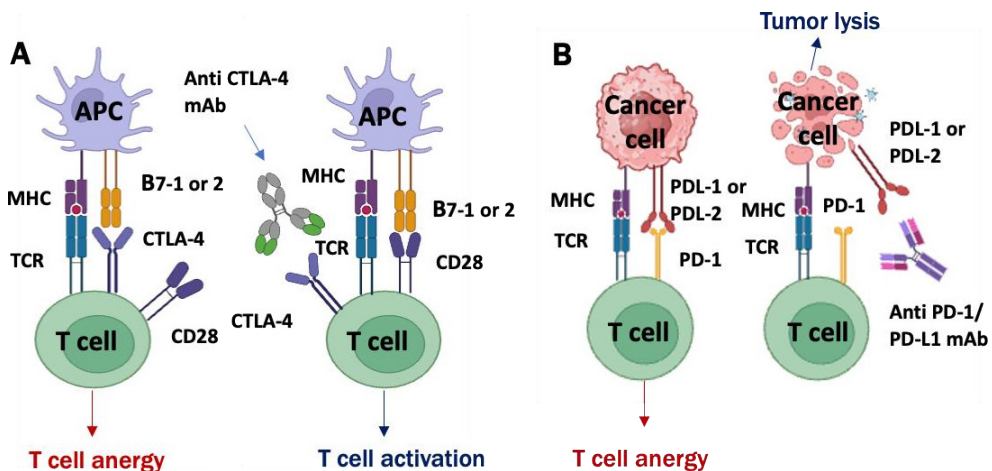


Figure 1: Schematic representation of the potential antitumor mechanism of CTLA-4 or PD1/PDL1 [2] axis blockade. A. CTLA-4 inhibition allows the interaction of CD28 with B7-1 or B7-2 thus allowing for T cell activation upon the presentation from the APC of the cancer neoantigen to the T cell. B. Inhibition of the PD1/PDL1 [2] axis allows for the T cell upon activation from the cancer neoantigen presented by the tumor cell to effectively exert its antitumoral effects.

Phase I trials of monoclonal antibodies that conferred CTLA-4 blockade [28] and PD-1 inhibition [29] demonstrated antitumoral activity and more importantly, prolonged responses or disease control to a subset of patients. These studies acted as a proof of concept for the possibility of application of immune therapy against cancer in a wide scale. Previous studies with high dose IL-2 [30] or the administration of autologous TILs [11,31] had demonstrated efficacy against especially melanoma or renal cell cancer, but these treatment modalities suffered from two major limitations for their wide application, high toxicity rates and the inability for reproducibility. The development of immune checkpoint inhibitors (ICIs), on the other hand, offered the possibility of the application of immune therapy in everyday clinical practice on a global level.

The promising results of the phase I trials of CTLA-4 and PD-1/PD-L1 inhibitors led to the further development of these class of drugs through the assessment of their activity and toxicity in larger scale, phase II and III trials. Ipilimumab was the first drug to be approved by the FDA for the treatment of metastatic melanoma in 2011 after the results of the phase III trial that compared ipilimumab plus gp100 versus gp100 versus ipilimumab monotherapy in 676 HLA-A*0201-positive patients with unresectable stage III or IV melanoma [32]. Administration of ipilimumab was associated with improved median survival 10 months in the patients that were treated with ipilimumab plus gp100 compared with 6,4 months in the patients that received gp100 (hazard ratio for death (HR)=0.68, $p<0.001$). Noticeably, in accordance with the previous reports from the phase I trials [28], the administration of ipilimumab was associated with prolonged responses or prolonged disease stabilization which was unprecedented at the time [32].

In the March of 2015, Nivolumab, an igG4 anti-PD-1 fully humanized monoclonal antibody, received FDA regulatory approval as 2nd line treatment for metastasized NSCLC with squamous histology that had progressed to one previous line of chemotherapy based on the results of the Checkmate 017 trial [33]. Checkmate 017 was a randomized phase III trial, that compared Nivolumab with standard of treatment docetaxel in individuals was metastatic squamous NSCLC that had progressive or refractory disease to previous 1st line platinum based cytotoxic chemotherapy. The primary endpoint was overall survival. The patients treated with nivolumab experienced improved overall survival compared to the individuals that received treatment with docetaxel, median Overall Survival (OS) 9,2 months vs 6 months (HR: 0.59, Confidence Intervals (CI): 0.44-0.79, $p < 0.001$).

Checkmate 057 was a phase III randomized trial investigated the activity of nivolumab against docetaxel as 2nd line treatment for patients with non-squamous metastatic NSCLC that had progressed after first line treatment with chemotherapy with a platinum backbone [34]. The primary endpoint of the study was overall survival. Nivolumab group had improved survival compared to docetaxel group at a statistical significant level, HR=0.73 (96% CI: 0.59 to 0.89; $p=0.002$) [33]. Checkmate 057 led to FDA regulatory approval of nivolumab as a second line treatment for patients with non-squamous NSCLC that have progressed after 1st line treatment with a platinum doublet.

Several months later, on October of 2015, Pembrolizumab, an IgG4, fully humanized monoclonal antibody received also regulatory approval as 2nd line treatment for individuals with metastatic NSCLC that had experienced treatment failure with a 1st line platinum based chemotherapy based on the results of Keynote-010 and Keynote-001 [35,36]. Keynote-010 was a phase III randomized trial that compared the activity of pembrolizumab against

docetaxel in individuals with metastatic NSCLC that had progressed to 1st line platinum based treatment in PD-L1 positive patients [35]. The primary end points of the study were overall survival and progression-free survival in the total population and in patients with PD-L1 expression on at least 50% of malignant cells. PD-L1 positivity was defined as the number of cancer cells that stained positive with the monoclonal antibody assay 22C3. PD-L1 positive patients were defined as the individuals with PD-L1 positivity in $\geq 1\%$ of neoplastic cells [35,36]. Pembrolizumab administration 2 mg/kg was associated with improved overall survival compared to docetaxel, (HR=0.71, 95% CI: 0.58–0.88; $p<0.001$).

Atezolizumab, an anti-PD-L1 IgG1 monoclonal antibody, was approved by FDA also as 2nd line treatment for patients with metastatic NSCLC that had progressed to first line platinum-based chemotherapy in October of 2016. The trial that led to the regulatory approval of atezolizumab was the OAK trial [37]. OAK was a phase III randomized trial that compared the efficacy of atezolizumab versus docetaxel as 2nd line treatment [37]. OAK study had co-primary endpoints, overall survival in the intention to treat population (ITT) and PD-L1 expression populations TC1/TC2/TC3 or IC1/IC2/IC3 [37]. In OAK study a different antibody assay for PD-L1 immunochemistry quantitative analysis was applied, the VENTANA SP142 PD-L1 immunohistochemistry assay. TC1/TC2/TC3 were defined as PD-L1 expression on 1% or more of cancer cells and IC1/IC2/IC3 as PD-L1 expression on 1% or more of tumor-infiltrating cells of the immune system [37]. Overall survival was improved with atezolizumab compared with docetaxel in the ITT population, 13.8 months vs 9.6 months, HR= 0.73 (95% CI: 0.62–0.87, $p<0.001$).

In the first line treatment setting, Pembrolizumab received FDA regulatory approval in 2016 as a result of Keynote-024 [38]. Keynote-024 was a randomized phase III trial that compared the activity of pembrolizumab as first line treatment against platinum-based chemotherapy in individuals with metastatic NSCLC without epidermal growth factor (*EGFR*) or anaplastic lymphoma kinase (*ALK*) genetic aberrations [38]. The primary endpoint of the study was progression free survival whereas overall survival was the secondary endpoint. Pembrolizumab administration was statistically improved in the pembrolizumab group compared with chemotherapy group, HR=0.60 (95% CI: 0.41-0.89, $p=0.005$). Noticeably, The results from keynote-024 are made even more impressive if someone considers also the crossover rate to pembrolizumab after progression to chemotherapy which was more than 50% [38].

Finally, on November 2017, the initial results of the PACIFIC trial were published [39]. PACIFIC trial was a phase III randomized trial that investigated the activity of durvalumab, an igG1k anti-PD-L1 monoclonal antibody, as a maintenance therapy after concomitant chemoradiotherapy with curative intent for locally advanced NSCLC, stage IIIA or stage IIIB by TNM. The co-primary endpoints were progression free survival and overall survival. The trial was positive as the patients in the durvalumab group had an improved progression free survival compared to placebo, 16.8 months vs 5.6 months, HR= 0.52, 95% CI: 0.42 to 0.65, $p<0.001$). PACIFIC trial acted as a proof-of-concept study by demonstrating the efficacy of immune checkpoint inhibitors in the maintenance setting.

A timeline of the regulatory approvals by FDA of immune checkpoint inhibitors for the management of metastatic NSCLC until the end of 2017 is demonstrated in diagram 1.

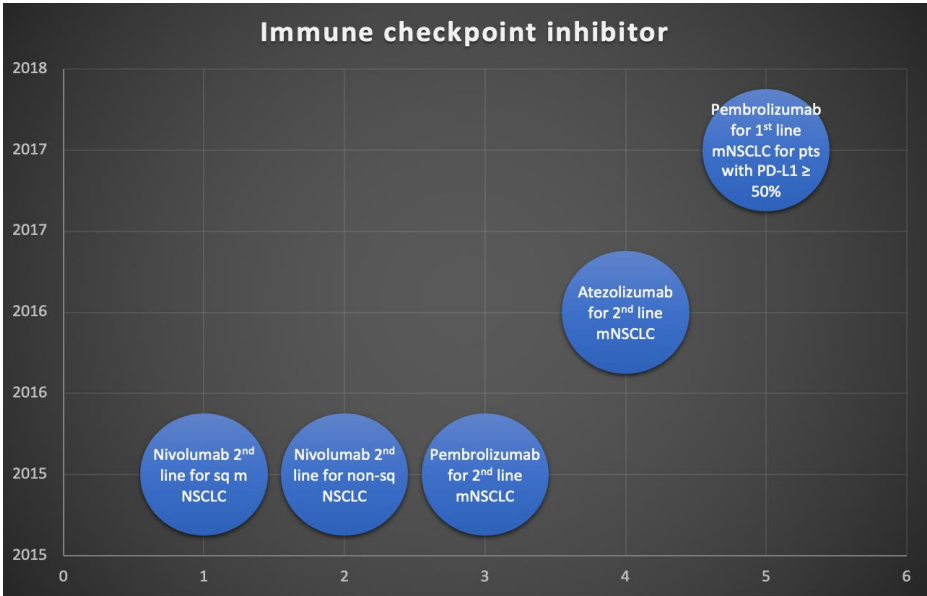


Diagram 1: Timeline of FDA approval of immune checkpoint inhibitors for the treatment of metastatic Non-Small Cell Lung Cancer (NSCLC).

In addition, since 2013, published data from phase I study NCT01024231 acted as proof of point of synergistic modulation of antitumor immunity by the combined inhibition of CTLA-4 and PD-1 [40]. Furthermore, new proteins that act as immune checkpoints have been recognized and their role as potential immunotherapy targets is under active ongoing research(25,27,41).

Through the conceptualization of the aforementioned data, the introduction of immune checkpoint inhibitors introduced a new era of medical oncology by offering the chance to harness the sophisticated force and competency of adaptive immunity in every day patient care. Nevertheless, every big step is accompanied with an increasing number of questions that emerge as a natural causal reality.

1.2 Definition of Cancer Cachexia Syndrome and interrelated molecular pathways between Cancer Cachexia and immune response

A. Cancer cachexia syndrome definition, epidemiology and clinical impact

The term cachexia originates from the Hellenic word «καχεξία» which is a complex word that combines two derivatives, 'κακός' that means bad and 'έξις' which means condition. Cachexia is defined as a distinct clinical syndrome characterized by depletion of body weight, muscle mass, and adipose tissue, along with a perturbation in the equilibrium governing energy and protein homeostasis, which remains refractory to amelioration through the provision of sufficient dietary nutrients [42]. The cachexia syndrome can manifest as a pathophysiological consequence of both malignant and non-malignant conditions, encompassing ailments like congestive heart failure, chronic obstructive pulmonary disease, and acquired immunodeficiency syndrome (AIDS). Thus, the ancient Hellenes, describe with the term cachexia the phenotypical imprinting of a complex underlying metabolic pathophysiologic process associated with a wide spectrum of medical conditions.

Within the domain of cancer, the cachexia syndrome (CCS) exhibits a notable prevalence, impacting as many as 80% of terminal-stage cancer patients, and has been correlated with heightened postoperative complications, diminished responsiveness and augmented toxicity in relation to chemotherapy, as well as overall untoward prognoses [43]. Additionally, it closely correlates with a progressive decline in performance status and an impaired quality of life, directly contributing to approximately 20% of all cancer-related mortalities [42].

CCS exhibits a multifaceted underlying pathophysiological framework triggered by a plethora of soluble signaling agents and cell-cell interactions, originating either directly from neoplastic cells or as a result of their intricate interplay with constituents of the tumor microenvironment (TME) and the host's immune system. These cellular networks orchestrate the emergence of a systemic inflammatory reaction, activation of biochemically disadvantageous cycles, and perturbation of fundamental endocrine and metabolic cascades [44]. The onset of cachexia is not an inescapable outcome of cancer; instead, it appears to hinge upon the initiation and continual sustenance of an underlying inflammatory response that drives the disruption of the intricate equilibrium regulating metabolic pathways [42,44]. Moreover, the systemic inflammatory process at the core of CCS exerts a profound influence on the operational dynamics of both the innate and adaptive immune systems, operating across multiple tiers, thereby rendering individuals afflicted with cancer cachexia more susceptible to infections [45].

Furthermore, CCS as a syndrome is associated with adipose tissue wasting and a biochemical process which has been identified as browning of the adipose tissue [46]. Browning of the adipose tissue has been characterized as the result of the uncoupling of mitochondrial respiration in brown and beige adipose cells [46] which is mediated through the activity of uncoupling protein 1 (UCP1) which, in turn, is characterized by its expression only in thermogenic fat tissue (46–48). Adipose tissue is known to be a body compartment with an important role in the modulation of the immune response [49,50]. Moreover, adipose tissue composition has been reported as an important prognostic biomarker in cancer patients

undergoing treatment(51–53). More analytically, high visceral fat percentage has been associated with poor clinical outcomes [51] where on the other hand, high subcutaneous adiposity has been associated with improved survival outcomes in individuals suffering from a wide spectrum of malignancies [52,53].

From a clinical standpoint, diagnosis of CCS is done by applying the criteria set by the international consensus of cancer cachexia [1]. These criteria encompass instances of physiological changes characterized by a reduction in body weight exceeding 5% during the preceding 6 months, or a body mass index (BMI) falling below 20 kg/m², coupled with any degree of weight decline surpassing 2% or any extent of weight loss exceeding 2% in an individual with an appendicular skeletal muscle index that is consistent of sarcopenia.

B. Cancer Cachexia Syndrome and Cancer-Immunity-Cycle

From an immunological standpoint, many of the mechanisms that have been proposed to be involved in CCS pathogenesis have also been recognized as important immune system modulators. Many cytokines that have been involved in CCS pathogenesis, either in pre-clinical models or in translational studies have been shown to be involved in the orchestration of immune response(54– 59,59–65,65–67). In addition, dysregulated autophagy, P-selectin/PSGL-1 interaction, myeloid derived suppressor cells (MDSCs), cancer associated fibroblasts (CAFs) and M2 polarized macrophages (M2) are biological processes and cell subtypes that have been associated both with CCS pathogenesis and sustainment and as immune suppressors(41,58,68–72). These findings raise the possibility of a potential dual role of these cellular interaction networks, acting both as inducers of metabolism equilibrium disruption, thus, causing the cachexic phenotype and participating in the process of immunoediting towards the successful evasion of the host's immune surveillance during the malignant process trajectory. The dual role of these mediators and mechanisms and their role on cancer-immunity- cycle [73] is depicted on figure 2.

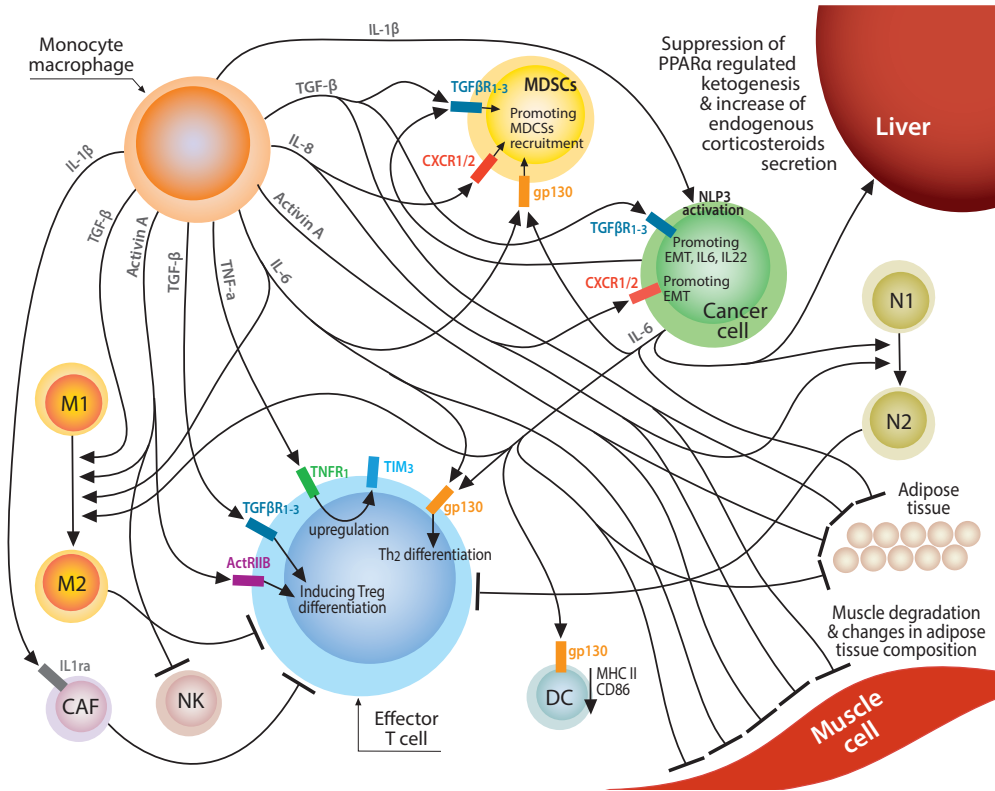


Figure 2: The dual role of a wide range spectrum of cachexia pathogenetic mechanisms and their contribution both on the phenotypical changes of cancer cachexia syndrome such as muscle wasting and adipose tissue remodeling and the inhibition of a successful anti-tumor immune response.

Abbreviations: MDSC: Myeloid derived suppressor cell, M1 & M2: M1 and M2 macrophage subtypes, N1 & N2: N1 and N2 tumor infiltrating neutrophils subtypes, CAF: Cancer associated fibroblast, DC: Dendritic cell, NK: Natural killer cell, EMT: Epithelial-to- mesenchymal transition, PPARα: Peroxisome proliferator-activated receptor alpha, ActRIIB: Type IIβ activin receptor, gp130: Glycoprotein 130, TGFβR1-3: Transforming growth factor beta receptors 1-3, TIM3: T-cell immunoglobulin and mucin-domain containing- 3, TNFR1: Tumor necrosis factor receptor 1, CXCR1/2: C-X-C motif chemokine receptor 1-2, NLP3: Nodule inception protein-like protein 3

TNF- α superfamily

More analytically, Tumor Necrosis Factor- α (TNF- α) is an acute phase reactant secreted by immune cells in the setting of stress such as infection or cancer [74]. TNF- α has shown in a variety of cachexia models to contribute to muscle wasting through the blockade of myocyte differentiation and promoting muscle degeneration through the process of ubiquitination by stimulating the activity of ubiquitin E3 ligase pathway [75] and administration of exogenous TNF- α has shown to induce cachexia in preclinical models [76]. Also it has been reported to be involved in blockade of the adipocytes differentiation process through the inhibition of adipocyte differentiation transcription factors [54] and has been implicated to be involved in the sickness behavior caused by cachexia through its effect on hypothalamic function [77]. Translation data about the role of TNF- α levels for cachexia development in cancer patients have not been consistent [78,79] and the administration anti-TNF- α monoclonal antibodies failed to reverse the cachexia phenotype in patient with pancreatic adenocarcinoma when combined with cytotoxic chemotherapy [56,80]. Nonetheless, preclinical data demonstrated that TNF- α inhibition can overcome resistance to PD-1 administration in mouse melanoma models [55]. The researchers reported that Tumor Necrosis Factor Receptor 1 (TNFR1) activation through TNF- α stimulation resulted in reduced effector CD-8+ effector T cell accumulation and upregulation of secondary immune checkpoint T-cell immunoglobulin and mucin-domain containing- 3 (TIM-3) [55]. TNF- α inhibition in patients receiving immunotherapy with checkpoint inhibitors because of immune related adverse events (irAEs) was not associated with worse clinical outcomes [81]. NCT03293784 is a phase I clinical study studying the safety of concomitant administration of certolizumab, a TNF- α inhibitor in combination with nivolumab and ipilimumab in patients with metastatic melanoma. It may be possible that continuous TNF- α /TNFR1 interaction can led to T cell exhaustion and abrasion of immune response and checkpoint inhibition efficacy in conjunction with cancer cachexia phenotype, but because of the multifactorial pathogenesis and pathophysiology of CCS it is possible this effect to be diluted and further research is required.

TNF-Related Weak Inducer of Apoptosis (TWEAK) is another member of the TNF- α superfamily that has been associated with CCS pathogenesis [82]. TWEAK binds to the TNF receptor superfamily member 12A (TNFRSF12A; also known as fibroblast growth factor-inducible 14 (Fn14) and TWEAKR) and TNFRSF12A activation in CCS study models has been reported to cause muscle atrophy through ubiquitination and activation of the NF- κ B intracellular pathway [67]. More interestingly, TNFRSF12A blockade was associated with CCS development prevention and improved survival in mouse embryonic fibroblast (MEF) Fn14 tumor models [82]. TWEAK also assumes the function of an immune modulator. More analytically, the binding of TWEAK to Fn14 impedes the activation of signal transducer and activator of transcription protein (STAT)-1, thereby dampening the generation of interferon (IFN-) and interleukin-12 (IL-12), thus demonstrating as an important factor for the effective transition from innate to adaptive immunity [65]. In the same report, TWEAK^{-/-} mice exhibited vigorous antitumor responses from natural killer (NK) cells and Th1 T cells, manifesting the capacity to reject B16 melanoma model tumor, in contrast to their wild-type (wt) counterparts [65]. Furthermore, TWEAK/Fn14 inhibition has been reported to induce an antitumoral effect by increasing the number of intratumoral

immune cells, mostly CD45+ memory cell by activating the Monocyte Chemoattractant Protein-1 [66]. A phase I study of RG7212, an IgGk1 anti-TWEAK monoclonal antibody, in patient with solid tumors has yielded modest results [83] whereas other studies are ongoing. There is paucity of clinical and preclinical data on a potential synergistic effect of combining TWEAK/Fn14 inhibitors with immune checkpoint inhibitors, but TWEAK/Fn14 pathway is an interesting pharmacodynamic target, both as anti-cachexia agent and the attenuation of immune checkpoint inhibitors antitumor activity.

Interleukins (IL)-1 α , IL-1 β , IL-6 and IL-8

Interleukin (IL)-1 α and IL-1 β , cytokines belonging to the interleukin 1 family, have been associated with cachexia pathogenesis and have been also implicated in the immunoediting process by tumors [58,72,84–87]. Nevertheless, data have been conflicting since IL-1R blockade, the receptor that both IL-1 α and IL-1 β are binding, did not show to effectively ameliorate weight loss and the CCS phenotype in mouse models [57]. IL-1 β , has been reported to exert an important role in tumor progression and immune evasion in various tumor models (58,58,85) suggesting a potential synergistic effect when combined with immune checkpoint inhibitors.

Interleukin-6 (IL-6) represents a multifaceted cytokine originating from activated macrophages, playing a cardinal role in the genesis of cancer cachexia syndrome (CCS). In experimental models, IL-6 has been demonstrated to contribute to CCS through diverse mechanisms, including augmented autophagy and elevation of transcriptional factors promoting degradation of myofibrillar proteins [42]. Plasma concentrations of IL-6 have shown a direct positive correlation with the pathogenesis of CCS and poor clinical outcomes in translational studies performed in cancer-afflicted individuals [88]. In the pre-clinical front, in a study model of colorectal cancer development, *Apc*^{Min/+} mice, harboring a germline mutation in the adenomatous polyposis coli gene (APC), exhibited heightened serum IL-6 levels, resulting in muscle tissue atrophy and the ensuing cachexia phenotype. In contrast, *Apc*^{Min/+IL-6^{-/-}} mice, which were double knock down for the IL-6 gene and had also the germline APC mutation, did not expressed the cachectic phenotype. Introduction of exogenous IL-6 into *Apc*^{Min/+IL-6^{-/-}} mice led to the emergence of the cachexia phenotype, underscoring the potential central role of IL-6 in CCS development [89]. Furthermore, administration of tocilizumab, an anti-IL-6 monoclonal antibody, in 3 cancer patients with CCS has been reported to minimize the cachectic phenotype and to led to improved clinical outcomes [90,91]. Moreover, congruent with its catabolic impact and propensity for muscle wasting, IL-6 concurrently exerts suppressive effects on antitumor immunity on multiple checkpoints of the cancer-immunity-cycle ranging from hindering dendritic cell function and development [92] to the inhibition of CD4+ T cells maturation and their polarization towards a tumor promoting Th2 phenotype [62,93], the stimulation of intra-tumoral accumulation of MDSCs [94] and the polarization of the macrophages into an M2 phenotype [95]. Notably, in two murine cachexia models, tumor- derived IL-6 prompted hepatic metabolic reprogramming by suppressing Peroxisome Proliferator-Activated Receptor alpha (PPAR α)-regulated ketogenesis, consequently leading to heightened endogenous glucocorticoid secretion. This, in turn, impaired antitumor immunity and resistance to immunotherapy [59]. Translational studies of metastatic melanoma patients treated with

the anti-CTLA-4 monoclonal antibody ipilimumab revealed a correlation between lower IL-6 serum levels and extended survival [96]. The prospect of targeting IL-6 has emerged as an appealing strategy to augment tumor responsiveness to immunotherapy.

Interleukin-8 (IL-8), serves as a chemokine predominantly synthesized by macrophages and monocytes, carrying out its actions by binding with differential affinity to multiple receptors with the C-X-C motif chemokine receptors (CXCR) 1 and 2 being the most well studied [97,98]. Elevated circulating concentrations of IL-8 in individuals with lung and pancreatic cancer have been linked to the onset of cancer cachexia syndrome (CCS) and unfavorable survival outcomes [99,100]. In addition to its capacity to incite an inflammatory and catabolic state, IL-8 has demonstrated associations with attenuated antitumor immune responses across a diverse array of experimental models. Tumor cell-derived IL-8 has been correlated with recruiting N2-type tumor-associated neutrophils (TANs) [101] and myeloid-derived suppressor cells (MDSCs) [94], driving forward immunoediting towards malignancy progression. Clinical data in patients with metastatic melanoma and non-small cell lung cancer (NSCLC) undergoing treatment with immune checkpoint inhibitors demonstrated an association between high IL-8 levels and the emergence of secondary resistance to immunotherapy [102]. In light of the available experimental evidence, the IL-8/CXCR1/2 axis emerges as a promising target for fostering robust antitumor immune responses and enhancing the efficacy of presently employed immunotherapeutic modalities.

Transforming growth factor β (TGF- β) family

Three member of the transforming growth factor β (TGF- β) family have been linked to the ontogenesis of CCS, Activin A(103–105), TGF- β [106] and Growth Differentiation Factor 15 (GDF15) [107].

Activin A is a protein complex engaged in a broad array of physiological processes from programmed cell death (apoptosis), and the recuperation of tissue injuries [104]. Activin A has demonstrated to propagate muscular wasting and cachexia in experimental models [103] and pharmacological blockade of the activin type II receptors (ActRIIB) pathway reversed cancer-related cachexia and muscular degeneration, consequently extending survival in C26 Tumor-Bearing Mice [108]. A clinical study also evidenced a positive correlation between serum levels of Activin A and the emergence of CCS, coupled with diminished survival rates among individuals with pancreatic malignancies [105]. In concurrence with its catabolic manifestations, Activin A has exhibited the ability to suppress antitumor immune responses by facilitating the differentiation of CD4⁺ T cells into T regulatory cells (Tregs) in vitro [109] and inducing the polarization of tumor-associated macrophages (TAMs) into an M2 phenotype [110]. A phase I study is investigating the effect of STM 434, an activin A inhibitor, in combination with liposomal doxorubicin in patients with advanced solid tumors (NCT02262455). Consequently, the signaling cascade governed by Activin A and ActRIIB emerges as a compelling target, holding potential for both the mitigation of cachexia and the fortification of an efficacious antitumor immune reaction. Nonetheless, further clinical and translational inquiries are warranted in this realm.

Since 1991, TGF- β has been implicated as a pathogenetic factor of CCS and fibrosis [111]. Preclinical models have unveiled that the release of TGF- β into circulation, attributed

to osteolysis stemming from bone metastases within murine models, activates the Mothers Against Decapentaplegic Homolog 3 (SMAD3)-NADPH oxidase 4 (NOX4)-ryanodine receptor 1 (RyR1) pathway, culminating in muscular malfunction and the onset of cachexia [106]. Its paramount role within the immune system is the preservation of immune tolerance. By exerting pleiotropic influences on a diverse spectrum of immune cells, TGF- β averts the genesis of autoimmune disorders while upholding immune reactions against pathogens. Nonetheless, hijacking of this signaling pathway from the cancer cells can precipitate the immunoediting process leading to tumor evasion and progression, thus, this pathway emerges as a compelling candidate for targeted interventions in antitumor therapeutic strategies [112]. Phase I and II clinical trials are underway to evaluate the safety and effectiveness of agents targeting TGF- β 1-2-3, either in isolation or cytotoxic chemotherapy or in conjunction with immune checkpoint inhibitors ICIs (NCT03192345, NCT02699515, NCT02517398 and NCT03315871).

The engagement of mitogen-activated protein kinase 11 (MAP3K11) by the interaction between GDF-15 and GDNF family receptor alpha-like (GFRAL) has been identified as the principal initiator of weight loss in animal models of cancer-associated cachexia [107]. Additionally, heightened levels of GDF15 within serum have been linked to the emergence of CCS, anorexia, escalated tumor burden, and unfavorable survival outcomes in cancer-afflicted individuals [113]. It curbs the maturation of dendritic cells within the TME, leading to impaired activation of T cells and abrogating antitumor immunity [114]. Conversely, the depletion of GDF-15 within orthotopic pancreatic cancer models reinstated immunosurveillance within the TME [115] and analogously, downregulation of GDF-15 via short hairpin RNA (shRNA) in a glioblastoma model elicited enhanced T cell infiltration within the TME and elevated survival rates [116]. Summarizing the aforementioned, TGF- β family related biological networks constitute promising pharmacological targets both as cachectic treatment and for the enhancement of the activity of ICIs.

Autophagy, cancer cachexia and immune response

Autophagy embodies a multi-stage process intricately orchestrating the ordered degradation and recycling of cellular constituents [117]. Its association with the CCS pathogenesis and its phenotypical imprinting as the persistent depletion of muscle mass in cancer-afflicted individuals has been demonstrated in translational studies [118,119]. Beclin-1 and microtubule-associated protein 1A/1B light chain 3B II (LC3 B-II), two proteins that have been reported to exert central roles in the structure and regulation of the autophagic machinery, exhibit elevated expression within the skeletal musculature of cancer patients [119]. The involvement of autophagy manifests a dual role within the realm of tumorigenesis and progression. Baseline autophagy stands as an antagonistic process against tumorigenesis, whereas dysregulated autophagy fosters the generation and evolution of tumors through aberrant processing and accumulation of byproducts of cellular metabolism that drive forward the malignant process [68].

On top of that, autophagy holds cardinal significance within both the innate and adaptive facets of immunity, particularly concerning the processes of antigen presentation and the nexus between innate and adaptive immune responses. Autophagosomes engulf intracellularly perturbed proteins, subsequently presenting the resulting peptide products

within MHC-II-bearing compartments for antigen display to a specific subset of CD4+ T cells [120]. The autophagic machinery exhibits an important role in the process of MHC-I-mediated cross-presentation to CD8+ T cells, while simultaneously tempering the cross-priming dynamics of CD8+ T cells [121]. In parallel, autophagy's role looms significant in maintaining the metabolic and oxidative equilibrium of T cells, as compromised autophagy instigates impaired degradation of mitochondrial elements, instigating a consequential surge in ROS generation and consequent T cell anergy [69]. Contrastingly, autophagy occupies a pivotal niche in the survival and immune regulatory function of Tregs, as the ablation of *Atg5* or *Atg7*, genes fundamentally essential in the construction and operation of the autophagic protein complex, leads to Treg dysfunction and apoptosis [69]. Tregs bereft of autophagic capabilities witness a waning expression of the transcription factor Forkhead Box P3 (FOXP3), which concurrently augments the elevation of metabolic mediators, resulting in a compromised immune suppressing role [69]. Equally pivotal, autophagy serves as a determinant for steering macrophages towards an M2 immunosuppressive phenotype [122] and the autophagic biological network orchestrated by high mobility group box 1 (HMGB1) has emerged as a critical driver for the perpetuation of myeloid-derived suppressor cells (MDSCs) viability [123].

Amidst the intricate landscape, while autophagy appears to wield a noteworthy influence in the trajectory of CCS and its perturbations align with the dampening of antitumor immune responses, a dearth of comprehensive data necessitates further exploration. Further research at a preclinical and translational level is warranted to fathom whether the escalated inflow of autophagy in the skeletal musculature of CCS-affected cancer patients correlates with a corresponding surge in autophagy within specific immune cellular components of the tumor microenvironment (TME), ultimately culminating in the aggregation of Tregs and M2 macrophages. The validation of this hypothesis could emphasize the role of dysregulated autophagy in the context of primary and/or secondary resistance to checkpoint blockade and position components of the autophagic machinery as potential targets for the development of novel treatments.

SELP gene and cachexia

Cancer patients harboring the C allele of the rs6136 single nucleotide polymorphism (SNP) within the *SELP* gene, which encodes the adhesion molecule P-selectin, exhibit a diminished susceptibility to Cancer Cachexia Syndrome (CCS) [124]. This aforementioned specified genetic variation is associated with reduced serum levels of P-selectin [125]. The family of selectins, encompassing E-selectin, P-selectin, and L-selectin, stands as a collective of adhesion molecules that exert a central role in the orchestration of the inflammatory cascade mainly through the regulation of the recruitment of immune cells and platelets at sites of inflammation [126]. P-selectin glycoprotein ligand-1 (PSGL-1) emerges ubiquitously across all leukocyte subpopulations, serving as the primary ligand for P-, E-, and L-selectins [90].

Experimental models, employing mice deficient in selectins (P-, L-, and E-selectin), have underscored the role of these molecules in promoting metastasis while also facilitating the recruitment of CD11b+Ly6C+Ly6G+ myeloid-derived suppressor cells (MDSCs) within the tumor microenvironment (TME) [127]. Furthermore, PSGL-1 has been implicated to as an immune checkpoint regulator [41]. In a murine model of melanoma,

mice lacking PSGL-1 (Selp^{g^{-/-}}) exhibited an augmented antitumor immune response, attributable to the downregulation of inhibitory checkpoints. This led to a heightened intratumoral accumulation of effector CD44^{hi}CD8⁺ and CD4⁺ T cells in comparison to their wild-type counterparts and higher numbers of IFN- γ and IL-2 producing T cells [41]. There exists a paucity of data pertaining to the potential of a blockade targeting the P-selectin/PSGL-1 axis in effecting the reversal of the CCS phenotype or investigating a potential synergistic effect of dual inhibition of PD1 or CTLA-4 dual inhibition and the selectin/PSGL-1 axis.

Nevertheless, the prospect of targeting the PSGL-1/P-selectin pathway for immunotherapy presents itself as a compelling avenue, particularly for individuals afflicted by preexisting CCS (Figure 3).

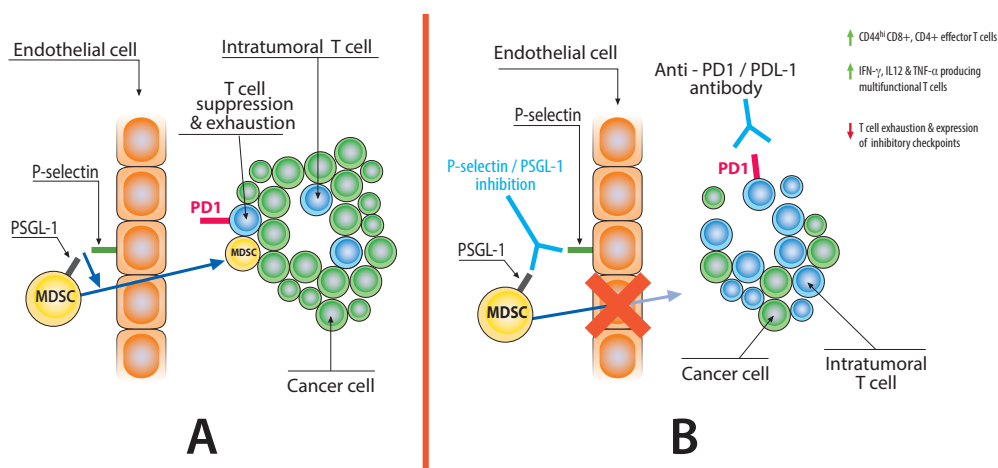


Figure 3: Potential synergistic mechanism potentiating immunotherapy effect derived from the dual inhibition of PD-1/PD-L1 and P-Selectin/PSGL-1 interactions. MDSC: Myeloid derived suppressor cell, PSGL-1: P-selectin glycoprotein ligand 1, PD-1: Programmed cell death protein 1, PD-L1: Programmed cell death protein 1 ligand

Myeloid derived suppressor cells (MDSCs)

MDSCs encompass a heterogeneous assemblage of myeloid-derived cells intricately linked with the dampening of antitumor immune responses [70]. MDSCs, whether as circulating cells or within the TME, have been associated with the genesis of CCS across studies in experimental models and in cancer patients [71,128]. MDSCs exercise multifaceted negative influence over the antitumor immune response. They have been reported to facilitate the recruitment of intratumoral regulatory T cells (Tregs) and elicit the polarization of macrophages toward an M2 immunosuppressive phenotype [70,94]. The role of MDSCs is hypothesized to precipitate CCS through the provocation and perpetuation of an underlying inflammatory milieu, consequently triggering amplified energy expenditure and protein turnover [71].

The pursuit of strategies targeting MDSCs is fraught with challenges due to the intricate heterogeneity intrinsic to divergent human MDSC populations. Nevertheless, such endeavors stand forth as one of the most promising avenues for augmenting the tumor's

sensitivity to immunotherapy. The overarching inquiry concerning the potential of MDSC depletion to ameliorate the CCS phenotype or to surmount established immunotherapeutic resistance beckons for more thorough investigation.

C. Conclusions

As discerned from the aforementioned preclinical and clinical data, a significant subset of factors implicated in the pathogenesis of cancer cachexia exhibit a dual role. This dual role encompasses the phenotypic footprint of cancer cachexia and diminished immune responsiveness against malignant processes. When one contemplates the prevalence of the cancer cachexia syndrome in cancer afflicted individuals, coupled with the escalating population of patients afflicted by neoplasms and undergoing immunotherapy, the investigation into the influence of the aforementioned syndrome on the clinical outcome of these individuals becomes an anticipated causal cognitive correlation.

1.3 The necessity for the discovery of immunotherapy biomarkers

The introduction of ICIs unraveled an new era in metastatic lung cancer management offering the possibility of prolonged remission in a small, but significant subset of patients with metastatic malignancies [32–34,36–38,40,129]. However, sufficient biomarkers in order to predict the individuals that will derive benefit from the administration of ICIs are lacking. From a financial standpoint, the extensive implementation of ICIs is correlated with noteworthy expenditures for the healthcare framework, thereby engendering deliberations on the viability of their cost-effectiveness [130]. Further research on the discovery of biomarkers would improve not only patient selection but could also drive forward research towards the therapeutic field by further unraveling the underlying mechanisms of primary and secondary resistance to ICIs.

PD-L1 expression on cancer cells or in the immune cells of the TME has been the only biomarker that has demonstrated to be associated with improved clinical outcomes in prospective studies [33,34,36,129]. At 2017, three different immunohistochemistry (IHC) assays had been developed to evaluate PD-L1 expression and they have received approval from the FDA as companion diagnostic assays. PD-L1 IHC 22C3 pharmDx assay (Dako North America) has been applied for the estimation of PD-L1 expression in pembrolizumab clinical trials [29,35,36,38,129]. Dako 28-8, a rabbit PD-L1 antibody, has been used for testing the PD-L1 expression in nivolumab clinical trials [33,34,40]. Ventana SP263 has been the IHC test applied in the atezolizumab trials [37]. It is worth noting that 22C3 and 28-8 assessed PD-L1 expression levels, as the percentage of cancer cells in the biopsy material that stained positive with the test antibodies [33–36,38,40] whereas SP263 Ventana assessed PD-L1 expression in the cancer cells and immune cells of the TME [37].

Despite the different IHC assays applied in the clinical trials that led to regulatory approval of ICIs, PD-L1 expression levels have demonstrated consistently, across different studies, a positive correlation with improved clinical outcomes [29,33–35,37,38]. In Keynote-001, individuals with positive PD-L1 expression experienced longer Progression-Free Survival (PFS) and OS when compared with the rest of the treated patient in the study cohort [36]. Interestingly, duration of response (DOR) was not affected by PD-L1 expression levels [36]. In Keynote-010, PD-L1 expression $\geq 50\%$ was associated with a numerical higher overall survival compared to patients with PD-L1 expression ranging from 1–49% [35]. In Keynote-042, which investigated pembrolizumab effect in patients with PD-L1 expression $\geq 50\%$, ICI administration was associated with high response rates $\sim 45\%$ and an unprecedented PFS of 10,3 months [38].

In accordance with the Keynote studies, Checkmate-057 trial demonstrated also that high PD-L1 expression consists a positive predictive and prognostic biomarker for ICI efficacy in NSCLC [34]. In the aforementioned trial, individuals with PD-L1 expression $\geq 1\%$ expressed 31% response rates when treated with nivolumab, compared to 9% for ICI treated patients with PD-L1 expression levels $< 1\%$ [34]. However, correspondingly with Keynote-001 DOR was not associated with PD-L1 expression and responders with negative PD-L1 expression experienced a prolonged clinical benefit from ICI administration [34,36]. Hazard Ratios (HR) for OS were similar for PD-L1 negative and PD-L1 positive patients ranging from 0.58 to 0.69, respectively [34]. In Checkmate-017, PD-L1 expression in the intention-to-treat (ITT) population was not correlated with response or survival outcomes [33]. This result could be

attributed to a statistical type error II, the fact that the study was not designed to evaluate PD-L1 expression and clinical outcomes as the primary end-point and to the inherent divergent biology of squamous NSCLC compared to LADC.

OAK study, evaluated PD-L1 expression by applying the Ventana SP263 assay [37]. According to percentage of tumor cell or immune cell positivity for PD-L1 expression they were classified as TC0, TC1, TC2, TC3 and IC0, IC1, IC2 and IC3 respectively [37]. TC0 was classified as 0% PD-L1 expression on tumor cells, TC1 as 1% or more but less than 5%, TC2 as PD-L1 expression 5-49% and TC3 as PD-L1 expression 50% or higher in the tumor cells [37]. In an analogous manner, patients were classified as IC0, IC1, IC2 and IC3 [37]. TC3 or IC3 patients demonstrated improved clinical outcomes compared to rest of the patient cohort [37].

Consequently, as derived from the data from the phase III studies that led to the regulatory approval for ICI treatment in NSCLC, PD-L1 is an important biomarker for patient selection, especially for individuals with PD-L1 equal or higher to 50%, because it determines first line treatment options. Moreover, it has been the only validated biomarker on prospective large-scale trials. On the other hand, even the patients with negative PD-L1 expression can derive a significant clinical benefit if they respond to treatment [33,34,37]. Importantly, PD-L1 expression has not been correlated with DOR in the aforementioned studies, so all the patients independently of its expression can achieve a prolonged disease control [33,34,37]. However, the Kaplan-Meier survival curves of the majority of the studies have shown that a number of patients receiving immunotherapy as monotherapy have worse survival than those treated with cytotoxic chemotherapy in the first 3-6 months of treatment (Figure 4).

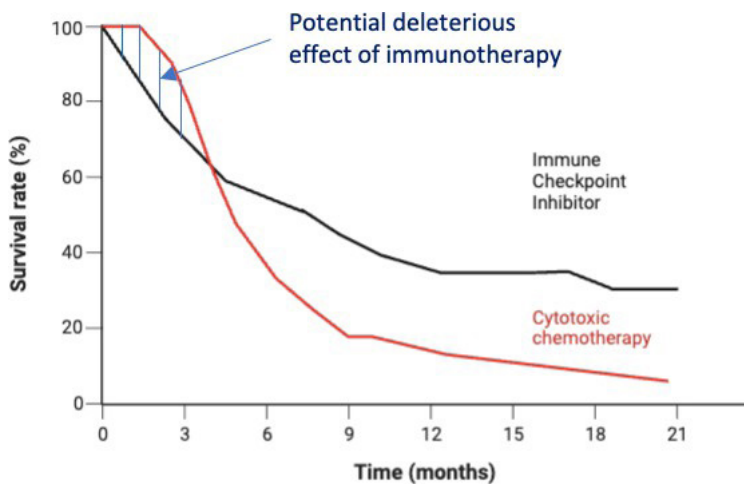


Figure 4: Hypothetic Kaplan-Meier curve that depicts the observed phenomenon in phase 3 trials where patients in the immunotherapy arm experience worse survival than the patients in the chemotherapy arm in the first 3-6 months after treatment initiation.

There has not been a sufficient explanation for this phenomenon but several underlying etiologies have been proposed. One hypothesis that has been proposed associates this phenomenon with the prolonged time to response (TTR) to ICI [131]. More analytically, certain individuals with rapid progressive disease do not have sufficient time to respond

to ICI and as a consequence, they experience worse survival. Another explanation is that PD-L1 inhibition can lead to the expansion of an immune suppressive compartment of the adaptive immunity, such as the Tregs [132]. None of the previous hypotheses, however, has been validated in translational or clinical data. Nonetheless, there is a group of patients that does not derive benefit from ICI administration and maybe there hinders a potential deleterious effect of immunotherapy and PD-L1 status is not sufficient for the identification of this subgroup.

TME has been characterized by significant inter-tumoral (tumor by tumor) and intra-tumoral (inside the tumor) heterogeneity [133]. This heterogeneity is based on the different immune phenotypes of TME ranging from cold tumors, tumors that do not have the capacity to induce immune stimulation, immune-excluded tumor, tumors that have induced immune stimulation but the effector T cells are excluded mechanically from the tumor so that they cannot reach and exterminate efficiently the cancer cells and inflamed tumors, tumors with infiltration of immune cells that have been activated against cancer neoantigens [133]. In colorectal cancer, the immune-score, a score based on the enumeration of two immune cell populations (CD3+/CD45RO+, CD3+/CD8+ or CD8+/CD45RO+) in the core of the tumor and in the invasive margin has proved an effective prognostic marker in prospective studies [134]. Despite the promising preclinical results and the robust biologic rationale behind this approach, there has not been any prospective study that has evaluated the effect of the TME context on ICI efficacy and clinical outcomes in NSCLC patients.

Mutational Burden (TMB) is defined as the number of mutation in certain number of DNA bases [135]. Higher TMB led to higher number of cancer-related neoantigens that can potentially be identified and eliminated by the immune cells. Patients with solid tumors deficient in the gene products responsible for mismatch repair (*MLH1*, *MSH2*, *MSH6*, and *PMS2*), that have consequently high TMB, demonstrated high response rates and prolonged clinical benefit from the administration of single pembrolizumab in a tumor agnostic setting [136]. High TMB has been associated with clinical benefit from ICI administration in retrospective studies [137,138] but his role as a biomarker has not been confirmed in prospective studies in NSCLC. In concordance with high TMB, high number of tumor infiltrating lymphocytes have been associated with improved clinical outcomes after ICI administration [139] and as a positive prognostic indicator in individuals with surgical resected NSCLC [140] but data from prospective studies in NSCLC affected patients undergoing ICI treatment are lacking.

However besides molecular and histopathological characteristics clinical co-factors can potentially affect ICI outcomes in NSCLC patients. Body mass index (BMI) and percentage of weight loss (WL%) has been identified as a negative prognostic factor in large scale retrospective data [141]. In addition, the presence of cancer dissemination in the central nervous system (CNS) [142], liver [143] and skeletal system [144] has been associated with poor survival outcomes in patients with metastatic NSCLC treated with cytotoxic chemotherapy. In addition, tumor burden as defined by the number of organ systems affected by metastatic disease has also been negatively correlated with clinical outcomes [145]. Large scale retrospective or prospective data that investigated the effect of the aforementioned factors and co-factor on the clinical outcomes of ICI treated patients with NSCLC had not been available by 2017. Nevertheless, further clinical research is warranted for further delineation of these factors as prognostic and predictive factors in ICI treated cancer afflicted individuals.

The configuration of the intestinal microbiome plays a crucial role in influencing the development of a proficient immune response [146]. Preclinical data have underscored the significance of the gut microbiota composition in relation to the effectiveness of immunotherapy in experimental models involving mice afflicted with melanoma [147]. Interestingly, tumors manifested an unresponsive nature to CTLA blockade in mice subjected to antibiotic treatment or raised under germ-free conditions. However, this inherent deficiency was effectively circumvented by means of oral administration of *Bacteroides fragilis*, immunization with *Bacteroides fragilis* polysaccharides, or the transfer of T cells specifically targeting *Bacteroides fragilis* [147]. At the clinical level, antibiotics (ATB) administration holds the potential to induce substantial modifications in the composition of the microbiome, consequently giving rise to a prolonged state of gut dysbiosis and compromised immune function [146]. In addition to antibiotics, proton pump inhibitors (PPIs), widely prescribed pharmaceutical agents, have been associated with a marked reduction in the diversity measured by Shannon's index. Furthermore, these agents have been shown to bring about alterations affecting up to around 20% of the bacterial taxa residing within the intestinal flora [148]. ATBs and PPIs are commonly administered drugs in NSCLC patients, however their effect on ICI clinical outcomes had not been researched on this particular oncological setting.

For over fifty years, the administration of exogenous corticosteroids has stood as a fundamental therapeutic approach for managing autoimmune disorders. Corticosteroids execute their immunosuppressive effects through a complex mechanism, concurrently targeting both innate and adaptive immune responses. They act as agonists for the glucocorticoid receptor (GR), initiating subsequent transcriptional modifications in an array of genes implicated in the initiation of innate immune reactions [149]. Given these well-established immunosuppressive attributes, the clinical trials leading to the approval of ICIs incorporated the criterion of excluding patients who were administered steroids in doses exceeding 10 mg of prednisolone equivalent [28,28,29,33,34,36–38,40]. However, patients afflicted with NSCLC frequently necessitate steroid doses surpassing 10 mg of prednisolone equivalent for a spectrum of underlying causes, ranging from managing cerebral edema due to brain metastases to addressing exacerbations of chronic obstructive pulmonary disease (COPD). The application of steroids in individuals undergoing ICI therapy raises concerns about potentially impeding the efficacy of ICIs, thus worsening the patients' survival. Retrospective analysis of metastatic NSCLC patients treated with ICIs has indicated poorer outcomes, including diminished response rates, decreased PFS, and OS when steroid doses exceeded 10 mg of prednisolone equivalent [150]. Additionally, for the management of severe grade III–IV immune-related adverse events (irAEs) occurring in 10–15% of ICI recipients [81], high-dose steroid administration (≥ 1 mg/kg/day) constitutes the primary therapeutic intervention. Information regarding the clinical ramifications for patients receiving steroids due to irAEs is primarily derived from studies focused on melanoma [81]. Nevertheless, in addition to oral or intravenous steroids, individuals with NSCLC commonly resort to inhalational steroids due to the heightened prevalence of chronic obstructive pulmonary disease (COPD) within this demographic. Inhalational steroids trigger a multitude of immune-modulating effects on the bronchial mucosa [151]; however, their potential influence on the effectiveness of ICIs remains a subject yet to be explored. In conclusion, high dose steroids for the palliation of cancer related symptoms and the management of irAEs has been an understudied subject but with important clinical relevance.

Artificial Intelligence (AI) constitutes an expansive domain encompassing the application of technologies in the construction of machinery and computing systems endowed with the capacity to emulate cognitive processes inherent to human intelligence. This emulation encompasses faculties like visual perception, linguistic comprehension and articulation, data analysis, generation of suggestions, and various other cognitive operations. Machine learning, as a distinct facet of artificial intelligence, facilitates the autonomous acquisition and refinement of knowledge by machines or systems through experiential input. Instead of traditional, explicit programming, machine learning harnesses algorithms to meticulously analyze extensive datasets, internalize the recognized patterns, and subsequently formulate judicious conclusions. Advancements in the efficacy of machine learning algorithms transpire incrementally as they iteratively encounter additional data throughout the training phase. The outcome of this developmental trajectory materializes in the form of machine learning models, which encapsulate the distilled insights gleaned from algorithmic execution on training datasets. The efficacy of these models is inherently linked to the quantum of data engaged, with augmented data volumes resulting in heightened model performance. AI possesses the capacity to employ sophisticated algorithms to extract discernible attributes from extensive healthcare datasets. The resultant insights acquired from this process substantially contribute to the enhancement of clinical practices. Furthermore, AI demonstrates the capability to exhibit self-learning and self-correcting attributes, thereby refining its accuracy through feedback mechanisms. In the field of medicine, AI is poised to provide vital support to healthcare professionals by granting access to contemporaneous medical knowledge originating from authoritative journals, textbooks, and well-established clinical protocols. This provision of information serves to elevate the quality of patient care, informed by well-grounded decisions. Additionally, the application of AI holds the potential to mitigate the unavoidable diagnostic and therapeutic errors intrinsic to human clinical practices. Moreover, AI holds the ability to distill invaluable insights from expansive patient cohorts, facilitating real-time deductions that contribute to health risk alerts and predictive assessments concerning health outcomes [152]. JADBio, a machine learning platform, has been used reported previously to been able to accurately predict secretory sequences of the cellular proteome and to identify prominent differences in amino acid content between secreted and cytoplasmic proteins [153].

As evidenced by the cognitive summation of the aforementioned clinical and experimental data, there exists a significant number of unanswered questions regarding the specific clinical and molecular characteristics of patient subgroups that would benefit from immunotherapy administration. Furthermore, the presence of a group of patients for whom immunotherapy administration has negative implications becomes apparent. Further research at both clinical and translational levels is needed to clarify these inquiries, as it has the potential to lead not only to the discovery of new biomarkers and improved patient selection but also to the deciphering of mechanisms underlying primary and secondary resistance to immunotherapy.

2. Aims of the thesis

The primary objective driving the execution of this doctoral dissertation was to conduct a prospective, single center, observational study involving individuals diagnosed with metastatic NSCLC, who were undergoing treatment with ICIs. This pursuit aimed at the discernment and delineation of clinical, radiological and laboratory factors that could affect immunotherapy outcomes. The results of this study could lead potentially to an improved patient selection for ICI treatment and to help us acquire the knowledge of the intrinsic characteristic of the subset of patients that might attain benefit from immunotherapy in the metastatic NSCLC setting. Owing to a scarcity of available data during the proposal and commencement of this doctoral thesis, the study endeavored to assess an extensive array of clinical, radiological, and laboratory variables, employing a diverse range of methodological analyses. For the creation of the appropriate patient cohort in order to investigate the initial hypotheses we collected prospective data from individuals with metastatic NSCLC that received ICIs in the Oncology Department of the University Hospital of Heraklion, Crete from November 15, 2017 until November 15, 2019. All the patients that received ICIs in the Oncology Department of the University Hospital of Heraklion were screened for inclusion and upon signing the consent form they were included in the study for further analysis.

In the first publication, an array of clinical and fundamental laboratory data was analyzed in patients afflicted with metastatic NSCLC undergoing second-line ICI treatment. Specifically, an in-depth statistical analysis was conducted to elucidate potential correlations between patient outcomes and the co-administration of antibiotics, proton pump inhibitors, and corticosteroids, along with their disease burden which was further defined by the type and number of organs affected by metastatic dissemination. Subsequently, these data were subjected to further analysis utilizing the JADbio machine learning platform to establish the foundation of a predictive model.

In the second publication, we explored the impact of the phenomenon of cancer cachexia on the efficacy of immunotherapy by utilizing clinical data (weight loss within 6 months prior to the initiation of immunotherapy) and radiological data (skeletal muscle index at the level of third lumbar vertebra which was calculated using computed tomography scans of the abdomen at the beginning of ICIs and every 3 months thereafter). Within this publication, data were analyzed from patients receiving ICIs as both first-line, second-line or subsequent-line treatments. This study was undertaken to investigate the role of the cachexia phenotype imprinting in the anti-tumor response in ICI treated NSCLC patients and its effect both on response and survival outcomes.

In the third publication, we investigated the impact of the differential body compositions of the patients in our cohort using radiological data acquired before the initiation of ICIs and during the course of the treatment. We explored the potential effect of adipose tissue composition through estimating the density of its differential compartments (intramuscular, subcutaneous and visceral adipose tissue) on clinical outcomes in NSCLC patient undergoing treatment with ICIs by analyzing abdominal data tomography scans before the initiation of the ICIs and every three months thereafter. In addition, we investigated the impact of reduced skeletal muscle mass, as an indirect indicator of an underlying inflammatory process, in the clinical outcomes of the patients in our cohort.

3. Methods

3.1 Study design

We systematically gathered prospective clinical, radiological and laboratory data from patients diagnosed with non-oncogene driven metastatic NSCLC who underwent treatment with immunotherapy, either as a single modality or in combination with chemotherapy. The decision for the treatment with ICIs in these individuals was taken by the treating physician according to ESMO guidelines [154]. All consecutive patients who were eligible candidates for PD-1/PD-L1 inhibitor treatment for metastatic NSCLC in the Oncologic Department of the University Hospital of Heraklion were screened from November 15, 2017 until November 15, 2019 for potential inclusion in the study. Individuals with *EGFR* mutations or *ALK* translocations were excluded from initial screening. *EGFR* mutational status was evaluated using polymerase chain reaction (PCR), while *ALK* genomic changes were analyzed using immunohistochemistry (ICH) or fluorescence in situ hybridization (FISH), respectively.

This study was conducted as an observational study with no interference with the patients' treatment plan on any clinical decisions. Ethical approval for the study was granted by the Ethics Committee of the University Hospital of Heraklion (ID: 2644), and the study was conducted in adherence to the principles outlined in the declaration of Helsinki (revised in 2013).

Prior to enrollment, written informed consent was acquired from all participating patients.

The **inclusion criteria** for this study were:

- Histological confirmation of metastatic NSCLC.
- Age > 18 years.
- Eastern Cooperative Oncology Group (ECOG) performance status 0-2.
- Adequate hepatic and renal function.
- Administration of ICIs according to ESMO guidelines [154].
- Patient's signed informed consent.

Exclusion Criteria:

- Active, unrelated malignancy.
- Active infection.

Methods:

The patient parameters that were analyzed are:

Clinical Parameters:

- **Basic demographic data:** gender, age, smoking history
- Performance status by ECOG [155].
- **Anthropometric characteristics:** height, weight, Body Mass Index (BMI), self-reported weight fluctuation over the past 6 and the past three months.

- A cut-off for BMI 25 kg/m² would be applied to dichotomize the patients as having low or high BMI in order to investigate any associations of the aforementioned parameters with clinical outcomes.
- Co-morbidities of the patient population.
- **Type and duration of co-administered drugs (pos, iv or inhalational steroids, antibiotics and proton-pump inhibitors):** Patients were classified based on their utilization of steroids, either taken orally or intravenously. This classification was applied if the steroid dosage exceeded 10 mg prednisone equivalent and was administered for a minimum duration of 10 days within the initial 12 weeks of treatment or within 15 days prior to its commencement. Further differentiation was made within this patient group: one subgroup encompassed individuals who had been prescribed steroids to manage immune-related adverse effects (irAEs) [156], while the other subgroup included those who had received steroids for supportive purposes (such as addressing brain edema due to brain metastases, anorexia, dyspnea, or COPD exacerbations). The administration of antibiotics (ATBs) was also categorized; this classification encompassed patients who had taken antibiotics within the 30 days preceding the start of immunotherapy and/or within the first 12 weeks of treatment. Extended ATB usage was defined as the administration of antibiotics for a minimum period of 14 days. If a patient underwent multiple shorter courses of antibiotics, the cumulative duration was calculated. For long-term proton-pump inhibitor (PPIs) usage, the criteria were set as the usage of PPIs for a duration of 3 months before commencing immunotherapy. Similarly, the chronic usage of inhalational steroids was defined as the consumption of these steroids for 3 months before initiating immunotherapy. It's important to note that the specific cutoffs of 10 days, 14 days, and 3 months for steroids, ATBs, and PPIs use, respectively, were determined arbitrarily before the commencement of data collection to ensure consistency in analysis.
- **Immunotherapy treatment type:** Single PD-1(PDL-1) inhibitor, PD-1-CTLA-4 inhibitors combination, chemotherapy-PD-1 combination and previous treatments (surgery, chemotherapy, radiation therapy).

Radiological Parameters:

- **Disease characteristics:** Sites of metastatic lesions, previous treatments, response to previous treatments according to RECIST 1.1 [157] and their duration, disease progression pattern in prior treatments.
- **Disease burden:** Patients were classified according to their disease burden in a dichotomous manner. High disease burden was classified as more than two organ systems affected with metastatic dissemination whereas low disease burden was classified as two or less organ systems affected with metastatic disease.
- **Response assessment to immunotherapy according to RECIST 1.1 [157]:** Time from initiation to response onset, degree and duration of response, disease progression type.

- **Body composition radiological markers:** Assessment of the appendicular skeletal muscle density, the intramuscular adipose tissue density, the visceral adipose tissue density and the subcutaneous adipose tissue density at the level of the third lumbar vertebra (L3) by analyzing the patients' abdominal computed tomography (CT) scans before the initiation of I-O through the application of slice-o-matic tomovision(158–160) and every three months thereafter. The densities would after be converted to indices [Intramuscular Fat Index (IMFI), Visceral Fat Index (VFI), Subcutaneous Fat Index (SFI), Lumbar Skeletal Muscle Index (LSMI)] by dividing them by height in meters squared.

Histological data:

- **Patients underlying histological subtype:** Squamous cell lung cancer (sqLC) vs non-squamous cell lung cancer.
- PD-L1 expression levels. The assessment of PD-L1 expression involved determining the percentage of tumor cells or immune cells of TME (if VENTANA SP142 was applied) exhibiting positive membranous staining. A positivity threshold of 1% was established as the point of reference to dichotomize patients as PD-L1 positive ($\geq 1\%$) or PD-L1 negative ($<1\%$).

Cancer cachexia indicators:

- **Cancer cachexia indicators:** Patient's average body weight 6 months before the initiation of immunotherapy (BW) and body weight at the beginning of immunotherapy (WOIM). Calculation of weight fluctuation percentage at the beginning of immunotherapy compared with patient's average body weight 6 months before its initiation $[(WOIM - BW)/100]$.

Laboratory Parameters:

- Total white blood cell count, neutrophil count, lymphocyte count, neutrophil-to-lymphocyte ratio at the beginning of immunotherapy. The cut-off for neutrophil/ lymphocyte ratio (NLR) for the further classification of the patients as having high or low NLR was set at > 3 .
- Serum albumin at the beginning of immunotherapy. The threshold for albumin levels was established at 3.5 g/dl, which corresponds to the lower limit of normal within the hospital's laboratory where the study took place.
- Lactate dehydrogenase levels (LDH) at the beginning of immunotherapy. Elevated LDH levels were defined according to the upper limit of normal value range (UNL) (247 units/liter) in the laboratory of the hospital where the study was conducted.

The analysis of plasma levels of cytokines TNF- α , IL-1, IL-6, and IL-8 using the ELISA method and their correlation with the clinical outcomes of the patients was not performed, despite being proposed in the context of this doctoral dissertation. The reason for this was that, at the time of data collection, a plethora of publications existed [102,161–163],

and the aforementioned analysis would not contribute to the originality of the research. For the same reason, we did not proceed with further analysis of the correlations between the levels of CRP and erythrocyte sedimentation rate (ESR) with the clinical outcome, as proposed in the initial proposal of this doctoral dissertation [164].

On the other hand, we decided to conduct more detailed analysis on the adipose tissue composition of the patients in our cohort and its association with clinical outcomes. The underlying reason was the accumulation of clinical and preclinical data on a potential association between obesity and favorable clinical outcomes with ICIs treatment in patients afflicted with a wide spectrum of underlying malignancies [165–168].

3.2 Definition of cachexia syndrome and adipose tissue indices in the study population

Patients' classification as having or not cancer cachexia was executed utilizing the criteria established by Fearon et al [1]. These criteria encompassed body weight loss exceeding 5% within the preceding 6 months before the first administration of immunotherapy or a BMI below 20 kg/m², coupled with any extent of weight loss beyond 2%, or a diminished appendicular skeletal muscle index indicative of sarcopenia, combined with any degree of weight loss surpassing 2%.

The assessment of patients' appendicular skeletal muscle index involved the quantification of skeletal muscle thickness at the third lumbar vertebra level (L3), performed by analyzing abdominal computed tomography (CT) scans obtained prior to the initiation of ICI treatment, utilizing the Slice-o-matic Tomovision software (sliceOmatic 5.0 Rev-9 Alberta Protocol) (Figure 5). Muscle area thickness was normalized by the square of each individual's height, establishing a baseline Lumbar Skeletal Muscle Index (LSMI) measured in cm²/m². The LSMI threshold values (LNL: lower normal limit) employed to define sarcopenia were determined as <55 cm²/m² for males and <39 cm²/m² for females, as outlined by the international consensus for cancer cachexia definition [1].

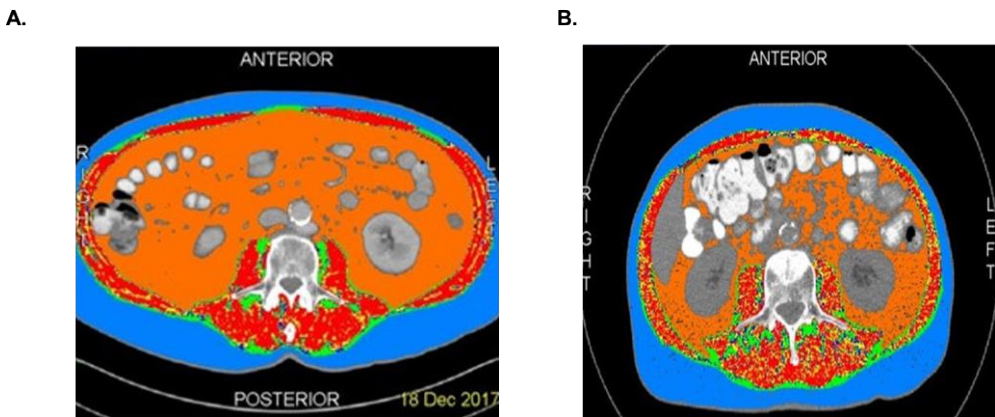


Figure 5: Tomovision analysis of the abdominal computed tomography scans of two individuals in our cohort A. A male patient with baseline LSMI = 55.02 cm²/m² without sarcopenia B. A male patient with baseline LSMI=39.45 cm²/m² consistent with sarcopenia.

LSMI=Lumbar Skeletal Muscle Index (cm²/m²) (At the level of 3rd lumbar vertebra)

The final analysis encompassed solely those individuals for whom adequate radiological (LSMI) and/or clinical data (BMI, weight fluctuations within the last six months) were available, facilitating classification as cachectic or non-cachectic based on Fearon et al.'s criteria [1](Diagram 2). Additionally, we conducted LSMI assessments during patients' ICI treatment, aiming to explore potential associations between LSMI fluctuations and treatment outcomes. In this context, we contrasted baseline LSMI values with LSMI values from the initial radiological evaluation subsequent to the commencement of ICI therapy. Categorization of patients during treatment was carried out using a binary approach, classifying individuals according to their median LSMI reduction % during I-O.

Density computations for distinct adipose tissue compartments and skeletal muscle were executed using precise Hounsfield Unit (HU) threshold references unique to each tissue compartment (-190 HU to -30 HU for intramuscular fat, -150 HU to -50 HU for visceral fat, -190 HU to -30 HU for subcutaneous fat, -29 HU to +150 for skeletal muscle) (Figure 6). Subsequently, the density measurements for both fat (in cm^2) and muscle (in cm^2) were transformed into indices (in cm^2/m^2) through division by the square of the individual's height in meters (Intramuscular Fat Index: IMFI, Visceral Fat Index: VFI, Subcutaneous Fat Index: SFI, and Lumbar Skeletal Muscle Index: LSMI).

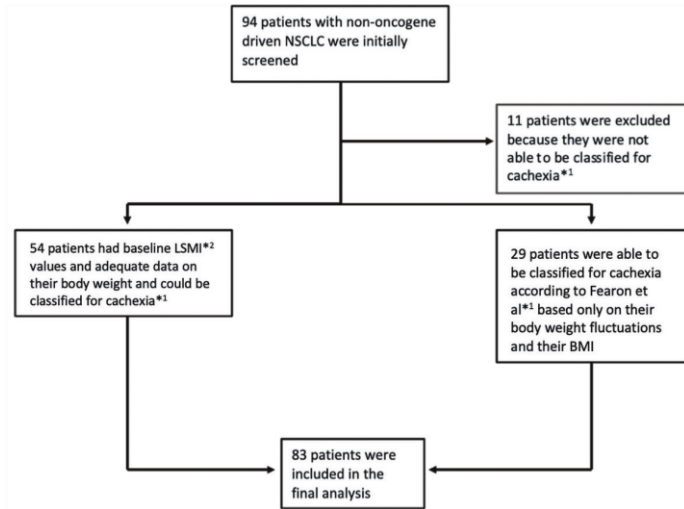


Diagram 2: Flow chart of our study. *1: Classification for cachexia was conducted according to the criteria by Fearon *et al.* [1]. *2: LSMI: Lumbar Skeletal Muscle Index.

Patients were stratified into categories based on their baseline IMFI, VFI, and SFI values, determined by the gender-specific median value for each respective index. Individuals with baseline values falling below the median were designated as possessing low values, while those with values surpassing the median were categorized as possessing high values.

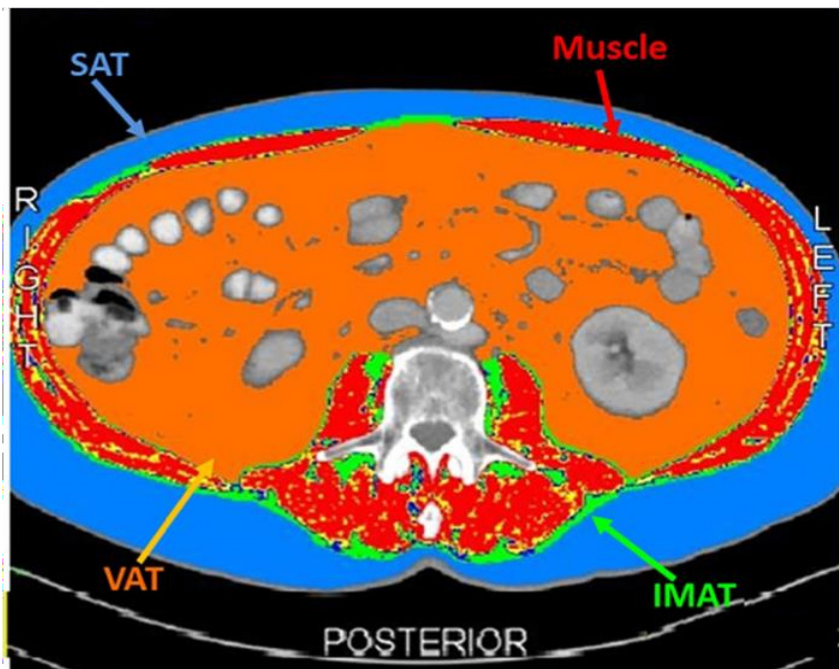


Figure 6: SliceOmatic tomovision analysis of the computed tomography scan of a male patient distinguishing the different context of Visceral Adipose Tissue (VAT), Intramuscular Adipose Tissue (IMAT), Subcutaneous Adipose Tissue (SAT) and skeletal muscle according to their differential Hounsfield Units (HU) references.

3.3 Statistical analysis and model design analysis

Statistical analysis

The statistical analyses were conducted using IBM SPSS Statistics version 25.0.0 (IBM Corp., Armonk, NY, USA). Descriptive statistics were applied to define categorical and continuous nominal variables. The threshold for statistical significance was set at $p < 0.05$ (two-tailed test).

Associations between each investigated parameter and objective partial response (ORR) and disease control rate (DCR) were assessed through the utilization of the chi-square test (X^2). Furthermore, the chi-square test was employed to explore potential associations between a plethora of categorical parameters. The impact of the duration of ATB administration in days, as a continuous variable, on DCR rates was assessed via the Mann-Whitney U test. This test was also employed to discern potential disparities in the distributions of Intramuscular Fat Index (IMFI), Visceral Fat Index (VFI), Subcutaneous Fat Index (SFI), and Lumbar Skeletal Muscle Index (LSMI) values between responders and non-responders, as well as between individuals who achieved disease control as the best response to immune checkpoint inhibitor therapy (ICIS) versus those who experienced disease progression.

Kruskal-Wallis test was applied to analyze potential differences in baseline LSMI distributions in relation to the presence of cancer cachexia syndrome (CCS). Additionally, Kruskal-Wallis test was used to explore any variations in the distributions of LSMI percentage changes during immune checkpoint inhibitor (ICI) treatment concerning objective response rate (ORR), disease control rate (DCR), and duration of disease control of ≥ 6 months.

To examine potential correlations, Spearman's rank correlation coefficient was utilized to explore associations between BMI values and IMFI, VFI, SFI, as well as LSMI.

Univariate binary logistic regression was employed to ascertain the odds ratios (OR) of the analyzed parameters on the probability of achieving disease control response (DCR) or progressive disease (PD) as best response to treatment. For the variables that displayed statistical significance in the univariate analysis, multivariate logistic regression was applied.

The Kaplan-Meier method was adopted to evaluate the influence of the studied parameters on Progression-Free Survival (PFS) and Overall Survival (OS). Comparison of curves was performed using the log-rank test. Individuals who had not progressed or they were alive at the time of data analysis they were censored at the time of their last follow-up. In the context of the second paper, which examined the effect of cancer cachexia on ICI treatment outcomes, the log-rank test was used to evaluate the impact of baseline CCS on OS within subgroups of patients receiving ICI as first-line or second-line treatment. Additionally, the log-rank test was utilized to assess the effect of cancer cachexia on 6-month survival after ICI initiation, employing a cut-off value of six months. For individuals who were alive but had a follow-up duration less than six months, their data were censored at the time of their last follow-up.

In the initial paper of this PhD thesis, the Cox Regression Method was initially employed to investigate the effect of the duration of ATB administration, as a continuous nominal variable in days, on both PFS and OS. Similarly, in the third publication, univariate Cox

regression analysis was employed to examine the influence of BMI, IMFI, VFI, SFI, and LSMI as continuous nominal variables on PFS and OS by using gender was used as a stratification factor.

In all three published papers, a univariate Cox Regression Analysis was executed to calculate Hazard Ratios (HR) for all analyzed categorical co-variables in relation to PFS and OS. For the first and second papers, variables that reached statistical significance in the univariate analysis underwent multivariate Cox Regression Analysis. However, in the third paper, due to a limited number of events (less than ten in specific variables) and a small statistical sample, a multivariate analysis was not performed on the variables that achieved statistical significance in the univariate analysis.

The decision not to perform a sample size and power calculation was influenced by the scarcity of published reports concerning the effect of the examined parameters on the outcome of immunotherapy- treated cancer patients at the time of data collection initiation. Given this lack of available data for necessary calculations, this proof-of-concept exploratory study deemed such calculations to hold little value.

Multivariate analysis by JADBIO tool

To facilitate a multivariate analysis of our dataset, we employed JADBIO, a fully automated machine learning (AutoML) system available at www.jadbio.com. JADBIO employs an artificial intelligence (AI) system to select algorithms and methods suited to the specific problem, based on data type and user-defined preferences. This encompassed data transformation, pre-processing, feature selection, model selection, and result visualization. The system also determined the hyperparameters to optimize for each method. The amalgamation of methods and their corresponding hyperparameters constitutes a configuration, which is applied using a 10-fold cross-validation protocol. Consequently, JADBIO generates numerous models, ranked by a performance metric – in our case, the area under the receiver operating characteristic (ROC) curve (AUC) – and outputs the highest-performing model (figure 7). To mitigate potential overestimation of predictive performance, JADBIO employs a bootstrap-based correction method [169] and calculates confidence intervals for the resulting performance using the same approach.

In our analysis, we employed JADBIO for binary classification modeling to predict the likelihood of an individual achieving Disease Stabilization (PR or SD vs. PD) with immune checkpoint inhibitors (ICIs) as a second-line treatment. The tool harnessed various modeling algorithms, including support vector machines (SVM) with polynomial and Gaussian kernels, random forests [170], ridge logistic regression [171], and decision trees [172]. Among the available performance metrics in JADBIO, we selected the AUC. It is noteworthy that the outcomes of such analyses often yield complex models, which may prove challenging for human comprehension. In this context, JADBIO also furnishes the best interpretable model. For our study, we present the performance estimation derived from the best- performing model.

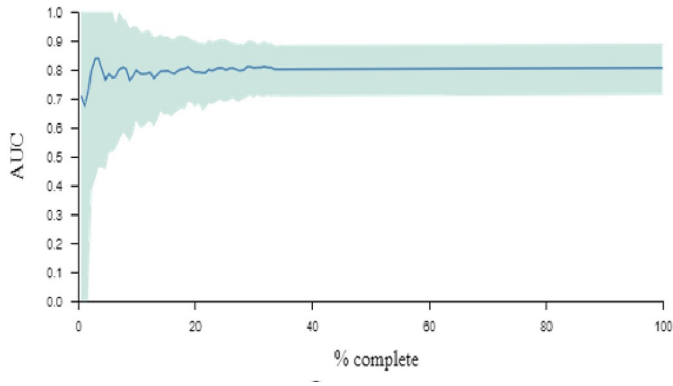


Figure 7: Illustration of the learning procedure undertaken by JADbio for the classification analysis of our dataset. JADbio explored 3017 configurations and conducted training for a total of 211190 models.

4. Results

4.1 Clinical parameters as determinants of outcome in patients with Non-Small Cell Lung Cancer treated with PD-1/PD-L1 inhibitors

In the first paper that was published as a result of this doctoral dissertation [173] we analyzed clinical and laboratory data of the 66 patients in our cohort that were treated with ICIs as second line therapy after progress in first line platinum based cytotoxic chemotherapy. The patients' data were prospectively collected from 15 of November 2017 until 21 of November 2019.

Patient Characteristics

Detailed information about the patients' characteristics can be found in Table 1. The median age was 69 years (range: 39-81 years old) and 55 (83.3%) of the individuals in our cohort were of male gender. In addition, 51 (77.3%) were classified as having performance status (PS) = 0-1 by ECOG and the rest 11 (16.7%) were classified as PS=2. 60 (91%) patients were active smokers or former smokers. From a histological perspective, 37 (56.1%) patients were diagnosed with non-squamous NSCLC and the rest 29 (43.9%) had squamous NSCLC as an underlying histology. PD-L1 status was evaluated in 32 patients out of 66 patients. 12 out of the 32 evaluable patients were classified as PD-L1 negative (PD-L1 < 1%) whereas the rest 20 were having PD-L1 expression $\geq 1\%$, thus they were deemed as PD-L1 positive. 24 patients (36.3%) were categorized as having received steroids according to the predetermined definition, 34 (51.5%) had received antibiotics (ATBs) and 22 (33.3%) had undergone an extended course of ATBs (≥ 14 days of cumulative exposure to ATBs).

Impact of Analyzed Variables on Response Outcomes

Response assessment revealed that 10 patients (15.2%) experienced partial response (PR) as best response to second line ICIs, 23 (34.8%) had stable disease (SD), and 33 (50%) exhibited progressive disease (PD). There was no patient that was able to achieve a complete response (CR) to ICIs. The responders experienced prolonged responses with the median duration of response to be 7.97 months, ranging from 2.8 to 26.9 months.

Low BMI ($< 25 \text{ kg/m}^2$) ($p = 0.030$, 95% confidence interval) consisted the only parameter to be associated with lower RR at a statistically significant level ($p = 0.030$, 95% confidence interval). Moreover, parameters such as low BMI ($p = 0.003$), presence of bone metastases ($p = 0.007$), liver dissemination ($p = 0.014$), and high disease burden (> 2 organs with metastatic disease) ($p = 0.017$) were significantly associated with reduced disease stabilization rates (DCR) (table 2). Co-medications such as ATB administration ($p = 0.014$), extended ATB administration ($p = 0.002$), and the use of systemic steroids ($p = 0.040$) exhibited statistically significant negative correlations with DCR (Fig 8A– 8C). In addition, we investigated the duration of ATB administration in days as a continuous nominal variable. The days of ATB administration was negatively correlated with disease stabilization rates ($p = 0.004$; Fig 9). None of the other assessed parameters displayed significant impacts on disease stabilization rates (Table 2).

In the univariate logistic regression analysis, we investigated the odds ratios (OR) of each examined covariate on its effect the probability of achieving disease stabilization with ICIs are illustrated in Fig 10A. Steroid administration ($p=0.049$), ATB administration ($p=0.015$), prolonged ATB administration ($p=0.003$), BMI ≤ 25 kg/m² ($p=0.004$), liver ($p=0.018$) and bone metastases ($p=0.010$) were all significantly associated with reduced probability to achieve DCR. However, in the multivariate logistic regression analysis only bone metastases [OR: 0.153, $p = 0.019$] and prolonged ATB administration [OR: 0.085, $p= 0.002$] were found to independently predict a lower likelihood of disease stabilization with ICIs (Fig 10B).

All Patients		
Variable	N	%
Number of patients	66	
Age (years) Median (range)	69 (39—81)	
Gender		
Male	55	83.3
Female	11	16.7
Performance status		
0-1	51	77.3
2	15	22.7
Smoking status		
Active smokers	39	59.1
Former smokers	21	31.8
Never smokers	6	9.1
Body mass index (BMI)		
> 25 kg/m ²	82	48.5
< 25 kg/m ²	34	51.5
Histology		
Non-squamous	37	56.1
Squamus	29	43.9
Number of organs with metastases		
1-2	45	68.2
>2	21	31.8
Brain metastases		
Yes	14	21.2
No	52	78.8
Liver metastases		
Yes	19	28.8
No	47	71.2
Bone metastases		
Yes	20	30.3
No	46	69.7
Lymph node metastases		
Yes	39	59.1
No	27	40.9

All Patients		
Variable	N	%
Baseline albumin levels		
< 3.5 g/dl	12	18.2
≥ 3.5 g/dl	51	77.2
Not available	3	4.5
Baseline LDH levels		
> UNL	20	30.3
≤ UNL	36	54.5
Not available	10	15.2
PDU levels		
< 1%	12	18.2
≥ 1%	20	30.3
Not available	34	51.5
Steroid administration <10mg of daily prednisolone equivalent for more than 10 days within 15 days before initiation of immunotherapy or during the course of it (first 12 weeks)		
Steroids naive	42	63.6
Steroids due to irAEs	8	12.1
Steroids for supportive reasons	16	24.2
Antibiotics administration within 30 days before the initiation of immunotherapy or during the course of it (first 12 weeks)		
Yes	34	51.5
No	32	48.5
Duration of antibiotics administration (days) Median (range)	5 (0—37)	
Prolonged administration of antibiotics > 14 days within 30 days before the initiation of immunotherapy or during the course of it (first 12 weeks)		
Yes	22	33.3
No	44	66.7
Use of inhalation steroids for > 3 months before the initiation of immunotherapy		
Yes	10	15.2
No	56	84.8
Use of proton pump inhibitors for > 3 months before the initiation of immunotherapy		
Yes	23	34.8
No	43	65.2
Grade III or IV iRAEs		
Yes	8	12.1
No	58	87.9
Response to immunotherapy	0	0
CR		
PR	10	15.2
SD	23	34.8
PD		50.0
Disease progression		
Yes	55	83.3
No	11	16.7

All Patients		
Variable	N	%
Death		
Yes	55	83.3
No	11	16.7
Duration of response (months) Median (range)	7.97 (2.8–26.9)	
Progression free survival (months) Median (range)	3.50 (0.16–26.9)	
Overall survival (months) Median (range)	6.77 (0.6–26.9)	
Follow up (months) Median (range)	6.37 (0.6–26.9)	

Table 1: Baseline patwient characteristics

Variable	N=66	PR or SD	PD	P value (chi-square test,95% CI)
ATB ^a administration				
Yes	34	12	22	p=0.014
No	32	21	11	
Prolonged ATB administration				
Yes	22	5	17	p=0.002
No	44	28	16	
Baseline Steroid administration >10 mg ≥10 days				
N=58				
Yes	16	4	12	p=0.040
No	42	23	19	
Use of inhalational steroids				
Yes	10	4	6	p=0.367
No	56	29	27	
PPis ^b administration				
Yes	23	9	14	p=0.151
No	43	14	19	
BMI ^c < 25 kg/m ²				
Yes	34	11	23	p=0.003
No	32	22	10	
Liver metastases				
Yes	19	5	14	p=0.014
No	47	28	19	
Brain metastases				
Yes	14	6	8	p=0.382
No	52	27	25	
Bone metastases				
Yes	20	5	15	p=0.007
No	46	28	18	
LN ^d metastases				
Yes	39	22	17	p=0.158
No	27	11	16	

Variable	N=66	PR or SD	PD	P value (chi-square test,95% CI)
Disease burdens				
High	21	6	15	p=0.017
Low	45	27	18	
Performance status				
0-1	51	28	23	p=0.120
2	15	5	10	
LDH ^f levels>UNL ^g	N=56			
Yes	20	6	14	p=0.059
No	36	20	16	
Albumin < 3.5 g/dl	N=63			
Yes	12	3	9	p=0.076
No	51	27	24	
NLR ^h >3	N=62			
Yes	41	18	23	p=0.236
No	21	12	9	
PDL1i ≥ 1%	N=32			
Yes	20	11	9	p=0.234
No	12	4	8	

Table 2: Effect of the studied parameters on disease stabilization rates (PR or SD). ATB=Antibiotics, b: PPis=Proton pump inhibitors, c: BMI=Body mass index, d: LN=Lymph nodes, e: Disease burden high=More than 2 organs affected with metastatic disease, f: LDH=Lactate dehydrogenase, g: UNL=Upper normal limit (247 units/liter), h: NLR=Neutrophil to lymphocyte ratio, i: PDL1=Programmed death ligand 1

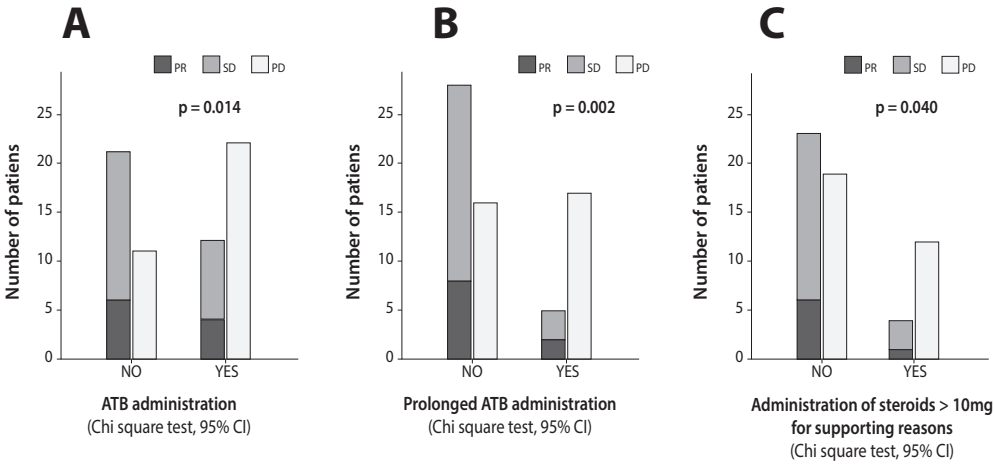


Figure 8: Bar plots visualizing the effect of (A) antibiotic administration (B) prolonged antibiotic (More that 14 cumulative days of antibiotic usage 30 days before the initiation of immunotherapy and within the first 12 weeks of treatment) administration and (C) steroid administration >10 mg on disease stabilization rates (PR or SD; Chi-square test, 95%).

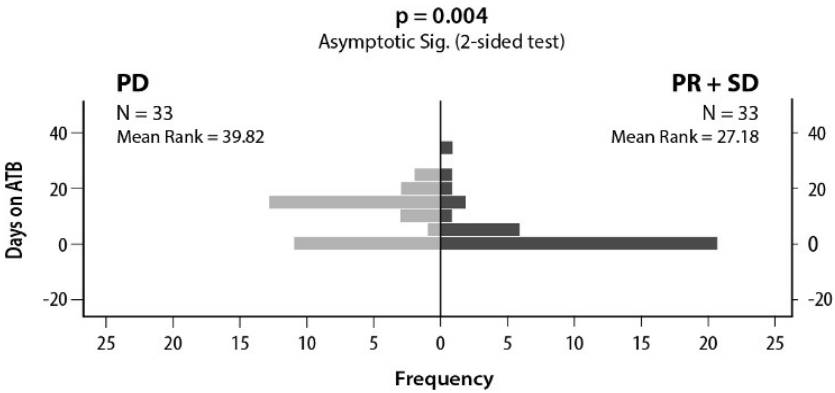


Figure 9: Mann-Whitney U test examining the effect of the duration of ATB administration in days on Disease Control Rates (DCR). On the left side are the days on ATB of the patients that experienced progressive disease (PD) and on the right side the days on ATB of those who had DCR (PR or SD) as response to immune checkpoint inhibitors administration.

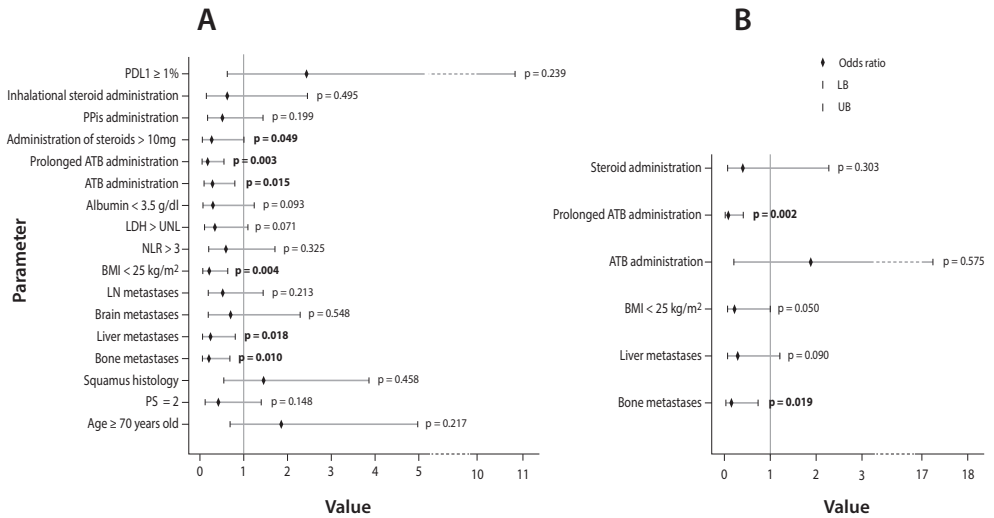


Figure 10: Forest plot depicting the odds ratios of the studied parameters for disease stabilization (PR or SD) in (A) univariate binary regression analysis and (B) multivariate binary regression analysis that included the variables that reached statistical significance ($p < 0.05$) in the univariate analysis. (LB: Lower border, UB: Upper border).

Survival Analysis

The study encompassed a cohort of patients with a median follow-up duration of 6.37 months, ranging from 0.6 to 26.9 months. Following data censoring, the median progression-free survival (PFS) was observed to be 3.50 months (95% CI: 1.49–5.50), and the median overall survival (OS) was 6.77 months (95% CI: 2.29–11.24) for the entire patient cohort. Comprehensive results pertaining to the influence of analyzed variables on PFS and OS can be found in Table 3.

Significantly, several factors were associated with decreased PFS, including a BMI below 25 kg/m² (2.33 vs. 4.93 months, $p = 0.009$), a high disease burden (1.77 vs. 4.67 months, $p = 0.008$), the presence of liver metastases (1.73 vs. 4.80 months, $p = 0.002$), and the presence of bone metastases (2.10 vs. 4.80 months, $p = 0.024$). Additionally, baseline albumin levels below 3.5 g/dl (1.70 vs. 4.40 months, $p = 0.005$) and a baseline neutrophil-to-lymphocyte ratio (NLR) above 3 (2.53 vs. 4.93, $p = 0.024$) were correlated with reduced PFS. While the administration of antibiotics (ATB) was not linked to lower PFS in a statistically significant level ($p = 0.062$), prolonged ATB courses and steroid administration more than 10 mg for the palliation of cancer related morbidity were significantly associated with inferior PFS (1.57 vs. 4.93 months, $p < 0.001$ and 1.27 vs. 4.70 months, $p = 0.013$, respectively). Other covariates did not demonstrate statistically significant associations with PFS (Table 3).

In terms of their impact on patient survival, parameters such as performance status 2 (3.17 vs. 9.60 months, $p = 0.027$), baseline albumin levels below 3.5 g/dl (1.70 vs. 9.57 months, $p = 0.003$), baseline lactate dehydrogenase (LDH) levels above the upper normal limit (3.70 vs. 9.90 months, $p = 0.040$), and the presence of bone metastases (3.77 vs. 10.33 months, $p = 0.011$) exhibited a negative correlation with OS (table 3). Prolonged ATB administration was significantly associated with reduced OS (2.50 vs. 9.93 months, $p = 0.001$; refer to Figure 11B), whereas the use of steroids (2.53 vs. 9.60 months, $p = 0.051$) or antibiotics (4.00 vs. 9.67 months, $p = 0.301$) did not exhibit statistically significant correlations with diminished survival (table 3). No other associations indicating inferior OS were noted (table 3).

Univariate and multivariate survival analysis using Cox Regression indicated that the duration of ATB administration, assessed as a continuous nominal variable, exhibited an inverse correlation with both PFS ($p = 0.007$, 95% CI) and OS ($p = 0.027$, 95% CI; see Figure 11C and 11D).

The univariate analysis for PFS excluded baseline albumin levels due to an insufficient number of events, and the results are outlined in Table 4. In a multivariate analysis, factors such as steroid usage for supportive reasons [HR = 2.556, $p = 0.004$], prolonged ATB administration [HR = 3.403, $p = 0.0001$], and the presence of liver [HR = 3.266, $p = 0.001$] or bone metastases [HR = 2.244, $p = 0.017$] were identified as independent predictors of reduced PFS (refer to Table 4). For OS, multivariate analysis revealed that prolonged ATB use [HR = 2.945, $p = 0.0001$] and the presence of bone metastases [HR = 1.890, $p = 0.049$] were independently associated with decreased survival (detailed in Table 4).

	Median PFS (months)	p value (log-rank test)	Median OS (months)	p value (log-rank test)
All patients (n=66)	3.50			
Age				
< 70 years old	3.23	0.659	5.43	0.545
≥ 70 years old	4.40		10.80	
Performance status				
0-1	4.70	0.140	9.60	0.027
2	2.37		3.17	
BMI ^a				
<25 kg/m ²	2.33	0.009	3.77	0.106
≥25 kg/m ²	4.93		9.60	
Histology				
Squamous	4.00	0.628	6.37	0.847
Non squamous	2.37		9.43	
Disease burden ^b				
High	1.77	0.008	9.60	0.139
Low	4.67		4.83	
Brain metastases				
Yes	1.63	0.506	4.80	0.953
No	3.97		9.47	
Liver metastases				
Yes	1.73	0.002	4.83	0.238
No	4.80		9.47	
Bone metastases				
Yes	2.10	0.024	3.77	0.011
No	4.80		10.33	
LN ^c metastases				
Yes	4.67	0.607	9.47	0.758
No	2.37		6.77	
Baseline albumin levels				
< 3.5 g/dl	1.70	0.005	1.70	0.003
≥ 3.5 g/dl	4.40		9.57	
Baseline LDH ^d levels				
≤ 247 units/liter	3.97	0.078	9.90	0.040
> 247 units/liter	1.53		3.70	
NLR ^e				
≤ 3	4.93	0.024	9.60	0.139
> 3	2.53		5.27	
Steroid administration ^f for supportive reasons				
Yes	1.27	0.013	2.53	0.051
No	4.70		9.60	
ATB ^g administration				
Yes	1.97	0.062	4.00	0.301
No	4.80		9.47	

	Median PFS (months)	p value (log-rank test)	Median OS (months)	p value (log-rank test)
Prolonged ATB administration				
Yes	1.57	<0.001	2.53	0.001
No	4.93		9.90	
PPis ^b administration				
Yes	2.33	0.119	6.37	0.099
No	4.70		9.47	
Inhalational steroid administration				
Yes	2.10	0.467	4.00	0.558
No	4.00		9.43	

Table 3: Log-rank test demonstrating the effect of the analyzed variables on progression-free survival (PFS) and overall survival (OS). a: BMI=Body mass index, b: High disease burden: > 2 organs with metastatic disease, low disease burden: ≤ 2 organs with metastatic disease, c: LN=Lymph Nodes, d: LDH=Lactate dehydrogenase, e: NLR=neutrophil/lymphocyte ratio, f: Administration of > 10 mg of prednisolone equivalent for ≥ 10 days, g: ATB=Antibiotics, h: PPis=Proton pump inhibitors

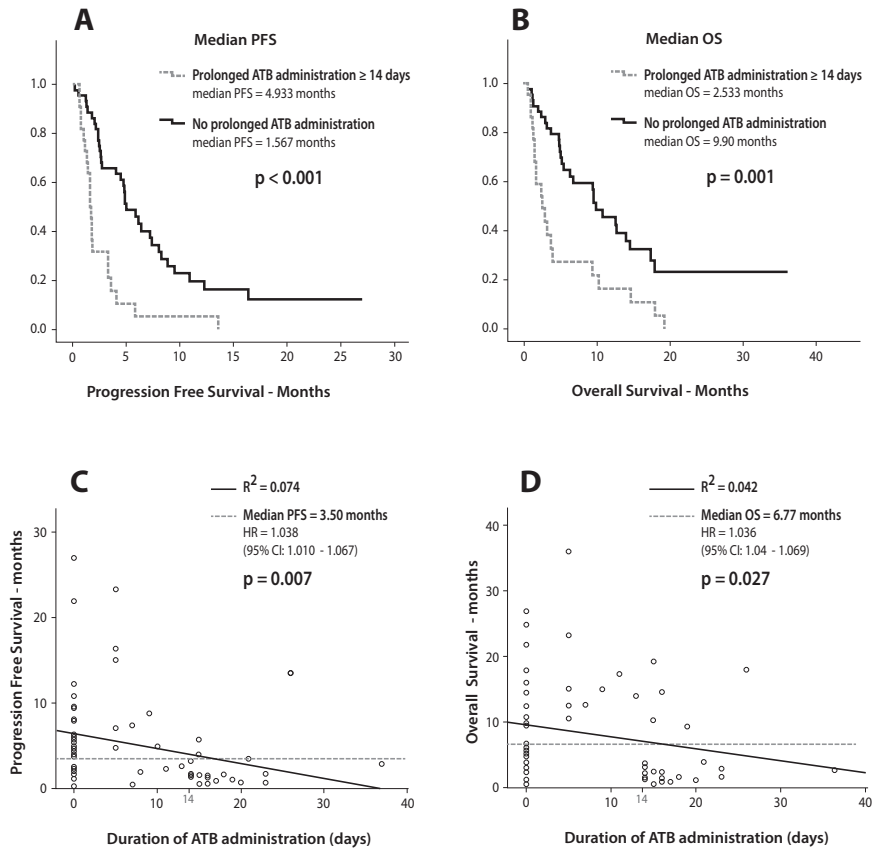


Figure 11: Survival Analysis Utilizing Kaplan-Meier Method and Cox Regression. A. Impact of Extended Antibiotic (ATB) Usage on Progression-Free Survival (PFS). B. Influence of Extended ATB Usage on Overall Survival (OS). C. Scatterplot Illustrating the Influence of ATB Duration in Days as a Continuous Variable on PFS. D. Scatterplot Demonstrating the Relationship Between ATB Duration in Days as a Continuous Variable.

Cox regression	PFS		OS	
Univariate analysis	HR (95% CI)	p value	HR (95%CI)	p value
Performance status	1.574(0.855–2.899)	0.145	1.999(1.068–3.740)	0.030
Age ≥ 70 years old	1.127(0.661–1.922)	0.660	1.193(0.673–2.114)	0.546
Smoker of former smoker	1.126(0.404–3.135)	0.821	2.361(0.571–9.757)	0.235
Female gender	1.033(0.504–2.120)	0.929	1.144(0.535–2.445)	0.729
Brain metastases	1.242(0.653–2.364)	0.509	1.022(0.493–2.118)	0.953
Bone metastases	1.913(1.078–3.394)	0.027	2.135(1.171–3.893)	0.013
Liver metastases	2.503(1.390–4.506)	0.002	1.443(0.781–2.665)	0.241
Disease burden	2.115(1.201–3.725)	0.009	1.562(0.860–2.840)	0.142
Steroid administration > 10 mg	2.156(1.158–4.013)	0.015	1.908(0.985–3.698)	0.055
ATB ^a administration	1.655(0.068–2.830)	0.065	1.353(0.761–2.406)	0.304
Prolonged ATB administration ≥14 days	3.181(1.795–5.637)	0.0001	2.646(1.476–4.741)	0.001
NLR ^b	1.939(1.050–3.559)	0.033	1.588(0.855–2.947)	0.143
LDH>UNL	1.674(0.935–2.997)	0.083	1.868(1.018–3.425)	0.044
Multivariate analysis	HR (95% CI)	p value	HR (95%CI)	p value
Performance status			1.878(0.963–3.661)	0.075
Bone metastasis	2.244(1.155–4.360)	0.017	1.890(1.017–3.512)	0.049
Liver metastasis	3.266(1.653–6.375)	0.001		
Disease burden	1.552(0.555–4.329)	0.401		
Steroid administration > 10 mg	2.566(1.347–4.887)	0.004		
Prolonged ATB administration ≥14 days	3.403(1.817–6.375)	0.0001	2.945(1.619–5.358)	0.0001
NLR	1.147(0.580–2.269)	0.693		
LDH > UNL ^c			1.618(0.877–2.985)	0.123

Table 4: Univariate and multivariate analysis utilizing Cox Regression Method.

^a: ATB = Antibiotics, ^b: NRL = Neutrophil to Lymphocyte ratio, ^c: UNL = Upper normal limit (247 Units/liter).

Multivariate Analysis Using JADBio Tool

To address the classification task pertaining the probability of achieving DCR as best response to ICIs, patients were stratified into two groups: responders, characterized by Partial Response (PR) or Stable Disease (SD), and non-responders, experiencing Progressive Disease (PD) as best response to ICIs. JADBio employed an extensive array of configurations (3017) and trained a multitude of models (211190) for the classification analysis, as shown in Figure 7. LASSO feature selection was performed by JADbio with specific parameters (penalty = 0.5, lambda = 0.027), leading to the identification of four crucial features: extended Antibiotic (ATB) administration, presence of bone metastases, presence of liver metastases, and a Body Mass Index (BMI) below 25 kg/m². This selection process resulted in a singular signature. The predictive algorithm of the best-performing model was a Support Vector Machine (SVM) of the C-SVC type with a Polynomial Kernel and the following hyper-parameters (cost = 0.01, gamma = 1.0, degree = 4), achieving an Area Under the Curve (AUC) value of 0.806 (0.714– 0.889), as illustrated in Figure 12A. The Receiver Operating Characteristic (ROC) curve for the top- performing model is depicted in Figure 12B. Furthermore, the classification analysis provided valuable insights into the feature importance of the selected variables, demonstrating the reduction in predictive performance when each feature was excluded from the model, as shown in Figure 13A. Box

plots, visually contrasting the cross-validated predicted probability of class membership with the actual class labels of samples, are presented in Figure 13B.

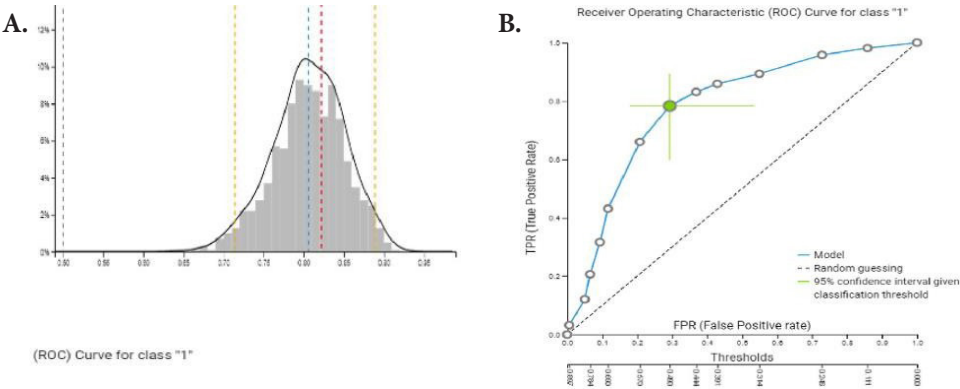


Figure 12: **A.** Distribution of the performance metric (AUC) of our model. The distribution is computed on out of sample predictions of the current model. **B.** Receiver Operating Characteristic (ROC) Curve for the best performing model (Support Vector Machines (SVM) of type C-SVC with Polynomial Kernel and hyper-parameters: cost = 0.01, gamma = 1.0, degree = 4). The classification threshold for the 95% confidence intervals has been set at the average F1/accuracy/Balance accuracy.

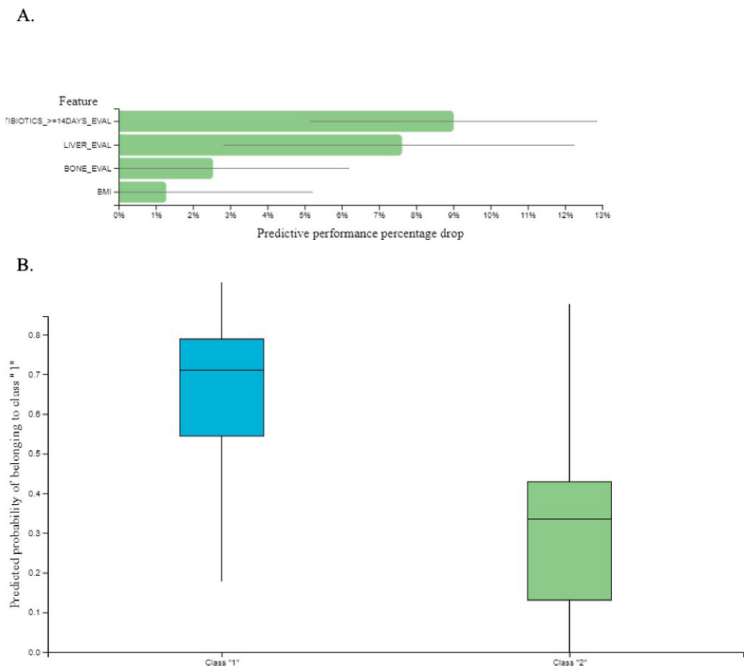


Figure 13: **A.** Feature importance plot: This chart reports feature importance defined as the percentage drop in predictive performance when the feature is removed from the model. Grey lines indicate 95% confidence intervals. **B.** The Box-Plot contrasts the cross-validated predicted probability of belonging to a specific class against the actual class of the samples. Well-performing models are expected to provide predictions that are close to 1 for the actual class and close to 0 for all other class. Class 1 is the probability of achieving PR or SD as response to immunotherapy and class 2 is the probability of developing disease progression.

4.2 Cancer cachexia syndrome as a biomarker of immunotherapy outcomes in metastatic Non-Small Cell Lung Cancer

In the second publication we investigated the effect of the impact of underlying CCS [174] on the clinical outcomes of ICIs in patients with metastatic NSCLC. In contrast with the first publication, we included individuals that were treated with ICIs for metastatic NSCLC in the first and subsequent line settings. In order to achieve this purpose, we analyzed data of 94 patients with metastatic NSCLC that were treated with ICIs in the Oncology Department of the University Hospital of Heraklion, Crete. Only in 83 patients we were able to collect sufficient clinical or radiological data in order for them to be diagnosed with underlying CCS (diagram 2).

Patient characteristics

A total of 83 patients were enrolled in this analysis. The median follow-up duration stood at 9.53 months. A detailed breakdown of patients' characteristics can be found in Table 5. The median age was 66 years, with 70 (84.3%) being male, and 77 (92.8%) were either active or former smokers. The majority of the patients in our cohort, 65 patients (78.3%) were clinically evaluated to have performance status (PS)=0-1 by ECOG and the rest 18 were classified as having PS=2.

In addition, 51 patients (61.4%) that were included in the final analysis had non-squamous NSCLC as underlying histology and the rest 32 (38.6%) were afflicted by squamous cell metastatic NSCLC. We further assessed the disease burden of the individuals in our cohort that was determined as the number of organs afflicted with metastatic dissemination and 57 patients (68.7%) had metastatic disease in ≤ 2 organs and the rest 26 (31.3%) had metastases in more than 2 organs. PD-L1 status was estimated in 52 (61.4%) out of 83 patients in our cohort. In the subgroup of the 52 individuals in our cohort with calculated PD-L1 values, 16 (30.7%) had PD-L1 $< 1\%$, 22 (42.3%) had PD-L1 expression in the range of equal or higher to 1% and lower than 50% and the rest 15 (18.1%) had PD-L1 expression equal or higher than 50%.

The mean baseline Body Mass Index (BMI) was 26.69 kg/m^2 , and 38.6% of patients had a baseline BMI of less than 25 kg/m^2 . Albumin levels at the initiation of immunotherapy were available in 76 (91.5%) patients and only 12 patients (14.5%) had serum albumin lower than 3.5 g/L which represents the lower normal limit.

The majority of patients in our cohort (79.5%) received ICIs as their second line of treatment, while the rest were administered as a first-line treatment. All patients who received ICIs as a second-line treatment had previously progressed on a platinum doublet regimen. The ICIs administered to the individuals in our cohort were Nivolumab in 54 patients, Pembrolizumab in 26 patients and Atezolizumab in 3 patients. Only 2 patients (2.4%) received ICIs in combination with platinum-based chemotherapy as first line treatment, while the remaining patients received ICIs as monotherapy. The Overall Response Rate (ORR) was 20.5%, and 48.2% of patients experienced Progressive Disease (PD) as the best response to treatment. Grade III-IV irAEs were observed in 7 patients (8.4%). The median Progression-Free Survival (PFS) was 4.80 months, and the median Overall Survival (OS) was 9.90 months.

Variable	All patients	
	N	%
Number of patients	83	
Age, median (range)	66 (39–81)	
Gender		
Male	70	84.3
Female	13	15.7
Performance status		
0–1	65	78.3
2	18	21.7
Smoking status		
Active or former smokers	77	92.8
Never smokers	6	7.2
Histology		
Squamous	32	38.6
Non-squamous	51	61.4
Mean baseline BMI (SD)	26.69 (4.69)	
Baseline BMI		
<25 kg/m ²	32	38.6
≥25 kg/m ²	51	61.4
Brain metastases		
Yes	20	24.1
No	63	75.9
Liver metastases		
Yes	23	27.7
No	60	72.3
Bone metastases		
Yes	29	34.9
No	54	65.1
Number of organs with metastatic disease		
1–2	57	68.7
>2	26	31.3
Baseline albumin levels		
≥3.5 g/dL	64	77.1
<3.5 g/dL	12	14.5
Missing values	7	8.4
PD-L1 levels		
<1%	14	16.9
1% < PD-L1 < 50%	22	26.5
≥50%	15	18.1
Missing values	32	38.5

Variable	All patients	
	N	%
Line of treatment of ICI administration		
1 st line	17	20.5
2 nd line	66	79.5
Immunotherapy agent		
Nivolumab	54	65.1
Pembrolizumab	26	31.3
Atezolizumab	3	3.6
Mode of ICI administration		
Monotherapy	81	97.6
Combination with chemotherapy	2	2.4
Baseline cancer cachexia		
Yes	43	51.8
No	40	48.2
Baseline LSMI		
Male [mean (SD)]	46.26 (10.07)	
Female [mean (SD)]	34.6 (6.74)	
Baseline LSMI		
Below LNV	39	47.0
Above LNV	15	18.1
Missing values	29	34.9
LSMI change during ICI treatment %, median (range)	4.96 (Min: –28.08, Max: 14.61)	
Response to ICIs		
CR	1	1.2
PR	16	19.3
SD	26	31.3
PD	40	48.2
Duration of disease control* (N=38)		
<6 months	10	26.3
≥6 months	28	73.7
Grade III–IV irAEs		
Yes	7	8.4
No	76	91.6
PFS (months), median (95% CI)	4.80 (3.10–6.50)	
OS (months), median (95% CI)	9.90 (6.81–12.98)	
Follow up (months), median (95% CI)	9.53 (6.05–13.01)	

Table 5: Baseline patient characteristics

Baseline Cancer Cachexia Syndrome (CCS) was observed in 43 patients (51.8%), with only 15 out of 54 patients having baseline Lean Skeletal Muscle Index (LSMI) values not indicative of sarcopenia (above the Lower Normal Limit). In 29 patients the available computed tomography images were not of sufficient quality in order to calculate the LSMI of the patients, but

it was possible to be categorized as cachectic or not based on their weight fluctuations in the last 6 months before ICIs initiation. The distribution of baseline LSMI differed significantly between cachectic and non-cachectic males ($P=0.001$) but not among females ($P=0.606$) (Figure 14). Twenty-eight patients had evaluable LSMI values at their first evaluation post ICI initiation. The median LSMI percentage change during ICIs treatment was -4.96% (ranging from -28.08% to 14.61%). Patients were categorized based on their percent LSMI reduction during IO, using the median LSMI reduction during treatment (5%) as a cutoff.

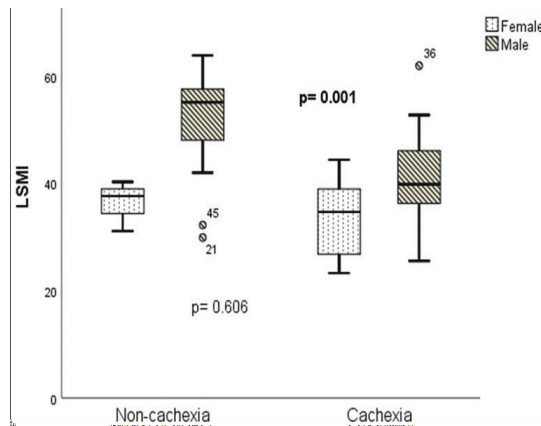


Figure 14: The Kruskal-Wallis test was employed to assess potential distinctions in the distributions of baseline Lean Skeletal Muscle Index (LSMI) values between males with cachexia and those without, as well as between females with cachexia and those without.

Effect of the studied parameters on response outcomes

The associations of all analyzed parameters with ORR are detailed in table 6. Baseline BMI below 25 kg/m^2 ($P=0.047$) and the presence of CCS ($P \leq 0.001$) were significantly associated with a lower Overall Response Rate (ORR). Similarly, CCS was significantly linked with reduced Disease Control Rate (DCR) ($P \leq 0.001$), along with baseline LSMI below the Lower Normal Limit (LNL) ($P \leq 0.001$), BMI below 25 kg/m^2 ($P=0.039$), and metastatic spread in more than two organs ($P=0.034$). PD-L1 status (PD-L1 $< 1\%$ vs PD-L1 $\geq 1\%$) did not affect ORR or DCR at a statistically significant level in our cohort. The effects of all the analyzed variables on DCR are presented in Table 7.

The distribution of LSMI percent change during IO did not significantly differ between individuals who achieved Complete Response (CR) or Partial Response (PR) compared to those with Stable Disease (SD) or PD ($P=0.446$) (Figure 15A). Similarly, the distribution of LSMI percent change during IO did not differ between individuals with disease control compared to those who experienced PD ($P \geq 0.99$) (Figure 15B) or among those who achieved prolonged disease control for at least six months versus those who did not ($P=0.424$) (Figure 15C).

In univariate logistic regression analysis, BMI below 25 kg/m^2 [OR = 2.58 (95% CI: 1.04–6.19), $P=0.041$] and the presence of baseline CCS [OR = 8.89 (95% CI: 3.28–24.12), $P \leq 0.001$] were significantly associated with an increased probability of PD as the best response to ICI treatment (Figure 16A, Table 8). However, in the multivariate analysis, only CCS remained

as an independent predictor for an increased probability of PD as the best response to treatment [OR =8.11 (95% CI: 2.95–22.94), $P \leq 0.001$], with an Area Under the Curve (AUC) of 0.748 (95% CI: 0.640–0.856) (Figure 16B and Table 8).

Effect of the studied variables on survival outcomes

Patients with baseline CCS experienced significantly shorter PFS (2.36 vs. 7.33 months, $P \leq 0.001$) (Figure 17A) and OS (3.70 vs. 17.93 months, $P \leq 0.001$) (Figure 17B) compared to non- cachectic individuals. Similarly, patients with baseline LSMI values indicative of sarcopenia had significantly reduced PFS (2.96 vs. 7.96 months, $P = 0.032$) (Figure 17C) and OS (5.43 months vs. not reached, $P = 0.006$) (Figure 17D) compared to those with baseline LSMI values not indicating sarcopenia.

However, LSMI reduction greater than 5% during IO did not significantly affect PFS (7.96 vs. 7.33 months, $P = 0.193$) (Figure 18A) or OS (19.20 vs. 14.03 months, $P = 0.400$) (Figure 18B). The effects of all other studied covariates on survival outcomes are summarized in Table 9.

The presence of baseline cachexia significantly reduced survival in the subgroup of patients who received IO as a first-line treatment (not reached vs. 13.37 months, $P = 0.028$) (Figure 19A) and in the subgroup of patients who received IO as a second-line treatment (12.70 vs. 3.23 months, $P = 0.003$) (Figure 19B). Additionally, the presence of baseline cancer cachexia was significantly associated with inferior 6-month survival from the initiation of IO ($P < 0.001$) (Figure 20).

Variable	N=83	CR or PR	SD or PD	P value (chi-square test, 95% CI)
Age				
<70 years old	51	12	39	0.385
≥70 years old	32	5	27	
Gender				
Male	70	14	56	0.801
Female	13	3	10	
Performance status				
0–1	65	14	51	0.650
2	18	3	15	
Histology				
Non-squamous	51	12	39	0.385
Squamous	32	5	27	
Brain metastases				
Yes	20	4	16	0.951
No	63	13	50	
Liver metastases				
Yes	23	3	20	0.298
No	60	14	46	
Bone metastases				
Yes	29	7	22	0.545
No	54	10	44	
Disease burden*				
High	26	5	21	0.849
Low	57		45	

Variable	N=83	CR or PR	SD or PD	P value (chi-square test, 95% CI)
PD-L1 status	N=51	12		
<1%	14	3	11	0.988
≥1%	37		29	
Baseline albumin levels	N=76	8		
<3.5 g/dL	12	0	12	0.085
≥3.5 g/dL	64	13	51	
BMI				
<25 kg/m ²	32	3	29	0.047
≥25 kg/m ²	51	14	37	
Cancer Cachexia				
Yes	43	2	41	<0.01
No	40		25	
Baseline LSMI	N=54	15		
<LNV	39	6	33	0.051
≥LNV	15	6	9	

Table 6: Effect of the analyzed parameters on objective response rates (ORR). CR: Complete response, PR: Partial response, SD: Stable disease, PD: Progressive disease

Variable	N=83	CR or PR or SD	PD	P value (chi-square test, 95% CI)
Age				
<70 years old	51	24	27	0.274
≥70 years old	32	19	13	
Gender				
Male	70	38	32	0.294
Female	13	5	8	
Performance status				
0–1	65	37	28	0.076
2	18	6	12	
Histology				
Non-squamous	51	24	27	0.274
Squamous	32	19	13	
Brain metastases				
Yes	20	8	12	0.225
No	63	35	28	
Liver metastases				
Yes	23	8	15	0.055
No	60	35	25	
Bone metastases				
Yes	29	11	18	0.064
No	54	32	22	
Disease burden*				
High	26	9	17	0.034
Low	57	34	23	
PD-L1 status	N=51			

Variable	N=83	CR or PR or SD	PD	P value (chi-square test, 95% CI)
<1%	14	5	9	0.180
≥1%	37	21	16	
Baseline albumin levels	N=76			
<3.5 g/dL	12	4	8	0.174
≥3.5 g/dL	64	35	29	
BMI				
<25 kg/m ²	32	12	20	0.039
≥25 kg/m ²	51	31	20	
Cancer Cachexia				
Yes	43	12	31	<0.01
No	40	31	9	
Baseline LSMI	N=54			
<LNV	39	13	26	<0.01
≥LNV	15	13	2	

Table 7: Effect of the analyzed parameters on disease control rates (DCR). CR: Complete response, PR: Partial response, SD: Stable disease, PD: Progressive disease

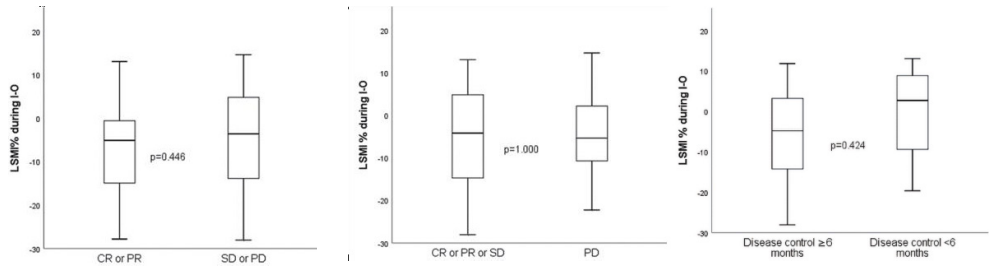


Figure 15: The Kruskal-Wallis test was employed to examine potential disparities in the distributions of Lean Skeletal Muscle Index (LSMI) change percentages during Immune-Oncology (I-O) treatment A) Between patients who achieved Complete Response (CR) or Partial Response (PR) and those who experienced Stable Disease (SD) or Progressive Disease (PD). B) Between patients who achieved CR, PR, or PD and those who experienced PD. C) Between individuals who attained prolonged disease control for six months or more and those who did not.

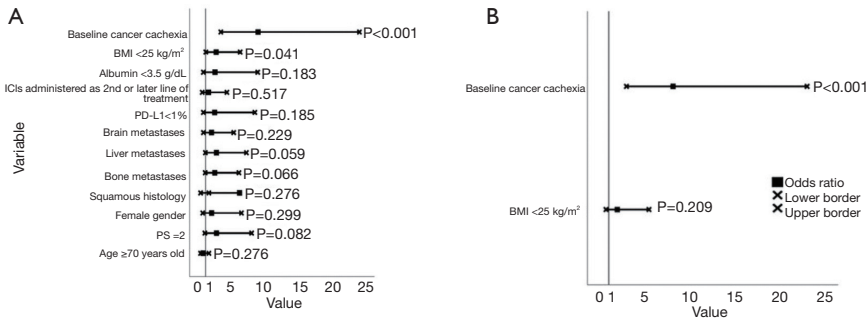


Figure 16: Forest plots illustrating the odds ratios of the analyzed variables concerning the likelihood of experiencing disease progression as the best response to Immune Checkpoint Inhibitor (ICI) treatment, delineated as follows: (A) Univariate analysis; and (B) Multivariate analysis. The variables include ICI (Immune Checkpoint Inhibitor), BMI (Body Mass Index), PD-L1 (Programmed Death-Ligand 1), and PS (Performance Status).

Variable	Univariate			Multivariate		
	OR (95% CI)	P value	AUC (95% CI)	OR (95% CI)	P value	AUC (95% CI)
Age ≥70 years old	0.61 (0.25–1.49)	0.276	0.558 (0.434–0.682)			
PS=2	2.64 (0.88–7.91)	0.082	0.580 (0.456–0.704)			
Female gender	1.90 (0.56–6.39)	0.299	0.542 (0.417–0.667)			
Squamous histology	0.61 (0.25–1.49)	0.276	0.558 (0.434–0.682)			
Bone metastases	2.38 (0.94–6.01)	0.066	0.597 (0.474–0.720)			
Liver metastases	2.63 (0.97–7.13)	0.059	0.594 (0.471–0.718)			
Brain metastases	1.88 (0.67–5.22)	0.229	0.557 (0.432–0.681)			
PD-L1 <1%	2.36 (0.66–8.40)	0.185	0.584 (0.426–0.742)			
ICIs administered as 2 nd or later line of treatment	1.43 (0.49–4.20)	0.517	0.529 (0.404–0.653)			
Albumin <3.5 g/dL	2.41 (0.66–8.83)	0.183	0.557 (0.427–0.687)			
BMI <25 kg/m ²	2.58 (1.04–6.19)	0.041	0.610 (0.488–0.733)	1.94 (0.69–5.44)	0.209	
Baseline cancer cachexia	8.89 (3.28–24.12)	<0.001	0.748 (0.640–0.856)	8.11 (2.95–22.94)	<0.001	
Overall						0.748 (0.640–0.856)

Table 8: Univariate and multivariate logistic regression on the odds ratio (OR) of the analyzed parameters on the probability of developing disease progression (PD) as response to treatment with ICIs. OR: Odds Ratio, AUC: Area under the curve, PS: Performance status by ECOG.

Univariate and multivariate analyses

Univariate and multivariate analyses examining the impact of the analyzed variables on Progression-Free Survival (PFS) and Overall Survival (OS) are presented with detail in Table 10.

In the univariate analysis for PFS, the administration of ICIs as a second-line treatment [Hazard Ratio (HR)=2.22 (95% Confidence Interval: 1.19–4.40), P=0.023] and the presence of baseline Cancer Cachexia Syndrome (CCS) [HR =2.72 (95% CI: 1.64–4.50), P≤0.001] achieved statistical significance. However, in the multivariate analysis, only the presence of baseline CCS [HR =2.49 (95% CI: 1.49– 4.16), P≤0.001] emerged as an independent predictor associated with a shorter PFS (Table 10).

In the univariate analysis for OS, factors such as performance status 2, a high disease burden, ICI administration as a second-line treatment, and the presence of baseline CCS were all significantly correlated with diminished OS. Nevertheless, in the multivariate analysis, performance status 2 [HR=1.98 (95% CI: 1.10–3.58), P=0.023], ICI administration as a second-line treatment [HR =2.91 (95% CI: 1.13–7.49), P=0.027], and the presence of CCS [HR =2.52 (95% CI: 1.40–4.55), P=0.002] emerged as independent adverse prognostic factors for shorter survival (Table 10).

In the univariate analysis concerning the impact of baseline cancer cachexia on the likelihood of death within six months from the initiation of the ICIs, cancer cachexia was significantly associated with an increased risk of death within the first six months of IO [HR =3.90 (95% CI: 1.75–8.70), P=0.001)] (Figure 20).

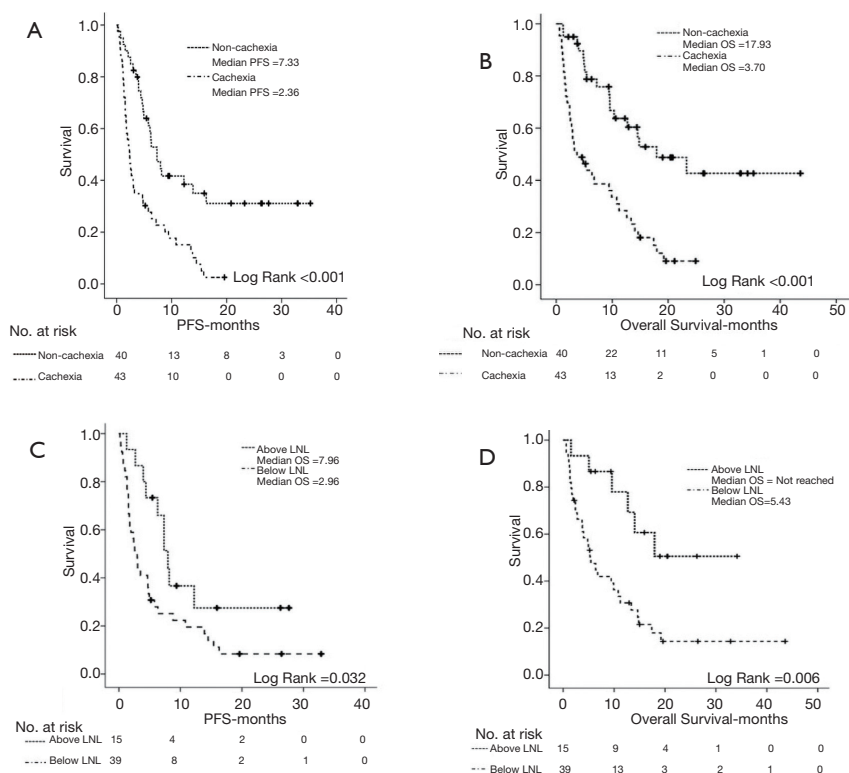


Figure 17: Kaplan-Meier survival curves illustrating the impact of baseline Cancer Cachexia Syndrome (CCS) on Progression-Free Survival (PFS) (A) and Overall Survival (OS) (B), as well as the influence of baseline Lumbar Skeletal Muscle Index (LSMI) values on PFS (C) and OS (D). CCS, cancer cachexia syndrome; PFS, progression free survival (months); OS, overall survival (months); LSMI, lumbar skeletal muscle index (cm^2/m^2) (at the level of 3rd lumbar vertebra); LNL, lower normal limit ($55 \text{ cm}^2/\text{m}^2$ for males and $<39 \text{ cm}^2/\text{m}^2$ for females).

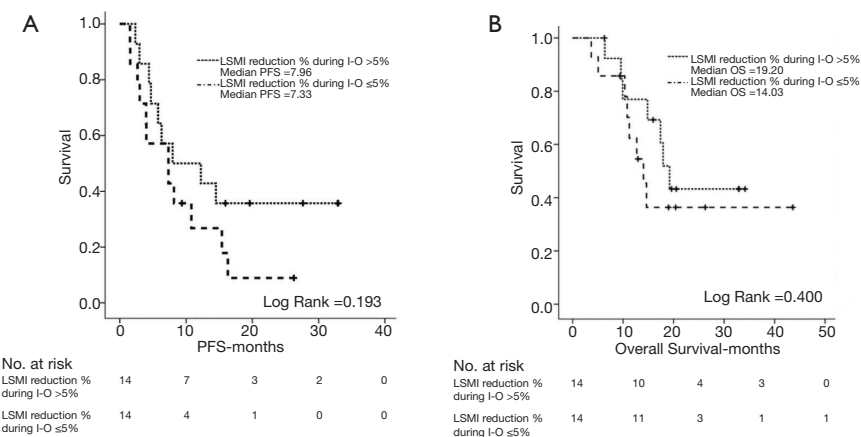


Figure 18: Log-rank test demonstrating the effect of LSMI reduction% >5 during I-O on PFS (A) and OS (B). LSMI, lumbar skeletal muscle index (cm^2/m^2) (at the level of 3rd lumbar vertebra); I-O, immunotherapy; PFS, progression free survival; OS, overall survival.

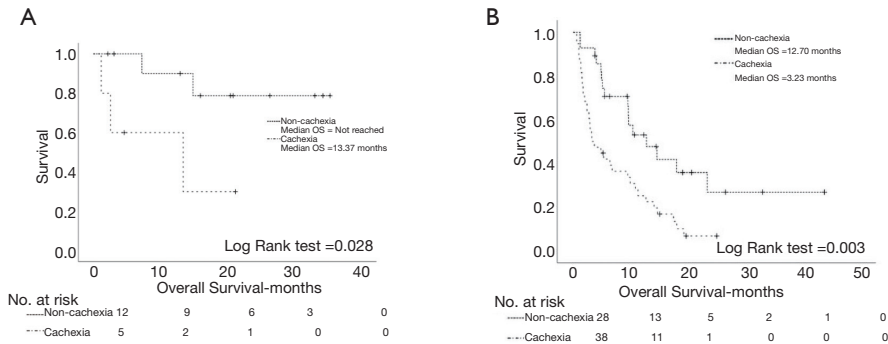


Figure 19: Log rank test demonstrating the effect of cancer cachexia syndrome on overall survival amongst the patients' subgroups that received PD-1/PD-L1 inhibitors as first line treatment (A) and second line treatment (B). OS, overall survival; PD-1, programmed death-1; PD-L1, programmed death ligand 1.

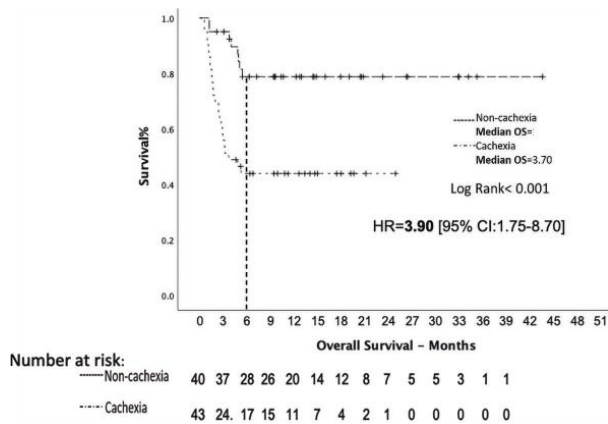


Figure 20: Log-rank test demonstrating the effect of cancer cachexia syndrome on 6 months survival.

Variable	Median PFS (Months)	P value (log-rank test)	Median OS (Months)	P value (log-rank test)
Age				
<70 years old	4.00	0.803	9.47	0.957
≥70 years old	7.17		12.70	
Gender				
Male	4.80	0.253	10.33	0.531
Female	2.10		9.43	
Performance Status				
0-1	5.77	0.217	12.60	0.008
2	2.40		3.17	
Histology				
Squamous	5.77	0.580	9.57	0.572
Non-squamous	3.00		9.90	
BMI				
<25 kg/m ²	2.53	0.153	4.00	0.273
≥25 kg/m ²	6.20		10.33	
Line of treatment of ICI administration				

Variable	Median PFS (Months)	P value (log-rank test)	Median OS (Months)	P value (log-rank test)
1 st line	13.80	0.019	Not reached	0.002
2 nd or later lines	4.40		9.43	
Brain metastases				
Yes	2.17	0.203	6.77	0.299
No	4.93		10.80	
Bone metastases				
Yes	4.80	0.674	7.23	0.198
No	3.23		12.70	
Liver metastases				
Yes	2.10	0.056	6.77	0.405
No	5.77		10.80	
Disease burden*				
High	2.53	0.057	4.83	0.038
Low	4.93		13.37	
Baseline albumin levels				
<3.5 g/dL	1.77	0.008	2.40	0.017
≥3.5 g/dL	5.77		11.23	
PD-L1 levels				
<1%	2.57	0.880	7.23	0.184
≥1%	4.80		12.60	
Baseline Cancer Cachexia				
Yes	2.37		3.70	<0.001
No	7.33	<0.001	17.93	
Baseline LSMI				
<LNV	2.97	0.032	5.43	0.006
≥LNV	7.97		Not reached	
LSMI reduction % during ICI treatment				
<-5%	7.97	0.193	19.20	0.400
≥-5%	7.33		14.03	

Table 9: Log-rank test on the effect of the studied variables on PFS and OS (n=83). *, high disease burden was defined as > 2 organs with metastatic spread. ICI: Immune checkpoint inhibitor; LSMI: lumbar skeletal muscle index (at the level of 3rd lumbar vertebra); LNV, lower normal value that was set for males =55 cm/m² and for females =39 cm/m².

Cox regression	PFS		OS	
	HR (95% CI)	P value	HR (95% CI)	P value
Univariate analysis				
Age ≥70 years old	0.94 (0.57–1.54)	0.803	0.98 (0.58–1.69)	0.957
Performance status 2	1.42 (0.81–2.50)	0.220	2.18 (1.21–3.90)	0.009
Female gender	1.46 (0.76–2.80)	0.257	1.26 (0.61–2.57)	0.523
Squamous histology	0.582 (0.53–1.43)	0.869	1.17 (0.68–1.99)	0.573
Brain metastases	1.43 (0.82–2.48)	0.207	1.38 (0.75–2.53)	0.302
Liver metastases	1.65 (0.98–2.77)	0.059	1.28 (0.72–2.29)	0.406
Bone metastases	1.11 (0.68–1.18)	0.675	1.42 (0.83–2.43)	0.200
High disease burden*	1.63 (0.98–2.70)	0.060	1.77 (1.02–3.06)	0.041
PD-L1 <1%	0.95 (0.46–1.95)	0.880	0.60 (0.28–1.29)	0.189
ICIs as 2 nd or later line of treatment	2.22 (1.19–4.40)	0.023	3.90 (1.55–9.82)	0.001
Baseline cancer cachexia	2.72 (1.64–4.50)	<0.001	3.22 (1.82–5.69)	<0.001
Multivariate analysis				
Age ≥70 years old				
Performance status 2			1.98 (1.10–3.58)	0.023
Female gender				
Squamous histology				
Brain metastases				
Liver metastases				
Bone metastases				
High disease burden			1.16 (0.64–2.11)	0.618
PD-L1 <1%				
ICIs as 2 nd or later line of treatment	1.83 (0.91–3.66)	0.088	2.91 (1.13–7.49)	0.027
Baseline cancer cachexia	2.49 (1.49–4.16)	<0.001	2.52 (1.40–4.55)	0.002

Table 10: Univariate and multivariate analysis using Cox regression method in the whole patient population.
*: high disease burden = metastatic dissemination in > 2 organs, PFS: Progression free survival; OS: Overall survival; HR: Hazard Ratio; ICI: Immune checkpoint inhibitor; PD-L1: Programmed death ligand-1

4.3 Adipose tissue composition as a prognostic and predictive biomarker of immunotherapy outcomes in metastatic Non-Small Cell Lung Cancer

In the third paper that resulted from the analysis of the data from the patient cohort that was created [175] we investigated the role of adipose tissue composition as a prognostic and predictive factor of ICI efficacy in NSCLC. To this end, we analyzed the radiological and clinical data of the 52 patients in the cohort that we had sufficient radiological data that were suitable for the quantitative estimation of adipose and skeletal muscle composition. In this publication, in the same manner as the second publication, we included patients that received ICIs as first or subsequent lines of therapy.

Patient characteristics

A total of 52 patients were enrolled in the analysis. Comprehensive individual patient characteristics are detailed in Table 11. Among these patients, 43 (82.7%) were male, with a median age of 68 years (ranging from 39 to 81 years). Notably, 43 (82.7%) individuals had received ICIs as a second-line treatment, while 9 patients received it as a first-line treatment. It's noteworthy that all patients who received immunotherapy as a second-line treatment had previously experienced disease progression while on a platinum doublet regimen. The vast majority of the individuals in the studied cohort, 48 (92.3%) were active or former smokers. PD-L1 status data were available for 32 (61.5%) patients. Among the individuals with estimated PD-L1 status, 10 (31.3%) had PD-L1 < 1%, 15 (46.9%) had $1\% \leq \text{PD-L1} < 50\%$ and 7 (21.9%) had PD-L1 expression $\geq 50\%$. In the patients of our cohort, the greater part, 50 individuals (96.2%), received ICIs as monotherapy, whereas two patients received ICIs in combination with chemotherapy. The individuals in our cohort were all treated with PD-1 or PD-L1 inhibitors and more specifically 34 (65.4%) were administrated Nivolumab, 16 (30.8%) received Pembrolizumab and 2 (3.8%) were treated with Atezolizumab.

The mean baseline Body Mass Index (BMI) was calculated to be 26.67 kg/m^2 . Thirteen patients (25%) were classified as obese, with a BMI exceeding 30 kg/m^2 , while 21 patients (40.4%) fell within the BMI range of 25 kg/m^2 to $< 30 \text{ kg/m}^2$. The remaining 34.6% of patients had a BMI below 25 kg/m^2 . The median values for intramuscular fat index (IMFI), visceral fat index (VFI), and subcutaneous fat index (SFI) for both males and females are presented in Table 11. Notably, 36 patients (69.2%) met the criteria for sarcopenia, according to predefined thresholds that were set by the international consensus, as their lumbar skeletal muscle index (LSMI) values were below the lower normal limit (LNL).

Adipose tissue and skeletal muscle indices correlation with BMI

VFI demonstrated a substantial positive correlation with BMI values ($\rho = 0.810$, $p < 0.001$) (Figure 21A), as did SFI ($\rho = 0.623$, $p < 0.001$) (Figure 21B), and LSMI ($\rho = 0.429$, $p = 0.002$) (Figure 21C) when applying the Spearman correlation co-efficiency method. However, IMFI did not exhibit a significant correlation with BMI values ($\rho = 0.242$, $p = 0.084$) (Figure 21D). Furthermore, when investigating any potential correlation of the adipose tissue indices with LSMI, IMFI showed no correlation with LSMI ($\rho = -0.172$, $p = 0.222$) (Figure 22A). In contrast, VFI ($\rho = 0.466$, $p = 0.001$) (Figure 22B) and SFI ($\rho = 0.289$, $p = 0.042$) (Figure 22C) displayed a positive correlation with LSMI at a statistically significant level.

All patients		
Variable	N	%
Number of patients	52	
Age (years) Median (range)	68 (39–81)	
Gender		
Male	43	82.7
Female	9	17.3
Performance status		
0–1	41	78.8
2	11	21.2
Smoking status		
Active or former smokers	48	92.3
Never smokers	4	7.7
Histology		
Squamous	22	42.3
Non-squamous	30	57.7
Mean baseline BMI (SD)	26.67 (4.39)	
Baseline BMI		
< 25 kg/m ²	18	34.6
25 kg/m ² ≤ BMI < 30 kg/m ²	21	40.4
BMI > 30 kg/m ²	13	25
Brain metastases		
Yes	10	19.2
No	42	80.8
Liver metastases		
Yes	14	26.9
No	38	73.1
Bone metastases		
Yes	15	28.8
No	37	71.2
Baseline albumin levels		
≥3.5 g/dl	41	78.8
<3.5 g/dl	6	11.5
Missing values	5	9.6
PD-L1 levels		
< 1%	10	19.2
1% < PD-L1 < 50%	15	28.8
≥ 50%	7	13.5
Missing values	20	38.5
Line of treatment of ICI administration		
1 st line	9	17.3
2 nd line	43	82.7
Immunotherapy agent		
Nivolumab	34	65.4
Pembrolizumab	16	30.8
Atezolizumab	2	3.8

All patients		
Variable	N	%
Mode of ICI administration		
Monotherapy	50	96.2
Combination with chemotherapy	2	3.8
Baseline LSMI		
< LNL	16	30.8
≥ LNL	36	69.2
Median baseline IMFI (cm ² /m ²)		
Males (N = 43) (range)	9.87 (3.53–35.13)	
Females (N = 9) (range)	10.52 (4.24–39.45)	
Median baseline VFI (cm ² /m ²)		
Males (N = 43) (range)	45.15 (6.34–172.82)	
Females (N = 9) (range)	31.20 (12.78–92.75)	
Baseline SFI (cm ² /m ²)		
Males (N = 43) (range)	50.73 (4.61–136.65)	
Females (N = 7) (range)	55.36 (44.24–149.26)	

Table 11: Baseline patient characteristics. BMI = Body mass index, SD = Standard deviation, PD-L1 = Programmed death ligand-1, ICI = Immune checkpoint inhibitor, LSMI: Lumbar skeletal muscle index (At the level of 3rd lumbar vertebra), LNL: Lower normal limit, 55 cm²/m² for males and 39 cm²/m² for females, IMFI = Intramuscular Fat Index (At the level of 3rd lumbar vertebra), VFI = Visceral Fat Index (At the level of 3rd lumbar vertebra), SFI = Subcutaneous Fat Index (At the level of 3rd lumbar vertebra)

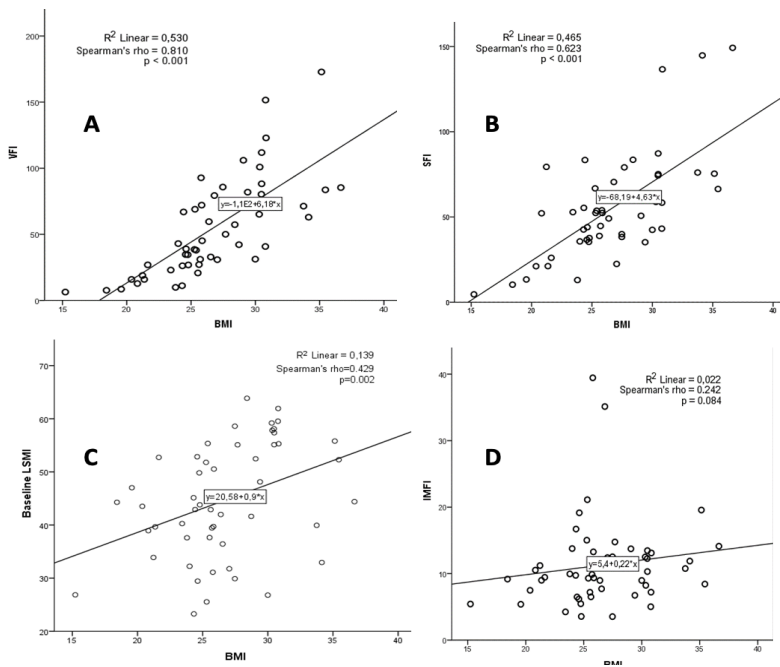


Figure 21: Scatter-plots demonstrating the correlation between baseline BMI values and A. baseline VFI values, B. baseline SFI values C. baseline LSMI values D. baseline IMFI values. BMI=Body mass index, LSMI: Lumbar skeletal muscle index (At the level of 3rd lumbar vertebra), IMFI=Intramuscular Fat Index (At the level of 3rd lumbar vertebra), VFI=Visceral Fat Index (At the level of 3rd lumbar vertebra), SFI=Subcutaneous Fat Index (At the level of 3rd lumbar vertebra)

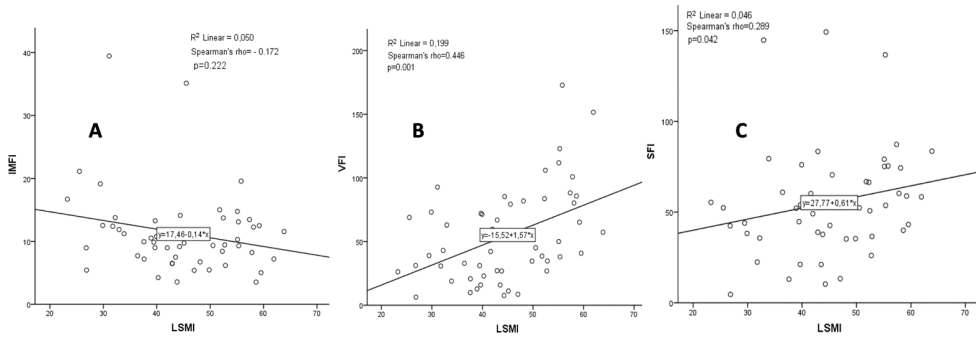


Figure 22: Scatter-plots demonstrating the correlation between baseline LSMI values and A. baseline IMFI values, B. baseline VFI values, C. baseline SFI values.

LSMI: Lumbar skeletal muscle index (At the level of 3rd lumbar vertebra), IMFI=Intramuscular Fat Index (At the level of 3rd lumbar vertebra), VFI=Visceral Fat Index (At the level of 3rd lumbar vertebra), SFI=Subcutaneous Fat Index (At the level of 3rd lumbar vertebra)

Response assessment

In terms of treatment outcomes, the Objective Response Rate (ORR) within our cohort was 23.1%, and 7 patients (13.5%) encountered grade 3 or 4 immune-related adverse events (irAEs) attributable to immunotherapy administration (table 12).

The distributions of BMI ($p = 0.391$), IMFI ($p = 0.688$), VFI ($p = 0.460$), and LSMI ($p = 0.501$) did not exhibit statistically significant differences between individuals who achieved complete or partial response (CR or PR) as best response to immunotherapy treatment compared with those who did not [stable disease (SD) or progressive disease (PD)] (figure 23A-23D). Notably, responders displayed statistically significantly higher Subcutaneous Fat Index (SFI) values compared to non-responders ($p = 0.040$) (Fig 24A).

Furthermore, individuals who achieved disease control demonstrated significantly elevated SFI values ($p = 0.005$) (Fig 24B), higher BMI values ($p = 0.029$) (Fig 24C), and increased VFI values ($p = 0.011$) (Fig 24D) when compared to patients who experienced disease progression as their best response to treatment. However, no significant differences were observed in Intramuscular Fat Index (IMFI) values ($p = 0.164$) and Lumbar Skeletal Muscle Index (LSMI) values ($p = 0.105$) between individuals who achieved disease control and those who experienced disease progression (Figure 23E-23F).

None of the analyzed categorical parameters had a statistically significant impact on Objective Response Rate (ORR), as indicated in table 13.

All patients		
Variable	N	%
Response to ICIs		
CR	1	1.9
PR	11	21.2
SD	15	28.8
PD	25	48.1
Grade 3-4 irAEs		
Yes	7	13.5
No	45	86.5

All patients		
Variable	N	%
Progression-free survival (months)		
Median (95% CI)	4.67 (3.53–5.81)	
Overall survival (months)		
Median (95% CI)	10.33 (6.83–13.84)	
Follow-up (months)		
Median (95% CI)	9.90 (5.07–14.73)	

Table 12: Response, survival and follow-up results for the whole patient population. CR: Complete response, PR: Partial response, SD: Stable disease, PD: Progressive disease, irAEs = Immune-related Adverse Events

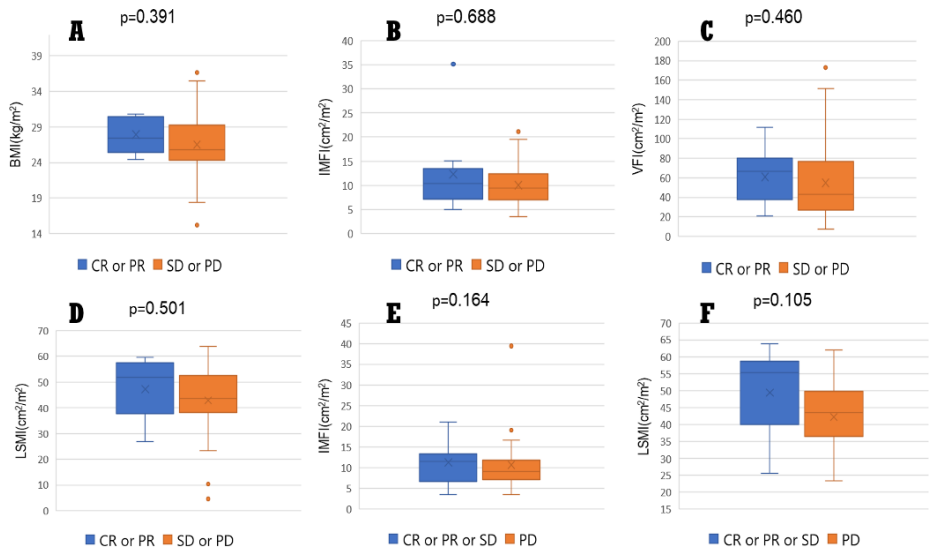


Figure 23: Box-plots demonstrating the differential distributions (Mann Whitney U test) of A. Baseline* BMI values between responders and non-responders B. IMFI values between responders and non-responders C. VFI values between responders and non-responders D. LSMI values between responders and non-responders E. IMFI values in patients who achieved disease control (CR or PR or SD) versus those who experienced PD F. LSMI values of individuals who achieved disease control versus those who had disease progression. BMI=Body mass index, LSMI: Lumbar skeletal muscle index (At the level of 3rd lumbar vertebra), IMFI=Intramuscular Fat Index (At the level of 3rd lumbar vertebra), VFI=Visceral Fat Index (At the level of 3rd lumbar vertebra), SFI=Subcutaneous Fat Index (At the level of 3rd lumbar vertebra), CR: Complete response, PR: Partial response, SD: Stable disease, PD: Progressive disease
* Baseline: At the beginning of immunotherapy

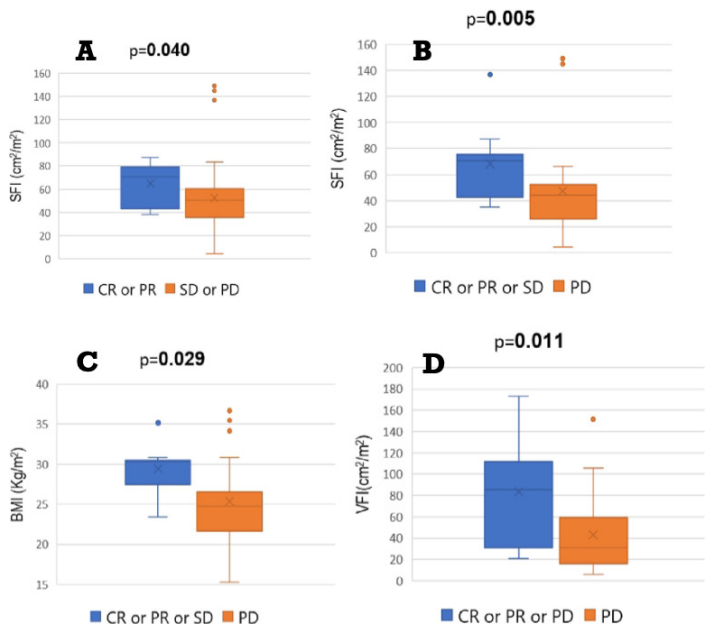


Figure 24: Box-plots depicting the baseline* differential distributions (Mann Whitney U test) of **A.** SFI (cm²/m²) between responders (CR or PR) and non-responders (SD or PD) to I-O **B.** SFI (cm²/m²) between patients who achieved disease control (CR or PR or SD) as result of I-O versus those who developed disease progression (PD) **C.** BMI (kg/m²) between patients who achieved disease control as result of I-O administration in comparison to those who developed disease progression and **D.** VFI (cm²/m²) between individuals who experienced disease control under I-O versus those who had disease progression.

I-O = Immunotherapy; **BMI** = Body mass index; **VFI** = Visceral Fat Index (At the level of 3rd lumbar vertebra); **SFI** = Subcutaneous Fat Index (At the level of 3rd lumbar vertebra); **CR** = Complete response; **PR** = Partial response; **SD** = Stable disease, **PD** = Progressive disease. * **Baseline** = At the beginning of immunotherapy.

Variable	N=52	CR or PR	SD or PD	P value (chi-square test, 95% CI)
Age				
< 70 years old	31	7	25	0.918
≥ 70 years old	21	5	16	
Gender				
Male	43	10	33	0.947
Female	9	2	7	
Performance status				
0-1	41	10	31	0.664
2	9	2	11	
Histology				
Non-squamous	30	7	23	0.959
Squamous	22	5	17	
Brain metastases				
Yes	10	1	9	0.275
No	42	11	31	

Variable	N=52	CR or PR	SD or PD	P value (chi-square test, 95% CI)
Liver metastases				
Yes	14	3	11	0.864
No	38	9	29	
Bone metastases				
Yes	15	4	11	0.696
No	37	8	29	
PD-L1 status				
N=33				
< 1 %	10	2	8	0.708
≥ 1 %	23	6	17	
Baseline albumin levels				
N=47				
< 3.5 g/dl	6	0	6	0.202
≥ 3.5 g/dl	41	9	32	
BMI				
< 25 kg/m ²	18	2	16	0.136
≥ 25 kg/m ²	34	10	24	
Baseline LSMI				
< LNL	36	6	30	0.100
≥ LNL	16	6	10	
Baseline IMFI				
Low	26	5	21	0.510
High	26	7	19	
Baseline VFI				
Low	26	6	20	1.000
High	26	6	20	
Baseline SFI				
N=50				
Low	25	3	22	0.088
High	25	8	17	

Table 13: Effect of the studied variables on objective response rate (ORR). BMI=Body mass index; SD=Standard deviation; LSMI=Lumbar skeletal muscle index (At the level of 3rd lumbar vertebra), LNL: Lower normal limit, 55 cm²/m² for males and 39 cm²/m² for females; IMFI=Intramuscular Fat Index (At the level of 3rd lumbar vertebra); VFI=Visceral Fat Index (At the level of 3rd lumbar vertebra); SFI=Subcutaneous Fat Index (At the level of 3rd lumbar vertebra)

Survival outcomes

The median Progression-Free Survival (PFS) for the patients in our cohort was 4.67 months (95% CI: 3.53 – 5.81 months) and their median Overall Survival (OS) was 10.33 months (95% CI: 6.83 - 13.84 months), respectively (table 12). Median follow-up time was 9.90 months (95% CI: 5.07 – 14.73 months).

The impact of the examined variables on PFS and OS has been summarized in table 14. Patients with baseline LSMI values below the lower normal limit (LNL), thus classified as sarcopenic, experienced significantly shorter PFS (3.30 vs. 7.33 months, $p = 0.040$) (Fig 25A) and OS (6.37 vs. not reached months, $p = 0.009$) (Fig 25B), respectively. On the other hand, low Subcutaneous Fat Index (SFI) did not significantly affect PFS (2.97 vs. 5.77 months, $p=0.135$) (Fig 25C), but it was also associated with a reduced OS (5.43 vs. 14.03 months, $p=0.020$)

(Fig 25D) at a statistically significant level. Additionally, the presence of brain metastases demonstrated a substantial association with shorter PFS (1.57 vs. 4.93 months, $p = 0.006$), although it did not reach statistical significance for OS (4.80 vs. 12.70 months, $p = 0.083$) (table 14). Furthermore, albumin levels below 3.5 g/dl were linked to inferior PFS (1.70 vs. 4.80 months, $p = 0.011$) and OS (1.70 vs. 11.23 months, $p = 0.001$). None of the other analyzed parameters displayed any significant associations with either PFS or OS (Table 14).

In the subgroup analysis investigating the combined effect of SFI and LSMI values on survival outcomes, it was observed that the three subgroups created exhibited significant differences in OS ($p = 0.004$) (figure 26A). However, survival outcomes did not significantly differ between patients with high SFI and LSMI below LNL and patients with both high SFI and LSMI above LNL (9.90 vs. 17.93 months, $p = 0.285$) (figure 26B).

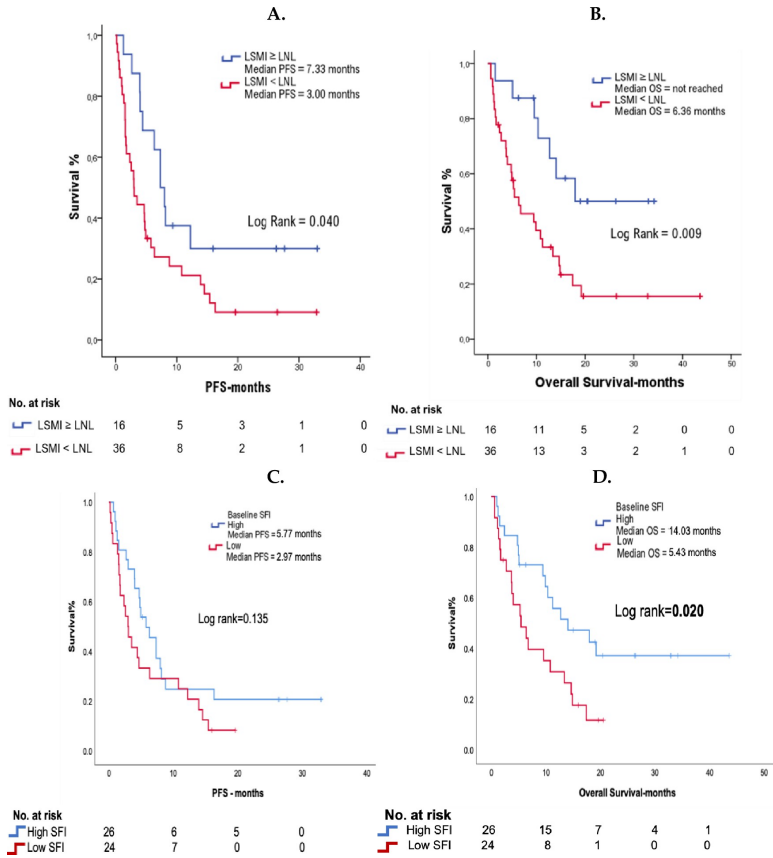


Figure 25: Kaplan-Meier curves demonstrating the effect of **A.** Baseline*¹ LSMI*² values on PFS **B.** Baseline LSMI values on OS **C.** Baseline SFI*³ values on PFS **D.** Baseline SFI values on OS. LSMI = Lumbar skeletal muscle index (At the level of 3rd lumbar vertebra); SFI = Subcutaneous Fat Index (At the level of 3rd lumbar vertebra); OS = Overall survival; PFS = Progression free survival.

*¹ Baseline: At the beginning of immunotherapy with PD-1/PD-L1 inhibitors.

*² LNL: Lower normal limit, 55 cm²/m² for males and 39 cm²/m² for females.

*³ High and low classification for SFI represents above and below gender specific median value, respectively.

	Median PFS (Months)	p value (log-rank test)	Median OS (Months)	p value (log-rank test)
All patients (n=52)				
Age				
< 70 years old	4.00	0.754	9.43	0.512
≥ 70 years old	7.33		13.37	
Gender				
Male	4.80	0.104	11.23	0.370
Female	1.53		6.77	
Performance Status				
0-1	4.80	0.360	12.70	0.140
2	3.50		5.27	
Histology				
Squamous	5.77	0.222	10.80	0.812
Non-squamous	2.57		9.90	
BMI				
< 25 kg/m²	1.77	0.196	3.77	0.175
25 kg/m² ≤ BMI < 30 kg/m²	6.30		10.30	
BMI ≥ 30 kg/m²	7.33		14.03	
Line of treatment of ICI administration				
1 st line	7.33	0.088	Not reached	0.005
2 nd or later lines	4.67		9.43	
Brain metastases				
Yes	1.57	0.006	4.80	0.083
No	4.93		12.70	
Bone metastases				
Yes	4.70	0.983	10.80	0.638
No	4.67		10.33	
Liver metastases				
Yes	1.53	0.120	3.77	0.059
No	4.80		12.70	
Baseline albumin levels				
< 3.5 g/dl	1.70	0.011	1.70	0.001
≥ 3.5 g/dl	4.80		11.23	
PD-L1 levels				
< 1%	2.57	0.786	5.27	0.290
≥ 1%	4.67		11.23	

	Median PFS (Months)	p value (log-rank test)	Median OS (Months)	p value (log-rank test)
Baseline LSMI				
< LNL	3.00	0.040	6.37	0.009
≥ LNL	7.33		Not reached	
Baseline IMFI				
Low	3.03	0.647	10.80	0.229
High	4.80		12.70	
Baseline VFI				
Low	3.03	0.975	6.37	0.231
High	4.93		11.23	
Baseline SFI				
Low	2.97	0.135	5.43	0.020
High	5.77		14.03	

Table 14: Log-rank test on the effect of the studied variables on PFS and OS. BMI=Body mass index, ICI=Immune check-point inhibitor, PD- L1=Programmed death ligand-1, LSMI=Lumbar skeletal muscle index (cm²/m²) (At the level of 3rd lumbar vertebra), LNL=Lower normal limits, 55 cm²/m² for males and 39 cm²/m² for females, IMFI=Intramuscular fat index (cm²/m²) (At the level of 3rd lumbar vertebra), Low: Below gender specific median value, VFI=Visceral fat index (cm²/m²) (At the level of 3rd lumbar vertebra), Low: Below gender specific median value, SFI=Subcutaneous fat index (cm²/m²) (At the level of 3rd lumbar vertebra), Low: Below gender specific median value

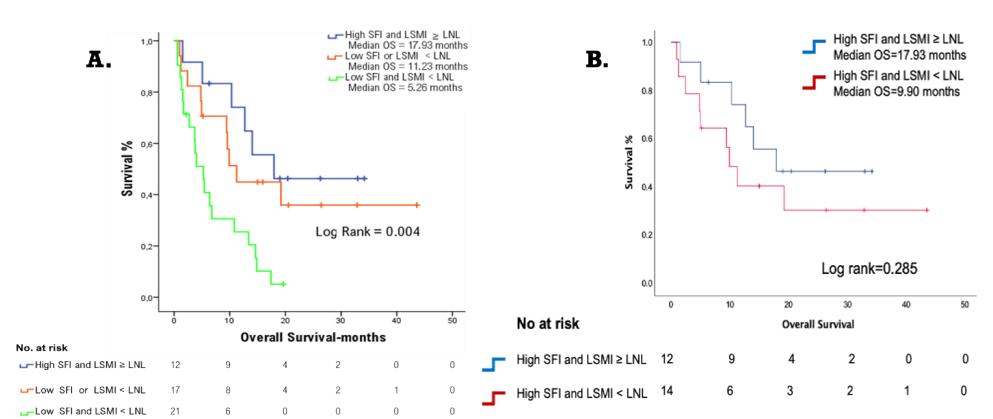


Figure 26: Log-rank test demonstrating the different survival outcomes of A. The patients in our cohort according to the combination of their baseline^{*1} SFI and LSMI values B. Between patients with high^{*2} SFI and LMSI ≥ LNL^{*3} and patients with high SFI and LMSI < LNL.

LSMI=Lumbar skeletal muscle index (cm²/m²) (At the level of 3rd lumbar vertebra), SFI=Subcutaneous fat index (cm²/m²) (At the level of 3rd lumbar vertebra), OS=Overall survival. ^{*1} Baseline: At the beginning of immunotherapy; ^{*2} Low: Below gender specific median value; High: Above gender specific median value; ^{*3} LNL: Lower normal limit, 55 cm²/m² for males and 39 cm²/m² for females

Cox Regression Analysis

In the Cox Regression Analysis, Intramuscular Fat Index (IMFI), Visceral Fat Index (VFI), Subcutaneous Fat Index (SFI), Lumbar Skeletal Muscle Index (LSMI), and Body Mass Index (BMI) considered as continuous nominal variables did not reveal any statistically significant associations with Progression-Free Survival (PFS) as outlined in Table 15. However, it was demonstrated that SFI values as continuous nominal variables in cm²/m² were positively correlated with improved survival at a statistically significant level, indicated by HR = 0.983 (95% CI: 0.970–0.987, p = 0.014) (Table 15 and figure 27). No other body composition indices, when treated as continuous variables, exhibited statistically significant associations with OS.

Among the analyzed parameters, only the presence of brain metastases, with HR = 2.71 (95% CI: 1.299–5.667, p = 0.008), and baseline LSMI below the lower normal limit (LNL), with HR = 2.03 (95% CI: 1.018–4.032, p = 0.044), were identified as predictors for an increased likelihood of experiencing disease progression (figure 28A and table 16). In the univariate analysis for OS, baseline LSMI below LNL demonstrated an HR of 2.90 (95% CI: 1.261–6.667, p = 0.012), while low SFI displayed an HR of 2.20 (1.114–4.333, p= 0.023), both predicting for inferior survival (figure 28B and table 16).

COX REGRESSION	PFS		OS	
UNIVARIATE ANALYSIS	HR (95% Confidence Intervals)	p value	HR (95% Confidence Intervals)	p value
BMI (kg/m ²)	0.973 (0.895–1.059)	0.528	0.936 (0.853–1.028)	0.165
LSMI (cm ² /m ²)	0.981 (0.950–1.013)	0.236	0.973 (0.941–1.006)	0.102
IMFI (cm ² /m ²)	0.996 (0.955–1.039)	0.866	0.950 (0.890–1.014)	0.121
VFI (cm ² /m ²)	0.998 (0.989–1.007)	0.646	0.991 (0.980–1.002)	0.095
SFI (cm ² /m ²)	0.993 (0.982–1.005)	0.246	0.983 (0.970–0.997)	0.014

Table 15: Univariate analysis using Cox regression method investigating the hazard ratios of the BMI*, IMFI, VFI and SFI as continuous nominal variables (cm²/m²) on PFS and OS. Gender was used as a stratification factor. BMI: Body mass index (kg/m²), LSMI: Lumbar skeletal muscle index (cm²/m²), IMFI = Intramuscular fat index (cm²/m²), VFI = Visceral fat index (cm²/m²), SFI = Subcutaneous fat index (cm²/m²); * BMI, IMFI, VFI and SFI were calculated at the beginning of immunotherapy

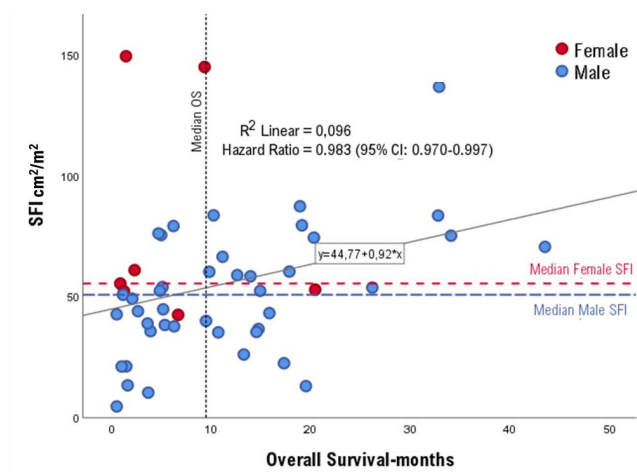


Figure 27: Scatter-plot demonstrating the overall survival values of the patients according to their baseline SFI. Univariate Cox Regression analysis for OS for SFI as continuous variable HR=0.983 (0.970-0.997), p=0.014. Gender was used as a stratification factor.

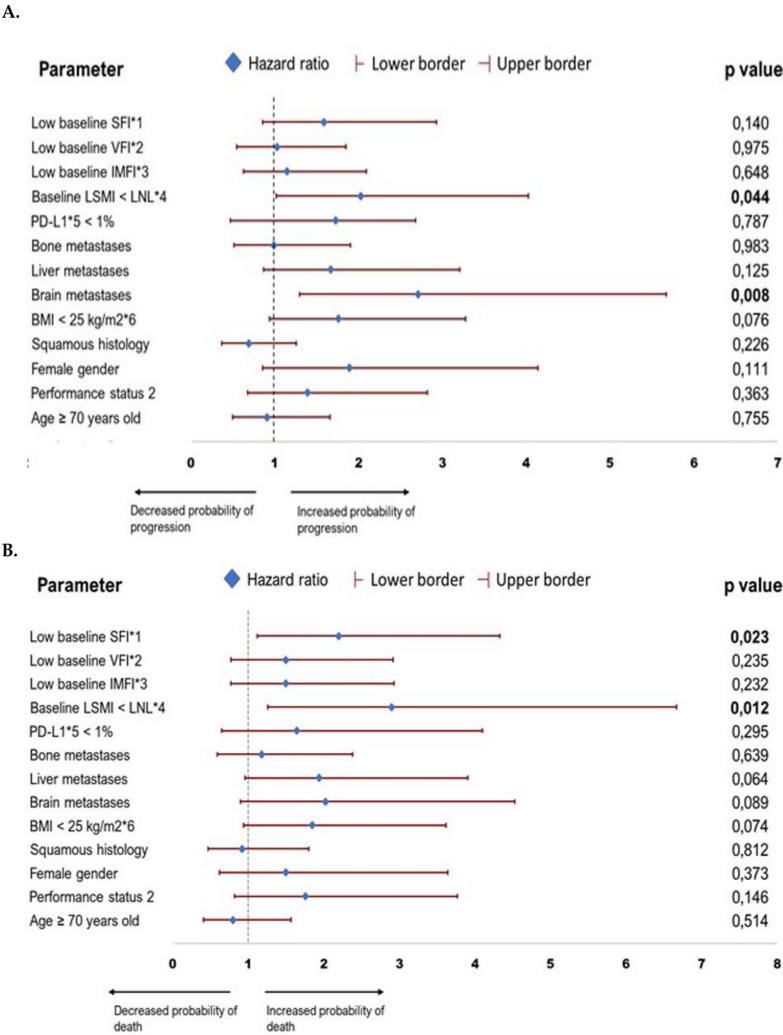


Figure 28: Forest plots demonstrating the hazard ratios and their 95% confidence intervals of the analyzed parameters on A. Probability of disease progression B. Probability of death under treatment with ICIs. BMI = Body mass index; PD-L1 = Programmed death ligand-1, ICI = Immune checkpoint inhibitor; LSMI: Lumbar skeletal muscle index (At the level of 3rd lumbar vertebra); LNL: Lower normal limit, 55 cm²/m² for males and 39 cm²/m² for females; IMFI = Intramuscular Fat Index (At the level of 3rd lumbar vertebra); VFI = Visceral Fat Index (At the level of 3rd lumbar vertebra); SFI = Subcutaneous Fat Index (At the level of 3rd lumbar vertebra). *1,2,3,4,5,6 SFI, VFI, IMFI, LSMI, PD-L1 and BMI values were calculated at the beginning of treatment with ICIs. *1,2,3 Low for SFI, VFI and IMFI means below gender specific median value.

COX REGRESSION	PFS		OS	
UNIVARIATE ANALYSIS	HR (95% Confidence Intervals)	p value	HR (95% Confidence Intervals)	p value
Age ≥ 70 years old	0.91 (0.496-1.663)	0.755	0.80 (0.407-1.568)	0.514
Performance status 2	1.39 (0.684-2.823)	0.363	1.76 (0.821-3.773)	0.146
Female gender	1.89 (0.864-4.141)	0.111	1.50 (0.616-3.636)	0.373
Squamous histology	0.69 (0.374-1.262)	0.226	0.92 (0.473-1.798)	0.812
BMI < 25 kg/m2	1.76 (0.942-3.282)	0.076	1.85 (0.942-3.618)	0.074
Brain metastases	2.71 (1.299-5.667)	0.008	2.02 (0.898-4.529)	0.089
Liver metastases	1.67 (0.868-3.213)	0.125	1.94 (0.962-3.905)	0.064
Bone metastases	0.99 (0.517-1.905)	0.983	1.18 (0.588-2.378)	0.639
PD-L1 < 1%	1.73 (0.474-2.677)	0.787	1.64 (0.652-4.081)	0.295
Baseline LSMI < LLN	2.03 (1.018-4.032)	0.044	2.90 (1.261-6.667)	0.012
Low baseline IMFI	1.15 (0.631-2.096)	0.648	1.50 (0.770-2.931)	0.232
Low baseline VFI	1.03 (0.551-1.848)	0.975	1.50 (0.769-2.919)	0.235
Low baseline SFI	1.59 (0.860-2.925)	0.140	2.20 (1.114-4.333)	0.023

Table 16: Univariate analysis using Cox regression method investigating the hazard ratios of the analyzed categorical covariates on PFS and OS. BMI=Body mass index, PD-L1=Programmed death ligand-1, LSMI=Lumbar skeletal muscle index (cm²/m²), LNL: 55 cm²/m² for males and 39 cm²/m² for females, IMFI=Intramuscular fat index (cm²/m²). Low: Below gender specific median value, VFI=Visceral fat index (cm²/m²). Low: Below gender specific median value, SFI=Subcutaneous fat index (cm²/m²). Low: Below gender specific median value

5. Discussion

The primary aim of this doctoral dissertation was to conduct a prospective investigation of clinical, laboratory and radiological data of individuals with metastatic NSCLC that were treated with PD-1/PD-L1 inhibitors in a single academic center, from 2017 until 2019, in order to identify specific parameters that can potentially affect patients' clinical outcomes. The results of our research, which were published in three scientific publications, demonstrated the prognostic importance of skeletal dissemination, the central role of microbiome on the orchestration of a robust immune response, the cardinal role of cancer cachexia as a negative predictive and prognostic indicator and provided clinical proof on the importance of adipose tissue composition as an immune system modulator. Finally, in this new age of artificial intelligence, we proved that easily obtainable patient and disease characteristics can be linked to treatment responses and integrated into a multifaceted model using machine learning for predicting individual clinical benefits from ICIs.

5.1 Disease characteristics and antibiotic usage as determinants of immunotherapy outcomes

More specifically, in the subgroup of patients in our cohort that received ICIs as 2nd line treatment after 1st line progression to platinum doublet, we observed that the presence of bone metastases was indicative of a poor prognosis for NSCLC. This finding is consistent with previous retrospective studies suggesting that the effectiveness of ICIs may be influenced by the specific sites of metastasis [176,177]. These findings could be potentially mechanistically explained by the demonstrated release of TGF- β in circulation, a known immune suppressive factor, as result of cancerous osseous dissemination [106]. Furthermore, our analysis revealed that patients with a lower body mass index (BMI) and low levels of albumin experienced shorter periods of progression-free survival (PFS) compared to those with higher BMI or normal albumin values, respectively. However, it is important to note that BMI and albumin levels, when considered independently, are insufficient for a comprehensive evaluation of patients' nutritional status, necessitating a more comprehensive analysis to fully understand the impact of body composition on treatment outcomes in cancer patients receiving immunotherapy which we further investigated in the second and third publication of this doctoral dissertation. It is also worth mentioning that performance status 2 did not emerge as an independent negative prognostic factor in our study, possibly due to the small sample size of our cohort and the limited number of patients with performance status 2, which increased the risk of statistical error type I. The same principle can apply why PD-L1 status did not emerge as an important prognostic or predictive factor in our cohort.

Our analysis indicated that the use of common co-medications had a significant impact on patient outcomes. To mitigate potential biases, particularly among patients experiencing prolonged clinical remissions, we established a 12-week timeframe from the initiation of ICIs to classify patients based on their use of steroids and antibiotics (ATBs). While categorizing ATB administration as a binary variable did not yield significant effects on PFS or OS, however, when analyzing the duration of ATB administration as a continuous nominal variable revealed a statistically significant negative association with both PFS and OS.

Notably, prolonged ATB administration independently predicted a reduced likelihood of disease stabilization, as well as inferior PFS and OS. These findings support existing evidence of a dose-dependent relationship between ATB exposure and reduced ICI efficacy, as also demonstrated by Tinsley et al [178]. Furthermore, the are in accordance with large scale retrospective and prospective data that have shown that ATB administration in ICI treated cancer afflicted individuals abates immunotherapy efficacy [179–181]. All these accumulated data delineate the central role of gut bacterial composition [182] for the development of a robust immune function and highlight caution with the administration of ATB in immunotherapy treated cancer patients.

Within our analysis, the use of steroids for supportive reasons independently correlated with shorter PFS in our patient cohort, although no significant associations with OS were discerned. Regrettably, due to the limited number of patients, we were unable to conduct a more detailed subgroup analysis regarding the specific reasons for the supportive use of steroids. Nonetheless, our findings echo prior reports that have raised concerns regarding the use of >10 mg prednisone equivalent in patients receiving ICIs [150,183,184]. Conversely, the administration of inhalational steroids or proton pump inhibitors (PPIs) did not exhibit detrimental effects on treatment outcomes within our analysis, suggesting their safe utilization. Interestingly, our results concerning PPIs contrast with retrospective analyses by Hopkins et al. [185] and a recent metanalysis of 33 studies [186], which indicated that PPIs adversely impacted survival outcomes in individuals with cancer treated with ICIs. Therefore, additional research is warranted to elucidate the effects of PPIs on the efficacy of ICIs in order to clarify if it consists an independent factor that leads to poor treatment outcomes.

Furthermore, we integrated all the recorded parameters into JADbio, an artificial intelligence (AI) system, to evaluate the interplay of these diverse features and assess the significance of each parameter in predicting individual treatment outcomes in an integrated manner. JADbio identified four clinical features and generated a signature that accurately predicted the likelihood of disease stabilization resulting from ICI treatment with an 81% accuracy rate. These four features encompassed prolonged ATB administration, the presence of bone metastases, liver metastases, and BMI < 25 kg/m². The elevated importance attributed to prolonged ATB administration underscores the critical role of microbiome composition in fostering an effective antitumor immune response. Intriguingly, these findings suggest that factors intrinsic to the biology of the primary tumor are linked not only to the specific patterns of metastatic spread but also to the response to ICIs.

Previous studies have utilized artificial intelligence (AI) to predict the outcomes of patients with a wide spectrum of malignancies undergoing treatment with immune checkpoint inhibitors (ICIs) either using as input radiomic [187,188] or even specific biochemical signatures [189]. Despite the relatively smaller size of our analyzed patient cohort, our investigation boasts several advantages. Notably, it encompasses a broader spectrum of routinely accessible and easily obtainable clinical parameters. Moreover, it affords the ability to quantify the significance of each parameter in shaping an individual's treatment response.

Utilizing the JADBio platform, we have developed an innovative multivariate model capable of predicting an individual's likelihood of achieving disease stabilization when undergoing second-line ICI treatment for metastatic NSCLC, demonstrating an impressive accuracy level of 81%. It is pertinent to highlight that alternative Automated Machine

Learning (AutoML) services might have yielded an inflated estimation of the final predictive performance. These services predominantly rely on cross-validation, a practice that can lead to overfitting when applied to sample-sample scenarios [190]. In contrast, JADBio is purpose-built for such scenarios and employs a technique to alleviate cross-validation bias, thereby furnishing a more conservative and dependable estimate of the ultimate predictive performance [169].

Our findings after machine learning analysis from JADBio underscore the potential utility of routinely accessible variables in distinguishing individuals who will attain disease control with ICIs from those likely to experience disease progression on treatment. For the latter group, we recommend closer monitoring, alternative treatment strategies, or participation in clinical trials. However, it's crucial to note that immunotherapy has now transitioned into the first-line treatment setting, either as monotherapy or in combination with chemotherapy, with only a minority of patients receiving ICIs in the second-line or subsequent settings so further research is warranted in this new clinical setting.

The strengths of our study lie in its prospective evaluation, which encompasses a wide array of common and easily obtainable clinical and laboratory parameters, along with the inclusion of common co-medications in a cohort of lung cancer patients undergoing immunotherapy. A significant novel aspect of our report lies in the additional multivariate analysis using an AutoML interface to ascertain the integrated feature importance of each parameter in shaping individual patient outcomes. Nevertheless, our study does have limitations, primarily stemming from its small sample size and the absence of PD-L1 levels in our model due to high rates of missing data. Furthermore, our results have yet to undergo validation in a separate patient cohort.

5.2 Cancer cachexia as predictive and prognostic factor in the immunotherapy era

In the second scientific report that resulted from the analysis of the prospectively gathered data from the cohort in the context of this doctoral dissertation, we demonstrated a significant association between cancer cachexia and diminished response rates to PD-1/ PD-L1 inhibitors, establishing it as an independent predictor for both reduced progression-free survival (PFS) and overall survival (OS). Additionally, we observed that individuals with lumbar skeletal muscle index (LSMI) values falling below the thresholds for sarcopenia experienced poorer survival outcomes. These results consist the clinical proof of our original hypothesis that the metabolic deregulation which leads to the cachexia phenotype is strongly associated with a diminished immune response.

However, the categorization of patients as cachectic or not poses a significant challenge, since the available criteria used of weight loss and sarcopenia represent merely a rough phenotypic imprint of an exceptionally complex phenomenon, possibly involving distinct pathogenetic mechanisms from patient to patient. In order to categorize patients within our cohort with cancer cachexia, we adopted the criteria established by Fearon et al [1] which remain to this day the most generally accepted classification and encompass radiological and clinical data. Their criteria specifically focus on cancer-related cachexia and incorporate assessments of pretreatment weight loss, body mass index (BMI), and body composition

analysis. After analyzing the data, the prevalence of cancer cachexia among the patients in our cohort was consistent with previously published reports [42,125,191].

In our data, the presence of cancer cachexia syndrome emerged as an independent factor of diminished responsiveness and survival in NSCLC patients under ICI treatment. The cachectic patients in our cohort demonstrated almost ninefold higher probability of disease progression as best response to ICIs in comparison to the non-cachectic one. In addition, they had more than twofold risk of death. Our findings align with previous retrospective studies that have explored the detrimental effects of weight loss and reduced muscle mass on immune-oncology treatment outcomes (table 17). Shiroyama et al. demonstrated in a retrospective cohort of metastatic NSCLC patients that sarcopenia, calculated by the psoas muscle index in CT scans, was associated with reduced response rates to PD-1 inhibitors and inferior PFS [192]. Moreover, retrospective cohorts by Miyawaki et al. [193] and Roch et al. [194] revealed that cachexia, defined as pretreatment weight loss exceeding 5% in the last 6 months, served as an independent predictor of adverse survival outcomes in metastatic NSCLC patients treated with ICIs. Finally, Chu et al. reported that skeletal muscle density holds predictive and prognostic value in melanoma patients in setting of CTLA-4 inhibition, as the patients in the analyzed cohort were treated with ipilimumab [195]. Notably, Turner et al. [196] conducted a pharmacokinetic analysis in patients with non-small cell lung cancer (NSCLC) and melanoma receiving pembrolizumab monotherapy. They reported an association between rapid baseline plasma clearance (C_{L0}) of pembrolizumab and poor OS, even in the absence of a direct association between plasma exposure and OS at pembrolizumab doses between 2 and 10 mg/kg. The researchers proposed that this substantial difference in OS could be attributed to an underlying increased catabolic status caused by cancer cachexia syndrome, providing indirect evidence that patients with elevated serum protein catabolism are refractory to ICIs.

Interestingly, the distributions of LSMI percent change during I-O treatment did not differ between responders and non-responders in our study. Moreover, LSMI reduction exceeding 5% was not significantly associated with diminished PFS or OS in our cohort. These findings contrast with the results reported by Roch et al. [194], who identified evolving sarcopenia (defined as a reduction in skeletal muscle index of more than 5% during I-O treatment) as linked to adverse survival outcomes. These discrepancies may be attributed to the relatively small sample size of 28 patients in our study and potential selection biases within this subgroup.

Our prospective data corroborate these earlier retrospective findings regarding the adverse effects of cachexia and reduced muscle composition on immunotherapy outcomes. Notably, we employed a comprehensive definition of cancer cachexia status, considering pretreatment weight loss, BMI, and skeletal muscle index, which distinguishes our approach from previous studies. This underscores the importance of considering cachexia as an additional classification factor in the design of future immunotherapy trials.

Experimental models have demonstrated that the molecular mechanisms underlying cachexia negatively impact a wide range of immune antitumor functions [42,44,191]. Additionally, inhibiting cytokine pathways implicated in cachexia development has shown potential to enhance antitumor immune responses [41,55,107,115,196]. Combined blockade of specific pro-cachexia mediators and the PD-1/PD-L1 axis has demonstrated synergistic effects. Thus, the co-administration of anti-cachexia treatments with immunotherapies may

be imperative to improve immunotherapy efficacy and patient outcomes in individuals with cancer cachexia. Nevertheless, in-depth research on the serum or tumor microenvironment of cachectic patients is essential to unravel the underlying processes contributing to higher rates of ICI treatment failure in this population.

To our knowledge, this is the first prospective study examining the influence of cancer cachexia on cancer immunotherapy treatment outcomes. Additionally, we applied the international consensus definition for the classification of cancer cachexia. Nevertheless, our study has limitations, including a relatively small sample size with limited statistical power, the inclusion of NSCLC patients receiving ICIs in different treatment lines, and the absence of translational and molecular data.

5.3 Subcutaneous adipose tissue density and sarcopenia as pivotal components in the orchestration of robust anti-tumor immune response

In the third and final publication of this doctoral dissertation we delved deeper on body tissue composition in order to investigate even further a potential link between the aforementioned parameters and immunotherapy outcomes in NSCLC patients. For the body composition analysis, we utilized radiological data from 52 patients of our cohort that had sufficient radiological data for the estimation of adipose tissue and skeletal muscle. In this prospective investigation, we demonstrated that diminished subcutaneous adiposity and skeletal muscle depletion may serve as potential adverse prognostic indicators for individuals with metastatic NSCLC undergoing treatment with ICIs. Interestingly, within our cohort, low SFI values, whether considered as a continuous or categorical variable, were significantly linked to poorer survival outcomes and responders to treatment exhibited higher SFI levels compared to non-responders. However, whether the link between high SFI and improved outcomes is causal or an epiphenomenon resulting from potential underlying cancer cachexia and subsequent browning of white adipose tissue and lipolysis remains unclear.

Large scale retrospective data that investigated the effect of BMI in the clinical outcomes of ICIs treated cancer afflicted individuals demonstrated a positive correlation between higher BMI values and improved survival outcomes [167]. In a similar manner, weight loss percentage in cancer patients has been a well-recognized adverse prognostic factor [141]. There have been translational studies that have tried to provide a mechanistic explanation for this obesity paradox. Degens et al [197] illustrated within a cohort comprising 106 individuals afflicted with non-small cell lung cancer (NSCLC) and subjected to nivolumab therapy, that a weight reduction exceeding 2% during the course of treatment was conspicuously associated with a substantial decrease in SFI and VFI. This phenomenon, characterized by a pronounced decline in body composition metrics, emerged as a pertinent adverse factor adversely influencing overall prognostic survival outcomes [197]. In a retrospective study involving clear cell renal carcinoma patients, obesity was associated with increased peritumoral adipose tissue inflammation and improved survival outcomes [198]. Another interesting retrospective analysis conducted by Martini et al., involving a diverse group of malignancies in phase I trials of immunotherapy, demonstrated that a high SFI/IMFI ratio independently predicted superior OS [165]. Conversely, Woodall et al. investigated

the impact of BMI and body composition on treatment outcomes in melanoma patients receiving ICIs and reported that a high index of total visceral and subcutaneous adipose tissue was associated with reduced PFS [199]. However, when examining the subcutaneous adipose tissue index alone, they found no association with reduced PFS or OS [199]. Our results align with those of Martini et al. [165], suggesting a potential positive correlation between increased subcutaneous adiposity and improved survival outcomes. Finally, Nishioka et al [200], in a retrospective analysis of clinical and radiological data of 74 patients with NSCLC treated with PD-1/PD-L1 inhibitors, reported that individuals with decreasing adiposity under immunotherapy without cachexia had a favorable outcome. What sets our findings apart is our demonstration of a potential link between baseline SFI values and clinical outcomes in a cohort characterized by a consistent underlying malignancy histology and the vast majority of the patients in our cohort received PD-1/PD-L1 inhibitors as monotherapy. The lack of association between BMI and immunotherapy outcomes in our study may be partly attributed to our relatively small sample size and a potential statistical type error I, as overweight/obese patients tended to have better outcomes, although this difference did not reach statistical significance. Discrepancies between our findings and those of Woodall et al. [199] can be explained by potential selection bias among patient populations, variations in underlying malignancies, and differences in the types of immunotherapies administered.

Nonetheless, our results, along with the majority of the aforementioned studies, suggest a connection between increased adiposity and enhanced antitumor immune responses that warrants further investigation. Although there is insufficient data to propose a robust biological link, subcutaneous adipose tissue is known to produce leptin. Wang et al. [168] demonstrated that leptin plays a role in PD-1 upregulation and immune aging in obese mice, acting as a counterbalance mechanism for the inflammatory status associated with obesity. This biological effect could potentially explain the increased sensitivity to PD-1 inhibition observed in obese individuals, as they rely on the PD-L1 axis as a feedback mechanism to maintain immune equilibrium in the face of underlying inflammation.

Furthermore, accumulating evidence suggests cellular pathways that connect adipose tissue composition to immune system regulation [201]. Adipose tissue serves as a reservoir for a wide spectrum of immune cells which participate both in innate and adaptive immunity [202]. Obese mice's adipose tissue showed increased numbers of effector T cells and a higher CD8+/CD4+ ratio, along with reduced Treg numbers [203]. In lean mice, Tregs act as negative regulators of inflammation in adipose tissue, but their numbers are greatly reduced in the adipose tissue of obese mice [204]. In obese mice, infiltration of macrophages into adipose tissue has been reported to shift them from an M2 anti-inflammatory phenotype to an M1 proinflammatory phenotype, a phenomenon not observed in non-obese mice [205,206]. Based on these experimental data, it is conceivable that obese individuals may be more susceptible to checkpoint inhibition when dealing with underlying malignancies, owing to an underlying pro-inflammatory state characterized by heightened Th1 responses, macrophage polarization toward an M1 phenotype, and reduced Treg numbers in their adipose tissue reservoirs. However, this hypothesis necessitates further investigation through additional preclinical and translational research.

Furthermore, LSMI levels consistent with sarcopenia were identified as an adverse prognostic factor within our cohort. Sarcopenia had previously been linked to unfavorable

outcomes in cancer patients across numerous studies before the introduction of ICIs [192,207]. Additionally, sarcopenia is one of the criteria used to define cancer cachexia, a widely recognized adverse prognostic factor in cancer patients [1]. Our findings align with previous studies on the role of skeletal muscle depletion as a negative prognostic and predictive factor in ICI-treated cancer patients.

In addition, we conducted a subgroup analysis to examine the survival outcomes of patients with both low adiposity and muscle depletion compared to patients with high adiposity but muscle depletion and individuals without muscle depletion but high adiposity. Patients with both low SFI and sarcopenia exhibited the poorest outcomes, whereas the other two subgroups did not exhibit significant differences. Woodall et al. [199] reported that patients with high adiposity and reduced muscle mass experienced worse outcomes. However, this discrepancy may be attributed to the small sample size in our cohort, potentially limiting the ability to establish statistically significant correlations. Nonetheless, further research is needed to redefine the prognostic significance of sarcopenic obesity in the era of immunotherapy.

To our knowledge, this study represents the first analysis of prospective data focusing on NSCLC patients treated with ICIs, investigating the influence of fat and muscle tissue composition on treatment outcomes. Our study encompasses a population with a degree of homogeneity, as the vast majority of NSCLC patients received immunotherapy as monotherapy with PD-1/PDL-1 inhibitors, and most were administered as second-line treatment.

However, the primary limitation of our study is the relatively small sample size, which limits statistical power. Due to the small sample size, we grouped patients treated with ICIs in both first and second-line settings, and we also included two patients treated with a chemotherapy-ICI combination; we believe this number is too small to significantly impact the results. Furthermore, due to the low number of events in the subgroup of patients with LSMI values inconsistent with sarcopenia, we were unable to perform a multivariate analysis for overall survival. Most patients in our statistical sample received second-line PD-1/PDL-1 inhibitors, but a significant portion received them as first-line treatment. Additionally, our cohort had a gender imbalance, with the majority of patients being male and only a small proportion being female. Fat tissue compositions can significantly differ between genders, and an imbalanced population can hinder the establishment of statistically significant associations. Moreover, age, a significant factor affecting body composition, was represented across all age groups in our study. Conducting a power calculation was not feasible primarily due to the exploratory nature of this study, and secondarily due to the absence of prior publications examining the effect of adipose tissue composition in ICI-treated NSCLC patients that could serve as a basis for an initial power calculation. Finally, a specified cut-off point for IMFI, VFI, and SFI was not available, so we arbitrarily selected the gender-specific median value for each respective variable as the cut-off point.

Clinical study	Study design	Number (n) of patients	Malignancy setting	Treatment	Primary study point	Results
Turner et al [196]	Retrospective	n=1453	Metastatic melanoma and NSCLC	pembrolizumab	Relationship between pembrolizumab pharmacokinetics and overall survival	Higher pembrolizumab clearance (CL0) was an adverse prognostic factor for OS and it paralleled disease parameters associated with CCS (multivariate-adjusted CL0 HR = 1.64; 95% CI, 1.06-2.52 for melanoma and HR = 1.88; 95% CI, 1.22-2.89 for NSCLC)
Kichenadasse et al [167]	Retrospective	N=2110	Metastatic NSCLC	atezolizumab	Association of baseline BMI (at the beginning of immunotherapy) with treatment outcomes and adverse events	A linear association between increasing values of BMI and overall survival was observed.
Martini et al [165]	Retrospective	N=90	Cancer patients that were treated with immunotherapy in the context of phase I clinical trials in a single center	Immunotherapy based treatments	Association of BMI, subcutaneous fat index (SFI), intermuscular fat index (IFI), and visceral fat index (VFI) with survival outcome.	Patients with an SFI ≥ 73 had a significantly longer OS (hazard ratio, 0.20; 95% CI, 0.09-0.46 [$P < .001$]) and PFS (hazard ratio, 0.38; 95% CI, 0.20-0.72 [$P = 0.003$]) compared with patients with an SFI < 73 and IFI < 3.4 and those with an SFI < 73 and IFI ≥ 3.4
Shiroyama et al [192]	Retrospective	N=42	Previously treated metastatic NSCLC patients	nivolumab, pembrolizumab	Association of sarcopenia (calculated by measuring the cross- sectional area of the psoas muscle at the caudal end of the 3 rd lumbar vertebrae) with treatment outcomes	Sarcopenia negatively affected PFS (median, 2.1 vs. 6.8 months, $p = 0.004$) and response rates (40.0% vs. 9.1%, $p = 0.025$)
Roch et al [194]	Retrospective	N=142	Metastatic NSCLC	PD1/PDL1 inhibitors	Effect of cachexia (defined as 5% loss of body within the last 6 months) or the effect of evolving sarcopenia (defined as 5% reduction in skeletal muscle index during treatment) on patient outcomes	Cachexia negatively affected disease control rates (59.9% vs 41.1 %, odds ratio: 2.60 (95% CI: 1.03-6.58) and OS HR: 6.26 (95% CI: 2.23- 17.57). Evolving sarcopenia was an adverse predictor for shorter PFS, HR: 2.45 (95% CI: 1.09-5.53) and OS, HR: 3.87 (95% CI: 1.60-9.34)
Rounis et al [174]	Prospective	N=55	Metastatic NSCLC	PD1/PDL1	Association of cachexia (defined as weight loss 5% during the last 6 months since the initiation of immunotherapy or any degree of weight loss $\geq 2\%$ and a BMI $< 20 \text{ kg/m}^2$) with treatment outcomes	Preliminary analysis demonstrated that the presence of cachexia was an independent predictor of disease progression as best response to immunotherapy OR:8.11 [(95% CI: 2.95- 22.94), $P < 0.001$] and that cachexia constituted an independent predictor for inferior OS, HR: 2.52 [(95% CI: 1.40-4.55), $P = 0.002$]

Table 17: Summary of the representative clinical studies that examine the effect of cachexia and body composition on treatment outcomes in cancer patients treated with immunotherapy.

6. Conclusions

The culmination of research within the scope of this doctoral dissertation addressed our initial research hypotheses and unveiled significant findings that have the potential to inaugurate novel and intriguing avenues of investigation.

The examination of readily accessible clinical data within the context of this doctoral thesis revealed that in patients undergoing monotherapy with PD-1/PD-L1 pathway inhibitors, the presence of secondary osteogenic lesions and prolonged antibiotic administration emerged as independent factors associated with diminished survival rates. Consequently, individuals with osseous metastases should likely undergo more frequent radiological evaluations, as the efficacy of immunotherapy remains questionable, and they should be considered for inclusion in clinical trials due to their unfavorable prognosis. Furthermore, these findings underscore the central role of the microbiome in orchestrating the immune response against tumors, and the composition of the microbial ecosystem residing within our gastrointestinal system could potentially represent a future pharmacological target to enhance the effectiveness of existing ICIs. Lastly, in a world gradually recognizing the transformative potential of artificial intelligence to revolutionize human daily life in ways *hitherto* unimaginable, the data analysis performed using the JADBio artificial intelligence platform, leading to the development of a predictive model with an approximately 80% disease stabilization probability, serves as a proof of concept that further patient data analysis may lead to the identification of pioneering biomarkers and could potentially reshape everyday medical practice.

Furthermore, in our endeavor to explore the impact of the exceedingly intricate phenomenon, in terms of pathogenesis and pathophysiology, of metabolic dysregulation arising as a consequence of neoplasms, we have delineated that its phenotypic manifestation, commonly referred to as cancer cachexia syndrome as per existing definitions, constitutes an independent adverse predictive and prognostic factor. This aforementioned syndrome, which had previously been recognized as a negative prognostic factor in earlier clinical data, now assumes a central role in the contemporary era of immunotherapy. The investigation into cachexia could take an intriguing turn, as further molecular- level research in cachectic patients could potentially pave the way for the development of novel therapies capable of serving a dual role as enhancers of the immune response and inhibitors of metabolic dysregulation.

Finally, in our most recent publication, we have elucidated an intriguing positive correlation between the composition of subcutaneous adipose tissue and the clinical outcomes of patients with NSCLC treated with ICIs. These findings warrant validation in larger-scale studies and necessitate clarification as to whether reduced subcutaneous fat density is an independent factor negatively impacting the immune response or simply a manifestation of an underlying metabolic dysregulation leading to lipolysis and the browning of white adipose tissue. Further exploration at the preclinical and translational levels is necessary to deepen our understanding of this association, potentially uncovering new drug targets and biomarkers.

7. References

1. Fearon K, Strasser F, Anker SD, Bosaeus I, Bruera E, Fainsinger RL, et al. Definition and classification of cancer cachexia: an international consensus. *Lancet Oncol*. 2011 May;12(5):489–95.
2. Sung H, Ferlay J, Siegel RL, Laversanne M, Soerjomataram I, Jemal A, et al. Global Cancer Statistics 2020: GLOBOCAN Estimates of Incidence and Mortality Worldwide for 36 Cancers in 185 Countries. *CA Cancer J Clin*. 2021 May;71(3):209–49.
3. SEER [Internet]. [cited 2023 Aug 15]. SEER Cancer Statistics Review, 1975–2016. Available from: https://seer.cancer.gov/csr/1975_2016/index.html
4. Tang M, Abbas HA, Negrao MV, Ramineni M, Hu X, Hubert SM, et al. The histologic phenotype of lung cancers is associated with transcriptomic features rather than genomic characteristics. *Nat Commun*. 2021 Dec 6;12(1):7081.
5. Barlesi F, Mazieres J, Merlio JP, Debieuvre D, Mosser J, Lena H, et al. Routine molecular profiling of patients with advanced non-small-cell lung cancer: results of a 1-year nationwide programme of the French Cooperative Thoracic Intergroup (IFCT). *Lancet*. 2016 Apr 2;387(10026):1415–26.
6. Sutani A, Nagai Y, Udagawa K, Uchida Y, Koyama N, Murayama Y, et al. Gefitinib for non-small-cell lung cancer patients with epidermal growth factor receptor gene mutations screened by peptide nucleic acid-locked nucleic acid PCR clamp. *Br J Cancer*. 2006 Dec 4;95(11):1483–9.
7. Shaw AT, Ou SHI, Bang YJ, Camidge DR, Solomon BJ, Salgia R, et al. Crizotinib in ROS1- rearranged non-small-cell lung cancer. *N Engl J Med*. 2014 Nov 20;371(21):1963–71.
8. Solomon BJ, Mok T, Kim DW, Wu YL, Nakagawa K, Mekhail T, et al. First-line crizotinib versus chemotherapy in ALK-positive lung cancer. *N Engl J Med*. 2014 Dec 4;371(23):2167–77.
9. Hajdu SI. Pathfinders in oncology from ancient times to the end of the Middle Ages. *Cancer*. 2016;122(11):1638–46.
10. Coley WB. II. Contribution to the Knowledge of Sarcoma. *Ann Surg*. 1891 Sep;14(3):199–220.
11. Rosenberg SA, Packard BS, Aebersold PM, Solomon D, Topalian SL, Toy ST, et al. Use of tumor-infiltrating lymphocytes and interleukin-2 in the immunotherapy of patients with metastatic melanoma. A preliminary report. *N Engl J Med*. 1988 Dec 22;319(25):1676–80.
12. Dunn GP, Bruce AT, Ikeda H, Old LJ, Schreiber RD. Cancer immunoediting: from immunosurveillance to tumor escape. *Nat Immunol*. 2002 Nov;3(11):991–8.
13. Hanahan D, Weinberg RA. Hallmarks of cancer: the next generation. *Cell*. 2011 Mar 4;144(5):646–74.
14. Waterhouse P, Penninger JM, Timms E, Wakeham A, Shahinian A, Lee KP, et al. Lymphoproliferative disorders with early lethality in mice deficient in Ctlα-4. *Science*. 1995 Nov 10;270(5238):985–8.
15. Tivol EA, Borriello F, Schweitzer AN, Lynch WP, Bluestone JA, Sharpe AH. Loss of CTLA-4 leads to massive lymphoproliferation and fatal multiorgan tissue destruction, revealing a critical negative regulatory role of CTLA-4. *Immunity*. 1995 Nov;3(5):541–7.
16. Ishida Y, Agata Y, Shibahara K, Honjo T. Induced expression of PD-1, a novel member of the immunoglobulin gene superfamily, upon programmed cell death. *EMBO J*. 1992 Nov;11(11):3887–95.
17. Ribas A. Releasing the Brakes on Cancer Immunotherapy. *N Engl J Med*. 2015 Oct 15;373(16):1490–2.
18. Yoshida T, Jiang F, Honjo T, Okazaki T. PD-1 deficiency reveals various tissue-specific autoimmunity by H-2b and dose-dependent requirement of H-2g7 for diabetes in NOD mice. *Proc Natl Acad Sci U S A*. 2008 Mar 4;105(9):3533–8.
19. Malissen B, Grégoire C, Malissen M, Roncagalli R. Integrative biology of T cell activation. *Nat Immunol*. 2014 Sep;15(9):790–7.
20. Alegre ML, Frauwirth KA, Thompson CB. T-cell regulation by CD28 and CTLA-4. *Nat Rev Immunol*. 2001 Dec;1(3):220–8.
21. Corse E, Allison JP. Cutting edge: CTLA-4 on effector T cells inhibits in trans. *J Immunol*. 2012 Aug 1;189(3):1123–7.
22. Qureshi OS, Zheng Y, Nakamura K, Attridge K, Manzotti C, Schmidt EM, et al. Trans- endocytosis of CD80 and CD86: a molecular basis for the cell-extrinsic function of CTLA-4. *Science*. 2011 Apr 29;332(6029):600–3.

23. Francisco LM, Sage PT, Sharpe AH. The PD-1 pathway in tolerance and autoimmunity. *Immunol Rev*. 2010 Jul;236:219–42.
24. Okazaki T, Honjo T. PD-1 and PD-1 ligands: from discovery to clinical application. *Int Immunol*. 2007 Jul;19(7):813–24.
25. Bousiotis VA. Molecular and Biochemical Aspects of the PD-1 Checkpoint Pathway. *N Engl J Med*. 2016 Nov 3;375(18):1767–78.
26. Grosso JF, Jure-Kunkel MN. CTLA-4 blockade in tumor models: an overview of preclinical and translational research. *Cancer Immun*. 2013;13:5.
27. Pardoll DM. The blockade of immune checkpoints in cancer immunotherapy. *Nat Rev Cancer*. 2012 Apr;12(4):252–64.
28. Weber JS, O'Day S, Urban W, Powderly J, Nichol G, Yellin M, et al. Phase I/II study of ipilimumab for patients with metastatic melanoma. *J Clin Oncol*. 2008 Dec 20;26(36):5950–6.
29. Patnaik A, Kang SP, Rasco D, Papadopoulos KP, Ellassaiss-Schaap J, Beeram M, et al. Phase I Study of Pembrolizumab (MK-3475; Anti-PD-1 Monoclonal Antibody) in Patients with Advanced Solid Tumors. *Clin Cancer Res*. 2015 Oct 1;21(19):4286–93.
30. Atkins MB, Lotze MT, Dutcher JP, Fisher RI, Weiss G, Margolin K, et al. High-dose recombinant interleukin 2 therapy for patients with metastatic melanoma: analysis of 270 patients treated between 1985 and 1993. *J Clin Oncol*. 1999 Jul;17(7):2105–16.
31. Betof Warner A, Corrie PG, Hamid O. Tumor-Infiltrating Lymphocyte Therapy in Melanoma: Facts to the Future. *Clin Cancer Res*. 2023 May 15;29(10):1835–54.
32. Hodi FS, O'Day SJ, McDermott DF, Weber RW, Sosman JA, Haanen JB, et al. Improved survival with ipilimumab in patients with metastatic melanoma. *N Engl J Med*. 2010 Aug 19;363(8):711–23.
33. Brahmer J, Reckamp KL, Baas P, Crinò L, Eberhardt WEE, Poddubska E, et al. Nivolumab versus Docetaxel in Advanced Squamous-Cell Non-Small-Cell Lung Cancer. *N Engl J Med*. 2015 Jul 9;373(2):123–35.
34. Borghaei H, Paz-Ares L, Horn L, Spigel DR, Steins M, Ready NE, et al. Nivolumab versus Docetaxel in Advanced Nonsquamous Non-Small-Cell Lung Cancer. *N Engl J Med*. 2015 Oct 22;373(17):1627–39.
35. Herbst RS, Baas P, Kim DW, Felip E, Pérez-Gracia JL, Han JY, et al. Pembrolizumab versus docetaxel for previously treated, PD-L1-positive, advanced non-small-cell lung cancer (KEYNOTE-010): a randomised controlled trial. *Lancet*. 2016 Apr 9;387(10027):1540–50.
36. Garon EB, Rizvi NA, Hui R, Leighl N, Balmanoukian AS, Eder JP, et al. Pembrolizumab for the treatment of non-small-cell lung cancer. *N Engl J Med*. 2015 May 21;372(21):2018–28.
37. Rittmeyer A, Barlesi F, Waterkamp D, Park K, Ciardiello F, von Pawel J, et al. Atezolizumab versus docetaxel in patients with previously treated non-small-cell lung cancer (OAK): a phase 3, open-label, multicentre randomised controlled trial. *Lancet*. 2017 Jan 21;389(10066):255–65.
38. Reck M, Rodríguez-Abreu D, Robinson AG, Hui R, Csőszi T, Fülöp A, et al. Pembrolizumab versus Chemotherapy for PD-L1-Positive Non-Small-Cell Lung Cancer. *N Engl J Med*. 2016 Nov 10;375(19):1823–33.
39. Antonia SJ, Villegas A, Daniel D, Vicente D, Murakami S, Hui R, et al. Durvalumab after Chemoradiotherapy in Stage III Non-Small-Cell Lung Cancer. *N Engl J Med*. 2017 Nov 16;377(20):1919–29.
40. Wolchok JD, Kluger H, Callahan MK, Postow MA, Rizvi NA, Lesokhin AM, et al. Nivolumab plus ipilimumab in advanced melanoma. *N Engl J Med*. 2013 Jul 11;369(2):122–33.
41. Tinoco R, Carrette F, Barraza ML, Otero DC, Magaña J, Rosenberg MW, et al. PSGL-1 Is an Immune Checkpoint Regulator that Promotes T Cell Exhaustion. *Immunity*. 2016 May 17;44(5):1190–203.
42. Baracos VE, Martin L, Korc M, Guttridge DC, Fearon KCH. Cancer-associated cachexia. *Nat Rev Dis Primers*. 2018 Jan 18;4:17105.
43. Shachar SS, Williams GR, Muss HB, Nishijima TF. Prognostic value of sarcopenia in adults with solid tumours: A meta-analysis and systematic review. *Eur J Cancer*. 2016 Apr;57:58–67.
44. Fearon KCH, Glass DJ, Guttridge DC. Cancer cachexia: mediators, signaling, and metabolic pathways. *Cell Metab*. 2012 Aug 8;16(2):153–66.

45. de Matos-Neto EM, Lima JDCC, de Pereira WO, Figuerêdo RG, Riccardi DMDR, Radloff K, et al. Systemic Inflammation in Cachexia - Is Tumor Cytokine Expression Profile the Culprit? *Front Immunol.* 2015;6:629.
46. Kir S, Spiegelman BM. CACHEXIA & BROWN FAT: A BURNING ISSUE IN CANCER. *Trends Cancer.* 2016 Sep;2(9):461–3.
47. Kir S, White JP, Kleiner S, Kazak L, Cohen P, Baracos VE, et al. Tumour-derived PTH- related protein triggers adipose tissue browning and cancer cachexia. *Nature.* 2014 Sep 4;513(7516):100–4.
48. Petruzzelli M, Schweiger M, Schreiber R, Campos-Olivas R, Tsoli M, Allen J, et al. A switch from white to brown fat increases energy expenditure in cancer-associated cachexia. *Cell Metab.* 2014 Sep 2;20(3):433–47.
49. Kershaw EE, Flier JS. Adipose tissue as an endocrine organ. *J Clin Endocrinol Metab.* 2004 Jun;89(6):2548–56.
50. Spoto B, Di Betta E, Mattace-Raso F, Sijbrands E, Vilardi A, Parlongo RM, et al. Pro- and anti-inflammatory cytokine gene expression in subcutaneous and visceral fat in severe obesity. *Nutr Metab Cardiovasc Dis.* 2014 Oct;24(10):1137–43.
51. Mauland KK, Eng Ø, Ytre-Hauge S, Tangen IL, Berg A, Salvesen HB, et al. High visceral fat percentage is associated with poor outcome in endometrial cancer. *Oncotarget.* 2017 Dec 1;8(62):105184–95.
52. Antoun S, Bayar A, Ileana E, Laplanche A, Fizazi K, di Palma M, et al. High subcutaneous adipose tissue predicts the prognosis in metastatic castration-resistant prostate cancer patients in post chemotherapy setting. *Eur J Cancer.* 2015 Nov;51(17):2570–7.
53. Ebadi M, Martin L, Ghosh S, Field CJ, Lehner R, Baracos VE, et al. Subcutaneous adiposity is an independent predictor of mortality in cancer patients. *Br J Cancer.* 2017 Jun 27;117(1):148–55.
54. Peyta L, Jarnouen K, Pinault M, Coulouarn C, Guimaraes C, Goupille C, et al. Regulation of hepatic cardioplipin metabolism by TNF α : Implication in cancer cachexia. *Biochim Biophys Acta.* 2015 Nov;1851(11):1490–500.
55. Bertrand F, Montfort A, Marcheteau E, Imbert C, Gilhodes J, Filleron T, et al. TNF α blockade overcomes resistance to anti-PD-1 in experimental melanoma. *Nat Commun.* 2017 Dec 22;8(1):2256.
56. Jatoti A, Dakhil SR, Nguyen PL, Sloan JA, Kugler JW, Rowland KM, et al. A placebo- controlled double blind trial of etanercept for the cancer anorexia/weight loss syndrome: results from N00C1 from the North Central Cancer Treatment Group. *Cancer.* 2007 Sep 15;110(6):1396–403.
57. Costelli P, Llovera M, Carbó N, García-Martínez C, López-Soriano FJ, Argilés JM. Interleukin-1 receptor antagonist (IL-1ra) is unable to reverse cachexia in rats bearing an ascites hepatoma (Yoshida AH-130). *Cancer Lett.* 1995 Aug 16;95(1–2):33–8.
58. Elkabets M, Ribeiro VSG, Dinarello CA, Ostrand-Rosenberg S, Di Santo JP, Apte RN, et al. IL-1 β regulates a novel myeloid-derived suppressor cell subset that impairs NK cell development and function. *Eur J Immunol.* 2010 Dec;40(12):3347–57.
59. Flint TR, Janowitz T, Connell CM, Roberts EW, Denton AE, Coll AP, et al. Tumor-Induced IL-6 Reprograms Host Metabolism to Suppress Anti-tumor Immunity. *Cell Metab.* 2016 Nov 8;24(5):672–84.
60. Jin L, Tao H, Karachi A, Long Y, Hou AY, Na M, et al. CXCR1- or CXCR2-modified CAR T cells co-opt IL-8 for maximal antitumor efficacy in solid tumors. *Nat Commun.* 2019 Sep 5;10(1):4016.
61. Coupland LA, Chong BH, Parish CR. Platelets and P-Selectin Control Tumor Cell Metastasis in an Organ-Specific Manner and Independently of NK Cells. *Cancer Res.* 2012 Sep 15;72(18):4662–71.
62. Diehl S, Anguita J, Hoffmeyer A, Zapton T, Ihle JN, Fikrig E, et al. Inhibition of Th1 differentiation by IL-6 is mediated by SOCS1. *Immunity.* 2000 Dec;13(6):805–15.
63. Scheede-Bergdahl C, Watt HL, Trutschnigg B, Kilgour RD, Haggarty A, Lucar E, et al. Is IL- 6 the best pro-inflammatory biomarker of clinical outcomes of cancer cachexia? *Clin Nutr.* 2012 Feb;31(1):85–8.
64. Koh J, Hur JY, Lee KY, Kim MS, Heo JY, Ku BM, et al. Regulatory (FoxP3+) T cells and TGF- β predict the response to anti-PD-1 immunotherapy in patients with non-small cell lung cancer. *Sci Rep.* 2020 Nov 4;10(1):18994.

65. Maecker H, Varfolomeev E, Kischkel F, Lawrence D, LeBlanc H, Lee W, et al. TWEAK attenuates the transition from innate to adaptive immunity. *Cell*. 2005 Dec 2;123(5):931–44.
66. Ye S, Fox MI, Belmar NA, Sho M, Chao DT, Choi D, et al. Enavatuzumab, a Humanized Anti-TWEAK Receptor Monoclonal Antibody, Exerts Antitumor Activity through Attracting and Activating Innate Immune Effector Cells. *J Immunol Res*. 2017;2017:5737159.
67. Padrão AI, Moreira-Gonçalves D, Oliveira PA, Teixeira C, Faustino-Rocha AI, Helguero L, et al. Endurance training prevents TWEAK but not myostatin-mediated cardiac remodelling in cancer cachexia. *Arch Biochem Biophys*. 2015 Feb 1;567:13–21.
68. Rosenfeldt MT, Ryan KM. The multiple roles of autophagy in cancer. *Carcinogenesis*. 2011 Jul;32(7):955–63.
69. Wei J, Long L, Yang K, Guy C, Shrestha S, Chen Z, et al. Autophagy enforces functional integrity of regulatory T cells by coupling environmental cues and metabolic homeostasis. *Nat Immunol*. 2016 Mar;17(3):277–85.
70. Gabrilovich DI, Ostrand-Rosenberg S, Bronte V. Coordinated regulation of myeloid cells by tumours. *Nat Rev Immunol*. 2012 Mar 22;12(4):253–68.
71. Cuenca AG, Cuenca AL, Winfield RD, Joiner DN, Gentile L, Delano MJ, et al. Novel role for tumor-induced expansion of myeloid-derived cells in cancer cachexia. *J Immunol*. 2014 Jun 15;192(12):6111–9.
72. Tjomsland V, Spånges A, Väilä J, Sandström P, Borch K, Druid H, et al. Interleukin 1 α sustains the expression of inflammatory factors in human pancreatic cancer microenvironment by targeting cancer-associated fibroblasts. *Neoplasia*. 2011 Aug;13(8):664–75.
73. Chen DS, Mellman I. Oncology meets immunology: the cancer-immunity cycle. *Immunity*. 2013 Jul 25;39(1):1–10.
74. Tracey KJ, Lowry SF, Cerami A. Cachectin: a hormone that triggers acute shock and chronic cachexia. *J Infect Dis*. 1988 Mar;157(3):413–20.
75. Siddiqui JA, Pothuraju R, Jain M, Batra SK, Nasser MW. Advances in cancer cachexia: Intersection between affected organs, mediators, and pharmacological interventions. *Biochim Biophys Acta Rev Cancer*. 2020 Apr;1873(2):188359.
76. Sherry BA, Gelin J, Fong Y, Marano M, Wei H, Cerami A, et al. Anticachectin/tumor necrosis factor- α antibodies attenuate development of cachexia in tumor models. *FASEB J*. 1989 Jun;3(8):1956–62.
77. Braun TP, Zhu X, Szumowski M, Scott GD, Grossberg AJ, Levasseur PR, et al. Central nervous system inflammation induces muscle atrophy via activation of the hypothalamic-pituitary-adrenal axis. *J Exp Med*. 2011 Nov 21;208(12):2449–63.
78. Karayiannakis AJ, Syrigos KN, Polychronidis A, Pitiakoudis M, Bounovas A, Simopoulos K. Serum levels of tumor necrosis factor- α and nutritional status in pancreatic cancer patients. *Anticancer Res*. 2001;21(2B):1355–8.
79. Maltoni M, Fabbri L, Nanni O, Scarpi E, Pezzi L, Flamini E, et al. Serum levels of tumour necrosis factor α and other cytokines do not correlate with weight loss and anorexia in cancer patients. *Support Care Cancer*. 1997 Mar;5(2):130–5.
80. Wiedenmann B, Malfertheiner P, Friess H, Ritch P, Arseneau J, Mantovani G, et al. A multicenter, phase II study of infliximab plus gemcitabine in pancreatic cancer cachexia. *J Support Oncol*. 2008 Jan;6(1):18–25.
81. Weber JS, Hodi FS, Wolchok JD, Topalian SL, Schadendorf D, Larkin J, et al. Safety Profile of Nivolumab Monotherapy: A Pooled Analysis of Patients With Advanced Melanoma. *J Clin Oncol*. 2017 Mar;35(7):785–92.
82. Johnston AJ, Murphy KT, Jenkinson L, Laine D, Emmrich K, Faou P, et al. Targeting of Fn14 Prevents Cancer-Induced Cachexia and Prolongs Survival. *Cell*. 2015 Sep 10;162(6):1365–78.
83. Lassen UN, Meulendijks D, Siu LL, Karanikas V, Mau-Sorensen M, Schellens JHM, et al. A phase I monotherapy study of RG7212, a first-in-class monoclonal antibody targeting TWEAK signaling in patients with advanced cancers. *Clin Cancer Res*. 2015 Jan 15;21(2):258–66.
84. McDonald JJ, McMillan DC, Laird BJA. Targeting IL-1 α in cancer cachexia: a narrative review. *Curr Opin Support Palliat Care*. 2018 Dec;12(4):453–9.

85. Oh K, Lee OY, Park Y, Seo MW, Lee DS. IL-1 β induces IL-6 production and increases invasiveness and estrogen-independent growth in a TG2-dependent manner in human breast cancer cells. *BMC Cancer*. 2016 Sep 8;16(1):724.
86. Zhang D, Zheng H, Zhou Y, Tang X, Yu B, Li J. Association of IL-1beta gene polymorphism with cachexia from locally advanced gastric cancer. *BMC Cancer*. 2007 Mar 14;7(1):45.
87. Strassmann G, Masui Y, Chizzonite R, Fong M. Mechanisms of experimental cancer cachexia. Local involvement of IL-1 in colon-26 tumor. *J Immunol*. 1993 Mar 15;150(6):2341–5.
88. Moses AGW, Maingay J, Sangster K, Fearon KCH, Ross JA. Pro-inflammatory cytokine release by peripheral blood mononuclear cells from patients with advanced pancreatic cancer: relationship to acute phase response and survival. *Oncol Rep*. 2009 Apr;21(4):1091–5.
89. Baltgalvis KA, Berger FG, Pena MMO, Davis JM, Muga SJ, Carson JA. Interleukin-6 and cachexia in ApcMin/+ mice. *Am J Physiol Regul Integr Comp Physiol*. 2008 Feb;294(2):R393–401.
90. Ando K, Takahashi F, Motojima S, Nakashima K, Kaneko N, Hoshi K, et al. Possible role for tocilizumab, an anti-interleukin-6 receptor antibody, in treating cancer cachexia. *J Clin Oncol*. 2013 Feb 20;31(6):e69–72.
91. Hirata H, Tetsumoto S, Kijima T, Kida H, Kumagai T, Takahashi R, et al. Favorable Responses to Tocilizumab in Two Patients With Cancer-Related Cachexia. *Journal of Pain and Symptom Management*. 2013 Aug;46(2):e9–13.
92. Kitamura H, Kamon H, Sawa SI, Park SJ, Katunuma N, Ishihara K, et al. IL-6-STAT3 controls intracellular MHC class II alphabeta dimer level through cathepsin S activity in dendritic cells. *Immunity*. 2005 Nov;23(5):491–502.
93. Tsukamoto H, Fujieda K, Hirayama M, Ikeda T, Yuno A, Matsumura K, et al. Soluble IL6R Expressed by Myeloid Cells Reduces Tumor-Specific Th1 Differentiation and Drives Tumor Progression. *Cancer Res*. 2017 May 1;77(9):2279–91.
94. Gabrilovich DI, Nagaraj S. Myeloid-derived suppressor cells as regulators of the immune system. *Nat Rev Immunol*. 2009 Mar;9(3):162–74.
95. Zhou J, Qu Z, Sun F, Han L, Li L, Yan S, et al. Myeloid STAT3 Promotes Lung Tumorigenesis by Transforming Tumor Immunosurveillance into Tumor-Promoting Inflammation. *Cancer Immunol Res*. 2017 Mar;5(3):257–68.
96. Damuzzo V, Solito S, Pinton L, Carrozzo E, Valpione S, Pigozzo J, et al. Clinical implication of tumor-associated and immunological parameters in melanoma patients treated with ipilimumab. *Oncoimmunology*. 2016;5(12):e1249559.
97. Dixit N, Simon SI. Chemokines, selectins and intracellular calcium flux: temporal and spatial cues for leukocyte arrest. *Front Immunol*. 2012;3:188.
98. Pekalski ML, García AR, Ferreira RC, Rainbow DB, Smyth DJ, Mashar M, et al. Neonatal and adult recent thymic emigrants produce IL-8 and express complement receptors CR1 and CR2. *JCI Insight*. 2(16):e93739.
99. Gioulbasanis I, Patrikidou A, Kitikidou K, Papadimitriou K, Vlachostergios PJ, Tsatsanis C, et al. Baseline plasma levels of interleukin-8 in stage IV non-small-cell lung cancer patients: relationship with nutritional status and prognosis. *Nutr Cancer*. 2012;64(1):41–7.
100. Hou YC, Wang CJ, Chao YJ, Chen HY, Wang HC, Tung HL, et al. Elevated Serum Interleukin-8 Level Correlates with Cancer-Related Cachexia and Sarcopenia: An Indicator for Pancreatic Cancer Outcomes. *J Clin Med*. 2018 Dec 1;7(12):502.
101. Mishalian I, Bayuh R, Eruslanov E, Michaeli J, Levy L, Zolotarov L, et al. Neutrophils recruit regulatory T-cells into tumors via secretion of CCL17--a new mechanism of impaired antitumor immunity. *Int J Cancer*. 2014 Sep 1;135(5):1178–86.
102. Sanmamed MF, Perez-Gracia JL, Schalper KA, Fusco JP, Gonzalez A, Rodriguez-Ruiz ME, et al. Changes in serum interleukin-8 (IL-8) levels reflect and predict response to anti-PD-1 treatment in melanoma and non-small-cell lung cancer patients. *Ann Oncol*. 2017 Aug 1;28(8):1988–95.
103. Ding H, Zhang G, Sin KWT, Liu Z, Lin RK, Li M, et al. Activin A induces skeletal muscle catabolism via p38 β mitogen-activated protein kinase. *J Cachexia Sarcopenia Muscle*. 2017 Apr;8(2):202–12.

104. Loumaye A, de Barse M, Nachit M, Lause P, Frateur L, van Maanen A, et al. Role of Activin A and myostatin in human cancer cachexia. *J Clin Endocrinol Metab.* 2015 May;100(5):2030–8.
105. Loumaye A, de Barse M, Nachit M, Lause P, van Maanen A, Trefois P, et al. Circulating Activin A predicts survival in cancer patients. *J Cachexia Sarcopenia Muscle.* 2017 Oct;8(5):768–77.
106. Wanig DL, Mohammad KS, Reiken S, Xie W, Andersson DC, John S, et al. Excess TGF- β mediates muscle weakness associated with bone metastases in mice. *Nat Med.* 2015 Nov;21(11):1262–71.
107. Lerner L, Tao J, Liu Q, Nicoletti R, Feng B, Krieger B, et al. MAP3K11/GDF15 axis is a critical driver of cancer cachexia. *J Cachexia Sarcopenia Muscle.* 2016 Sep;7(4):467–82.
108. Zhou X, Wang JL, Lu J, Song Y, Kwak KS, Jiao Q, et al. Reversal of cancer cachexia and muscle wasting by ActRIIB antagonism leads to prolonged survival. *Cell.* 2010 Aug 20;142(4):531–43.
109. Semitekolou M, Alissafi T, Aggelakopoulou M, Kourepini E, Kariyawasam HH, Kay AB, et al. Activin-A induces regulatory T cells that suppress T helper cell immune responses and protect from allergic airway disease. *J Exp Med.* 2009 Aug 3;206(8):1769–85.
110. Ogawa K, Funaba M, Chen Y, Tsujimoto M. Activin A functions as a Th2 cytokine in the promotion of the alternative activation of macrophages. *J Immunol.* 2006 Nov 15;177(10):6787–94.
111. Zugmaier G, Paik S, Wilding G, Knabbe C, Bano M, Lupu R, et al. Transforming growth factor beta 1 induces cachexia and systemic fibrosis without an antitumor effect in nude mice. *Cancer Res.* 1991 Jul 1;51(13):3590–4.
112. Wrzesinski SH, Wan YY, Flavell RA. Transforming growth factor-beta and the immune response: implications for anticancer therapy. *Clin Cancer Res.* 2007 Sep 15;13(18 Pt 1):5262–70.
113. Johnen H, Lin S, Kuffner T, Brown DA, Tsai VW, Bauskin AR, et al. Tumor-induced anorexia and weight loss are mediated by the TGF-beta superfamily cytokine MIC-1. *Nat Med.* 2007 Nov;13(11):1333–40.
114. Zhou Z, Li W, Song Y, Wang L, Zhang K, Yang J, et al. Growth differentiation factor-15 suppresses maturation and function of dendritic cells and inhibits tumor-specific immune response. *PLoS One.* 2013;8(11):e78618.
115. Ratnam NM, Peterson JM, Talbert EE, Ladner KJ, Rajasekera PV, Schmidt CR, et al. NF- κ B regulates GDF-15 to suppress macrophage surveillance during early tumor development. *J Clin Invest.* 2017 Oct 2;127(10):3796–809.
116. Roth P, Junker M, Tritschler I, Mittelbronn M, Dombrowski Y, Breit SN, et al. GDF-15 contributes to proliferation and immune escape of malignant gliomas. *Clin Cancer Res.* 2010 Aug 1;16(15):3851–9.
117. Takeshige K, Baba M, Tsuboi S, Noda T, Ohsumi Y. Autophagy in yeast demonstrated with proteinase-deficient mutants and conditions for its induction. *J Cell Biol.* 1992 Oct;119(2):301–11.
118. Pigna E, Berardi E, Aulino P, Rizzuto E, Zampieri S, Carraro U, et al. Aerobic Exercise and Pharmacological Treatments Counteract Cachexia by Modulating Autophagy in Colon Cancer. *Sci Rep.* 2016 May 31;6:26991.
119. Aversa Z, Pin F, Lucia S, Penna F, Verzaro R, Fazi M, et al. Autophagy is induced in the skeletal muscle of cachectic cancer patients. *Sci Rep.* 2016 Jul 27;6:30340.
120. Randow F, Münz C. Autophagy in the regulation of pathogen replication and adaptive immunity. *Trends Immunol.* 2012 Oct;33(10):475–87.
121. Hahn T, Akporiaye ET. α -TEA as a stimulator of tumor autophagy and enhancer of antigen cross-presentation. *Autophagy.* 2013 Mar;9(3):429–31.
122. Liu K, Zhao E, Ilyas G, Lalazar G, Lin Y, Haseeb M, et al. Impaired macrophage autophagy increases the immune response in obese mice by promoting proinflammatory macrophage polarization. *Autophagy.* 2015;11(2):271–84.
123. Parker KH, Horn LA, Ostrand-Rosenberg S. High-mobility group box protein 1 promotes the survival of myeloid-derived suppressor cells by inducing autophagy. *J Leukoc Biol.* 2016 Sep;100(3):463–70.
124. Tan BHL, Fladvad T, Braun TP, Vigano A, Strasser F, Deans DAC, et al. P-selectin genotype is associated with the development of cancer cachexia. *EMBO Mol Med.* 2012 Jun;4(6):462–71.

125. Johns N, Stretch C, Tan BHL, Solheim TS, Sørhaug S, Stephens NA, et al. New genetic signatures associated with cancer cachexia as defined by low skeletal muscle index and weight loss. *J Cachexia Sarcopenia Muscle*. 2017 Feb;8(1):122–30.
126. Ley K, Kansas GS. Selectins in T-cell recruitment to non-lymphoid tissues and sites of inflammation. *Nat Rev Immunol*. 2004 May;4(5):325–35.
127. Borsig L, Wong R, Hynes RO, Varki NM, Varki A. Synergistic effects of L- and P-selectin in facilitating tumor metastasis can involve non-mucin ligands and implicate leukocytes as enhancers of metastasis. *Proc Natl Acad Sci U S A*. 2002 Feb 19;99(4):2193–8.
128. Ohki S, Shibata M, Gonda K, Machida T, Shimura T, Nakamura I, et al. Circulating myeloid-derived suppressor cells are increased and correlate to immune suppression, inflammation and hypoproteinemia in patients with cancer. *Oncol Rep*. 2012 Aug;28(2):453–8.
129. Kang SP, Gergich K, Lubiniecki GM, de Alwis DP, Chen C, Tice MAB, et al. Pembrolizumab KEYNOTE-001: an adaptive study leading to accelerated approval for two indications and a companion diagnostic. *Ann Oncol*. 2017 Jun;28(6):1388–98.
130. Aguiar PN, Perry LA, Penny-Dimri J, Babiker H, Tadokoro H, de Mello RA, et al. The effect of PD-L1 testing on the cost-effectiveness and economic impact of immune checkpoint inhibitors for the second-line treatment of NSCLC. *Ann Oncol*. 2017 Sep 1;28(9):2256–63.
131. Sharma P, Hu-Lieskovan S, Wargo JA, Ribas A. Primary, Adaptive, and Acquired Resistance to Cancer Immunotherapy. *Cell*. 2017 Feb 9;168(4):707–23.
132. Sharpe AH, Pauken KE. The diverse functions of the PD1 inhibitory pathway. *Nat Rev Immunol*. 2018 Mar;18(3):153–67.
133. Pitt JM, Marabelle A, Eggermont A, Soria JC, Kroemer G, Zitvogel L. Targeting the tumor microenvironment: removing obstruction to anticancer immune responses and immunotherapy. *Ann Oncol*. 2016 Aug;27(8):1482–92.
134. Galon J, Mlecnik B, Bindea G, Angell HK, Berger A, Lagorce C, et al. Towards the introduction of the “Immunoscore” in the classification of malignant tumours. *J Pathol*. 2014 Jan;232(2):199–209.
135. Chalmers ZR, Connelly CE, Fabrizio D, Gay L, Ali SM, Ennis R, et al. Analysis of 100,000 human cancer genomes reveals the landscape of tumor mutational burden. *Genome Med*. 2017 Apr 19;9(1):34.
136. Le DT, Durham JN, Smith KN, Wang H, Bartlett BR, Aulakh LK, et al. Mismatch repair deficiency predicts response of solid tumors to PD-1 blockade. *Science*. 2017 Jul 28;357(6349):409–13.
137. Rizvi NA, Hellmann MD, Snyder A, Kvistborg P, Makarov V, Havel JJ, et al. Mutational landscape determines sensitivity to PD-1 blockade in non-small cell lung cancer. *Science*. 2015 Apr 3;348(6230):124–8.
138. Peters S, Creelan B, Hellmann MD, Socinski MA, Reck M, Bhagavatheswaran P, et al. Abstract CT082: Impact of tumor mutation burden on the efficacy of first-line nivolumab in stage iv or recurrent non-small cell lung cancer: An exploratory analysis of CheckMate 026. *Cancer Research*. 2017 Jul 1;77(13_Supplement):CT082.
139. Zeng DQ, Yu YF, Ou QY, Li XY, Zhong RZ, Xie CM, et al. Prognostic and predictive value of tumor-infiltrating lymphocytes for clinical therapeutic research in patients with non-small cell lung cancer. *Oncotarget*. 2016 Mar 22;7(12):13765–81.
140. Lin G, Fan X, Zhu W, Huang C, Zhuang W, Xu H, et al. Prognostic significance of PD-L1 expression and tumor infiltrating lymphocyte in surgically resectable non-small cell lung cancer. *Oncotarget*. 2017 Oct 13;8(48):83986–94.
141. Martin L, Senesse P, Gioulbasanis I, Antoun S, Bozzetti F, Deans C, et al. Diagnostic criteria for the classification of cancer-associated weight loss. *J Clin Oncol*. 2015 Jan 1;33(1):90–9.
142. Sperduto PW, Yang TJ, Beal K, Pan H, Brown PD, Bangdiwala A, et al. Estimating Survival in Patients With Lung Cancer and Brain Metastases. *JAMA Oncol*. 2017 Jun;3(6):827–31.
143. Ren Y, Dai C, Zheng H, Zhou F, She Y, Jiang G, et al. Prognostic effect of liver metastasis in lung cancer patients with distant metastasis. *Oncotarget*. 2016 Jul 18;7(33):53245–53.
144. Chia VM, Cetin K, Jacobsen JB, Nørgaard M, Jensen AØ, Christiansen CF, et al. The incidence and prognostic significance of bone metastases and skeletal-related events in lung cancer patients: A population-based cohort study in Denmark. *JCO*. 2010 May 20;28(15_suppl):e18074–e18074.

145. Oh Y, Taylor S, Bekele BN, Debnam JM, Allen PK, Suki D, et al. Number of metastatic sites is a strong predictor of survival in patients with nonsmall cell lung cancer with or without brain metastases. *Cancer*. 2009 Jul 1;115(13):2930–8.
146. Belkaid Y, Hand TW. Role of the microbiota in immunity and inflammation. *Cell*. 2014 Mar 27;157(1):121–41.
147. Vétizou M, Pitt JM, Daillère R, Lepage P, Waldschmitt N, Flament C, et al. Anticancer immunotherapy by CTLA-4 blockade relies on the gut microbiota. *Science*. 2015 Nov 27;350(6264):1079–84.
148. Imhann F, Bonder MJ, Vich Vila A, Fu J, Mujagic Z, Vork L, et al. Proton pump inhibitors affect the gut microbiome. *Gut*. 2016 May;65(5):740–8.
149. Coutinho AE, Chapman KE. The anti-inflammatory and immunosuppressive effects of glucocorticoids, recent developments and mechanistic insights. *Mol Cell Endocrinol*. 2011 Mar 15;335(1):2–13.
150. Arbour KC, Mezquita L, Long N, Rizvi H, Auclin E, Ni A, et al. Impact of Baseline Steroids on Efficacy of Programmed Cell Death-1 and Programmed Death-Ligand 1 Blockade in Patients With Non-Small-Cell Lung Cancer. *J Clin Oncol*. 2018 Oct 1;36(28):2872–8.
151. Brusselle G, Bracke K. Targeting immune pathways for therapy in asthma and chronic obstructive pulmonary disease. *Ann Am Thorac Soc*. 2014 Dec;11 Suppl 5:S322–328.
152. Jiang F, Jiang Y, Zhi H, Dong Y, Li H, Ma S, et al. Artificial intelligence in healthcare: past, present and future. *Stroke Vasc Neurol [Internet]*. 2017 Dec 1 [cited 2023 Aug 26];2(4). Available from: <https://svn.bmj.com/content/2/4/230>
153. Orfanoudaki G, Markaki M, Chatzi K, Tsamardinos I, Economou A. MatureP: prediction of secreted proteins with exclusive information from their mature regions. *Sci Rep*. 2017 Jun 12;7(1):3263.
154. Planchard D, Popat S, Kerr K, Novello S, Smit EE, Faivre-Finn C, et al. Metastatic non- small cell lung cancer: ESMO Clinical Practice Guidelines for diagnosis, treatment and follow-up. *Ann Oncol*. 2018 Oct 1;29(Suppl 4):iv192–237.
155. Sørensen JB, Klee M, Palshof T, Hansen HH. Performance status assessment in cancer patients. An inter-observer variability study. *Br J Cancer*. 1993 Apr;67(4):773–5.
156. Haanen JB a. G, Carboneel F, Robert C, Kerr KM, Peters S, Larkin J, et al. Management of toxicities from immunotherapy: ESMO Clinical Practice Guidelines for diagnosis, treatment and follow-up. *Ann Oncol*. 2017 Jul 1;28(suppl_4):iv119–42.
157. Eisenhauer EA, Therasse P, Bogaerts J, Schwartz LH, Sargent D, Ford R, et al. New response evaluation criteria in solid tumours: revised RECIST guideline (version 1.1). *Eur J Cancer*. 2009 Jan;45(2):228–47.
158. Mourtzakis M, Prado CMM, Lieffers JR, Reiman T, McCargar LJ, Baracos VE. A practical and precise approach to quantification of body composition in cancer patients using computed tomography images acquired during routine care. *Appl Physiol Nutr Metab*. 2008 Oct;33(5):997–1006.
159. Mitsiopoulos N, Baumgartner RN, Heymsfield SB, Lyons W, Gallagher D, Ross R. Cadaver validation of skeletal muscle measurement by magnetic resonance imaging and computerized tomography. *J Appl Physiol* (1985). 1998 Jul;85(1):115–22.
160. Miller KD, Jones E, Yanovski JA, Shankar R, Feuerstein I, Falloon J. Visceral abdominal- fat accumulation associated with use of indinavir. *Lancet*. 1998 Mar 21;351(9106):871– 5.
161. Montfort A, Colacios C, Levade T, Andrieu-Abadie N, Meyer N, Ségui B. The TNF Paradox in Cancer Progression and Immunotherapy. *Front Immunol*. 2019 Jul 31;10:1818.
162. Garrido P, Pujol JL, Kim ES, Lee JM, Tsuboi M, Gómez-Rueda A, et al. Canakinumab with and without pembrolizumab in patients with resectable non-small-cell lung cancer: CANOPY-N study design. *Future Oncology*. 2021 Apr;17(12):1459–72.
163. Liu C, Yang L, Xu H, Zheng S, Wang Z, Wang S, et al. Systematic analysis of IL-6 as a predictive biomarker and desensitizer of immunotherapy responses in patients with non-small cell lung cancer. *BMC Medicine*. 2022 May 13;20(1):187.
164. Riedl JM, Barth DA, Brueckl WM, Zeitler G, Foris V, Mollnar S, et al. C-Reactive Protein (CRP) Levels in Immune Checkpoint Inhibitor Response and Progression in Advanced Non-Small Cell Lung Cancer: A Bi-Center Study. *Cancers (Basel)*. 2020 Aug 17;12(8):2319.

165. Martini DJ, Kline MR, Liu Y, Shabto JM, Williams MA, Khan AI, et al. Adiposity may predict survival in patients with advanced stage cancer treated with immunotherapy in phase 1 clinical trials. *Cancer*. 2020 Feb 1;126(3):575–82.
166. McQuade JL, Daniel CR, Hess KR, Mak C, Wang DY, Rai RR, et al. Association of body- mass index and outcomes in patients with metastatic melanoma treated with targeted therapy, immunotherapy, or chemotherapy: a retrospective, multicohort analysis. *The Lancet Oncology*. 2018 Mar 1;19(3):310–22.
167. Kichenadasse G, Miners JO, Mangoni AA, Rowland A, Hopkins AM, Sorich MJ. Association Between Body Mass Index and Overall Survival With Immune Checkpoint Inhibitor Therapy for Advanced Non-Small Cell Lung Cancer. *JAMA Oncol*. 2020 Apr 1;6(4):512–8.
168. Wang Z, Aguilar EG, Luna JI, Dunai C, Khuat LT, Le CT, et al. Paradoxical effects of obesity on T cell function during tumor progression and PD-1 checkpoint blockade. *Nat Med*. 2019 Jan;25(1):141–51.
169. Tsamardinos I, Greasidou E, Borboudakis G. Bootstrapping the out-of-sample predictions for efficient and accurate cross-validation. *Mach Learn*. 2018;107(12):1895–922.
170. Breiman L. Random Forests. *Machine Learning*. 2001 Oct 1;45(1):5–32.
171. Hoerl AE, Kennard RW. Ridge Regression: Biased Estimation for Nonorthogonal Problems. *Technometrics*. 2000;42(1):80–6.
172. Breiman L. *Classification and Regression Trees*. New York: Routledge; 2017. 368 p.
173. Rounis K, Makrakis D, Papadaki C, Monastiriotti A, Vamvakas L, Kalbakis K, et al. Prediction of outcome in patients with non-small cell lung cancer treated with second line PD-1/PDL-1 inhibitors based on clinical parameters: Results from a prospective, single institution study. *PLoS One*. 2021;16(6):e0252537.
174. Rounis K, Makrakis D, Tsigkas AP, Georgiou A, Galanakis N, Papadaki C, et al. Cancer cachexia syndrome and clinical outcome in patients with metastatic non-small cell lung cancer treated with PD-1/PD-L1 inhibitors: results from a prospective, observational study. *Translational Lung Cancer Research* [Internet]. 2021 Aug [cited 2021 Sep 2];10(8). Available from: <https://tlcr.amegroups.com/article/view/55615>
175. Makrakis D, Rounis K, Tsigkas AP, Georgiou A, Galanakis N, Tsakonas G, et al. Effect of body tissue composition on the outcome of patients with metastatic non-small cell lung cancer treated with PD-1/PD-L1 inhibitors. *PLoS One*. 2023;18(2):e0277708.
176. Landi L, D'Inca F, Gelibter A, Chiari R, Grossi F, Delmonte A, et al. Bone metastases and immunotherapy in patients with advanced non-small-cell lung cancer. *J Immunother Cancer*. 2019 Nov 21;7(1):316.
177. Prelaj A, Ferrara R, Rebuzzi SE, Proto C, Signorelli D, Galli G, et al. EPSiLoN: A Prognostic Score for Immunotherapy in Advanced Non-Small-Cell Lung Cancer: A Validation Cohort. *Cancers (Basel)*. 2019 Dec 5;11(12):1954.
178. Tinsley N, Zhou C, Tan G, Rack S, Lorigan P, Blackhall F, et al. Cumulative Antibiotic Use Significantly Decreases Efficacy of Checkpoint Inhibitors in Patients with Advanced Cancer. *Oncologist*. 2020 Jan;25(1):55–63.
179. Derosa L, Hellmann MD, Spaziano M, Halpenny D, Fidelle M, Rizvi H, et al. Negative association of antibiotics on clinical activity of immune checkpoint inhibitors in patients with advanced renal cell and non-small-cell lung cancer. *Ann Oncol*. 2018 Jun 1;29(6):1437–44.
180. Derosa L, Zitvogel L. Antibiotics impair immunotherapy for urothelial cancer. *Nat Rev Urol*. 2020 Nov;17(11):605–6.
181. Jiang S, Geng S, Chen Q, Zhang C, Cheng M, Yu Y, et al. Effects of Concomitant Antibiotics Use on Immune Checkpoint Inhibitor Efficacy in Cancer Patients. *Frontiers in Oncology* [Internet]. 2022 [cited 2023 Sep 3];12. Available from: <https://www.frontiersin.org/articles/10.3389/fonc.2022.823705>
182. Villemain C, Six A, Neville BA, Lawley TD, Robinson MJ, Bakdash G. The heightened importance of the microbiome in cancer immunotherapy. *Trends Immunol*. 2023 Jan;44(1):44–59.
183. Skribek M, Rounis K, Afshar S, Grundberg O, Friesland S, Tsakonas G, et al. Effect of corticosteroids on the outcome of patients with advanced non-small cell lung cancer treated with immune-checkpoint inhibitors. *Eur J Cancer*. 2021 Mar;145:245–54.

184. Ricciuti B, Dahlberg SE, Adeni A, Sholl LM, Nishino M, Awad MM. Immune Checkpoint Inhibitor Outcomes for Patients With Non-Small-Cell Lung Cancer Receiving Baseline Corticosteroids for Palliative Versus Nonpalliative Indications. *J Clin Oncol*. 2019 Aug 1;37(22):1927–34.
185. Hopkins AM, Kichenadasse G, Karapetis CS, Rowland A, Sorich MJ. Concomitant Antibiotic Use and Survival in Urothelial Carcinoma Treated with Atezolizumab. *Eur Urol*. 2020 Oct;78(4):540–3.
186. Chen B, Yang C, Dragomir MP, Chi D, Chen W, Horst D, et al. Association of proton pump inhibitor use with survival outcomes in cancer patients treated with immune checkpoint inhibitors: a systematic review and meta-analysis. *Ther Adv Med Oncol*. 2022 Jul 15;14:1758835922111704.
187. Park W, Mezquita L, Okabe N, Chae YK, Kwon D, Saravia D, et al. Association of the prognostic model iSEND with PD-1/L1 monotherapy outcome in non-small-cell lung cancer. *Br J Cancer*. 2020 Feb 4;122(3):340–7.
188. Trebeschi S, Drago SG, Birkbak NJ, Kurilova I, Călin AM, Delli Pizzi A, et al. Predicting response to cancer immunotherapy using noninvasive radiomic biomarkers. *Ann Oncol*. 2019 Jun 1;30(6):998–1004.
189. Wei F, Azuma K, Nakahara Y, Saito H, Matsuo N, Tagami T, et al. Machine learning for prediction of immunotherapeutic outcome in non-small-cell lung cancer based on circulating cytokine signatures. *J Immunother Cancer*. 2023 Jul 1;11(7):e006788.
190. Cawley GC, Talbot NLC. On Over-fitting in Model Selection and Subsequent Selection Bias in Performance Evaluation. *J Mach Learn Res*. 2010 Aug 1;11:2079–107.
191. Argilés JM, Busquets S, Stemmler B, López-Soriano FJ. Cancer cachexia: understanding the molecular basis. *Nat Rev Cancer*. 2014 Nov;14(11):754–62.
192. Shiroyama T, Nagatomo I, Koyama S, Hirata H, Nishida S, Miyake K, et al. Impact of sarcopenia in patients with advanced non-small cell lung cancer treated with PD-1 inhibitors: A preliminary retrospective study. *Sci Rep*. 2019 Feb 21;9(1):2447.
193. Miyawaki T, Naito T, Kodama A, Nishioka N, Miyawaki E, Mamesaya N, et al. Desensitizing Effect of Cancer Cachexia on Immune Checkpoint Inhibitors in Patients With Advanced NSCLC. *JTO Clinical and Research Reports* [Internet]. 2020 Jun 1 [cited 2021 Jun 1];1(2). Available from: [https://www.jtocrr.org/article/S2666-3643\(20\)30020-5/abstract](https://www.jtocrr.org/article/S2666-3643(20)30020-5/abstract)
194. Roch B, Coffy A, Jean-Baptiste S, Palaysi E, Daures JP, Pujol JL, et al. Cachexia - sarcopenia as a determinant of disease control rate and survival in non-small lung cancer patients receiving immune-checkpoint inhibitors. *Lung Cancer*. 2020 May;143:19–26.
195. Chu MP, Li Y, Ghosh S, Sass S, Smylie M, Walker J, et al. Body composition is prognostic and predictive of ipilimumab activity in metastatic melanoma. *J Cachexia Sarcopenia Muscle*. 2020 Jun;11(3):748–55.
196. Turner DC, Kondic AG, Anderson KM, Robinson AG, Garon EB, Riess JW, et al. Pembrolizumab Exposure-Response Assessments Challenged by Association of Cancer Cachexia and Catabolic Clearance. *Clin Cancer Res*. 2018 Dec 1;24(23):5841–9.
197. Degens JHRJ, Dingemans AMC, Willemsen ACH, Gietema HA, Hurkmans DP, Aerts JG, et al. The prognostic value of weight and body composition changes in patients with non- small-cell lung cancer treated with nivolumab. *J Cachexia Sarcopenia Muscle*. 2021 Jun;12(3):657–64.
198. Sanchez A, Furberg H, Kuo F, Vuong L, Ged Y, Patil S, et al. Transcriptomic signatures related to the obesity paradox in patients with clear cell renal cell carcinoma: a retrospective cohort study. *Lancet Oncol*. 2020 Feb;21(2):283–93.
199. Woodall MJ, Neumann S, Campbell K, Pattison ST, Young SL. The Effects of Obesity on Anti-Cancer Immunity and Cancer Immunotherapy. *Cancers (Basel)*. 2020 May 14;12(5):1230.
200. Nishioka N, Naito T, Miyawaki T, Yabe M, Doshita K, Kodama H, et al. Impact of losing adipose tissue on outcomes from PD-1/PD-L1 inhibitor monotherapy in non-small cell lung cancer. *Thorac Cancer*. 2022 May;13(10):1496–504.
201. Wensveen FM, Valentić S, Šestan M, Wensveen TT, Polić B. Interactions between adipose tissue and the immune system in health and malnutrition. *Semin Immunol*. 2015 Sep;27(5):322–33.
202. Lu J, Zhao J, Meng H, Zhang X. Adipose Tissue-Resident Immune Cells in Obesity and Type 2 Diabetes. *Front Immunol*. 2019;10:1173.

203. Nishimura S, Manabe I, Nagasaki M, Eto K, Yamashita H, Ohsugi M, et al. CD8+ effector T cells contribute to macrophage recruitment and adipose tissue inflammation in obesity. *Nat Med.* 2009 Aug;15(8):914–20.
204. Ilan Y, Maron R, Tukpah AM, Maioli TU, Murugaiyan G, Yang K, et al. Induction of regulatory T cells decreases adipose inflammation and alleviates insulin resistance in ob/ob mice. *Proc Natl Acad Sci U S A.* 2010 May 25;107(21):9765–70.
205. Lumeng CN, Bodzin JL, Saltiel AR. Obesity induces a phenotypic switch in adipose tissue macrophage polarization. *J Clin Invest.* 2007 Jan;117(1):175–84.
206. Kratz M, Coats BR, Hisert KB, Hagman D, Mutskov V, Peris E, et al. Metabolic dysfunction drives a mechanistically distinct proinflammatory phenotype in adipose tissue macrophages. *Cell Metab.* 2014 Oct 7;20(4):614–25.
207. Nishioka N, Naito T, Notsu A, Mori K, Kodama H, Miyawaki E, et al. Unfavorable impact of decreased muscle quality on the efficacy of immunotherapy for advanced non-small cell lung cancer. *Cancer Med.* 2021 Jan;10(1):247–56.

8. Abbreviations

SCLC: Small cell lung cancer	NADPH: Nicotinamide adenine dinucleotide phosphate
NSCLC: Non-small cell lung cancer	NOX: NADPH oxidase 4
LADC: Lung adenocarcinoma	RyR1: Ryanodine receptor 1
sqLC: Squamous lung carcinoma	MAP3K11: Mitogen-activated protein kinase kinase kinase 11
TILs: Tumor infiltrating lymphocytes	GFRAL: GDNF family receptor alpha like
CTLA-4: Cytotoxic T-lymphocyte-associated protein 4	shRNA: short hairpin RNA
PD-1: Programmed cell death-1	LC3B-II: Microtubule-associated protein 1A/1B-light chain 3
PD-L1: Programmed cell death ligand-1	FOXP3: Forkhead box P3
TCR: T cell receptor	HMGB1: High mobility group box 1 protein
MHC: Major histocompatibility complex	ICH: Immunochemistry
CD: Cluster of Differentiation	DOR: Duration of response
IL: Interleukin	MTB: Mutational tumor burden
ICIs: Immune checkpoint inhibitors	MLH1: MutL protein homolog 1
HLA: Human leukocyte antigen	MSH2: MutS homolog 2
Ig: Immunoglobulin	MSH6: MutS homolog 6
TC: Tumor cells	PMS2: Mismatch repair endonuclease PMS2
IC: Immune cells	NLR: Neutrophil to lymphocyte ratio
ITT: Intention to treat	LDH: Lactate dehydrogenase
PFS: Progression free survival	AutoML: Automated machine learning
OS: Overall survival	ROC: Receiver operating characteristic curve
FDA: Food Drug Administration	AUC: Area under the curve
TNM: Tumor, nodes, metastasis	PS: Performance status by ECOG
AIDS: Acquired immunodeficiency syndrome	PR: Partial response
CCS: Cancer cachexia syndrome	CR: Complete response
TME: Tumor microenvironment	SD: Stable disease
PPis: Proton pump inhibitors	PD: Progressive disease
ATBs: Antibiotics	ORR: Objective response rate
GR: Glucocorticoids receptor	UNL: Upper normal limit
irAEs: Immune related adverse events	HR: Hazard ratio
AI: Artificial intelligence	LNL: Lower normal limit
EGFR: Epidermal growth factor receptor	CI: Confidence interval
ALK: Anaplastic lymphoma kinase	UCP-1: Uncoupling protein 1
PCR: Polymerase chain reaction	BMI: Body mass index
FISH: Fluorescence in situ hybridization	PSGL-1: P-selectin glycoprotein ligand-1
ESMO: European Society of Medical Oncology	MDSCs: Myeloid derived suppressor cells
ECOG: Eastern Cooperative Oncology Group	CAFs: Cancer associated fibroblasts
COPD: Chronic obstructive pulmonary disease	DC: Dendritic cells
IMFI: Intramuscular fat tissue index	NK: Natural killer cells
SFI: Subcutaneous fat tissue index	EMT: Epithelial to mesenchymal transition
VFI: Visceral fat tissue index	PPARα: Peroxisome proliferator-activated receptor alpha
LSMI: Lumbar skeletal muscle index	gp130: Glycoprotein 130
TNF: Tumor Necrosis Factor	TGFβRI-3: Transforming growth factor receptor 1-3
TWEAK: Tumor necrosis factor like weak inducer of apoptosis	TIM3: Transmembrane immunoglobulin and munin domain 3
MEF: Mouse embryonic factor	TNFR1: Tumor necrosis factor receptor 1
NF-κB: Nuclear factor kappa-light-chain-enhancer of activated B cells	CXCR1/2: C-X-C motif chemokine receptor 1-2
STAT: Signal transducer and activator of transcription protein	NLP3: Nodule inception protein-like protein 3
IFN: Interferon	
Fn14: Targeting fibroblast growth factor inducible 14	
TAN: Tumor associated neutrophils	
TGF-β: Transforming growth factor beta	
GDF-15: Growth differentiation factor 15	
SMAD3: Mothers against decapentaplegic homolog 3	

Finally, and perhaps the most significant note of all, I would like, from the depths of my heart, to express my gratitude to the patients and their families for their participation in this study and I want to convey my admiration for the courage and bravery with which they faced the emperor of all maladies.

10. Published scientific papers as result of this PhD Thesis

PLOS ONE

RESEARCH ARTICLE

Prediction of outcome in patients with non-small cell lung cancer treated with second line PD-1/PDL-1 inhibitors based on clinical parameters: Results from a prospective, single institution study

Konstantinos Rounis^{1*}, Dimitrios Makrakis^{1,2}, Chara Papadaki³, Alexia Monastirioti³, Lambros Vamvakas¹, Konstantinos Kalbakis¹, Krystallia Gourlia⁴, Ioannis Xanthopoulos⁴, Ioannis Tsamardinos⁴, Dimitrios Mavroudis^{1,3}, Sofia Agelaki^{1,3}

1 Department of Medical Oncology, University General Hospital, Heraklion, Crete, Greece, **2** Division of Oncology, University of Washington Medical School, Seattle, Washington, United States of America, **3** Laboratory of Translational Oncology, School of Medicine, University of Crete, Heraklion, Crete, Greece, **4** Department of Computer Science, University of Crete, Heraklion, Crete, Greece

* kostas@rounis.gr



OPEN ACCESS

Citation: Rounis K, Makrakis D, Papadaki C, Monastirioti A, Vamvakas L, Kalbakis K, et al. (2021) Prediction of outcome in patients with non-small cell lung cancer treated with second line PD-1/PDL-1 inhibitors based on clinical parameters: Results from a prospective, single institution study. PLoS ONE 16(6): e0252537. <https://doi.org/10.1371/journal.pone.0252537>

Editor: Ramon Andrade De Mello, Nine of July University (UNINOVE): Discipline of Medical Oncology - Post Graduation Program in Medicine, BRAZIL

Received: November 2, 2020

Accepted: May 17, 2021

Published: June 1, 2021

Copyright: © 2021 Rounis et al. This is an open access article distributed under the terms of the [Creative Commons Attribution License](https://creativecommons.org/licenses/by/4.0/), which permits unrestricted use, distribution, and reproduction in any medium, provided the original author and source are credited.

Data Availability Statement: All relevant data are within the paper and its [Supporting information files](#).

Funding: This work was partly supported by Anticancer Research Support Association (ARSA). The funders had no role in study design, data collection and analysis, decision to publish, or

Abstract

Objective

We prospectively recorded clinical and laboratory parameters from patients with metastatic non-small cell lung cancer (NSCLC) treated with 2nd line PD-1/PD-L1 inhibitors in order to address their effect on treatment outcomes.

Materials and methods

Clinicopathological information (age, performance status, smoking, body mass index, histology, organs with metastases), use and duration of proton pump inhibitors, steroids and antibiotics (ATB) and laboratory values [neutrophil/lymphocyte ratio, LDH, albumin] were prospectively collected. Steroid administration was defined as the use of > 10 mg prednisone equivalent for ≥ 10 days. Prolonged ATB administration was defined as ATB ≥ 14 days 30 days before or within the first 3 months of treatment. JADBio, a machine learning pipeline was applied for further multivariate analysis.

Results

Data from 66 pts with non-oncogenic driven metastatic NSCLC were analyzed; 15.2% experienced partial response (PR), 34.8% stable disease (SD) and 50% progressive disease (PD). Median overall survival (OS) was 6.77 months. ATB administration did not affect patient OS [HR = 1.35 (CI: 0.761–2.406, $p = 0.304$)], however, prolonged ATBs [HR = 2.95 (CI: 1.62–5.36, $p = 0.0001$)] and the presence of bone metastases [HR = 1.89 (CI: 1.02–3.51, $p = 0.049$)] independently predicted for shorter survival. Prolonged ATB administration, bone metastases, liver metastases and BMI < 25 kg/m² were selected by JADBio as

preparation of the manuscript. One of the co-authors, Dimitrios Makrakis, at the time of data collection, was receiving a scholarship for cancer research from ARSA (ID: 2440338).

Competing interests: The authors have declared that no competing interests exist.

the important features that were associated with increased probability of developing disease progression as response to treatment. The resulting algorithm that was created was able to predict the probability of disease stabilization (PR or SD) in a single individual with an AUC = 0.806 [95% CI:0.714–0.889].

Conclusions

Our results demonstrate an adverse effect of prolonged ATBs on response and survival and underscore their importance along with the presence of bone metastases, liver metastases and low BMI in the individual prediction of outcomes in patients treated with immunotherapy.

Introduction

Immune checkpoint inhibitors (ICIs) targeting the PD-1/PD-L1 axis have demonstrated substantial clinical activity in metastatic NSCLC and received regulatory approval for use as first or subsequent lines of therapy [1–5]. However, only a small proportion of individuals will experience durable clinical remissions and subsequent significant clinical benefit. In addition, beyond PD-L1 levels in tumor cells or the immune cells of the tumor microenvironment, there is currently a lack of biomarkers for the prediction of treatment outcomes. From the financial perspective, the large scale use of these inhibitors is associated with substantial expenditures for the healthcare system, thus rendering their cost-effectiveness debatable [6, 7].

Pretreatment weight loss and low body mass index values have been well-recognized adverse prognostic features in cancer patients [8]. Furthermore, several clinical studies have reported the prognostic value of systemic inflammation in malignancy and the role of routine blood parameters as potential inflammatory biomarkers [9]. Neutrophil/lymphocyte ratio (NLR) and low albumin levels have been associated with treatment outcomes in patients with advanced cancer, including lung cancer [10, 11]. Evidence is being progressively gathered on the application of the aforementioned parameters for the creation of predictive models in a wide spectrum of malignancies [12–14].

Intestinal microbiome composition exerts a pivotal impact in the shaping of an effective immune response [15]. Preclinical data have highlighted the importance of gut microbiota on immunotherapy efficacy in experimental mouse melanoma models [16]. More importantly, antibiotic (ATB) administration may significantly alter the microbiome composition leading to gut dysbiosis and immune dysfunction [17]. Beyond ATBs, proton pump inhibitors (PPis) are among the most common prescribed drugs worldwide and their administration has been linked with a significant decrease in Shannon's diversity accompanied with alterations at the range of 20% of the bacterial taxa of the intestinal flora [18].

Daily steroid requirements > 10 mg of prednisone equivalent consisted an exclusion criterion for the registrational trials of ICIs [1–5]. In retrospective studies steroid administration has been associated with poor outcomes in patients with NSCLC treated with ICIs [19]. However, besides per os or intravenous steroids, NSCLC patients commonly use inhalational steroids due to the high prevalence of chronic obstructive pulmonary disease (COPD) in these individuals. Inhalational steroids exert a plethora of immunomodulatory effects on bronchial mucosa [20] however their effect on ICI efficacy has not been investigated so far.

Based on the above data we assumed that routinely available clinical and laboratory parameters may have prognostic and predictive relevance in patients with advanced NSCLC treated with ICIs. To test our hypothesis we conducted a prospective observational study in order to

evaluate their role in the determination of clinical outcome in patients with metastatic NSCLC treated with ICIs in the second line treatment setting. In addition, we introduced these parameters in the Just Add Data Bio (JADBio) (www.jadbio.com) machine learning pipeline [21, 22] for further multivariate analysis in order to estimate their integrative predictive value in NSCLC.

Materials and methods

Study design

This is a prospective observational study enrolling patients with metastatic NSCLC, without EGFR mutations or ALK translocations, treated with ICIs following progression on previous platinum-based chemotherapy. Patients were recruited at the Department of Medical Oncology, University General Hospital of Heraklion, from November 15, 2017 until November 21, 2019. Patients were eligible if they received ICIs as second-line treatment as per standard treatment guidelines, according to the decision of the treating physician. Written informed consent was obtained from all patients before enrollment. The study was reviewed and approved by the institutional review board of the University Hospital of Heraklion and was conducted in accordance with the principles of the Declaration of Helsinki (ID 2644).

Data collection and outcome assessment

Patients with EGFR mutations or ALK translocations were excluded from the analysis. Radiological assessment was prospectively performed using CT scans (or MRI if clinically indicated) from the start of immunotherapy and every 8–9 weeks thereafter. Partial response (PR), stable disease (SD) and progressive disease (PD) were assessed according to RECIST 1.1 criteria [23]. Disease stabilization (DS) was defined as the achievement of PR or SD after ICI administration. Disease progression was defined as radiological progression or death during the course of treatment. Progression free survival (PFS) was defined as the time duration between the initiation of immunotherapy and disease progression or death. Overall survival (OS) was defined as the time duration between the initiation of immunotherapy and death. Individuals that had not progressed or were alive at the time of data analysis were censored for PFS and OS respectively at the date of last follow up.

Data on patient [age, gender, smoking status, performance status (PS), body mass index (BMI)], disease characteristics (histology, organs affected with metastatic disease) and context and duration of co-medications [per os (pos), intravenous (iv) or inhalational steroids, ATB and PPIs] were prospectively collected. Disease burden was classified as high and low (> 2 and ≤ 2 organs with metastases) at the beginning of immunotherapy. Patients were classified based on their BMI at the start of immunotherapy in a binary fashion with the value of 25 kg/m^2 used as the cut-off to define BMI high vs BMI low. Common laboratory parameters such as baseline lactate dehydrogenase (LDH) levels, albumin and absolute white blood cell counts were collected at the time of treatment initiation. Elevated LDH levels were defined according to the upper limit of normal value range (UNL) (247 units/liter) and the cut-off for neutrophil/lymphocyte ratio (NLR) was set at > 3 . The cut-off for albumin levels was set at 3.5 g/dl that represents the lower normal limit. PD-L1 assessment, when available, further categorized the patients as PD-L1 positive or negative. PD-L1 expression was scored as % of tumor cells showing membranous and/or cytoplasmic staining; the cut-off for positivity was set at $\geq 1\%$.

Patients were categorized as having received steroids per os or iv in case of steroid use at a dosage of $> 10 \text{ mg}$ prednisone equivalent for ≥ 10 days within the first 12 weeks of treatment or within 15 days before its initiation. Patients were further sub-classified into two different subgroups, those who had received steroids due to immune related adverse effects (irAEs) and

those who had received steroids for supportive reasons (e.g. brain edema due to brain metastases, anorexia, dyspnea, COPD exacerbations). We categorized patients as having been administered ATB if they had received ATBs within 30 days before the initiation of immunotherapy and/or within the first 12 weeks of treatment; prolonged ATB administration was defined as ATBs use for ≥ 14 days. In case of multiple courses of shorter periods, the total duration was calculated. Long-term PPis usage was defined as the use of PPis for a time duration ≥ 3 months before the initiation of immunotherapy. Chronic administration of inhalational steroids was defined as use for ≥ 3 months prior to the start of immunotherapy. The cut-offs of 10 days, 14 days and 3 months for steroids, ATBs and PPIs use, respectively, were set arbitrarily before the initiation of data collection.

Statistical analysis

Statistical analysis was performed using SPSS 25.00. Descriptive statistics were performed to define categorical and continuous nominal variables. Statistical significance was set at $p < 0.05$ (two-sided test). Chi square test was used to access any potential associations between each variable with PR and DS rates. In addition, chi-square test was applied to investigate any potential associations of various clinical characteristics with prolonged ATB administration. Mann-Whitney U test was applied to test the effect of duration of ATB administration in days as a continuous variable on DS rates. In addition, we performed binary logistic regression analysis in order to examine the odds ratios (OR) of the studied covariates on the probability of achieving DS as response to ICI administration.

The Kaplan Meier method was used to access any effect of the studied parameters on PFS and OS. Curves were compared with the log-rank test. We initially applied Cox Regression Method to examine the effect of the duration of ATB administration as a continuous nominal variable in days on PFS and OS. Finally, we conducted a univariate analysis for each studied categorical variable and afterwards a multivariate analysis including the parameters that had reached statistical significance in the univariate analysis using Cox Regression Method to investigate their effect on survival outcomes.

We did not perform a sample size and power calculation because at the time of the initiation of data collection there was a scarcity of published reports on the effect of the studied parameters on the outcome of immunotherapy treated cancer patients. Thus, it would have been of no value in this exploratory study due to the lack of available data on which to base the required calculations.

Multivariate analysis by JADBIO tool

For the purpose of conducting a multivariate analysis on our data, we applied JADBIO, a fully automated machine learning (AutoML) system (www.jadbio.com). JADBIO selects the algorithms and methods corresponding to the particular problem, according to the type of data used and possible preferences set by the user. To do this, it employs an artificial intelligence (AI) system responsible for selecting methods and performing tasks, such as data transformation, data pre-processing, feature selection, model selection and results visualization. Furthermore, the system is in charge of selecting which of their hyper-parameters to optimize. The combination of methods used and their corresponding hyper-parameters is defined as a configuration and these methods are applied using the 10-fold cross validation protocol. Thus, JADBIO produces thousands of different models, ranking them based on a scoring metric, in our case, area under the receiver operating characteristic (ROC) curve (AUC), and outputs the best performing one. To eliminate the possibility of overestimating the final predictive

performance, JADBio uses a bootstrap-based method to correct it [24]. Using the same method, it calculates the confidence intervals of the resulted performance.

In our analysis, we used JADBio for binary classification modelling for the prediction of the probability of a single individual to achieve DS (PR or SD vs PD) with ICIs as second line treatment. The feature classification of the parameters used as input in JADBio is demonstrated in [S1 Table](#). The tool applied the following modelling algorithms: support vector machines (SVM) with full polynomial and Gaussian kernels [25], random forests [26], ridge logistic regression [27], and decision trees [28]. The performance metric we chose over the several ones available at JADBio, is the AUC. In most cases, the result of an analysis will be a complex model, incomprehensible to the human user. To aid in that regard, JADBio additionally outputs the best interpretable model. In our work, we report the performance estimation of the best performing model.

Results

Patient characteristics

Patients' characteristics are shown in detail in [Table 1](#). All the individuals included in this study were Caucasian. All patients had received prior platinum-based chemotherapy. Median age was 69 years (range: 39–81 years), 24 patients (36.3%) had received steroids, 34 (51.5%) had received ATBs and 22 (33.3% of the total population) had been administered a prolonged course of ATBs. None of the studied clinical and laboratory parameters were associated at a statistical significant level with prolonged ATB administration ([S2 Table](#)).

Effect of the studied variables on response outcomes

Ten (15.2%) patients experienced PR, 23 (34.8%) SD and 33 (50%) had PD at the time of their first disease evaluation. Median duration of response was 7.97 months (range, 2.8–26.9 months).

Only low BMI ($p = 0.030$, CI 95%) was significantly associated with inferior response rates ([S3 Table](#)). Low BMI ($p = 0.003$, CI 95%), the presence of bone metastases ($p = 0.007$, CI 95%), liver metastases ($p = 0.014$, CI 95%) and high disease burden ($p = 0.017$, CI 95%) were significantly associated with inferior DS rates. ATB administration ($p = 0.014$, CI 95%), prolonged ATB administration ($p = 0.002$, CI 95%) and the use of pos or iv steroids for supportive reasons ($p = 0.040$, CI 95%), exhibited a statistically significant correlation with reduced DS rates ([Fig 1A–1C](#)). The duration of ATB administration in days as a continuous nominal variable was also negatively correlated with DS rates ($p = 0.004$, CI 95%) ([S1 Fig](#)). None of the other studied parameters affected DS rates at a significant level ([S4 Table](#)).

The odds ratio (OR) of each studied covariate on the probability of achieving DS as result of ICIs administration along with its statistical significance are depicted in [Fig 2A](#) and [S5 Table](#). In the multivariate logistic regression analysis, bone metastases [OR: 0.153 (CI: 0.032–0.734, $p = 0.019$)] and prolonged ATB administration [OR: 0.085 (CI: 0.017–0.411, $p = 0.002$)], independently predicted for lower probability of DS with ICIs ([Fig 2B](#) and [S5 Table](#)).

Effect of the studied variables on survival outcomes

Median duration of follow up was 6.37 months (range: 0.6–26.9 months). After data censoring, median PFS and OS for the whole patient population were 3.50 (95% CI: 1.49–5.50) and 6.77 (95% CI: 2.29–11.24) months, respectively.

The results on the effect of the studied variables on PFS and OS are depicted in [S6 Table](#). BMI <25 kg/m² (2.33 vs 4.93 months, $p = 0.009$), high disease burden (1.77 vs 4.67 months,

Table 1. Baseline patients' characteristics.

Variable	All patients	
	N	%
Number of patients	66	
Age (years)		
Median (range)	69 (39–81)	
Gender		
Male	55	83.3
Female	11	16.7
Performance status		
0–1	51	77.3
2	15	22.7
Smoking status		
Active smokers	39	59.1
Former smokers	21	31.8
Never smokers	6	9.1
Body mass index (BMI)		
≥ 25 kg/m ²	32	48.5
< 25 kg/m ²	34	51.5
Histology		
Non-squamous	37	56.1
Squamous	29	43.9
Number of organs with metastases		
1–2	45	68.2
> 2	21	31.8
Brain metastases		
Yes	14	21.2
No	52	78.8
Liver metastases		
Yes	19	28.8
No	47	71.2
Bone metastases		
Yes	20	30.3
No	46	69.7
Lymph node metastases		
Yes	39	59.1
No	27	40.9
Baseline albumin levels		
< 3.5 g/dl	12	18.2
≥ 3.5 g/dl	51	77.2
Not available	3	4.5
Baseline LDH levels		
$> \text{UNL}$	20	30.3
$\leq \text{UNL}$	36	54.5
Not available	10	15.2
PDL1 levels		
$< 1\%$	12	18.2
$\geq 1\%$	20	30.3
Not available	34	51.5

(Continued)

Table 1. (Continued)

	All patients	
Variable	N	%
Steroid administration <10mg of daily prednisolone equivalent for more than 10 days within 15 days before initiation of immunotherapy or during the course of it (first 12 weeks)		
Steroids naïve	42	63.6
Steroids due to irAEs	8	12.1
Steroids for supportive reasons	16	24.2
Antibiotics administration within 30 days before the initiation of immunotherapy or during the course of it (first 12 weeks)		
Yes	34	51.5
No	32	48.5
Duration of antibiotics administration (days)		
Median (range)	5 (0–37)	
Prolonged administration of antibiotics ≥ 14 days within 30 days before the initiation of immunotherapy or during the course of it (first 12 weeks)		
Yes	22	33.3
No	44	66.7
Use of inhalation steroids for ≥ 3months before the initiation of immunotherapy		
Yes	10	15.2
No	56	84.8
Use of proton pump inhibitors for ≥ 3 months before the initiation of immunotherapy		
Yes	23	34.8
No	43	65.2
Grade III or IV iRAEs		
Yes	8	12.1
No	58	87.9
Response to immunotherapy		
CR	0	0
PR	10	15.2
SD	23	34.8
PD	33	50.0
Disease progression		
Yes	55	83.3
No	11	16.7
Death		
Yes	48	72.7
No	18	27.3
Duration of response (months)		
Median (range)	7.97 (2.8–26.9)	
Progression free survival (months)		
Median (range)	3.50 (0.16–26.9)	
Overall survival (months)		
Median (range)	6.77 (0.6–26.9)	
Follow up (months)		
Median (range)	6.37 (0.6–26.9)	

<https://doi.org/10.1371/journal.pone.0252537.t001>

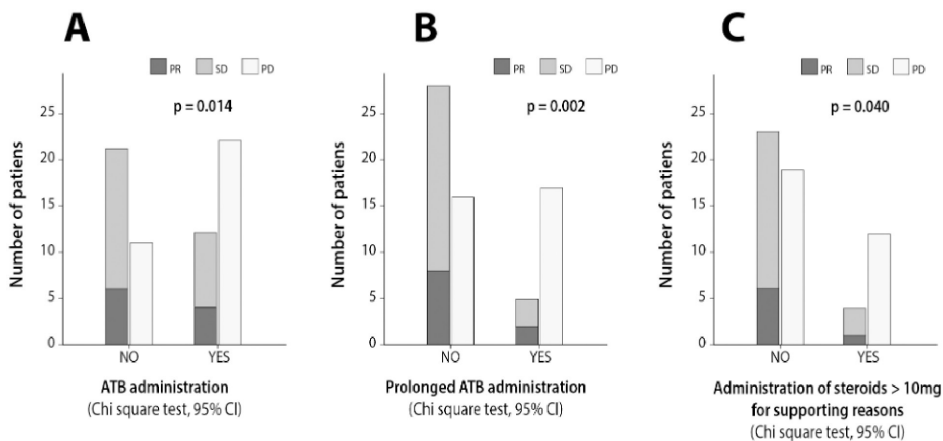


Fig 1. Bar plots depicting the effect of (A) ATB administration (B) prolonged ATB administration and (C) steroid administration > 10 mg on disease stabilization rates (PR or SD; Chi-square test, 95%).

<https://doi.org/10.1371/journal.pone.0252537.g001>

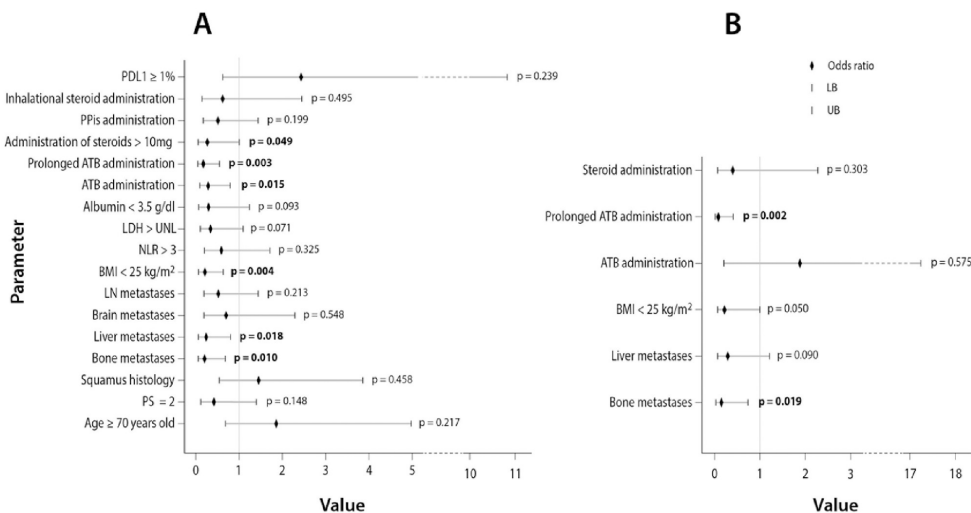


Fig 2. Forest plot depicting the odds ratios of the studied parameters for disease stabilization (PR or SD) in (A) univariate binary regression analysis and (B) multivariate binary regression analysis that included the variables that reached statistical significance ($p < 0.05$) in the univariate analysis. (LB: Lower border, UB: Upper border).

<https://doi.org/10.1371/journal.pone.0252537.g002>

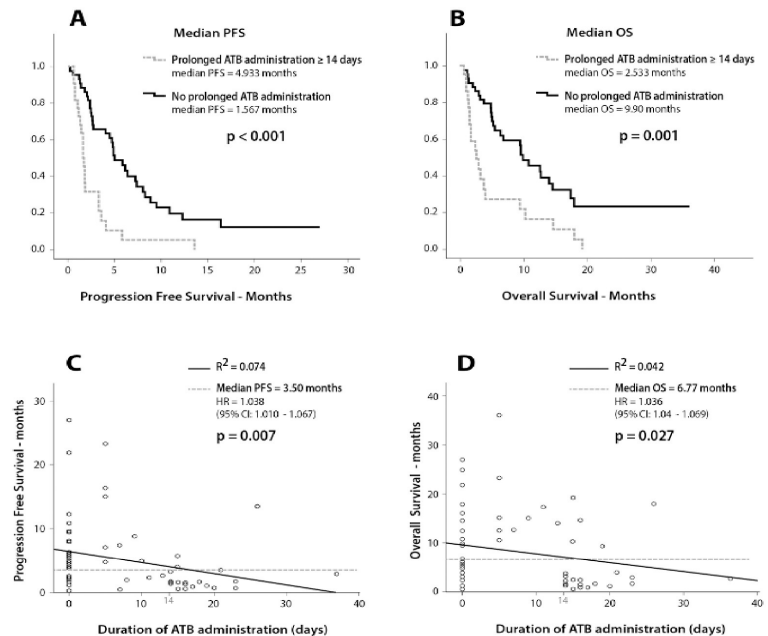


Fig 3. Survival analysis using Kaplan Meier and Cox regression. (A) Effect of prolonged ATB administration on PFS (B) Effect prolonged ATB administration on OS (C) Scatter plot depicting the effect of the duration of ATB administration in days as a continuous variable on PFS (D) Scatter plot depicting the effect of the duration of ATB administration in days as a continuous variable.

<https://doi.org/10.1371/journal.pone.0252537.g003>

$p = 0.008$) and the presence of liver (1.73 vs 4.80 months, $p = 0.002$) or bone metastases (2.10 vs 4.80 months, $p = 0.024$) were significantly associated with reduced PFS. In addition, baseline albumin levels < 3.5 g/dl (1.70 vs 4.40 months, $p = 0.005$) and baseline NLR > 3 (2.53 vs 4.93, $p = 0.024$) were also correlated with reduced PFS. Although ATB administration was not associated with lower PFS, ($p = 0.062$) (S2A Fig), prolonged ATB course (Fig 3A) and steroid administration > 10 mg for supportive reasons (S3A Fig) were significantly correlated with inferior PFS (1.57 vs 4.93 months, $p < 0.001$ and 1.27 vs 4.70 months, $p = 0.013$). None of the other analyzed covariates exhibited statistically significant correlations with PFS (S4A and S5A Figs and S6 Table).

Regarding their effect on patients' survival, PS 2 (3.17 vs 9.60 months, $p = 0.027$), baseline albumin levels < 3.5 g/dl (1.70 vs 9.57 months, $p = 0.003$), baseline LDH levels $> \text{UNL}$ (3.70 vs 9.90 months, $p = 0.040$) and the presence of bone metastases (3.77 vs 10.33 months, $p = 0.011$) exhibited a negative correlation with OS (S6A and S6B Fig). Prolonged ATB administration was associated with reduced OS (2.50 vs 9.93 months, $p = 0.001$) (Fig 3B), however, the use of steroids (2.53 vs 9.60 months, $p = 0.051$) or of ATB (4.00 vs 9.67 months, $p = 0.301$) (S2B and S3B Figs) were not correlated with reduced OS. No other associations with inferior OS were observed (S4B and S5B Figs and S6 Table).

Table 2. Univariate and multivariate analysis using Cox Regression Method.

Cox regression	PFS		OS	
Univariate analysis	HR (95% CI)	p value	HR (95%CI)	p value
Performance status	1.574(0.855–2.899)	0.145	1.999(1.068–3.740)	0.030
Age ≥ 70 years old	1.127(0.661–1.922)	0.660	1.193(0.673–2.114)	0.546
Smoker of former smoker	1.126(0.404–3.135)	0.821	2.361(0.571–9.757)	0.235
Female gender	1.033(0.504–2.120)	0.929	1.144(0.535–2.445)	0.729
Brain metastases	1.242(0.653–2.364)	0.509	1.022(0.493–2.118)	0.953
Bone metastases	1.913(1.078–3.394)	0.027	2.135(1.171–3.893)	0.013
Liver metastases	2.503(1.390–4.506)	0.002	1.443(0.781–2.665)	0.241
Disease burden	2.115(1.201–3.725)	0.009	1.562(0.860–2.840)	0.142
Steroid administration > 10 mg	2.156(1.158–4.013)	0.015	1.908(0.985–3.698)	0.055
ATB ^a administration	1.655(0.068–2.830)	0.065	1.353(0.761–2.406)	0.304
Prolonged ATB administration ≥ 14 days	3.181(1.795–5.637)	0.0001	2.646(1.476–4.741)	0.001
NLR ^b	1.939(1.050–3.559)	0.033	1.588(0.855–2.947)	0.143
LDH>UNL	1.674(0.935–2.997)	0.083	1.868(1.018–3.425)	0.044
Multivariate analysis	HR (95% CI)	p value	HR (95%CI)	p value
Performance status			1.878(0.963–3.661)	0.075
Bone metastasis	2.244(1.155–4.360)	0.017	1.890(1.017–3.512)	0.049
Liver metastasis	3.266(1.653–6.375)	0.001		
Disease burden	1.552(0.555–4.329)	0.401		
Steroid administration > 10 mg	2.566(1.347–4.887)	0.004		
Prolonged ATB administration ≥ 14 days	3.403(1.817–6.375)	0.0001	2.945(1.619–5.358)	0.0001
NLR	1.147(0.580–2.269)	0.693		
LDH > UNL ^c			1.618(0.877–2.985)	0.123

^a: ATB = Antibiotics,

^b: NRL = Neutrophil to Lymphocyte ratio,

^c: UNL = Upper normal limit (247 Units/liter).

<https://doi.org/10.1371/journal.pone.0252537.t002>

Univariate and multivariate survival analysis

Cox Regression analysis revealed that the duration of ATB administration evaluated as a continuous nominal variable was negatively correlated with PFS ($p = 0.007$, CI 95%) and OS ($p = 0.027$, 95% CI) (Fig 3C and 3D).

In the univariate analysis for PFS, baseline albumin levels were not included in the analysis due to insufficient number of events; results are shown in Table 2. Multivariate analysis demonstrated that steroids used for supportive reasons [HR = 2.556 (CI: 1.347–4.887, $p = 0.004$)], prolonged administration of ATBs [HR = 3.403 (CI: 1.817–6.375, $p = 0.0001$)] and the presence of liver [HR = 3.266 (CI: 1.653–6.375, $p = 0.001$)] or bone metastases [HR = 2.244 (CI: 1.155–4.360, $p = 0.017$)] were independent predictors for inferior PFS (Table 2).

In the multivariate analysis for OS, prolonged use of ATBs [HR = 2.945 (CI: 1.619–5.358, $p = 0.0001$)] and bone metastases [HR = 1.890 (CI: 1.017–3.512, $p = 0.049$)] were independently associated with reduced survival (Table 2).

Multivariate analysis using the JADBio tool

For the classification task (response to ICIs), patients were divided into two groups; responders were characterized as those experiencing PR or SD and non-responders were those experiencing PD as best response to treatment. For the classification analysis, JADbio tried 3017

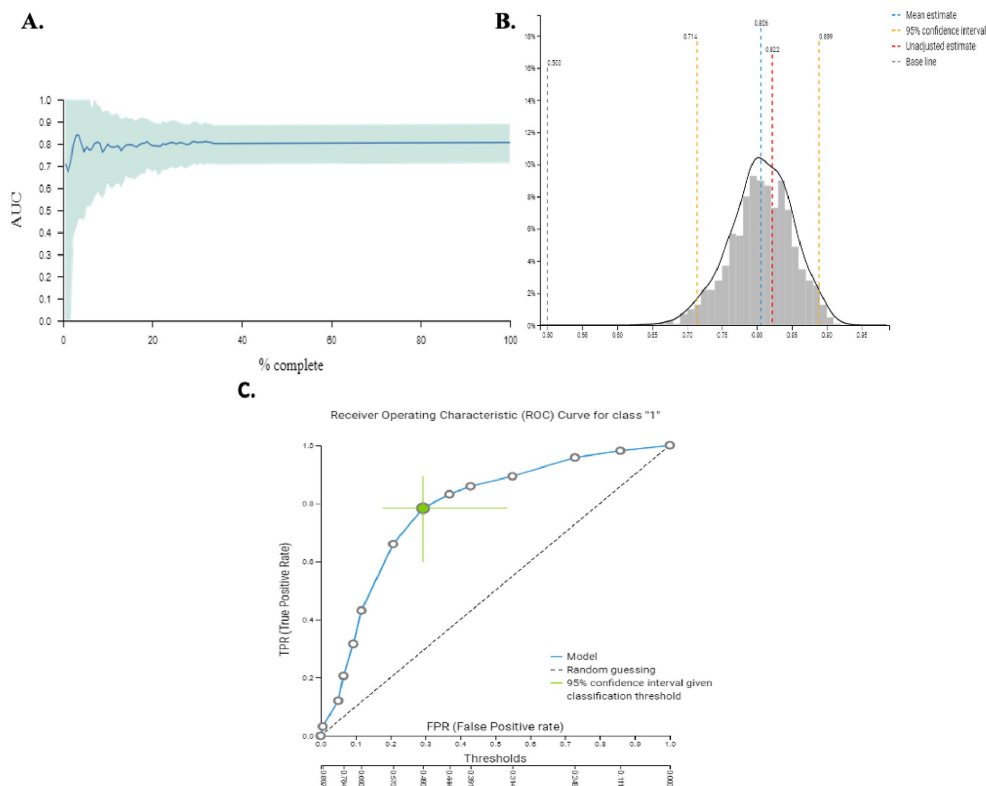


Fig 4. A. Visualization of the learning process of JADbio for the classification analysis of our data. JADbio tried 3017 configurations and trained 211190 models in total. B. Distribution of the performance metric (AUC) of our model. The distribution is computed on out of sample predictions of the current model. C. Receiver Operating Characteristic (ROC) Curve for the best performing model (Support Vector Machines (SVM) of type C-SVC with Polynomial Kernel and hyper-parameters: cost = 0.01, gamma = 1.0, degree = 4). The classification threshold for the 95% confidence intervals has been set at the average F1/accuracy/Balance accuracy.

<https://doi.org/10.1371/journal.pone.0252537.g004>

configurations and trained 211190 models (Fig 4A). JADbio performed LASSO feature selection (penalty = 0.5, lambda = 0.027) and selected 4 features: prolonged ATB administration, bone metastases, liver metastases and BMI < 25 kg/m² for the original signature. In total there was only one signature. The predictive algorithm of the best performing model was SVM of type C-SVC with Polynomial Kernel and hyper-parameters: cost = 0.01, gamma = 1.0, degree = 4 with an AUC = 0.806 [0.714–0.889] (Fig 4B). The ROC curve of the best performing model is demonstrated in Fig 4C. In addition, the classification analysis was able to calculate the feature importance of the selected features on the probability of achieving PR or SD which was defined as the percentage drop in predictive performance when each particular feature was removed from the model (Fig 5A). The box plots that visualize the contrast of the cross-validated predicted probability of belonging to a specific class against the actual class of the samples are depicted in Fig 5B.

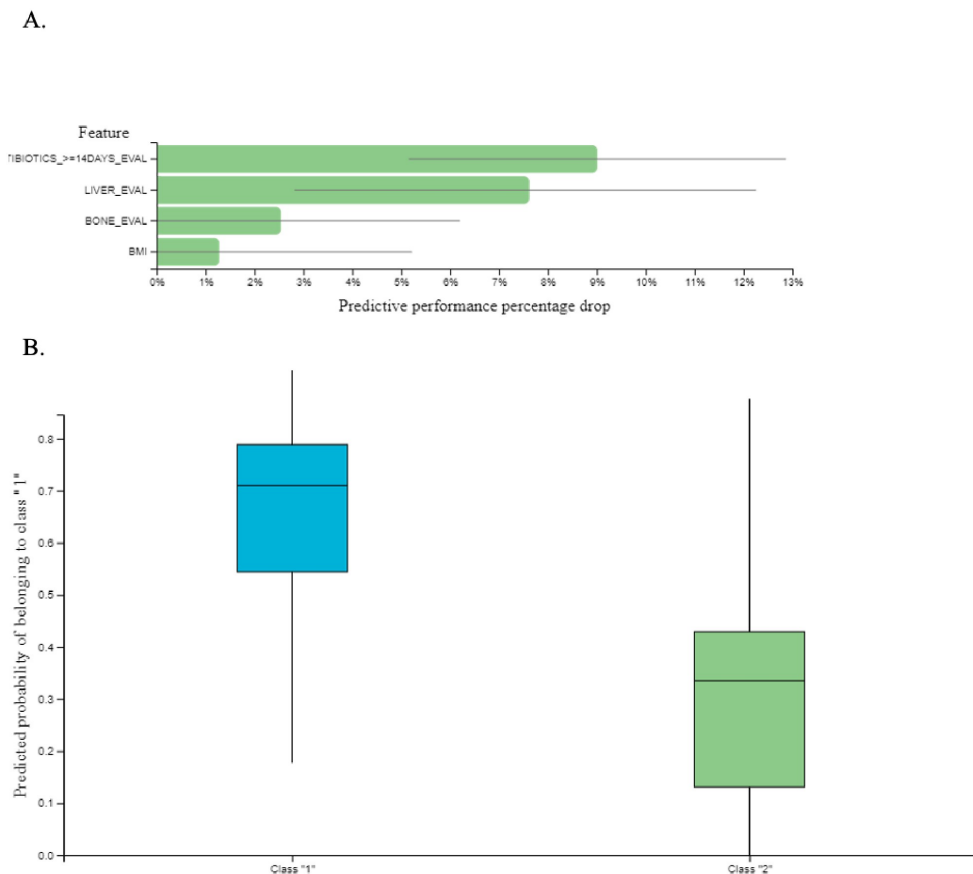


Fig 5. A. Feature importance plot: This chart reports feature importance defined as the percentage drop in predictive performance when the feature is removed from the model. Grey lines indicate 95% confidence intervals. B. The Box-Plot contrasts the cross-validated predicted probability of belonging to a specific class against the actual class of the samples. Well-performing models are expected to provide predictions that are close to 1 for the actual class and close to 0 for all other class. Class 1 is the probability of achieving PR or SD as response to immunotherapy and class 2 is the probability of developing disease progression.

<https://doi.org/10.1371/journal.pone.0252537.g005>

Discussion

The primary aim of our study was to prospectively evaluate the effect of common clinical and laboratory parameters on the outcome of patients with metastatic NSCLC receiving immunotherapy. We herein demonstrate that routinely available patient and disease characteristics are correlated with treatment outcomes and can be integrated into a multifactorial model predicting individual clinical benefit from ICIs using a machine learning approach.

In our cohort, bone metastases constituted an adverse prognostic factor in NSCLC patients treated with second line ICIs. In accordance, previous retrospective studies highlight that ICI

efficacy may vary according to the presence of specific disease sites [29, 30]. Furthermore, we observed that patients with low BMI had shorter PFS compared to patients with high BM. Low albumin levels were also significantly associated with both shorter PFS and OS in our cohort. However, it should be noted that BMI and/or albumin levels cannot be used alone for the evaluation of patients' nutritional status. More detailed analysis is required to further elucidate the impact of body composition in the outcome of cancer patients treated with immunotherapy [31, 32]. Performance status 2 did not emerge as an independent negative prognostic factor, however this could be attributed to the small sample size of our cohort and the fact that only 15 patients had performance status 2, leading to increased probability for a statistical type I error.

The administration of commonly used co-medications exerted a significant impact on patients' outcome in our analysis. The time frame of 12 weeks from the start of ICIs initiation employed for the classification of patients according to the use of steroids and ATBs was set to avoid a bias for those achieving long term clinical remissions, who thus, would have a higher possibility for steroid and ATB use during the course of their illness. ATB administration as a categorical variable did not affect PFS or OS, however when we examined the effect of their administration in days as a continuous nominal variable, a statistically significant negative correlation with PFS and OS was revealed. Importantly, prolonged ATBs administration emerged as an independent predictor for reduced probability of disease stabilization and for inferior PFS and OS. Our results are in accordance with previously published prospective and retrospective studies [33, 34] and further reinforce the data published by Tinsley et al [35] reporting worst outcomes with cumulative ATB administration in patients with metastatic malignancies receiving ICIs indicating a dose dependent effect between ATB exposure and reduced ICI efficacy. Our findings along with the results from previously published reports suggest that ATB administration, especially for longer time periods should be avoided in patients receiving immunotherapy.

In our analysis we classified patients who received steroids into two different subgroups, those who were administered steroids for supportive reasons and those who received high dose steroids due to immune related adverse effects (irAEs). In our cohort, the use of steroids for supportive reasons was independently associated with shorter PFS, however no associations with OS were revealed. Regrettably, due to the small number of patients we were not able to perform more detailed subgroup analysis regarding the specific reasons for the supportive administration of steroids, however, our findings reinforce previous reports raising concerns regarding the use of > 10 mg prednisone equivalent in patients receiving ICIs [36]. On the contrary, the administration of inhalational steroids or of PPIs did not impair treatment outcomes in our analysis and their administration seems safe. Our results regarding the effects of PPIs are in contrast with a recent published retrospective analysis by Hopkins et al [37] demonstrating that PPIs negatively affected survival outcomes in individuals with metastatic urothelial cancer treated with atezolizumab. Therefore, further research is needed in order to clarify their effects on the efficacy of ICIs.

We further incorporated all the recorded parameters into JADbio, an artificial intelligence (AI) system, with to evaluate how these different features interact with one another and to examine the feature importance of each particular parameter on individual treatment outcomes in an integrative manner. JADbio selected four clinical features and created a signature that was able to predict the possibility for disease stabilization as result of treatment with ICIs with an accuracy of 81%. These four features consisted of prolonged ATB administration, bone metastases, liver metastases and BMI < 25 kg/m². The higher feature importance obtained for prolonged ATB administration further underscores the importance of the microbiome composition for an effective antitumor immune response [16]. Interestingly, they

indicate that factors likely inherent to the biology of the primary tumour are related to both the specific patterns of metastatic spread and the response to ICIs.

Previous studies have employed AI for the prediction of outcome of patients with metastatic melanoma and NSCLC receiving treatment with ICIs [38, 39]. Despite the significant smaller sample of the cohort studied herein, our analysis provides the advantage of including a wider range of routinely available, easily obtainable clinical parameters and more importantly it allows the calculation of each parameter's feature importance on the determination of an individual's outcome. Using JADbio, we constructed a novel multivariate model predicting the individual possibility of achieving disease stabilization in patients with metastatic NSCLC treated with ICIs in the second line setting with accuracy at the level of 81%. Using other AutoML services, an overestimation of the final predictive performance might have resulted, as they mainly use cross-validation, which overfits in sample-sample scenarios [40]. JADBio is built for such scenarios and uses a technique [24] to remove this cross-validation bias, rendering the final performance estimation conservative and reliable.

Our results indicate that routinely available variables could be used to identify individuals who will achieve disease control with ICIs and to spot those who will likely progress on treatment for whom closer monitoring, alternative treatment regimens or participation in clinical trials should be advised. However, it should be also noted that immunotherapy has now moved into the first line treatment setting either as a monotherapy or in combination with chemotherapy and that only a minority of patients now receive ICIs in the second line or beyond.

Strengths of our study include the prospective evaluation and analysis of a wide range of common and easily accessible clinical and laboratory parameters and of common co-mediations in a cohort of lung cancer patients treated with immunotherapy to determine their prognostic role. A significant novelty of our report represents the additional multivariate analysis using an AutoML interface to further determine the integrated feature importance of each of these parameters on individual patient outcomes. Limitations of our study are the small statistical sample and the fact that PD-L1 levels were not included in our model due to high rates of missing data. In addition, our results were not validated in another patient cohort.

Conclusion

Our results corroborate previous evidence regarding the negative predictive role of liver and bone metastases in NSCLC patients treated with ICIs. Furthermore, they emphasize the negative effect of ATBs on patient outcomes and suggest that long-term ATBs use should be avoided in these patients. By incorporating our data into the JADbio machine learning system, we were able to distinguish the clinical variables that are most relevant for achieving disease control with immunotherapy. Importantly, we estimated the feature importance of these variables on individual patient outcomes in an integrative manner. Since immunotherapy is currently mostly used either as first line treatment, either as a single agent or in combination with chemotherapy, our findings merit further evaluation in these settings.

Supporting information

S1 Table. Binary classification of patients' feature input in JADBio.
(DOC)

S2 Table. Chi square test demonstrating the association of the analyzed clinical parameters with a prolonged ATB course.
(DOC)

S3 Table. Effect of the studied variables on response rates.

(DOC)

S4 Table. Effect of the studied variables on disease stabilization rates.

(DOC)

S5 Table. Univariate and multivariate logistic regression on the Odds Ratio (OR) of the analyzed covariates on the probability of achieving disease stabilization (PR or SD) as response to treatment with ICIs.

(DOC)

S6 Table. Kaplan Meier method (log-rank test) on the effect of the studied parameters on PFS and OS.

(DOC)

S1 Fig. Mann-Whitney U test examining the effect of the duration of ATB administration in days on DS rates. On the left side are the days on ATB of the patients that experienced PD and on the right side the days on ATB of those who had DS (PR or SD) as response to ICI administration.

(DOC)

S2 Fig. Kaplan-Meier curves on the effect of ATB administration on PFS (A) and OS (B).

(DOC)

S3 Fig. Kaplan-Meier curves on the effect of steroid administration > 10 mg on PFS (A) and OS (B).

(DOC)

S4 Fig. Kaplan-Meier curves on the effect of chronic PPIs administration on (A) PFS and (B) OS.

(DOC)

S5 Fig. Kaplan-Meier curves on the effect of inhalational steroids administration on (A) PFS and (B).

(DOC)

S6 Fig. Kaplan Meier curves depicting the effect of the following parameters on OS (A) Baseline albumin levels <3.5 g/dl (B) Presence of bone metastases.

(DOC)

Acknowledgments

We would like to thank Pavlos Charonyktakis (CTO and co-founder of JADBio) for his insights on the JADBio application methodology and the interpretation of results. We would also like to thank all the patients and their families who participated in this study.

Author Contributions

Conceptualization: Sofia Agelaki.

Data curation: Dimitrios Makrakis, Chara Papadaki, Alexia Monastirioti, Lambros Vamvakas, Konstantinos Kalbakis.

Formal analysis: Konstantinos Rounis, Chara Papadaki.

Investigation: Konstantinos Rounis, Dimitrios Makrakis, Alexia Monastiriotti, Lambros Vamvakas, Konstantinos Kalbakis.

Methodology: Konstantinos Rounis, Chara Papadaki, Sofia Agelaki.

Software: Krystallia Gourlia, Iordanis Xanthopoulos, Ioannis Tsamardinos.

Supervision: Ioannis Tsamardinos, Dimitrios Mavroudis, Sofia Agelaki.

Validation: Ioannis Tsamardinos.

Writing – original draft: Konstantinos Rounis.

Writing – review & editing: Konstantinos Rounis, Chara Papadaki, Dimitrios Mavroudis, Sofia Agelaki.

References

1. Brahmer J, Reckamp KL, Baas P, Crinò L, Eberhardt WEE, Poddubskaya E, et al. Nivolumab versus Docetaxel in Advanced Squamous-Cell Non–Small-Cell Lung Cancer. *New England Journal of Medicine* [Internet]. 2015 Jul 9 [cited 2020 May 15]; 373(2):123–35. <https://doi.org/10.1056/NEJMoa1504627> PMID: 26028407
2. Borghaei H, Paz-Ares L, Horn L, Spigel DR, Steins M, Ready NE, et al. Nivolumab versus Docetaxel in Advanced Nonsquamous Non–Small-Cell Lung Cancer. *N Engl J Med*. 2015 Oct 22; 373(17):1627–39. <https://doi.org/10.1056/NEJMoa1507643> PMID: 26412456
3. Rittmeyer A, Barlesi F, Waterkamp D, Park K, Ciardiello F, von Pawel J, et al. Atezolizumab versus docetaxel in patients with previously treated non-small-cell lung cancer (OAK): a phase 3, open-label, multi-centre randomised controlled trial. *Lancet*. 2017 21; 389(10066):255–65. [https://doi.org/10.1016/S0140-6736\(16\)32517-X](https://doi.org/10.1016/S0140-6736(16)32517-X) PMID: 27979383
4. Socinski MA, Jotte RM, Cappuzzo F, Orlandi F, Stroyakovskiy D, Nogami N, et al. Atezolizumab for First-Line Treatment of Metastatic Nonsquamous NSCLC. *N Engl J Med*. 2018 Jun 14; 378(24):2288–301. <https://doi.org/10.1056/NEJMoa1716948> PMID: 29863955
5. Gandhi L, Rodríguez-Abreu D, Gadgeel S, Esteban E, Felip E, De Angelis F, et al. Pembrolizumab plus Chemotherapy in Metastatic Non-Small-Cell Lung Cancer. *N Engl J Med*. 2018 May 31; 378(22):2078–92. <https://doi.org/10.1056/NEJMoa1801005> PMID: 29658856
6. Georgieva M, da Silveira Nogueira Lima JP, Aguiar P, de Lima Lopes G, Haaland B. Cost-effectiveness of pembrolizumab as first-line therapy for advanced non-small cell lung cancer. *Lung Cancer*. 2018; 124:248–54. <https://doi.org/10.1016/j.lungcan.2018.08.018> PMID: 30268469
7. Verma V, Sprave T, Haque W, Simone CB, Chang JY, Welsh JW, et al. A systematic review of the cost and cost-effectiveness studies of immune checkpoint inhibitors. *J Immunother Cancer*. 2018 23; 6(1):128. <https://doi.org/10.1186/s40425-018-0442-7> PMID: 30470252
8. Martin L, Senesse P, Gioulbasanis I, Antoun S, Bozzetti F, Deans C, et al. Diagnostic Criteria for the Classification of Cancer-Associated Weight Loss. *JCO* [Internet]. 2014 Nov 24 [cited 2020 May 16]; 33(1):90–9. Available from: <https://ascopubs.org/doi/full/10.1200/JCO.2014.56.1894> PMID: 25422490
9. Laird BJ, Kaasa S, McMillan DC, Fallon MT, Hjermstad MJ, Fayes P, et al. Prognostic factors in patients with advanced cancer: a comparison of clinicopathological factors and the development of an inflammation-based prognostic system. *Clin Cancer Res*. 2013 Oct 1; 19(19):5456–64. <https://doi.org/10.1158/1078-0432.CCR-13-1066> PMID: 23938289
10. Kazandjian D, Gong Y, Keegan P, Pazdur R, Blumenthal GM. Prognostic Value of the Lung Immune Prognostic Index for Patients Treated for Metastatic Non-Small Cell Lung Cancer. *JAMA Oncol*. 2019 Jul 25; <https://doi.org/10.1001/jamaoncol.2019.1747> PMID: 31343662
11. Sun H, Hu P, Shen H, Dong W, Zhang T, Liu Q, et al. Albumin and Neutrophil Combined Prognostic Grade as a New Prognostic Factor in Non-Small Cell Lung Cancer: Results from a Large Consecutive Cohort. *PLOS ONE*. 2015 Dec 14; 10(12):e0144663. <https://doi.org/10.1371/journal.pone.0144663> PMID: 26656866
12. Hopkins AM, Rowland A, Kichenadasse G, Wiese MD, Gurney H, McKinnon RA, et al. Predicting response and toxicity to immune checkpoint inhibitors using routinely available blood and clinical markers. *Br J Cancer* [Internet]. 2017 Sep 26 [cited 2020 May 15]; 117(7):913–20. Available from: <https://www.ncbi.nlm.nih.gov/pmc/articles/PMC5625676/> <https://doi.org/10.1038/bjc.2017.274> PMID: 28950287

13. Ren F, Zhao T, Liu B, Pan L. Neutrophil-lymphocyte ratio (NLR) predicted prognosis for advanced non-small-cell lung cancer (NSCLC) patients who received immune checkpoint blockade (ICB). *Onco Targets Ther*. 2019; 12:4235–44. <https://doi.org/10.2147/OTT.S199176> PMID: 31239702
14. Weide B, Martens A, Hassel JC, Berking C, Postow MA, Bisschop K, et al. Baseline Biomarkers for Outcome of Melanoma Patients Treated with Pembrolizumab. *Clin Cancer Res*. 2016 Nov 15; 22(22):5487–96. <https://doi.org/10.1158/1078-0432.CCR-16-0127> PMID: 27185375
15. Belkaid Y, Hand T. Role of the Microbiota in Immunity and inflammation. *Cell* [Internet]. 2014 Mar 27 [cited 2020 May 15]; 157(1):121–41. Available from: <https://www.ncbi.nlm.nih.gov/pmc/articles/PMC4056765/> <https://doi.org/10.1016/j.cell.2014.03.011> PMID: 24679531
16. Vétizou M, Pitt JM, Daillère R, Lepage P, Waldschmitt N, Flament C, et al. Anticancer immunotherapy by CTLA-4 blockade relies on the gut microbiota. *Science*. 2015 Nov 27; 350(6264):1079–84. <https://doi.org/10.1126/science.1255557> PMID: 26541610
17. Palleja A, Mikkelsen KH, Forslund SK, Kashani A, Allin KH, Nielsen T, et al. Recovery of gut microbiota of healthy adults following antibiotic exposure. *Nature Microbiology* [Internet]. 2018 Nov [cited 2020 May 15]; 3(11):1255–65. Available from: <https://www.nature.com/articles/s41564-018-0257-9> PMID: 30349083
18. Imhann F, Bonder MJ, Vich Vila A, Fu J, Mujagic Z, Vork L, et al. Proton pump inhibitors affect the gut microbiome. *Gut*. 2016 May; 65(5):740–8. <https://doi.org/10.1136/gutjnl-2015-310376> PMID: 26657899
19. Arbour KC, Mezquita L, Long N, Rizvi H, Auclin E, Ni A, et al. Impact of Baseline Steroids on Efficacy of Programmed Cell Death-1 and Programmed Death-Ligand 1 Blockade in Patients With Non-Small-Cell Lung Cancer. *J Clin Oncol*. 2018 1; 36(28):2872–8. <https://doi.org/10.1200/JCO.2018.79.0006> PMID: 30125216
20. Brusselle G, Bracke K. Targeting immune pathways for therapy in asthma and chronic obstructive pulmonary disease. *Ann Am Thorac Soc*. 2014 Dec; 11 Suppl 5:S322–328. <https://doi.org/10.1513/AnnalsATS.201403-118AW> PMID: 25525740
21. Orfanoudaki G, Markaki M, Chatzi K, Tsamardinos I, Economou A. MatureP: prediction of secreted proteins with exclusive information from their mature regions. *Sci Rep*. 2017 12; 7(1):3263. <https://doi.org/10.1038/s41598-017-03557-4> PMID: 28607462
22. Panagopoulou M, Karagiani M, Balgkouranidou I, Biziota E, Koukaki T, Karamitrous E, et al. Circulating cell-free DNA in breast cancer: size profiling, levels, and methylation patterns lead to prognostic and predictive classifiers. *Oncogene*. 2019; 38(18):3387–401. <https://doi.org/10.1038/s41388-018-0660-y> PMID: 30643192
23. Eisenhauer EA, Therasse P, Bogaerts J, Schwartz LH, Sargent D, Ford R, et al. New response evaluation criteria in solid tumours: revised RECIST guideline (version 1.1). *Eur J Cancer*. 2009 Jan; 45(2):228–47. <https://doi.org/10.1016/j.ejca.2008.10.026> PMID: 19097774
24. Tsamardinos I, Greasidou E, Tsagris M, Borboudakis G. Bootstrapping the Out-of-sample Predictions for Efficient and Accurate Cross-Validation. *Machine Learning*. 2017 Aug 23; 107.
25. Boser BE, Guyon IM, Vapnik VN. A training algorithm for optimal margin classifiers. In: *Proceedings of the fifth annual workshop on Computational learning theory* [Internet]. Pittsburgh, Pennsylvania, USA: Association for Computing Machinery; 1992 [cited 2020 May 15]. p. 144–152. (COLT '92).
26. Breiman L. Random Forests. *Machine Learning* [Internet]. 2001 Oct 1 [cited 2020 May 16]; 45(1):5–32. <https://doi.org/10.1023/A:1010933404324>
27. Ridge Regression: Biased Estimation for Nonorthogonal Problems: *Technometrics*: Vol 12, No 1 [Internet]. [cited 2020 May 15]. <https://www.tandfonline.com/doi/abs/10.1080/00401706.1970.10488634>
28. Breiman L, Friedman JH, Olshen RA, Stone CJ. *Classification and Regression Trees* [Internet]. 1983 [cited 2020 May 15]. <https://www.semanticscholar.org/paper/Classification-and-Regression-Trees-Breiman-Friedman/8017699564136f93af21575810d557dba1ee6fc6>
29. Prelaj A, Ferrara R, Rebuzzi SE, Proto C, Signorelli D, Galli G, et al. EPSiLoN: A Prognostic Score for Immunotherapy in Advanced Non-Small-Cell Lung Cancer: A Validation Cohort. *Cancers* [Internet]. 2019 Dec [cited 2020 May 15]; 11(12):1954. Available from: <https://www.mdpi.com/2072-6694/11/12/1954> <https://doi.org/10.3390/cancers11121954> PMID: 31817541
30. Landi L, D'Incà F, Gelibter A, Chiari R, Grossi F, Delmonte A, et al. Bone metastases and immunotherapy in patients with advanced non-small-cell lung cancer. *Journal for ImmunoTherapy of Cancer* [Internet]. 2019 Nov 21 [cited 2020 May 15]; 7(1):316. <https://doi.org/10.1186/s40425-019-0793-8> PMID: 31752994
31. Kichenadasse G, Miners JO, Mangoni AA, Rowland A, Hopkins AM, Sorich MJ. Association Between Body Mass Index and Overall Survival With Immune Checkpoint Inhibitor Therapy for Advanced Non-Small Cell Lung Cancer. *JAMA Oncol*. 2019 Dec 26;

32. Fearon K, Strasser F, Anker SD, Bosaeus I, Bruera E, Fainsinger RL, et al. Definition and classification of cancer cachexia: an international consensus. *Lancet Oncol*. 2011 May; 12(5):489–95. [https://doi.org/10.1016/S1470-2045\(10\)70218-7](https://doi.org/10.1016/S1470-2045(10)70218-7) PMID: 21296615
33. Derosa L, Hellmann MD, Spaziano M, Halpenny D, Fidelle M, Rizvi H, et al. Negative association of antibiotics on clinical activity of immune checkpoint inhibitors in patients with advanced renal cell and non-small-cell lung cancer. *Ann Oncol*. 2018 1; 29(6):1437–44. <https://doi.org/10.1093/annonc/mdy103> PMID: 29617710
34. Pinato DJ, Howlett S, Ottaviani D, Urus H, Patel A, Mineo T, et al. Association of Prior Antibiotic Treatment With Survival and Response to Immune Checkpoint Inhibitor Therapy in Patients With Cancer. *JAMA Oncol*. 2019 Sep 12; <https://doi.org/10.1001/jamaoncol.2019.2785> PMID: 31513236
35. Tinsley N, Zhou C, Tan G, Rack S, Lorigan P, Blackhall F, et al. Cumulative Antibiotic Use Significantly Decreases Efficacy of Checkpoint Inhibitors in Patients with Advanced Cancer. *Oncologist*. 2020; 25(1):55–63. <https://doi.org/10.1634/theoncologist.2019-0160> PMID: 31292268
36. Ricciuti B, Dahlberg SE, Adeni A, Sholl LM, Nishino M, Awad MM. Immune Checkpoint Inhibitor Outcomes for Patients With Non-Small-Cell Lung Cancer Receiving Baseline Corticosteroids for Palliative Versus Nonpalliative Indications. *J Clin Oncol*. 2019 1; 37(22):1927–34. <https://doi.org/10.1200/JCO.19.00189> PMID: 31206316
37. Hopkins AM, Kichenadasse G, Karapetis CS, Rowland A, Sorich MJ. Concomitant Proton Pump Inhibitor Use and Survival in Urothelial Carcinoma Treated with Atezolizumab. *Clin Cancer Res [Internet]*. 2020 Sep 15 [cited 2020 Sep 21]; <https://clincancerres.aacrjournals.org/content/early/2020/09/11/1078-0432.CCR-20-1876> PMID: 32933995
38. Park W, Mezquita L, Okabe N, Chae YK, Kwon D, Saravia D, et al. Association of the prognostic model iSENd with PD-1/L1 monotherapy outcome in non-small-cell lung cancer. *Br J Cancer*. 2020 Feb; 122(3):340–7. <https://doi.org/10.1038/s41416-019-0643-y> PMID: 31761899
39. Trebeschi S, Drago SG, Birkbak NJ, Kurilova I, Călin AM, Delli Pizzi A, et al. Predicting response to cancer immunotherapy using noninvasive radiomic biomarkers. *Ann Oncol [Internet]*. 2019 Jun [cited 2020 May 15]; 30(6):998–1004. Available from: <https://www.ncbi.nlm.nih.gov/pmc/articles/PMC6594459/> <https://doi.org/10.1093/annonc/mdz108> PMID: 30895304
40. Cawley GC, Talbot NLC. On Over-fitting in Model Selection and Subsequent Selection Bias in Performance Evaluation. *Journal of Machine Learning Research [Internet]*. 2010 [cited 2020 May 15]; 11(70):2079–107. Available from: <http://jmlr.org/papers/v11/cawley10a.html>

S1 Table: Binary classification of patients’ feature input in JADBio.

Parameter	Feature	JADBio input
Female gender	Yes	1
	No	2
Performance status 0-1	Yes	1
	No	2
Age ≥ 70 years old	Yes	1
	No	2
BMI < 25 kg/m ²	Yes	1
	No	2
Non-squamous histology	Yes	1
	No	2
Presence of brain metastases	Yes	1
	No	2
Presence of liver metastases	Yes	1
	No	2
Presence of lung or pleural metastases	Yes	1
	No	2
Presence of bone metastases	Yes	1
	No	2
Presence of LN metastases	Yes	1
	No	2
LDH ≤ UNL	Yes	1
	No	2
Albumin < 3.5 g/dl	Yes	1
	No	2
Baseline NLR > 3	Yes	1
	No	2
ATB administration	Yes	1
	No	2
Prolonged ATB administration ≥ 14 days duration	Yes	1
	No	2
Steroid administration > 10 mg for ≥ 10 days	Yes	1
	No	2
Chronic PPis administration	Yes	1
	No	2
Chronic administration of inhalational steroids	Yes	1
	No	2
PR or SD to 1st line platinum doublet	Yes	1
	No	2
PR or SD to immunotherapy	Yes	1
	No	2

Abbreviations: BMI=Body mass index, LDH=Lactate dehydrogenase, UNL=Upper normal limit (247 units/liter), NLR=Neutrophile to lymphocyte ratio, PR=Partial response, SD=Disease stabilization, ATB=Antibiotics, PPis=Proton pump inhibitors



Original Article

Cancer cachexia syndrome and clinical outcome in patients with metastatic non-small cell lung cancer treated with PD-1/PD-L1 inhibitors: results from a prospective, observational study

Konstantinos Rounis^{1^}, Dimitrios Makrakis², Alexandros-Pantelis Tsigkas³, Alexandra Georgiou³, Nikolaos Galanakis⁴, Chara Papadaki⁵, Alexia Monastiriotti⁵, Lambros Vamvakas¹, Konstantinos Kalbakis¹, Nikolaos Vardakis¹, Meropi Kontogianni³, Ioannis Gioulbasanis⁶, Dimitrios Mavroudis^{1,5}, Sofia Agelaki^{1,5}

¹Department of Medical Oncology, University General Hospital of Heraklion, Heraklion, Crete, Greece; ²Division of Oncology, University of Washington Medical School, Seattle, WA, USA; ³Department of Nutrition & Dietetics, School of Health Sciences and Education, Harokopio University, Athens, Greece; ⁴Department of Medical Imaging, University General Hospital, Heraklion, Crete, Greece; ⁵Laboratory of Translational Oncology, School of Medicine, University of Crete, Heraklion, Greece; ⁶Department of Medical Oncology, Animus Kyanus Stavros General Clinic, Larissa, Greece

Contributions: (I) Conception and design: S Agelaki; (II) Administrative support: None; (III) Provision of study materials or patients: K Rounis, L Vamvakas, K Kalbakis, N Vardakis, S Agelaki, D Mavroudis; (IV) Collection and assembly of data: K Rounis, D Makrakis, N Galanakis, C Papadaki, A Monastiriotti; (V) Data analysis and interpretation: K Rounis, AP Tsigkas, A Georgiou, M Kontogianni, I Gioulbasanis, D Mavroudis, S Agelaki; (VI) Manuscript writing: All authors; (VII) Final approval of manuscript: All authors.

Correspondence to: Konstantinos Rounis, MD. Medical Oncologist, University General Hospital of Heraklion, Crete, Greece. Email: kostas@rounis.gr.

Background: Cancer cachexia syndrome (CCS) is an adverse prognostic factor in cancer patients undergoing chemotherapy or surgical procedures. We performed a prospective study to investigate the effect of CCS on treatment outcomes in patients with non-oncogene driven metastatic non-small cell lung cancer (NSCLC) undergoing therapy with programmed cell death protein 1 (PD-1)/programmed death ligand 1 (PD-L1) inhibitors.

Methods: Patients were categorized as having cancer cachexia if they had weight loss >5% in the last 6 months prior to immunotherapy (I-O) initiation or any degree of weight loss >2% and body mass index (BMI) <20 kg/m² or skeletal muscle index at the level of third lumbar vertebra (LSMI) <55 cm²/m² for males and <39 cm²/m² for females. LSMI was calculated using computed tomography (CT) scans of the abdomen at the beginning of I-O and every 3 months thereafter.

Results: Eighty-three patients were included in the analysis and the prevalence of cancer cachexia at the beginning of I-O was 51.8%. The presence of CCS was associated with inferior response rates to ICIs (P≤0.001) and consisted an independent predictor of increased probability for developing disease progression as best response to treatment, OR =8.11 (95% CI: 2.95–22.40, P≤0.001). In the multivariate analysis, the presence of baseline cancer cachexia consisted an independent predictor for inferior survival, HR =2.52 (95% CI: 1.40–2.55, P=0.002). Reduction of LSMI >5% during treatment did not affect overall survival (OS; P=0.40).

Conclusions: CCS is associated with reduced PD-1/PD-L1 inhibitor efficacy in NSCLC patients and should constitute an additional stratification factor in future I-O clinical trials. Further research at a translational and molecular level is required to decipher the mechanisms of interrelation of metabolic deregulation and suppression of antitumor immunity.

Keywords: Cancer cachexia; immunotherapy; PD-1/PD-L1 inhibitors; non-small cell lung cancer (NSCLC); outcome; survival; response rate

^ ORCID: 0000-0002-6643-9855.

Submitted Jun 03, 2021. Accepted for publication Aug 19, 2021.

doi: 10.21037/tlcr-21-460

View this article at: <https://dx.doi.org/10.21037/tlcr-21-460>

Introduction

Immunotherapy (I-O) with immune checkpoint inhibitors (ICIs) has defined a new era in the management of patients with metastatic non-small cell lung cancer (NSCLC). However, beyond programmed death ligand 1 (PD-L1) expression levels in cancer tissues, there is a paucity of biomarkers for the prediction of outcome in patients with metastatic NSCLC treated with ICIs (1). In addition, only a small subset of NSCLC patients receiving PD-1/PD-L1 inhibitors will achieve a durable clinical benefit and the underlying mechanisms that lead to primary or secondary resistance to I-O have not been elucidated thus far (2).

Cancer cachexia syndrome (CCS) is a complex metabolic syndrome characterized by weight loss, alterations in body composition and a pathophysiologic background that is defined by a perpetually sustained inflammatory process (3). CCS has a high prevalence amongst cancer patients and has been associated with adverse survival outcomes and reduced treatment efficacy (4). Furthermore, it has been estimated that it directly accounts for approximately 20% of cancer-related mortality (5).

Beyond its well-recognized effect on host's metabolic homeostasis deregulation, CCS has been also associated with immune system dysfunction and increased susceptibility to infections (6). CCS is characterized by a composite molecular pathogenesis that involves a wide spectrum of inflammatory processes ranging from increased levels in the serum or the tumor microenvironment (TME) of certain cytokines such as tumor necrosis factor (TNF)- α (7), interleukins (IL)-6 (6), IL-8 (8) and growth differentiation factor (GDF)-15 (9) to increased plasma or TME concentrations of myeloid derived suppressor cells (MDSCs) (10). The vast majority of these processes have been demonstrated in experimental models to affect the Cancer-Immunity-Cycle (11) and to exert a negative effect on antitumor immunity (12-16).

Based on the aforementioned reports, we hypothesized that the activation of the cellular pathways that define CCS pathogenesis could have a negative effect on antitumor immunity, thus abrogating I-O efficacy. In order to test our hypothesis, we conducted a prospective observational study at the University Hospital of Heraklion, Crete amongst

patients with metastatic NSCLC that were treated with ICIs. We present the following article in accordance with the REMARK reporting checklist (available at <https://dx.doi.org/10.21037/tlcr-21-460>).

Methods

Patient selection

We prospectively collected clinical and radiological data from patients with non-oncogene driven metastatic NSCLC who received I-O either as monotherapy or in combination with chemotherapy according to ESMO guidelines (17) from 2017–2020 at the University Hospital of Heraklion, Crete. All consecutive patients that were deemed to be candidates for receiving treatment with PD-1/PD-L1 inhibitors for metastatic NSCLC were screened for inclusion in this study. Individuals with *EGFR* mutations or *ALK* translocations were excluded before the initial screening. *EGFR* mutational status was assessed using polymerase chain reaction (PCR) and *ALK* genomic alterations were examined using immunohistochemistry (ICH) or fluorescence *in situ* hybridization (FISH), respectively. The study was approved from the Ethics Committee of the University Hospital of Heraklion (ID: 2644) and was conducted according to principles of the declaration of Helsinki (as revised in 2013). Written informed consent was obtained from all patients before enrollment.

Cachexia assessment

Patients were categorized as having cachexia based on the criteria set by Fearon *et al.* (18). These consist of body weight loss >5% within the last 6 months or body mass index (BMI) <20 kg/m² and any degree of weight loss >2% or low appendicular skeletal muscle index consisted with sarcopenia and any degree of weight loss >2%.

We assessed the appendicular skeletal muscle index of the patients by measuring the skeletal muscle thickness at the level of the third lumbar vertebra by analyzing the patients' abdominal computed tomography (CT) scans before the initiation of I-O through the application of

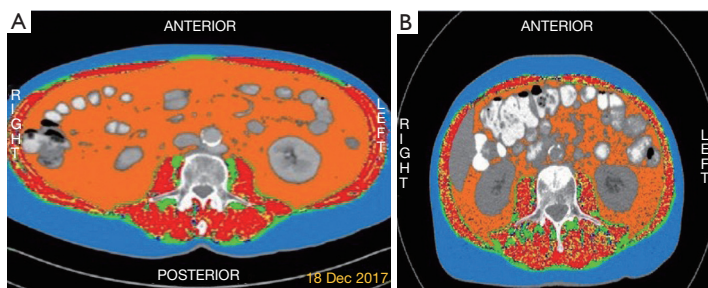


Figure 1 Tomovision analysis of the CT scans of two individuals in our cohort. (A) A male patient with baseline LSMI = $55.02 \text{ cm}^2/\text{m}^2$ without sarcopenia. (B) A male patient with baseline LSMI = $39.45 \text{ cm}^2/\text{m}^2$ consistent with sarcopenia. CT scan, computed tomography scan; LSMI, lumbar skeletal muscle index (cm^2/m^2) (at the level of 3rd lumbar vertebra).

Slice-o-matic Tomovision software (sliceOmatic 5.0 Rev-9 Alberta Protocol) (Figure 1). The muscle area thickness was divided by each individual's squared height, thus creating a baseline Lumbar Skeletal Muscle Index (LSMI) that was measured in cm^2/m^2 . The LSMI cut-off values (LNL: lower normal limit) used for the definition of sarcopenia were set at $<55 \text{ cm}^2/\text{m}^2$ for males and $<39 \text{ cm}^2/\text{m}^2$ for females, according to the international consensus for the definition of cancer cachexia (18). Only the individuals for whom we had sufficient radiological (LSMI) and/or clinical data (BMI, body weight fluctuations within the last six months) in order to be classified as cachectic or not, according to criteria set by Fearon *et al.* (18), were included in the final analysis (Figure S1).

We furthermore assessed, when available, the LSMI of patients during their treatment with I-O in order to investigate any potential correlation of LSMI fluctuations with treatment outcomes. For this purpose, we compared the baseline LSMI values with the LSMI values at the first radiological assessment of each individual after ICI therapy initiation. Patients were categorized according to their changes in LSMI during treatment in a binary fashion according to their median LSMI reduction% during I-O.

Data collection

We prospectively collected data on patient [age, gender, smoking status, ECOG performance status (PS), BMI, line of treatment of ICI administration], disease characteristics (histology, organs affected with metastases, PD-L1 status) and baseline albumin values at the timepoint of I-O

initiation.

Patients were classified in a dichotomous fashion based on their age (<70 vs. ≥ 70 years old), gender (male vs. female), PS (0–1 vs. 2), smoking status (smokers or former smokers vs. non-smokers), line of treatment of ICI administration (first line vs. second or later lines of treatment), brain metastases, liver metastases, bone metastases, disease burden (Low vs. high tumor burden), baseline BMI values (<25 vs. $\geq 25 \text{ kg}/\text{m}^2$), histology (squamous vs. non-squamous), PD-L1 status ($<1\%$ vs. $\geq 1\%$) and baseline albumin levels (<3.5 vs. $\geq 3.5 \text{ g}/\text{dL}$). PD-L1 expression levels, when available, were evaluated before the initiation of systemic treatment. 36 patients (26 individuals who received pembrolizumab and 10 that received nivolumab) had their samples evaluated using staining with 22C3 pharmDx assay. The remaining 12 patients with available PD-L1 status had their samples evaluated using Ventana SP142 assay. High disease burden was defined as metastatic spread in >2 organs. We decided to use this cut-off since it has been the only clinical factor significantly associated with the development of disease hyper-progression under treatment with ICIs (19). Finally, the cut-off values that were set for baseline albumin levels were the $3.5 \text{ g}/\text{dL}$ (which represents the lower normal limit in our laboratory).

Immune-related adverse events (irAEs) were recorded according to ESMO guidelines (20).

Outcome assessment

Response to treatment was evaluated according to RECIST 1.1 criteria (21). The images of the patients were reviewed specifically for this study in order to determine response

assessment according to RECIST 1.1 criteria. Patients were categorized according to their best response to ICIs as having complete response (CR), partial response (PR), stable disease (SD) and progressive disease (PD). Objective response rate (ORR) was defined as the percentage of individuals who achieved CR or PR as best response to treatment and disease control rate (DCR) was defined as the percentage of patients who achieved CR or PR or SD as best response to treatment. Prolonged duration of disease control was defined as absence of disease progression for a time period of ≥ 6 months amongst the patients who had achieved disease control (CR or PR or SD) at their first radiological assessment after ICI initiation.

Progression-free survival (PFS) was defined as the time from the initiation of ICI until the date of disease progression or death. Overall survival (OS) was defined as the time from the initiation of ICIs to death. Individuals who had not progressed or were still alive at the time of data analysis were censored at the date of last follow-up.

Statistical analysis

All statistical analyses were performed with SPSS 25.0.0 software (IBM Corp., Armonk, NY, USA). Descriptive statistics were applied to define and categorize nominal and categorical variables. Statistical significance was set at <0.05 . We furthermore applied Chi-square test to examine any potential associations between the studied variables with ORR and DCR. Kruskal-Wallis test was applied to examine any potential differences in baseline LSMI distributions according to the presence of CCS. In addition, any potential differences in the distributions of LSMI% changes during I-O with ORR, DCR and duration of disease control ≥ 6 months were examined with Kruskal-Wallis test.

A univariate binary logistic regression was performed to examine the odds ratios (OR) of the studied parameters on the probability of developing PD as best response to treatment. A multivariate logistic regression was performed for the variables that had reached statistical significance in the univariate analysis.

The Kaplan-Meier method was applied to investigate the effect of the studied variables on PFS and OS. Curves were compared with the log-rank test. In addition, we applied log-rank test in order to examine the effect of baseline cancer cachexia on OS in the subgroup of patients that received I-O as first line treatment and in the subgroup of patients that received it as second line treatment. A univariate Cox Regression Analysis was performed to

calculate the Hazard Ratios (HR) of age ≥ 70 years old, PS 2, female gender, squamous histology, bone metastases, liver metastases, brain metastases, PD-L1 $<1\%$, ICI administration as 2nd line of treatment, baseline albumin levels <3.5 g/dL and the presence of baseline CCS on PFS and OS. A multivariate Cox Regression Analysis was performed amongst the variables that had reached statistical significance in the univariate analysis.

Additionally, we applied log-rank test in order to estimate the effect of cancer cachexia on 6 months survival since the initiation of I-O. Six months survival time was used as a cut-off value. Individuals that were alive but had a follow-up time shorter than 6 months were censored at the time of their last follow-up. Using the 6 months survival time as a cut-off we also performed a univariate Cox regression analysis to estimate the hazard ratio of cancer cachexia on 6 months survival time.

A sample size and power calculation was not conducted because at the time of the initiation of data collection there were no published reports on the effect of cachexia on the outcome of I-O treated cancer patients. Thus, it would have been of no value in this exploratory, hypothesis generated study due to the lack of available data on which to base the required calculations for power calculation.

Results

Patient characteristics

A total of 83 patients were included in the analysis. Median follow-up duration was 9.53 months. Patients' characteristics are depicted in detail in *Table 1*. Median age was 66 years, 84.3% of patients were male and 92.8% were active or former smokers. Mean baseline BMI was 26.69 kg/m^2 and 38.6% of patients had baseline BMI values $<25 \text{ kg/m}^2$.

Most (79.5%) patients in our cohort had received ICIs as second line of treatment and the rest as first line treatment. All the patients who received ICIs as second line treatment had previously progressed on a platinum doublet. Only 2 patients (2.4%) had received I-O in combination with chemotherapy and the rest as monotherapy. ORR was 20.5% and 48.2% of patients experienced PD as best response to treatment. Median PFS and OS were 4.80 and 9.90 months, respectively.

Forty-three patients (51.8%) were classified as having baseline CCS at I-O initiation and only 15 patients out of the 54 with evaluable LSMI (27.8%) had baseline LSMI values not consistent with sarcopenia (Above NNL).

Table 1 Baseline patient characteristics

Variable	All patients	
	N	%
Number of patients	83	
Age, median (range)	66 (39–81)	
Gender		
Male	70	84.3
Female	13	15.7
Performance status		
0–1	65	78.3
2	18	21.7
Smoking status		
Active or former smokers	77	92.8
Never smokers	6	7.2
Histology		
Squamous	32	38.6
Non-squamous	51	61.4
Mean baseline BMI (SD)	26.69 (4.69)	
Baseline BMI		
<25 kg/m ²	32	38.6
≥25 kg/m ²	51	61.4
Brain metastases		
Yes	20	24.1
No	63	75.9
Liver metastases		
Yes	23	27.7
No	60	72.3
Bone metastases		
Yes	29	34.9
No	54	65.1
Number of organs with metastatic disease		
1–2	57	68.7
>2	26	31.3
Baseline albumin levels		
≥3.5 g/dL	64	77.1
<3.5 g/dL	12	14.5
Missing values	7	8.4

Table 1 (continued)

Table 1 (continued)

Variable	All patients	
	N	%
PD-L1 levels		
<1%	14	16.9
1% < PD-L1 < 50%	22	26.5
≥50%	15	18.1
Missing values	32	38.5
Line of treatment of ICI administration		
1 st line	17	20.5
2 nd line	66	79.5
Immunotherapy agent		
Nivolumab	54	65.1
Pembrolizumab	26	31.3
Atezolizumab	3	3.6
Mode of ICI administration		
Monotherapy	81	97.6
Combination with chemotherapy	2	2.4
Baseline cancer cachexia		
Yes	43	51.8
No	40	48.2
Baseline LSMI		
Male [mean (SD)]	46.26 (10.07)	
Female [mean (SD)]	34.6 (6.74)	
Baseline LSMI		
Below LNV	39	47.0
Above LNV	15	18.1
Missing values	29	34.9
LSMI change during ICI treatment %, median (range)	4.96 (Min: –28.08, Max: 14.61)	
Response to ICIs		
CR	1	1.2
PR	16	19.3
SD	26	31.3
PD	40	48.2
Duration of disease control* (N=38)		
<6 months	10	26.3
≥6 months	28	73.7

Table 1 (continued)

Table 1 (continued)

Variable	All patients	
	N	%
Grade III-IV irAEs		
Yes	7	8.4
No	76	91.6
PFS (months), median (95% CI)	4.80 (3.10–6.50)	
OS (months), median (95% CI)	9.90 (6.81–12.98)	
Follow up (months), median (95% CI)	9.53 (6.05–13.01)	

*, duration of disease control was calculated amongst the individuals who had achieved PR or SD during their first assessment after ICI administration and they had sufficient follow-up for 6 months or more. SD, standard deviation; ICI, immune checkpoint inhibitor; LSMI, lumbar skeletal muscle index (at the level of 3rd lumbar vertebra); LNV, lower normal value that was set for males, 55 cm/m² and for females, 39 cm/m²; irAEs, immune related adverse events; PFS, progression free survival; OS, overall survival; CI, confidence intervals.

Baseline LSMI distributions were significantly different between cachectic and non-cachectic males (P=0.001) but not females (P=0.606) (Figure S2).

Twenty-eight patients had evaluable LSMI values at their first evaluation post ICI initiation. Median LSMI percentage change during I-O was -4.96% (range, -28.08% to 14.61%). In order to access any potential associations of LSMI fluctuations during ICI treatment we categorized the patients according to their percent LSMI reduction during I-O using as a cut-off the median LSMI reduction during treatment which was 5%.

Effect of the studied variables on response outcomes

Baseline BMI <25 kg/m² (P=0.047) and the presence of CCS (P≤0.001) were significantly associated with inferior ORR. The associations of all the studied parameters with ORR are demonstrated in Table S1. Similarly, CCS was significantly associated with reduced DCR (P≤0.001) along with baseline LSMI <Lower Normal Limit (LNL) (P≤0.001), BMI <25 kg/m² (P=0.039) and metastatic spread in >2 organs (P=0.034). The effect of the analyzed variables on DCR are depicted in Table S2.

The distributions of LSMI percent change during I-O did not significantly differ amongst the individuals who achieved CR or PR as compared to those who experienced

SD or PD (P=0.446) (Figure S3A). In the same fashion, the distributions of LSMI percent change during I-O did not differ between the individuals with disease control as compared to those who experienced PD (P≥0.99) (Figure S3B) and amongst those who achieved prolonged disease control ≥6 months *vs.* those who did not (P=0.424) (Figure S3C).

In the univariate logistic regression analysis BMI <25 kg/m² [OR =2.58 (95% CI: 1.04–6.19), P=0.041] and the presence baseline CCS [OR =8.89 (95% CI: 3.28–24.12), P≤0.001] were significantly associated with increased probability of PD as best response to ICI treatment (Figure 2A, Table S3). However, in the multivariate analysis, only CCS, OR =8.11 (95% CI: 2.95–22.94, P≤0.001) with an area under the curve (AUC) =0.748 (95% CI: 0.640–0.856) independently predicted for increased probability of PD as best response to treatment (Figure 2B and Table S3).

Effect of the studied variables on survival outcomes

Patients with baseline CCS experienced significantly inferior PFS (2.36 *vs.* 7.33 months, P≤0.001) (Figure 3A) and inferior OS (3.70 *vs.* 17.93 months, P≤0.001) (Figure 3B) as compared to non-cachectic individuals. In a similar fashion, patients with baseline LSMI consistent with sarcopenia had significantly reduced PFS (2.96 *vs.* 7.96 months, P=0.032) (Figure 3C) and reduced OS (5.43 months *vs.* not reached, P=0.006) (Figure 3D) as compared to the individuals with baseline LSMI values not consistent with sarcopenia.

However, LSMI reduction >5% during I-O did not have any effect on PFS (7.96 *vs.* 7.33 months, P=0.193) (Figure 4A) nor OS (19.20 *vs.* 14.03 months, P=0.400) (Figure 4B).

The effect of all the other studied covariates on survival outcomes are summarized on Table S4.

The presence of baseline cachexia significantly reduced survival in the subgroup of patients that received I-O as first line treatment (not reached *vs.* 13.37 months, P=0.028) (Figure 5A) and to the subgroup of patients that received I-O as second line treatment (12.70 *vs.* 3.23 months, P=0.003) (Figure 5B). Finally, the presence of baseline cancer cachexia was significantly associated with inferior 6 months survival since the initiation of I-O (P<0.001) (Figure S4).

Univariate and multivariate analysis

Univariate and multivariate analyses on the effect of the analyzed variables on PFS and OS are summarized in Table 2.

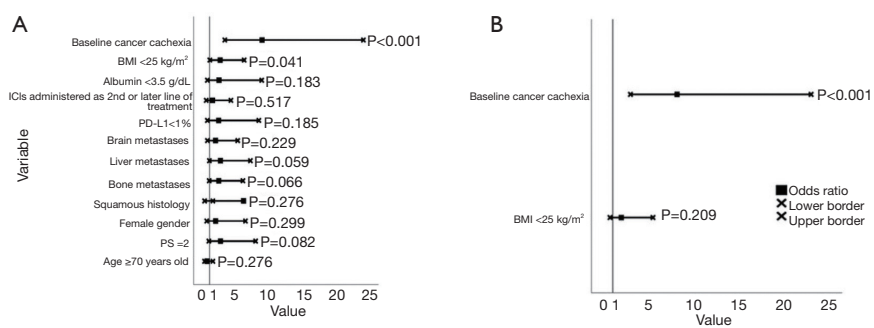


Figure 2 Forest plots depicting the odds ratios of the studied variables on the probability of having disease progression as best response to ICI treatment. (A) Univariate analysis; (B) multivariate analysis. ICI, immune checkpoint inhibitor; BMI, body mass index; PD-L1, programmed death-ligand 1; PS, performance status.

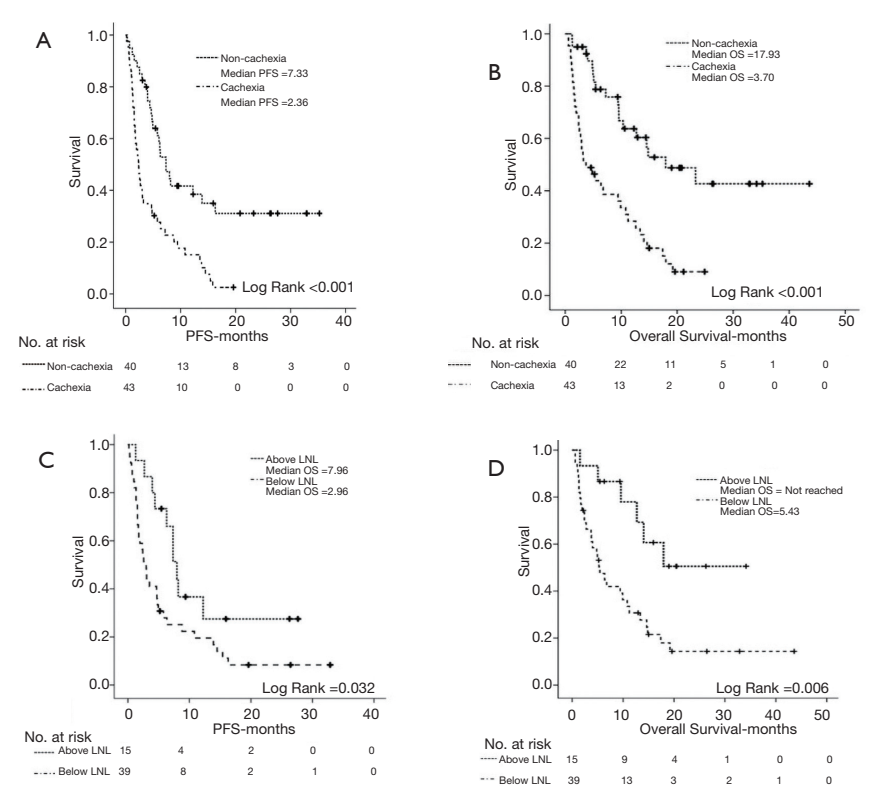


Figure 3 Kaplan-Meier curves depicting the effect of baseline CCS on PFS (A), OS (B) and the effect of baseline LSMI values on PFS (C) and OS (D). CCS, cancer cachexia syndrome; PFS, progression free survival (months); OS, overall survival (months); LSMI, lumbar skeletal muscle index (cm^2/m^2) (at the level of 3rd lumbar vertebra); LNL, lower normal limit ($55 \text{ cm}^2/\text{m}^2$ for males and $< 39 \text{ cm}^2/\text{m}^2$ for females).

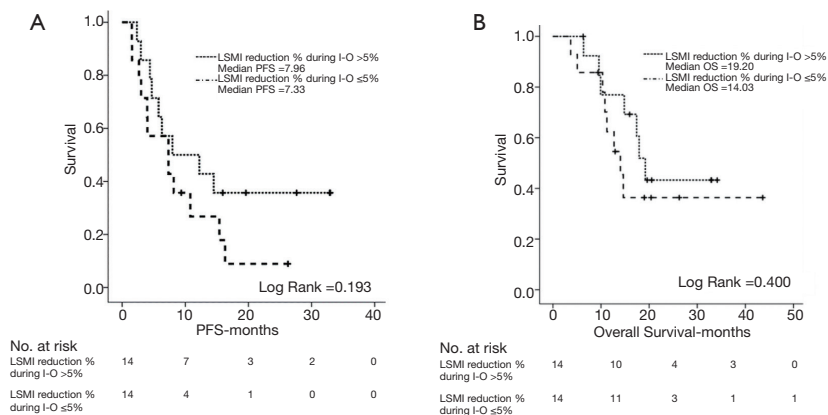


Figure 4 Log-rank test demonstrating the effect of LSMI reduction% >5 during I-O on PFS (A) and OS (B). LSMI, lumbar skeletal muscle index (cm^2/m^2) (at the level of 3rd lumbar vertebra); I-O, immunotherapy; PFS, progression free survival; OS, overall survival.

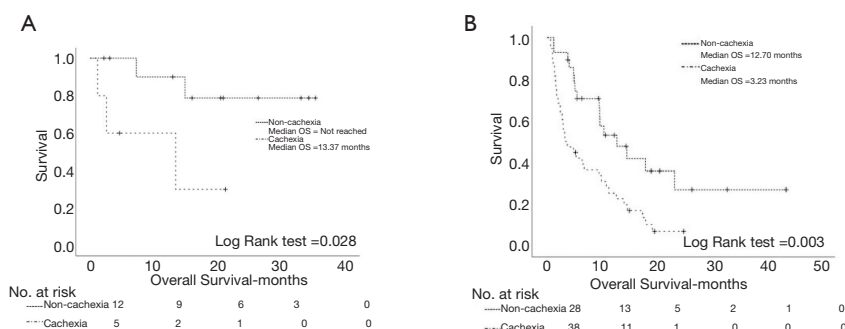


Figure 5 Log rank test demonstrating the effect of cancer cachexia syndrome on overall survival amongst the patients' subgroups that received PD-1/PD-L1 inhibitors as first line treatment (A) and second line treatment (B). OS, overall survival; PD-1, programmed death-1; PD-L1, programmed death ligand 1.

ICI administration as 2nd line of treatment [HR = 2.22 (95% CI: 1.19–4.40), $P=0.023$] and baseline CCS [HR = 2.72 (95% CI: 1.64–4.50), $P\leq 0.001$] reached statistical significance in the univariate analysis for PFS. However, in the multivariate analysis only the presence of baseline CCS [HR = 2.49 (95% CI: 1.49–4.16), $P\leq 0.001$] emerged as an independent predictor for shorter PFS.

In the univariate analysis performance status 2, high disease burden, ICI administration as 2nd line of treatment and baseline CCS were significantly associated with inferior OS. However, in the multivariate analysis, performance

status 2 [HR = 1.98 (95% CI: 1.10–3.58), $P=0.023$], ICI administration as 2nd line of treatment [HR = 2.91 (95% CI: 1.13–7.49), $P=0.027$] and the presence of CCS [HR = 2.52 (95% CI: 1.40–4.55), $P=0.002$] independently predicted for shorter survival (Table 2).

In the univariate analysis on the effect of baseline cancer cachexia on the probability of death within 6 months since the initiation of I-O, cancer cachexia was significantly associated with increased risk of death within the first 6 months of I-O [HR = 3.90 (95% CI: 1.75–8.70), $P=0.001$] (Figure S4).

Table 2 Univariate and multivariate analysis using Cox regression method in the whole patient population

Cox regression	PFS		OS	
	HR (95% CI)	P value	HR (95% CI)	P value
Univariate analysis				
Age ≥70 years old	0.94 (0.57–1.54)	0.803	0.98 (0.58–1.69)	0.957
Performance status 2	1.42 (0.81–2.50)	0.220	2.18 (1.21–3.90)	0.009
Female gender	1.46 (0.76–2.80)	0.257	1.26 (0.61–2.57)	0.523
Squamous histology	0.582 (0.53–1.43)	0.869	1.17 (0.68–1.99)	0.573
Brain metastases	1.43 (0.82–2.48)	0.207	1.38 (0.75–2.53)	0.302
Liver metastases	1.65 (0.98–2.77)	0.059	1.28 (0.72–2.29)	0.406
Bone metastases	1.11 (0.68–1.18)	0.675	1.42 (0.83–2.43)	0.200
High disease burden*	1.63 (0.98–2.70)	0.060	1.77 (1.02–3.06)	0.041
PD-L1 <1%	0.95 (0.46–1.95)	0.880	0.60 (0.28–1.29)	0.189
ICIs as 2 nd or later line of treatment	2.22 (1.19–4.40)	0.023	3.90 (1.55–9.82)	0.001
Baseline cancer cachexia	2.72 (1.64–4.50)	<0.001	3.22 (1.82–5.69)	<0.001
Multivariate analysis				
Age ≥70 years old				
Performance status 2			1.98 (1.10–3.58)	0.023
Female gender				
Squamous histology				
Brain metastases				
Liver metastases				
Bone metastases				
High disease burden			1.16 (0.64–2.11)	0.618
PD-L1 <1%				
ICIs as 2nd or later line of treatment	1.83 (0.91–3.66)	0.088	2.91 (1.13–7.49)	0.027
Baseline cancer cachexia	2.49 (1.49–4.16)	<0.001	2.52 (1.40–4.55)	0.002

*, high disease burden = metastatic dissemination in more than 2 organs. PFS, progression free survival; OS, overall survival; HR, hazard ratio; ICI, immune checkpoint inhibitor; PD-L1, programmed death ligand-1.

Discussion

In this prospective study, we demonstrated that cancer cachexia is associated with reduced response rates to PD-1/PD-L1 inhibitors and that it consists an independent predictor for both inferior PFS and OS. LSMI values below the thresholds for sarcopenia were also associated with inferior survival outcomes.

We decided to categorize the patients of our cohort according to the presence of cancer cachexia based on the criteria set by Fearon *et al.* (18) since they specifically focus on

cancer-related cachexia and take into account pretreatment weight loss, BMI and body composition analysis. Cancer cachexia had a high prevalence amongst the patients of our cohort in accordance with previously published reports (22).

Our results are in accordance with previous published retrospective reports addressing the negative effects of weight loss and reduced muscle mass on I-O outcomes (23–27). Turner *et al.* (23) performed a pharmacokinetic analysis in patients with NSCLC and melanoma that were treated with pembrolizumab monotherapy. An

association between rapid baseline plasma clearance (CL_0) of pembrolizumab and poor OS was reported despite a lack of association between plasma exposure and OS at pembrolizumab doses between 2 and 10 mg/kg. The researchers suggested that the substantial difference in OS was attributed to underlying increased catabolic status caused by CCS, providing indirect evidence that patients with elevated serum protein catabolism are refractory to ICIs. Shiroyama *et al.* (24) demonstrated in a retrospective cohort of metastatic NSCLC patients that sarcopenia, which was calculated by the psoas muscle index in CT scans, was associated with reduced response rates to PD-1 inhibitors and inferior PFS. Miyawaki *et al.* (25) and Roch *et al.* (26) in retrospective cohorts also demonstrated that cachexia, defined as pretreatment weight loss >5% in the last 6 months, was an independent predictor of adverse survival outcomes in metastatic NSCLC patients treated with ICIs. Finally, Chu *et al.* (27) reported that skeletal muscle density is predictive and prognostic in melanoma patients treated with ipilimumab. Our prospective data reinforce these previous retrospective reports on the adverse effects of cachexia and reduced muscle composition on I-O outcomes. However, in contrast to these studies we used a multifaceted definition of cancer cachexia status (18) for the classification of patients of our cohort, since we took into account pretreatment weight loss along with BMI and skeletal muscle index. Importantly, our findings along with the aforementioned retrospective data demonstrate that the presence of cachexia should constitute an additional classification factor in the design of future I-O trials.

Interestingly the distributions of LSMI percent change during I-O did not differ among responders and non-responders to treatment. In addition, LSMI reduction >5% was not associated with inferior PFS or OS in our cohort. These findings are in contrast with the results published by Roch *et al.* (26) who reported that evolving sarcopenia, defined as reduction in skeletal muscle index more than 5% during I-O, was associated with adverse survival outcomes. These differences can be attributed to the small number of 28 patients analyzed in our study and the possible selection bias for this subgroup in our cohort. However, body composition fluctuations and their effect on I-O outcomes is an interesting research subject that warrants further investigation.

It has been demonstrated using experimental models that the molecular cascades that govern the pathogenesis of cachexia also negatively affect a wide spectrum of immune antitumor functions (12-16). Furthermore, inhibition

of cytokine pathways implicated in the development of cachexia has been shown to invigorate antitumor immune responses (28-30) and combined blockade of specific pro-cachexia mediators and PD-1/PD-L1 axis was also reported to exert synergistic effects (31,32). Thus, the combination of anti-cachexia treatments along with immunotherapies might be necessary for the enhancement of I-O effectiveness and improvement of patient outcomes in patients with cancer cachexia. Nevertheless, further research of the serum or TME of patients with cachexia is required to decipher of the underlying processes that lead to higher rates of ICIs failure in cachectic individuals.

To our knowledge, this is the first prospective study investigating the effect of cancer cachexia on I-O treatment outcomes. In addition, we utilized the definition set by the international consensus for the classification of patients for cancer cachexia. Finally, our study sample consists exclusively from patients with NSCLC who received in their vast majority I-O as PD-1/PD-L1 monotherapy. The main limitations of our study are the relatively small sample size conferring limited statistical power and the fact that we included NSCLC patients receiving ICIs in different lines of therapy and the lack of translational and molecular data.

Conclusions

Cancer cachexia is an adverse independent factor predicting for poor outcomes in patients with metastatic NSCLC receiving ICIs and should constitute an additional stratification factor in the design of future immunotherapy trials. Finally, further research on the molecular pathogenesis of cachexia could result in the discovery of mechanisms that confer resistance to immunotherapy and the development of novel biomarkers and immunotherapy combinations.

Acknowledgments

We would like to thank Kyriaki Koutsoudaki and Marina Mavrogianni for their invaluable help in data collection and Sevasti Dara for her assistance in graphic design. Most importantly we would like to thank all the patients who participated in this study and their families.

Funding: None.

Footnote

Reporting Checklist: The authors have completed the

REMARK reporting checklist. Available at <https://dx.doi.org/10.21037/tlcr-21-460>

Data Sharing Statement: Available at <https://dx.doi.org/10.21037/tlcr-21-460>

Peer Review File: Available at <https://dx.doi.org/10.21037/tlcr-21-460>

Conflicts of Interest: All authors have completed the ICMJE uniform disclosure form (available at <https://dx.doi.org/10.21037/tlcr-21-460>). The authors have no conflicts of interest to declare.

Ethical Statement: The authors are accountable for all aspects of the work in ensuring that questions related to the accuracy or integrity of any part of the work are appropriately investigated and resolved. The study was approved from the Ethics Committee of the University Hospital of Heraklion (ID: 2644) and was conducted according to principles of the declaration of Helsinki (as revised in 2013). Written informed consent was obtained from all patients before enrollment.

Open Access Statement: This is an Open Access article distributed in accordance with the Creative Commons Attribution-NonCommercial-NoDerivs 4.0 International License (CC BY-NC-ND 4.0), which permits the non-commercial replication and distribution of the article with the strict proviso that no changes or edits are made and the original work is properly cited (including links to both the formal publication through the relevant DOI and the license). See: <https://creativecommons.org/licenses/by-nc-nd/4.0/>.

References

- Havel JJ, Chowell D, Chan TA. The evolving landscape of biomarkers for checkpoint inhibitor immunotherapy. *Nat Rev Cancer* 2019;19:133-50.
- Sharma P, Hu-Lieskovan S, Wargo JA, et al. Primary, Adaptive, and Acquired Resistance to Cancer Immunotherapy. *Cell* 2017;168:707-23.
- Baracos VE, Martin L, Koc M, et al. Cancer-associated cachexia. *Nat Rev Dis Primers* 2018;4:17105.
- von Haehling S, Anker SD. Prevalence, incidence and clinical impact of cachexia: facts and numbers-update 2014. *J Cachexia Sarcopenia Muscle* 2014;5:261-3.
- Argilés JM, Busquets S, Stemmler B, et al. Cancer cachexia: understanding the molecular basis. *Nat Rev Cancer* 2014;14:754-62.
- de Matos-Neto EM, Lima JD, de Pereira WO, et al. Systemic Inflammation in Cachexia - Is Tumor Cytokine Expression Profile the Culprit? *Front Immunol* 2015;6:629.
- Peyta L, Jarnouen K, Pinault M, et al. Regulation of hepatic cardioplin metabolism by TNF α : Implication in cancer cachexia. *Biochim Biophys Acta* 2015;1851:1490-500.
- Gioulbasanis I, Patrikidou A, Kitikidou K, et al. Baseline plasma levels of interleukin-8 in stage IV non-small-cell lung cancer patients: relationship with nutritional status and prognosis. *Nutr Cancer* 2012;64:41-7.
- Lerner L, Tao J, Liu Q, et al. MAP3K11/GDF15 axis is a critical driver of cancer cachexia. *J Cachexia Sarcopenia Muscle* 2016;7:467-82.
- Cuenca AG, Cuenca AL, Winfield RD, et al. Novel role for tumor-induced expansion of myeloid-derived cells in cancer cachexia. *J Immunol* 2014;192:6111-9.
- Chen DS, Mellman I. Oncology meets immunology: the cancer-immunity cycle. *Immunity* 2013;39:1-10.
- Bertrand F, Montfort A, Marcheteau E, et al. TNF α blockade overcomes resistance to anti-PD-1 in experimental melanoma. *Nat Commun* 2017;8:2256.
- Flint TR, Janowitz T, Connell CM, et al. Tumor-Induced IL-6 Reprograms Host Metabolism to Suppress Anti-tumor Immunity. *Cell Metab* 2016;24:672-84.
- Jin L, Tao H, Karachi A, et al. CXCR1- or CXCR2-modified CAR T cells co-opt IL-8 for maximal antitumor efficacy in solid tumors. *Nat Commun* 2019;10:4016.
- Roth P, Junker M, Tritschler I, et al. GDF-15 contributes to proliferation and immune escape of malignant gliomas. *Clin Cancer Res* 2010;16:3851-9.
- Gabrilovich DI, Nagaraj S. Myeloid-derived suppressor cells as regulators of the immune system. *Nat Rev Immunol* 2009;9:162-74.
- Planchard D, Popat S, Kerr K, et al. Metastatic non-small cell lung cancer: ESMO Clinical Practice Guidelines for diagnosis, treatment and follow-up. *Ann Oncol* 2018;29:iv192-237. Erratum in: *Ann Oncol* 2019;30:863-70.
- Fearon K, Strasser F, Anker SD, et al. Definition and classification of cancer cachexia: an international consensus. *Lancet Oncol* 2011;12:489-95.
- Ferrara R, Mezquita L, Texier M, et al. Hyperprogressive Disease in Patients With Advanced Non-Small Cell Lung Cancer Treated With PD-1/PD-L1 Inhibitors or With Single-Agent Chemotherapy. *JAMA Oncol* 2018;4:1543-52.

20. Haanen J, BLAG, Carbone F, Robert C, et al. Management of toxicities from immunotherapy: ESMO Clinical Practice Guidelines for diagnosis, treatment and follow-up. *Ann Oncol* 2017;28:iv119-42.
21. Eisenhauer EA, Therasse P, Bogaerts J, et al. New response evaluation criteria in solid tumours: revised RECIST guideline (version 1.1). *Eur J Cancer* 2009;45:228-47.
22. Tan BH, Fearon KC. Cachexia: prevalence and impact in medicine. *Curr Opin Clin Nutr Metab Care* 2008;11:400-7.
23. Turner DC, Kondic AG, Anderson KM, et al. Pembrolizumab Exposure-Response Assessments Challenged by Association of Cancer Cachexia and Catabolic Clearance. *Clin Cancer Res* 2018;24:5841-9.
24. Shiroyama T, Nagatomo I, Koyama S, et al. Impact of sarcopenia in patients with advanced non-small cell lung cancer treated with PD-1 inhibitors: A preliminary retrospective study. *Sci Rep* 2019;9:2447.
25. Miyawaki T, Naito T, Kodama A, et al. Desensitizing Effect of Cancer Cachexia on Immune Checkpoint Inhibitors in Patients With Advanced NSCLC. *JTO Clin Res Rep* 2020. doi: 10.1016/j.jtocrr.2020.100020
26. Roch B, Coffy A, Jean-Baptiste S, et al. Cachexia - sarcopenia as a determinant of disease control rate and survival in non-small lung cancer patients receiving immune-checkpoint inhibitors. *Lung Cancer* 2020;143:19-26.
27. Chu MP, Li Y, Ghosh S, et al. Body composition is prognostic and predictive of ipilimumab activity in metastatic melanoma. *J Cachexia Sarcopenia Muscle* 2020;11:748-55.
28. Maecker H, Varfolomeev E, Kischkel F, et al. TWEAK attenuates the transition from innate to adaptive immunity. *Cell* 2005;123:931-44.
29. Rautela J, Dagley LF, de Oliveira CC, et al. Therapeutic blockade of activin-A improves NK cell function and antitumor immunity. *Sci Signal* 2019;12:aat7527.
30. Tinoco R, Carrette F, Barraza ML, et al. PSGL-1 Is an Immune Checkpoint Regulator that Promotes T Cell Exhaustion. *Immunity* 2016;44:1190-203.
31. Li J, Xu J, Yan X, et al. Targeting Interleukin-6 (IL-6) Sensitizes Anti-PD-L1 Treatment in a Colorectal Cancer Preclinical Model. *Med Sci Monit* 2018;24:5501-8.
32. Kaplanov I, Carmi Y, Kornetsky R, et al. Blocking IL-1 β reverses the immunosuppression in mouse breast cancer and synergizes with anti-PD-1 for tumor abrogation. *Proc Natl Acad Sci U S A* 2019;116:1361-9.

Cite this article as: Rounis K, Makrakis D, Tsigkas AP, Georgiou A, Galanakis N, Papadaki C, Monastiriotti A, Vamvakas L, Kalbakis K, Vardakis N, Kontogianni M, Gioulbasanis I, Mavroudis D, Agelaki S. Cancer cachexia syndrome and clinical outcome in patients with metastatic non-small cell lung cancer treated with PD-1/PD-L1 inhibitors: results from a prospective, observational study. *Transl Lung Cancer Res* 2021;10(8):3538-3549. doi: 10.21037/tlcr-21-460

Supplementary

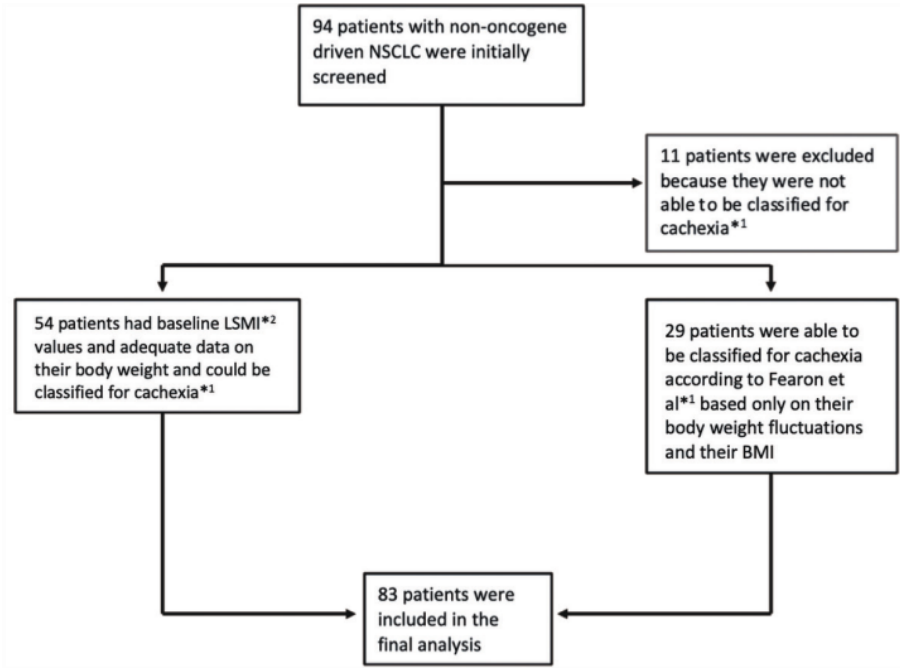


Figure S1: Flow chart of our study. ¹: Classification for cachexia was conducted according to the criteria by Fearon *et al.* [1]. ²: LSMI: Lumbar Skeletal Muscle Index.

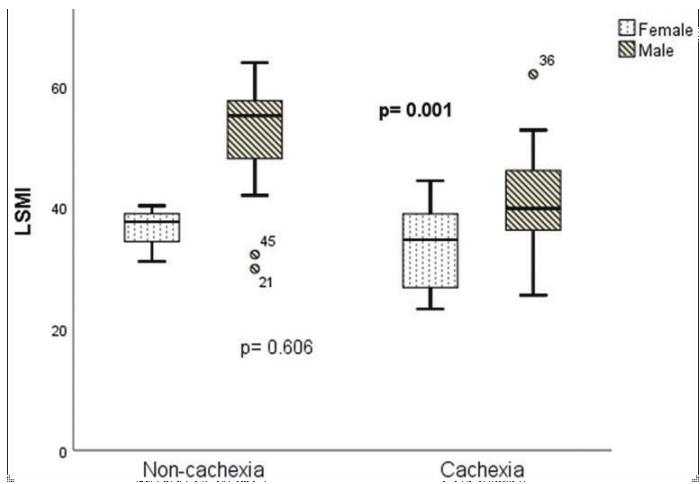


Figure S2: Kruskal-Wallis test examining potential differences in the distributions of baseline LSMI values between cachectic vs. non-cachectic males and cachectic vs. non-cachectic females.

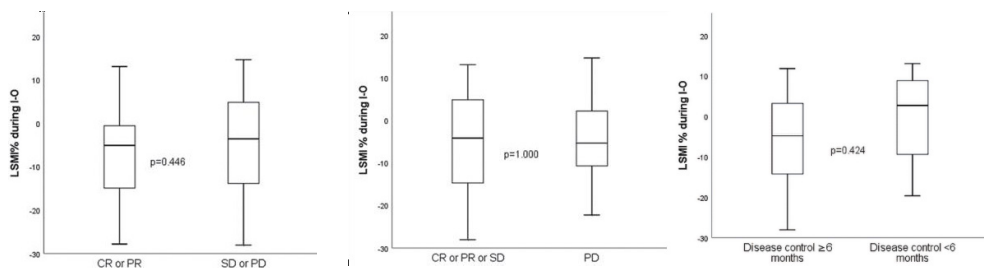


Figure S3: Kruskal-Wallis test investigating any potential difference in the distributions of LSMI change % during I-O. (A) Between patients who had CR or PR vs. those who experience SD or PD. (B) Between patients who had CR or PR or PD vs. those who experienced PD. (C) Between individuals who achieved prolonged disease control for [≥]6 months vs. those who did not.

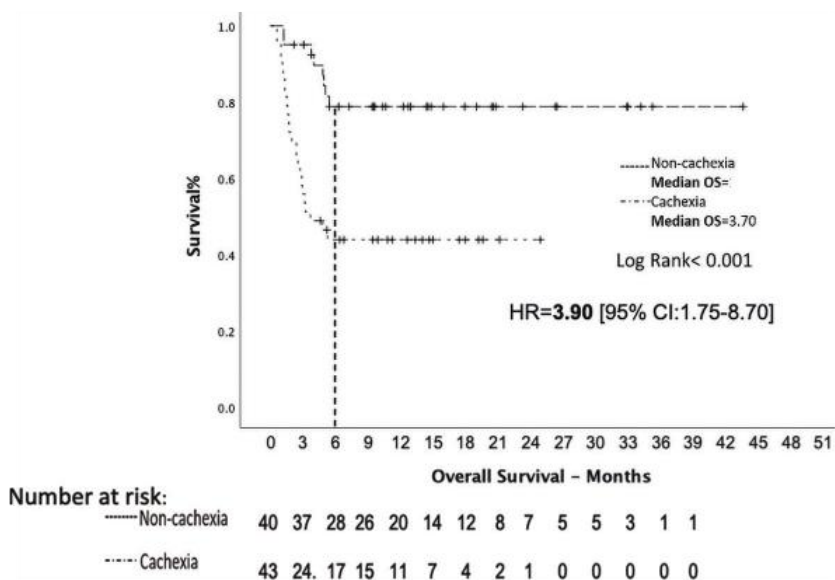


Figure S4: Log-rank test demonstrating the effect of cancer cachexia syndrome on 6 months survival.

Table S1: Effect of the studied variables on response rates

Variable	N=83	CR or PR	SD or PD	P value (chi-square test, 95% CI)
Age				
<70 years old	51	12	39	0.385
≥70 years old	32	5	27	
Gender				
Male	70	14	56	0.801
Female	13	3	10	
Performance status				
0–1	65	14	51	0.650
2	18	3	15	
Histology				
Non-squamous	51	12	39	0.385
Squamous	32	5	27	
Brain metastases				
Yes	20	4	16	0.951
No	63	13	50	
Liver metastases				
Yes	23	3	20	0.298
No	60	14	46	
Bone metastases				
Yes	29	7	22	0.545
No	54	10	44	
Disease burden*				
High	26	5	21	0.849
Low	57		45	
PD-L1 status				
<1%	14	3	11	0.988
≥1%	37		29	
Baseline albumin levels				
<3.5 g/dL	12	0	12	0.085
≥3.5 g/dL	64	13	51	
BMI				
<25 kg/m²	32	3	29	0.047
≥25 kg/m²	51	14	37	
Cancer Cachexia				
Yes	43	2	41	<0.01
No	40		25	
Baseline LSMI				
<LNV	39	6	33	0.051
≥LNV	15	6	9	

*, high disease burden was defined as >2 organs with metastatic spread. LSMI, lumbar skeletal muscle index (at the level of 3rd lumbar vertebra), LNV, lower normal value that was set for males =55 cm/m² and for females =39 cm/m².

Table S2: Effect of the studied variables on disease control (CR or PR or SD) rates.

Variable	N=83	CR or PR or SD	PD	P value (chi-square test, 95% CI)
Age				
<70 years old	51	24	27	0.274
≥70 years old	32	19	13	
Gender				
Male	70	38	32	0.294
Female	13	5	8	
Performance status				
0–1	65	37	28	0.076
2	18	6	12	
Histology				
Non-squamous	51	24	27	0.274
Squamous	32	19	13	
Brain metastases				
Yes	20	8	12	0.225
No	63	35	28	
Liver metastases				
Yes	23	8	15	0.055
No	60	35	25	
Bone metastases				
Yes	29	11	18	0.064
No	54	32	22	
Disease burden*				
High	26	9	17	0.034
Low	57	34	23	
PD-L1 status				
<1%	14	5	9	0.180
≥1%	37	21	16	
Baseline albumin levels				
<3.5 g/dL	12	4	8	0.174
≥3.5 g/dL	64	35	29	
BMI				
<25 kg/m²	32	12	20	0.039
≥25 kg/m²	51	31	20	
Cancer Cachexia				
Yes	43	12	31	<0.01
No	40	31	9	
Baseline LSMI				
<LNV	39	13	26	<0.01
≥LNV	15	13	2	

*, high disease burden was defined as >2 organs with metastatic spread. LSMI, lumbar skeletal muscle index (at the level of 3rd lumbar vertebra), LNV, lower normal value that was set for males =55 cm/m² and for females =39 cm/m².

Table S3: Univariate and multivariate logistic regression on the odds ratio (OR) of the analyzed covariates on the probability of developing disease progression (PD) as response to treatment with ICIs

Variable	Univariate			Multivariate		
	OR (95% CI)	P value	AUC (95% CI)	OR (95% CI)	P value	AUC (95% CI)
Age ≥70 years old	0.61 (0.25–1.49)	0.276	0.558 (0.434–0.682)			
PS=2	2.64 (0.88–7.91)	0.082	0.580 (0.456–0.704)			
Female gender	1.90 (0.56–6.39)	0.299	0.542 (0.417–0.667)			
Squamous histology	0.61 (0.25–1.49)	0.276	0.558 (0.434–0.682)			
Bone metastases	2.38 (0.94–6.01)	0.066	0.597 (0.474–0.720)			
Liver metastases	2.63 (0.97–7.13)	0.059	0.594 (0.471–0.718)			
Brain metastases	1.88 (0.67–5.22)	0.229	0.557 (0.432–0.681)			
PD-L1 <1%	2.36 (0.66–8.40)	0.185	0.584 (0.426–0.742)			
ICIs administered as 2 nd or later line of treatment	1.43 (0.49–4.20)	0.517	0.529 (0.404–0.653)			
Albumin <3.5 g/dL	2.41 (0.66–8.83)	0.183	0.557 (0.427–0.687)			
BMI <25 kg/m ²	2.58 (1.04–6.19)	0.041	0.610 (0.488–0.733)	1.94 (0.69–5.44)	0.209	
Baseline cancer cachexia	8.89 (3.28–24.12)	<0.001	0.748 (0.640–0.856)	8.11 (2.95–22.94)	<0.001	
Overall						0.748 (0.640–0.856)

OR, Odds Ratio; AUC, Area under the curve; PS, Performance status.

Table S4: Log-rank test on the effect of the studied variables on PFS and OS (n=83)

Variable	Median PFS (Months)	P value (log-rank test)	Median OS (Months)	P value (log-rank test)
Age				
<70 years old	4.00	0.803	9.47	0.957
≥70 years old	7.17		12.70	
Gender				
Male	4.80	0.253	10.33	0.531
Female	2.10		9.43	
Performance Status				
0–1	5.77	0.217	12.60	0.008
2	2.40		3.17	
Histology				
Squamous	5.77	0.580	9.57	0.572
Non-squamous	3.00		9.90	
BMI				
<25 kg/m ²	2.53	0.153	4.00	0.273
≥25 kg/m ²	6.20		10.33	
Line of treatment of ICI administration				
1 st line	13.80	0.019	Not reached	0.002
2 nd or later lines	4.40		9.43	
Brain metastases				
Yes	2.17	0.203	6.77	0.299
No	4.93		10.80	
Bone metastases				
Yes	4.80	0.674	7.23	0.198
No	3.23		12.70	

Table S4: Log-rank test on the effect of the studied variables on PFS and OS (n=83)

Variable	Median PFS (Months)	P value (log-rank test)	Median OS (Months)	P value (log-rank test)
Liver metastases				
Yes	2.10	0.056	6.77	0.405
No	5.77		10.80	
Disease burden*				
High	2.53	0.057	4.83	0.038
Low	4.93		13.37	
Baseline albumin levels				
<3.5 g/dL	1.77	0.008	2.40	0.017
≥3.5 g/dL	5.77		11.23	
PD-L1 levels				
<1%	2.57	0.880	7.23	0.184
≥1%	4.80		12.60	
Baseline Cancer Cachexia				
Yes	2.37		3.70	<0.001
No	7.33	<0.001	17.93	
Baseline LSMI				
<LNV	2.97	0.032	5.43	0.006
≥LNV	7.97		Not reached	
LSMI reduction % during ICI treatment				
<-5%	7.97	0.193	19.20	0.400
≥-5%	7.33		14.03	

*, high disease burden was defined as > 2 organs with metastatic spread. ICI, Immune checkpoint inhibitor; LSMI, lumbar skeletal muscle index (at the level of 3rd lumbar vertebra); LNV, lower normal value that was set for males =55 cm/m² and for females =39 cm/m².



Erratum to cancer cachexia syndrome and clinical outcome in patients with metastatic non-small cell lung cancer treated with PD-1/PD-L1 inhibitors: results from a prospective, observational study

Editorial Office

Translational Lung Cancer Research

Correspondence to: Editorial Office, Translational Lung Cancer Research. Email: editor@tlcr.org.

Submitted Sep 08, 2023. Accepted for publication Oct 10, 2023. Published online Oct 20, 2023.

doi: 10.21037/tlcr-2023-3

View this article at: <https://dx.doi.org/10.21037/tlcr-2023-3>

Erratum to: *Transl Lung Cancer Res* 2021;10:3538-49

This article (1) titled “Cancer cachexia syndrome and clinical outcome in patients with metastatic non-small cell lung cancer treated with PD-1/PD-L1 inhibitors: results from a prospective, observational study” (doi: 10.21037/tlcr-21-460), unfortunately contains errors in the authorship section.

The current affiliation 5 should be added under the names Konstantinos Rounis, Alexia Monastirioti, Dimitrios Mavroudis, and Sofia Agelaki.

In order to keep all affiliations appearing consecutively, the current affiliation 5 should be listed as affiliation 2. Following this change, the current affiliations 2–4 should be updated as affiliations 3–5. Affiliations 1 and 6 remain the same. Moreover, as Konstantinos Rounis is the corresponding author of this article, the correspondence information should be updated as well. The updated authorship section is presented below.

The authorship section should be updated as follows

Konstantinos Rounis^{1,2}△, Dimitrios Makrakis³, Alexandros-Pantelis Tsigkas⁴, Alexandra Georgiou⁴, Nikolaos Galanakis⁵, Chara Papadaki², Alexia Monastirioti², Lambros Vamvakas¹, Konstantinos Kalbakis¹, Nikolaos Vardakis¹, Meropi Kontogianni⁴, Ioannis Gioulbasanis⁶, Dimitrios Mavroudis^{1,2}, Sofia Agelaki^{1,2}

¹Department of Medical Oncology, University General Hospital of Heraklion, Heraklion, Greece; ²Laboratory of Translational Oncology, School of Medicine, University of Crete, Heraklion, Greece; ³Division of Oncology, University of Washington Medical School, Seattle, WA, USA; ⁴Department of Nutrition & Dietetics, School of Health Sciences and Education, Harokopio University, Athens, Greece; ⁵Department of Medical Imaging, University General Hospital, Heraklion, Greece; ⁶Department of Medical Oncology, Animus Kyanus Stavros General Clinic, Larissa, Greece

Correspondence to: Konstantinos Rounis, MD. Department of Medical Oncology, University General Hospital of Heraklion, Leoforos Panepistimiou, Iraklio 715 00, Heraklion, Greece; Laboratory of Translational Oncology, School of Medicine, University of Crete, Andrea Kalokerinou 13, Giorfirakia 715 00, Heraklion, Greece. Email: kostas@rounis.gr.

The authors apologize for the oversight.

Click [here](#) to view the updated version of the article.

Open Access Statement: This is an Open Access article distributed in accordance with the Creative Commons Attribution-NonCommercial-NoDerivs 4.0 International License (CC BY-NC-ND 4.0), which permits the non-commercial replication and distribution of the article with the strict proviso that no changes or edits are made and the original work is properly cited (including links to both the formal publication through the relevant DOI and the license). See: <https://creativecommons.org/licenses/by-nc-nd/4.0/>.

References

1. Rounis K, Makrakis D, Tsigkas AP, et al. Cancer cachexia syndrome and clinical outcome in patients with metastatic non-small cell lung cancer treated with PD-1/PD-L1 inhibitors: results from a prospective, observational study. *Transl Lung Cancer Res* 2021;10:3538-49.

Cite this article as: Editorial Office. Erratum to cancer cachexia syndrome and clinical outcome in patients with metastatic non-small cell lung cancer treated with PD-1/PD-L1 inhibitors: results from a prospective, observational study. *Transl Lung Cancer Res* 2023;12(10):2146-2147. doi: 10.21037/tlcr-2023-3

RESEARCH ARTICLE

Effect of body tissue composition on the outcome of patients with metastatic non-small cell lung cancer treated with PD-1/PD-L1 inhibitors

Dimitrios Makrakis^{1,2☯*}, Konstantinos Rounis^{1,3☯}, Alexandros-Pantelis Tsigkas⁴, Alexandra Georgiou⁴, Nikolaos Galanakis⁵, George Tsakonas^{3,6}, Simon Ekman^{3,6}, Chara Papadaki⁷, Alexia Monastirioti⁷, Meropi Kontogianni⁴, Ioannis Gioulbasanis⁸, Dimitris Mavroudis^{1,7}, Sofia Agelaki^{1,7}

1 Department of Medical Oncology, University General Hospital, Heraklion, Crete, Greece, **2** Jacobi Medical Center, Albert Einstein College of Medicine, The Bronx, NY, United States of America, **3** Comprehensive Cancer Center, Karolinska University Hospital, Stockholm, Sweden, **4** Department of Nutrition & Dietetics, School of Health Sciences and Education, Harokopio University, Athens, Greece, **5** Department of Medical Imaging, University General Hospital, Heraklion, Crete, Greece, **6** Department of Oncology-Pathology, Karolinska Institutet, Stockholm, Sweden, **7** Laboratory of Translational Oncology, School of Medicine, University of Crete, Heraklion, Greece, **8** Department of Medical Oncology, Animus Kyanus Stavros General Clinic, Larissa, Greece

☯ These authors contributed equally to this work.
* dmakrak@uw.edu



OPEN ACCESS

Citation: Makrakis D, Rounis K, Tsigkas A-P, Georgiou A, Galanakis N, Tsakonas G, et al. (2023) Effect of body tissue composition on the outcome of patients with metastatic non-small cell lung cancer treated with PD-1/PD-L1 inhibitors. PLoS ONE 18(2): e0277708. <https://doi.org/10.1371/journal.pone.0277708>

Editor: Matteo Bauckneht, IRCCS Ospedale Policlinico San Martino, Genova, Italy, ITALY

Received: May 19, 2022

Accepted: November 1, 2022

Published: February 10, 2023

Copyright: © 2023 Makrakis et al. This is an open access article distributed under the terms of the [Creative Commons Attribution License](https://creativecommons.org/licenses/by/4.0/), which permits unrestricted use, distribution, and reproduction in any medium, provided the original author and source are credited.

Data Availability Statement: For the conduction of this study, we analyzed prospective data derived from the study (ID:2644) previously conducted from our group (DOI: <https://doi.org/10.21037/tlcr-21-460>). Because these are a third-party dataset, they will be available upon request. In order to share the full dataset we will need specific permission from the Ethics Committee of the University Hospital of Heraklion. To request access to the full dataset, for researchers meeting the

Abstract

Obesity and sarcopenia have been reported to affect outcomes in patients with non-small cell lung cancer (NSCLC) treated with immune checkpoint inhibitors (ICIs). We analyzed prospective data from 52 patients with non-oncogene driven metastatic NSCLC treated with ICIs. Body tissue composition was calculated by measuring the fat and muscle densities at the level of 3rd lumbar vertebra in each patient computed tomography scan before ICI initiation using sliceOmatic tomosision. We converted the densities to indices [Intramuscular Fat Index (IMFI), Visceral Fat Index (VFI), Subcutaneous Fat Index (SFI), Lumbar Skeletal Muscle Index (LSMI)] by dividing them by height in meters squared. Patients were dichotomized based on their baseline IMFI, VFI and SFI according to their gender-specific median value. The cut-offs that were set for LSMI values were 55 cm²/m² for males and 39 cm²/m² for females. SFI distribution was significantly higher (p = **0.040**) in responders compared to non-responders. None of the other variables affected response rates. Low LSMI HR: **2.90** (95% CI: 1.261–6.667, p = **0.012**) and low SFI: **2.20** (95% CI: 1.114–4.333, p = **0.023**) values predicted for inferior OS. VFI and IMFI values did not affect survival. Subcutaneous adipose and skeletal muscle tissue composition significantly affected immunotherapy outcomes in our cohort.

criteria for access, please contact: konstantinos.rounis@regionstockholm.se.

Funding: The author(s) received no specific funding for this work.

Competing interests: The authors have declared that no competing interests exist.

1. Introduction

Immunotherapy (I-O) in the form of immune checkpoint inhibitors (ICIs) has significantly improved survival outcomes in the setting of a plethora of metastatic malignancies, including non-small cell lung cancer (NSCLC) [1], since it offers the possibility for durable remissions in a significant proportion of affected individuals. However, there is a scarcity of available biomarkers for the prediction of outcome in I-O treated patients with metastatic NSCLC [2]. Programmed death ligand- (PD-L)1 expression in tumor cells or immune cells of the tumor micro-environment (TME) consists the only approved biomarker thus far and its use suffers from significant limitations [3, 4].

Obesity poses one of the major health issues on a global scale [5] and it has been recognized as a risk factor for a wide range of malignancies [6]. More specifically, it has been proposed as the second most common risk factor for cancer development after tobacco exposure [7] and it has been linked with adverse treatment and survival outcomes in cancer patients [7, 8].

In contrast with these findings, large scale retrospective data have reported that obese individuals with higher Body Mass Index (BMI) values treated with ICIs for a variety of underlying malignancies experienced favorable outcomes compared to non-obese ones [9–11].

However, BMI as a marker of adipose tissue composition has limited accuracy since it is not able to distinguish between the differential fat depositions amongst different body compartments. Adipose tissue compartments are known to have substantial differences concerning their endocrine and immune properties [12, 13]. Furthermore, adipose tissue composition has been correlated with survival outcomes in cancer patients. High visceral fat percentage has been associated with poor outcomes in patients with endometrial cancer [14], whereas high subcutaneous fat density has been associated with favorable outcomes among patients with prostate, colorectal, and renal cancer [15, 16].

In addition, skeletal muscle depletion has been consistently associated with adverse outcomes in cancer patients across several studies [17–19] and serves as a criterion for the definition of cancer cachexia syndrome [20]. Recently, low skeletal muscle density has been reported as a negative predictive and prognostic factor in patients with metastatic melanoma [21] and NSCLC [22, 23] receiving treatment with ICIs. Finally, the presence of low muscle mass density was associated with increased toxicities from ipilimumab administration in individuals with metastatic melanoma [24].

Based on the above data we hypothesized that adipose and skeletal muscle tissue composition influences I-O outcomes in cancer patients. In order to further test our hypothesis, we analyzed clinical and radiological data from patients with metastatic NSCLC that received treatment with ICIs at the University Hospital of Heraklion, Crete from 2017 to 2020.

2. Materials and methods

2.1 Patient selection

We analyzed prospective clinical and radiological data which were acquired from a prospective observational study at the University Hospital of Heraklion, Crete (ID: 2644). Our population sample consisted of patients with non-oncogene driven metastatic NSCLC that were treated with ICIs either as monotherapy or in combination with chemotherapy according to ESMO guidelines [25]. Individuals with *EGFR* mutations or *ALK* translocations were excluded before the initial screening. Our study was approved by the ethical board of the University Hospital of Heraklion, Crete (ID: 2644) and was conducted according to principles of the declaration of Helsinki. Written informed consent was obtained from all patients before enrollment.

2.2 Body tissue composition assessment

For the assessment of body tissue composition we analyzed images from the abdominal Computed Tomography (CT) scans of the patients before the initiation of ICIs at the level of 3rd lumbar vertebra (L3) [26]. We analyzed the images using slice-o-matic tomovision software (sliceOmatic 5.0 Rev-9 Alberta Protocol). The densities of the different adipose tissue compartments and skeletal muscle were calculated through the application of differential Hounsfield Unit (HU) threshold references for each tissue compartment, respectively (−190 HU to −30 HU for intramuscular fat, −150 HU to −50 HU for visceral fat, −190 HU to −30 HU for subcutaneous fat, −29 HU to +150 for skeletal muscle) (Fig 1) [27, 28]. The fat densities (in cm^2) and muscle density (in cm^2) for each individual were converted to indices (in cm^2/m^2) by dividing them by height in meters squared (Intramuscular Fat Index: IMFI, Visceral Fat Index: VFI, Subcutaneous Fat Index: SFI and Lumbar Skeletal Muscle Index: LSMI).

We categorized the patients in a binary fashion according to their baseline IMFI, VFI and SFI based on the gender specific median value of each perspective index. Patients with baseline IMFI, VFI and SFI values below median were classified as low and those with above median values were classified as high, respectively. Patients were categorized according to their baseline LSMI according to the cut-offs for skeletal muscle depletion which were set by Fearon et al. [20]. They consist of $55 \text{ cm}^2/\text{m}^2$ for males and $39 \text{ cm}^2/\text{m}^2$ for females. Individuals with LSMI below the aforementioned cut-offs were categorized as < Lower Normal Limit (LNL) and the rest as \geq LNL.

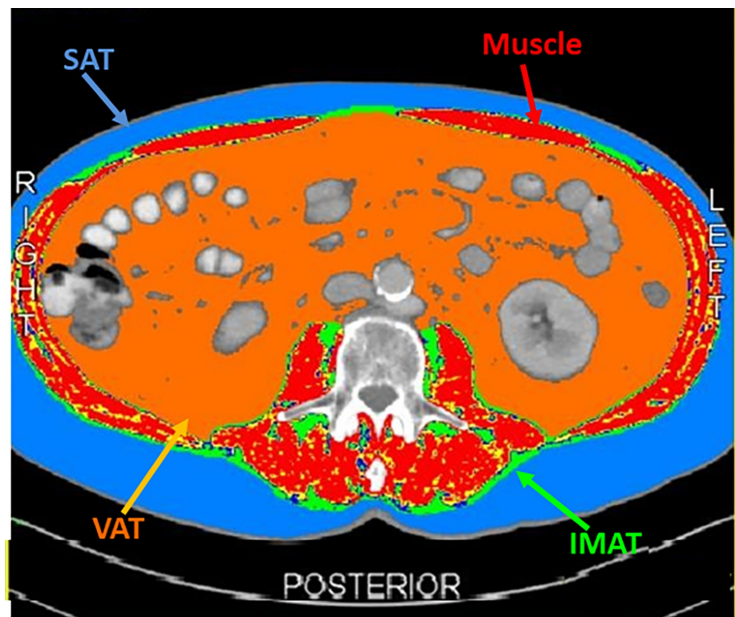


Fig 1. SliceOmatic tomovision analysis of the computed tomography scan of a male patient distinguishing the different context of Visceral Adipose Tissue (VAT), Intramuscular Adipose Tissue (IMAT), Subcutaneous Adipose Tissue (SAT) and skeletal muscle according to their differential Hounsfield Units (HU) references.

<https://doi.org/10.1371/journal.pone.0277708.g001>

2.3 Clinical data collection

The following clinical variables: age, gender, smoking status, ECOG performance status (PS), baseline BMI, histology, organs affected with metastases, PD-L1 status and line of treatment of ICI administration were analyzed. Individuals were classified in a dichotomous fashion based on their age (<70 years old vs ≥ 70 years old), gender (male vs female), PS (0–1 vs 2), smoking status (smokers or former smokers vs non-smokers), line of treatment of ICI administration (1st line vs 2nd or later lines of treatment), presence of brain, liver or bone metastases, histology (squamous vs non-squamous), PD-L1 status (<1% vs $\geq 1\%$) and baseline albumin levels (<3.5 g/dl vs ≥ 3.5 g/dl). The cut-off value that was set for baseline albumin levels was 3.5 gram (g)/deciliter (dl) which represents the lower normal limit in our laboratory.

We classified patients in our cohort according to their baseline BMI in a trichotomous fashion, those with BMI < 25 kg/m², overweight individuals with BMI values ≥ 25 kg/m² but < 30 kg/m² and obese with a BMI ≥ 30 kg/m².

Grade 3 or 4 immune related adverse events (irAEs) were recorded according to ESMO guidelines [29].

2.3.1 Response and survival outcomes assessment. Response assessment to treatment was conducted according to RECIST 1.1 criteria [30]. Patients were categorized according to their best response to ICIs as having complete response (CR), partial response (PR), stable disease (SD) and progressive disease (PD). Patients that had achieved CR or PR were classified as responders and the rest as non-responders. Objective response rate (ORR) was defined as the percentage of individuals who achieved CR or PR as best response to treatment. Patients were also categorized as achieving disease control (DC) if they had experienced CR or PR or SD as best response to treatment. We also compared response SFI scores both between patients with vs without disease control (defined as CR, PR or SD) and between patients with or without response (defined as CR or PR). This approach allowed for more detailed presentation of findings.

Progression-free survival (PFS) was calculated from the initiation of ICI until the date of disease progression or death. Overall survival (OS) was calculated from the beginning of ICI until the date of death. Individuals who had not progressed or were still alive at the time of data analysis were censored at the date of last follow-up.

2.3.2 Statistical analysis. Statistical analyses were performed with SPSS 25.0.0 software (IBM Corp., Armonk, NY, USA). Descriptive statistics were applied to define and analyze nominal and categorical variables. Statistical significance was set at < 0.05. Spearman's rank correlation coefficient was applied to examine any potential correlations between BMI values with IMFI, VFI, SFI and LSMI and between the fat indices with LSMI. Mann-Whitney U test was used to examine any potential differences amongst the distributions of IMFI, VFI, SFI and LSMI values between responders and non-responders and amongst those who achieved disease control as best response to I-O vs those who experienced disease progression. Chi-square test was applied to investigate any potential associations of the analyzed categorical parameters with ORR.

The Kaplan-Meier method was applied in order to investigate the effect of the studied parameters on PFS and OS. Curves were compared with the log-rank test. We performed initially a univariate Cox regression analysis to examine the effect of BMI, IMFI, VFI, SFI and LSMI as continuous nominal variables on PFS and OS using gender as a stratification factor. In addition, a univariate Cox regression analysis was performed to calculate the Hazard Ratios (HR) of age ≥ 70 years old, PS = 2, squamous histology, bone metastases, liver metastases, brain metastases, PD-L1 < 1%, BMI < 25 kg/m², low IMFI, low VFI, low SFI and LSMI < LNL on PFS and OS. We did not perform a multivariate analysis on the values that

had reached statistical significance in the univariate analysis due to low number of events and small statistical sample.

A sample size and power calculation was not conducted because at the time of the initiation of data collection there were no published reports on the effect of adipose or muscle tissue composition on the outcome of patients with malignancies receiving immunotherapy. Due to the lack of available statistical information on which to base the calculations for power analysis, it would have been of no value in this exploratory, hypothesis generated study.

3. Results

3.1 Patient characteristics

A total of 52 patients were included in the analysis. Individual patient characteristics are depicted in [Table 1](#). Median follow-up time was 9.9 months. Forty three patients (82.7%) were male and median age was 68 years old (range: 39–81 years). Forty three (82.7%) patients had received I-O as second-line treatment and 9 as a first line. All the patients that received immunotherapy as second line of treatment had previously progressed on a platinum doublet regimen. Fifty (96.2%) patients received ICIs as monotherapy and the other two in combination with chemotherapy. Objective Response Rate (ORR) was 23.1% in our cohort and 7 (13.5%) patients experienced grade 3 or 4 immune related adverse events (irAEs) as a result of I-O administration.

Mean baseline body mass index (BMI) was 26.67 kg/m². Thirteen patients (25%) were classified as obese with BMI > 30 kg/m², 21 patients (40.4%) had BMI values \geq 25 kg/m² but < 30 kg/m², and the rest 34.6% of patients had a BMI < 25 kg/m². The median values for intramuscular fat index (IMFI), visceral fat index (VFI) and subcutaneous fat index (SFI) for males and females, respectively, are demonstrated in [Table 1](#). Thirty-six (69.2%) patients were categorized as sarcopenic with lumbar skeletal muscle index (LSMI) values < lower normal limit (LNL).

VFI ($\rho = 0.810$, $p = <0.001$) (S1A Fig in [S1 File](#)), SFI ($\rho = 0.623$, $p = <0.001$) (S1B Fig in [S1 File](#)) and LSMI ($\rho = 0.429$, $p = 0.002$) (S1C Fig in [S1 File](#)) showed a significant positive correlation with BMI values whereas IMFI ($\rho = 0.242$, $p = 0.084$) did not (S1D Fig in [S1 File](#)). In addition, IMFI was not correlated with LSMI ($\rho = -0.172$, $p = 0.222$) (S2A Fig in [S1 File](#)). On the contrary, VFI ($\rho = 0.466$, $p = 0.001$) (S2B Fig in [S1 File](#)) and SFI ($\rho = 0.289$, $p = 0.042$) (S2C Fig in [S1 File](#)) were positively correlated with LSMI.

3.2 Response assessment

The distributions of BMI ($p = 0.391$), IMFI ($p = 0.688$), VFI ($p = 0.460$) and LSMI ($p = 0.501$) did not differ significantly between responders and non-responders to I-O (S3A–S3D Fig in [S1 File](#)). Responders had higher SFI values in comparison to non-responders at a statistically significant level ($p = 0.040$) ([Fig 2A](#)).

In addition, individuals who achieved disease control had higher SFI values ($p = 0.005$) ([Fig 2B](#)), higher BMI values ($p = 0.029$) ([Fig 2C](#)) and higher VFI values ($p = 0.011$) ([Fig 2D](#)) at a statistically significant level in comparison to patients who demonstrated disease progression as best response to treatment. IMFI values ($p = 0.164$) and LSMI values ($p = 105$) did not differ significantly among the individuals who demonstrated disease control vs those who experienced PD (S3E and S3F Fig in [S1 File](#)). None of the analyzed categorical parameters affected ORR at a statistically significant level (S1 Table in [S1 File](#)). Information on response to ICIs, rate of Grade 3–4 irAEs and patient survival (median progression free survival, median overall survival) can be found on [Table 2](#).

Table 1. Baseline (At the beginning of immunotherapy) patient characteristics.

	All patients	
Variable	N	%
Number of patients	52	
Age (years)		
Median (range)	68 (39–81)	
Gender		
Male	43	82.7
Female	9	17.3
Performance status		
0–1	41	78.8
2	11	21.2
Smoking status		
Active or former smokers	48	92.3
Never smokers	4	7.7
Histology		
Squamous	22	42.3
Non-squamous	30	57.7
Mean baseline BMI (SD)	26.67 (4.39)	
Baseline BMI		
< 25 kg/m ²	18	34.6
25 kg/m ² ≤ BMI < 30 kg/m ²	21	40.4
BMI > 30 kg/m ²	13	25
Brain metastases		
Yes	10	19.2
No	42	80.8
Liver metastases		
Yes	14	26.9
No	38	73.1
Bone metastases		
Yes	15	28.8
No	37	71.2
Baseline albumin levels		
≥3.5 g/dl	41	78.8
<3.5 g/dl	6	11.5
Missing values	5	9.6
PD-L1 levels		
< 1%	10	19.2
1% < PD-L1 < 50%	15	28.8
≥ 50%	7	13.5
Missing values	20	38.5
Line of treatment of ICI administration		
1 st line	9	17.3
2 nd line	43	82.7
Immunotherapy agent		
Nivolumab	34	65.4
Pembrolizumab	16	30.8
Atezolizumab	2	3.8
Mode of ICI administration		

(Continued)

Table 1. (Continued)

	All patients	
Variable	N	%
Monotherapy	50	96.2
Combination with chemotherapy	2	3.8
Baseline LSMI		
< LNL	16	30.8
≥ LNL	36	69.2
Median baseline IMFI (cm ² /m ²)		
Males (N = 43) (range)	9.87 (3.53–35.13)	
Females (N = 9) (range)	10.52 (4.24–39.45)	
Median baseline VFI (cm ² /m ²)		
Males (N = 43) (range)	45.15 (6.34–172.82)	
Females (N = 9) (range)	31.20 (12.78–92.75)	
Baseline SFI (cm ² /m ²)		
Males (N = 43) (range)	50.73 (4.61–136.65)	
Females (N = 7) (range)	55.36 (44.24–149.26)	

Abbreviations: BMI = Body mass index, SD = Standard deviation, PD-L1 = Programmed death ligand-1, ICI = Immune checkpoint inhibitor, LSMI: Lumbar skeletal muscle index (At the level of 3rd lumbar vertebra), LNL: Lower normal limit, 55 cm²/m² for males and 39 cm²/m² for females, IMFI = Intramuscular Fat Index (At the level of 3rd lumbar vertebra), VFI = Visceral Fat Index (At the level of 3rd lumbar vertebra), SFI = Subcutaneous Fat Index (At the level of 3rd lumbar vertebra)

<https://doi.org/10.1371/journal.pone.0277708.t001>

3.3 Survival outcomes

The effect of the studied variables on PFS and OS is summarized in S2 Table in [S1 File](#). Patients with baseline LSMI < LNL experienced inferior PFS (3.30 vs 7.33 months, $p = 0.040$) ([Fig 3A](#)) and OS (6.37 vs not reached months, $p = 0.009$) ([Fig 3B](#)), respectively. Low SFI did not affect PFS (2.97 vs 5.77 months, $p = 0.135$) ([Fig 3C](#)) but it was negatively associated with OS (5.43 vs 14.03 months, $p = 0.020$) ([Fig 3D](#)) at a statistically significant level. In addition, the presence of brain metastases demonstrated a significant association with inferior PFS (1.57 vs 4.93 months, $p = 0.006$) but not OS (4.80 vs 12.70 months, $p = 0.083$). Albumin levels < 3.5 g/dl were associated with inferior PFS (1.70 vs 4.80 months, $p = 0.011$) and OS (1.70 vs 11.23 months, $p = 0.001$). None of the other analyzed parameters demonstrated any significant association with PFS or OS (S2 Table in [S1 File](#)).

The subgroup analysis investigating the effect of the combination of SFI and LSMI values on survival outcomes demonstrated that the three subgroups that were created differed significantly in terms of OS ($p = 0.004$) (S4A Fig in [S1 File](#)). However, survival outcomes did not differ significantly between patients with high SFI and LSMI < LNL and patients with both high SFI and LSMI ≥ LNL (9.90 vs 17.93 months, $p = 0.285$) (S4B Fig in [S1 File](#)).

IMFI, VFI, SFI, LSMI and BMI as continuous nominal variables did not demonstrate any significant association with PFS ([Table 3](#)). However, SFI values exhibited a positive association with improved survival HR = **0.983** (95% CI: 0.970–0.987, $p = 0.014$) ([Table 3](#) and S5 Fig in [S1 File](#)). None of the other body composition indices as a continuous variable was associated with OS at a statistically significant level.

The presence of brain metastases HR = **2.71** (95% CI: 1.299–5.667, $p = 0.008$) and baseline LSMI < LNL HR = **2.03** (95% CI: 1.018–4.032, $p = 0.044$) were the only two parameters that predicted for increased probability of disease progression ([Fig 4A](#) and S3 Table in [S1 File](#)). In

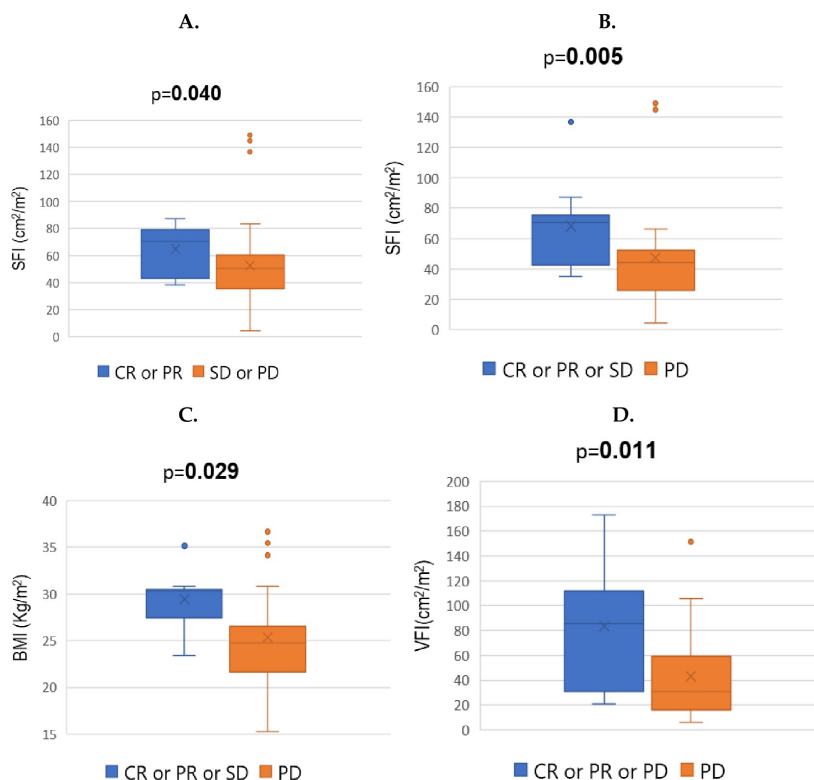


Fig 2. Box-plots depicting the baseline* differential distributions (Mann Whitney U test) of A. SFI (cm²/m²) between responders (CR or PR) and non-responders (SD or PD) to I-O B. SFI (cm²/m²) between patients who achieved disease control (CR or PR or SD) as result of I-O versus those who developed disease progression (PD) C. BMI (kg/m²) between patients who achieved disease control as result of I-O administration in comparison to those who developed disease progression and D. VFI (cm²/m²) between individuals who experienced disease control under I-O versus those who had disease progression. Abbreviations: I-O = Immunotherapy; BMI = Body mass index; VFI = Visceral Fat Index (At the level of 3rd lumbar vertebra); SFI = Subcutaneous Fat Index (At the level of 3rd lumbar vertebra); CR = Complete response; PR = Partial response; SD = Stable disease, PD = Progressive disease. *Baseline = At the beginning of immunotherapy.

<https://doi.org/10.1371/journal.pone.0277708.g002>

the univariate analysis for OS baseline LSMI < LNL HR = **2.90** (95% CI:1.261–6.667, p = **0.012**) and low SFI HR = **2.20** (1.114–4.333, p = **0.023**) predicted for inferior survival (Fig 4B and S3 Table in S1 File).

4. Discussion

In this study we demonstrated that reduced subcutaneous adiposity and skeletal muscle depletion could possibly constitute negative prognostic factors for individuals with metastatic NSCLC treated with ICIs. In our cohort, low SFI values (either as a continuous variable or as a categorical variable) were significantly associated with inferior survival outcomes. In addition, responders to treatment exhibited higher SFI distributions in comparison to non-responders.

Table 2. Treatment and response characteristics.

	All patients	
Variable	N	%
Response to ICIs		
CR	1	1.9
PR	11	21.2
SD	15	28.8
PD	25	48.1
Grade 3–4 irAEs		
Yes	7	13.5
No	45	86.5
Progression-free survival (months)		
Median (95% CI)	4.67 (3.53–5.81)	
Overall survival (months)		
Median (95% CI)	10.33 (6.83–13.84)	
Follow-up (months)		
Median (95% CI)	9.90 (5.07–14.73)	

Abbreviations: CR: Complete response, PR: Partial response, SD: Stable disease, PD: Progressive disease, irAEs = Immune-related Adverse Events

<https://doi.org/10.1371/journal.pone.0277708.t002>

Several clinical studies on cancer patients treated with ICIs have demonstrated that high BMI values are associated with favorable outcomes [9–11]. In a retrospective study of patients with clear cell renal carcinoma, obese patients were found to have increased peritumoral adipose tissue inflammation and better survival outcomes [31]. Martini et al. [32] performed a retrospective analysis of 90 patients that had received immunotherapy for a wide range of malignancies in the context of phase I trials and demonstrated that high SFI/IMFI ratio consisted an independent predictor of superior OS. On the contrary, Woodall et al. [33] investigated the effect of BMI and body composition on treatment outcomes in melanoma patients receiving ICIs. They reported that high total visceral and subcutaneous adipose tissue index was associated with reduced PFS [33]. However, when they investigated the effect of subcutaneous adipose tissue index it was not associated with reduced PFS or OS [33]. Finally Schols et al. [34] (citation: [10.1002/jcsm.12698](https://doi.org/10.1002/jcsm.12698)) demonstrated in a cohort of 106 NSCLC patients treated with nivolumab that the weight loss > 2% under treatment which was reflected with a significant loss in SFI and VFI consisted a negative prognostic survival factor. Our results are consistent with the results of Martini et al. [32] demonstrating a potential positive link between increased subcutaneous adiposity and improved survival outcomes. The novelty of our findings is that we demonstrate a potential link between baseline SFI values and clinical outcomes in a population with homogeneous underlying malignancy histology. The fact that we were not able to demonstrate any association between BMI and immunotherapy outcomes can be partially attributed to the small population sample since overweight/obese patients in our cohort had better outcomes but this difference did not reach statistical significance. The discordance between our results and the results from Woodall et al. [33] can be explained by selection bias among patient populations, different underlying malignancies and different immunotherapies.

However, our findings along with the results of the majority of the aforementioned studies could suggest a link between adiposity and improved antitumor immune response that merits further evaluation. There are insufficient data for the proposal of a robust biological link, but

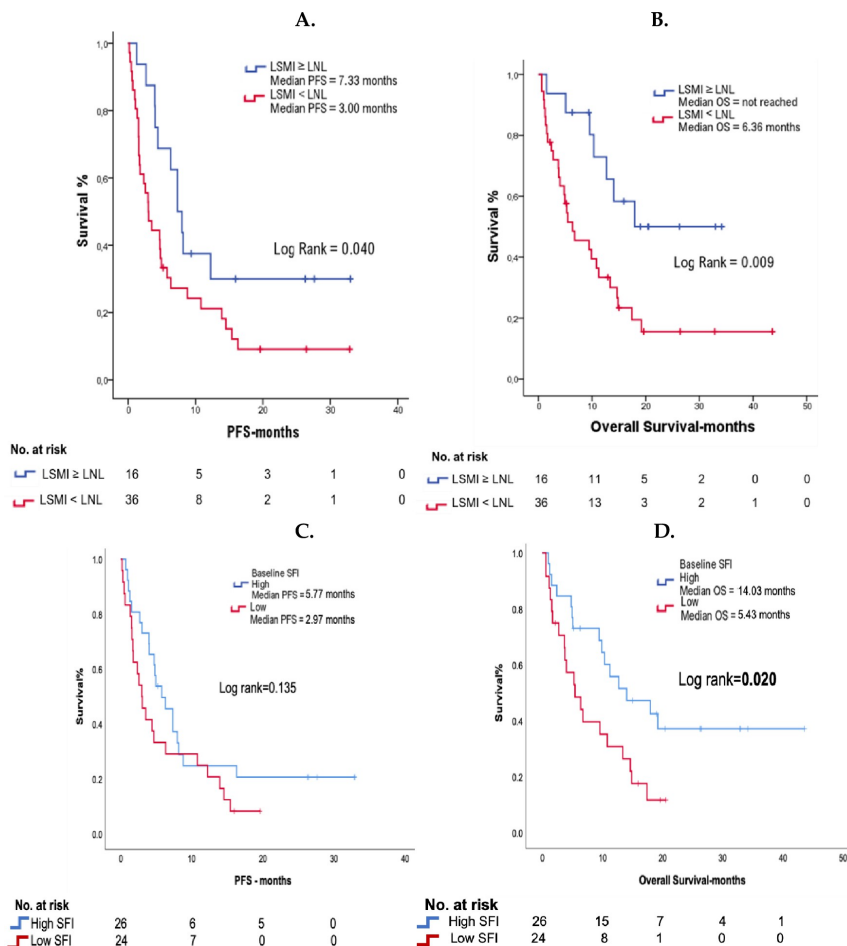


Fig 3. Kaplan-Meier curves demonstrating the effect of A. Baseline¹ LSMI² values on PFS B. Baseline LSMI values on OS C. Baseline SFI³ values on PFS D. Baseline SFI values on OS. Abbreviations: LSMI = Lumbar skeletal muscle index (At the level of 3rd lumbar vertebra); SFI = Subcutaneous Fat Index (At the level of 3rd lumbar vertebra); OS = Overall survival; PFS = Progression free survival. ¹**Baseline:** At the beginning of immunotherapy with PD-1/PD-L1 inhibitors. ²**LNL:** Lower normal limit, 55 cm²/m² for males and 39 cm²/m² for females. ³**High and low classification for SFI** represents above and below gender specific median value, respectively.

<https://doi.org/10.1371/journal.pone.0277708.g003>

subcutaneous adipose tissue is the compartment responsible for the production of leptin [35]. Leptin was demonstrated by Wang et al. [36] to be at least partially responsible for the effects of PD-1 upregulation and immune aging in obese mice as a counterbalance mechanism for the inflammatory status that accompanies obesity. However, the same biological effect may be responsible for the increased sensitivity to PD-1 inhibition in obese mice and humans, since they rely on PD-L1 axis as a feedback mechanism for the immunologic equilibrium of their

Table 3. Univariate analysis using Cox regression method investigating the hazard ratios of the BMI*, IMFI, VFI and SFI as continuous nominal variables (cm²/m²) on PFS and OS. Gender was used as a stratification factor.

COX REGRESSION	PFS		OS	
UNIVARIATE ANALYSIS	HR (95% Confidence Intervals)	p value	HR (95% Confidence Intervals)	p value
BMI (kg/m ²)	0.973 (0.895–1.059)	0.528	0.936 (0.853–1.028)	0.165
LSMI (cm ² /m ²)	0.981 (0.950–1.013)	0.236	0.973 (0.941–1.006)	0.102
IMFI (cm ² /m ²)	0.996 (0.955–1.039)	0.866	0.950 (0.890–1.014)	0.121
VFI (cm ² /m ²)	0.998 (0.989–1.007)	0.646	0.991 (0.980–1.002)	0.095
SFI (cm ² /m ²)	0.993 (0.982–1.005)	0.246	0.983 (0.970–0.997)	0.014

Abbreviations: BMI: Body mass index (kg/m²), LSMI: Lumbar skeletal muscle index (cm²/m²), IMFI = Intramuscular fat index (cm²/m²), VFI = Visceral fat index (cm²/m²), SFI = Subcutaneous fat index (cm²/m²)

* BMI, IMFI, VFI and SFI were calculated at the beginning of immunotherapy

<https://doi.org/10.1371/journal.pone.0277708.t003>

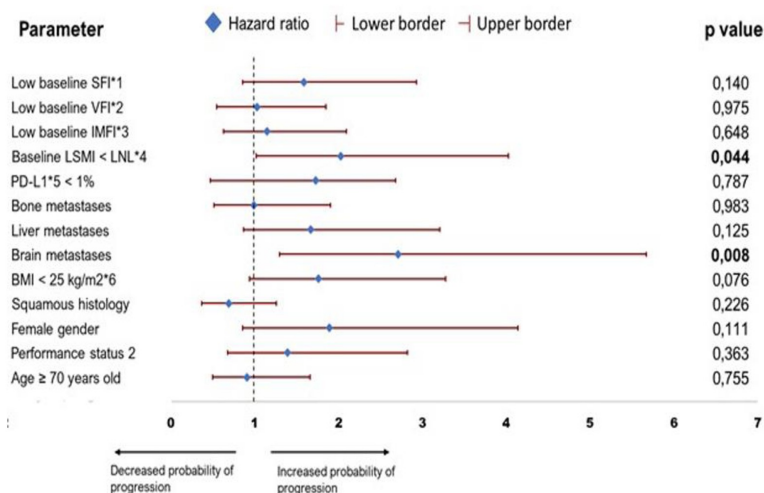
underlying inflammatory process and the release of this inhibition might result in more effective antitumor responses. On the other hand, it is unclear whether the link between high SFI and improved outcomes is causal and not an epiphenomenon due to a potential underlying cancer cachexia syndrome and a subsequent process of browning of white adipose tissue [37].

Furthermore, there is accumulation of evidence on the cellular pathways that connect adipose tissue composition and immune system regulation [38]. Adipose tissue serves as a nest for a plethora of immune cells such as macrophages, CD4+ T cells, CD8+ T cells, T regulatory (Treg) cells, iNKT cells and $\gamma\delta$ T cells [39]. The infiltration of macrophages into the adipose tissue of obese mice has been reported to switch them from the M2 phenotype to M1 proinflammatory phenotype, a phenomenon that has not been observed in non-obese mice [40, 41]. Furthermore, the adipose tissue of obese mice was found to be infiltrated by increased numbers of effector T cells and to demonstrate a high CD8+/CD4+ ratio with diminished number of Tregs [42]. Tregs act as a negative regulator of the inflammatory process in the adipose tissue of normal weight mice, but their numbers are greatly reduced in the adipose tissue of obese mice [43]. Based on these experimental data it is possible that obese individuals are more susceptible to checkpoint inhibition in the setting of underlying malignancies, due to an underlying pro-inflammatory status characterized by increased Th1 responses, macrophage polarization to an M1 phenotype and reduced number of Tregs in their adipose tissue reservoirs. However, this hypothesis needs to be further tested with additional preclinical and translational data.

LSMI levels consistent with sarcopenia were also an adverse prognostic factor in our cohort. Sarcopenia has been linked to adverse outcomes in cancer patients in multiple studies [17, 18] before the introduction of ICIs. In addition, it is one of the criteria for the definition of cancer cachexia, which consists one of the most well recognized adverse prognostic factors in cancer patients [20]. Our results are in accordance with other studies on the role of skeletal muscle depletion as a negative prognostic and predictive factor in ICI treated cancer patients [19, 21, 22, 34, 44].

In addition, we performed a subgroup analysis to examine the survival outcomes of patients with both low adiposity and muscle depletion in comparison to the patients with high adiposity but muscle depletion and the individuals without muscle depletion and high adiposity. Patients with both low SFI and sarcopenia had the worst outcome whereas the other two subgroups did not differ significantly. Woodall et al. [33] reported that patients with adiposity and reduced muscle mass had worse outcomes. This discordance might be due to the small sample size in our cohort that can hinder possible statistically significant correlations. Nevertheless,

A.



B.

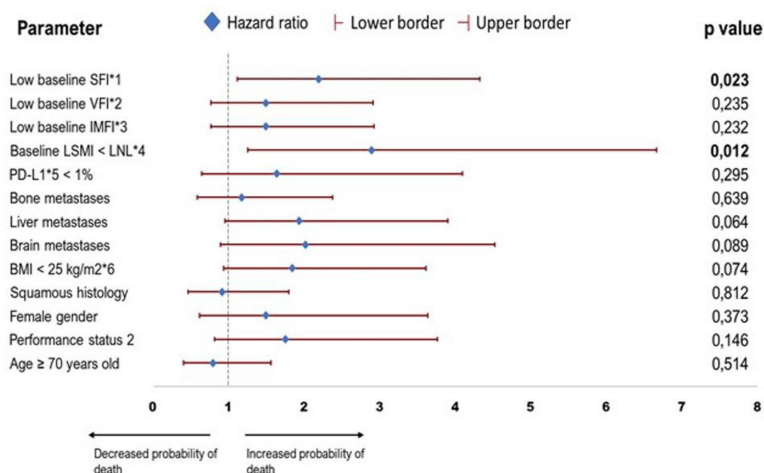


Fig 4. Forest plots demonstrating the hazard ratios and their 95% confidence intervals of the analyzed parameters on A. Probability of disease progression B. Probability of death under treatment with ICIs. Abbreviations: BMI = Body mass index; PD-L1 = Programmed death ligand-1, ICI = Immune checkpoint inhibitor; LSMI: Lumbar skeletal muscle index (At the level of 3rd lumbar vertebra); LNL: Lower normal limit, 55 cm²/m² for males and 39 cm²/m² for females; IMFI = Intramuscular Fat Index (At the level of 3rd lumbar vertebra); VFI = Visceral Fat Index (At the level of 3rd lumbar vertebra); SFI = Subcutaneous Fat Index (At the level of 3rd lumbar vertebra). *^{1,2,3,4,5,6} SFI, VFI, IMFI, LSMI, PD-L1 and BMI values were calculated at the beginning of treatment with ICIs. *^{1,2,3} Low for SFI, VFI and IMFI means below gender specific median value.

<https://doi.org/10.1371/journal.pone.0277708.g004>

further research is required in order to redefine the prognostic importance of sarcopenic obesity in the era of immunotherapy.

To our knowledge this is first analysis of prospective data in NSCLC patients who are treated with ICIs which investigates the effect of fat and muscle tissue composition on treatment outcomes. Our study consists of a population with a certain degree of homogeneity since the vast majority of the NSCLC patients received immunotherapy as a monotherapy with PD-1/PDL-1 inhibitors and most of the patients received it as 2nd line treatment.

The major limitation of our study is the small statistical sample with limited statistical power. Due to the small sample size, we analyzed together patients treated with ICIs in the 1st and 2nd line setting, while we also included two patients treated with chemotherapy-ICI combination; we consider this number too small to significantly affect results. In addition, due to low number of events in the subgroup of patients with LMSI values not consistent with sarcopenia we were not able to perform a multivariate analysis for overall survival. Our sample group was treated mostly with 2nd line PD-1/PDL-1 inhibitors, however a significant number of patients received them as 1st line. In addition, our cohort was imbalanced according to gender with the majority of our patients being male and only a small proportion being female. Fat tissue compositions can differ significantly between the two genders and an imbalanced population can hinder significant statistical associations. Moreover, age is one of the most significant factors that affects body composition and in this study patients from all age groups were included. A power calculation was not feasible mainly due to the exploratory nature of this study and secondary because of the lack of previous publications on the effect of adipose tissue composition in ICI treated NSCLC patients in which to base an initial power calculation. Finally, due to the lack of a specified cut-off for IMFI, VFI and SFI we arbitrarily chose as a cut-off point the gender specific median value of each perspective variable.

5. Conclusions

Our findings demonstrate that subcutaneous adipose tissue and muscle tissue composition could be associated with outcomes with ICI treatment in NSCLC patients. Validation of these results in larger cohorts is required.

The results from our study and from similar published articles propose a potential link between subcutaneous adiposity and sensitivity to PD-1/PD-L1 inhibition. Further research on preclinical and translational lever is required to further decipher a potential association between adiposity composition and immune system function towards the finding of novel drug targets or novel biomarkers.

Supporting information

S1 File.
(DOCX)

Acknowledgments

We would like to thank all the patients and their families for their participation in this study.

Institutional review board statement

Our study was approved by the ethical board of the University Hospital of Heraklion, Crete (ID: 2644) and was conducted according to principles of the declaration of Helsinki.

Informed consent statement

Written informed consent was obtained from all patients before enrollment.

Author Contributions

Conceptualization: Konstantinos Rounis, Sofia Agelaki.

Data curation: Dimitrios Makrakis, Nikolaos Galanakis, Chara Papadaki, Alexia Monastirioti.

Formal analysis: Dimitrios Makrakis, Konstantinos Rounis.

Funding acquisition: Dimitris Mavroudis, Sofia Agelaki.

Investigation: Dimitrios Makrakis, Nikolaos Galanakis, Chara Papadaki, Alexia Monastirioti.

Methodology: Dimitrios Makrakis, Konstantinos Rounis, Meropi Kontogianni, Ioannis Gioulbasanis, Sofia Agelaki.

Project administration: Sofia Agelaki.

Software: Alexandros-Pantelis Tsigkas, Alexandra Georgiou.

Supervision: Dimitris Mavroudis, Sofia Agelaki.

Validation: Konstantinos Rounis, Meropi Kontogianni, Ioannis Gioulbasanis, Dimitris Mavroudis, Sofia Agelaki.

Writing – original draft: Dimitrios Makrakis, Konstantinos Rounis, Nikolaos Galanakis.

Writing – review & editing: Dimitrios Makrakis, Konstantinos Rounis, Alexandros-Pantelis Tsigkas, Alexandra Georgiou, Nikolaos Galanakis, George Tsakonas, Simon Ekman, Chara Papadaki, Alexia Monastirioti, Meropi Kontogianni, Ioannis Gioulbasanis, Dimitris Mavroudis, Sofia Agelaki.

References

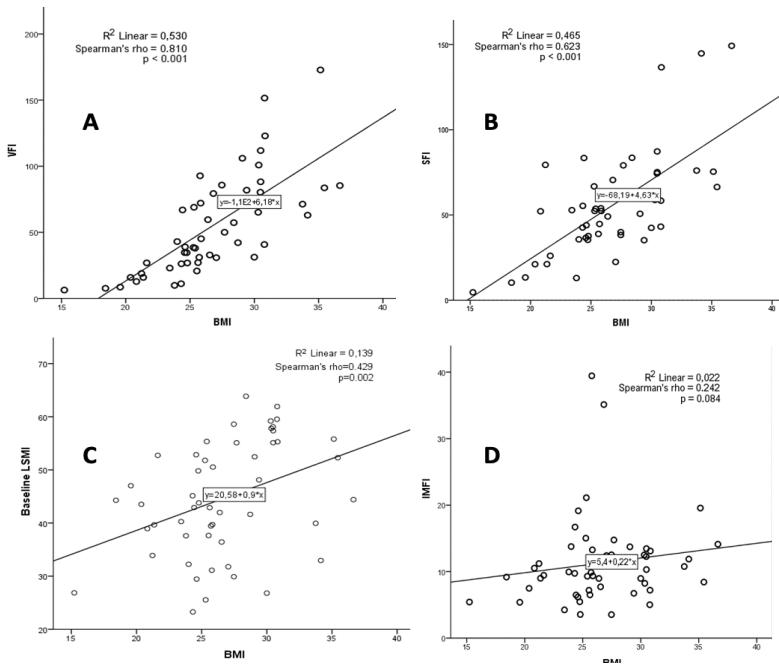
1. Robert C. A decade of immune-checkpoint inhibitors in cancer therapy. *Nature Communications*. 2020; 11(1):3801. <https://doi.org/10.1038/s41467-020-17670-y> PMID: 32732879
2. Camidge DR, Doebele RC, Kerr KM. Comparing and contrasting predictive biomarkers for immunotherapy and targeted therapy of NSCLC. *Nature Reviews Clinical Oncology*. 2019; 16(6):341–355. <https://doi.org/10.1038/s41571-019-0173-9> PMID: 30718843
3. Munari E, Zamboni G, Lunardi G, et al. PD-L1 Expression Heterogeneity in Non-Small Cell Lung Cancer: Defining Criteria for Harmonization between Biopsy Specimens and Whole Sections. *J Thorac Oncol*. 2018; 13(8):1113–1120. <https://doi.org/10.1016/j.jtho.2018.04.017> PMID: 29704674
4. Dong P, Xiong Y, Yue J, Hanley SJB, Watari H. Tumor-Intrinsic PD-L1 Signaling in Cancer Initiation, Development and Treatment: Beyond Immune Evasion. *Front Oncol*. 2018; 8. <https://doi.org/10.3389/fonc.2018.00386> PMID: 30283733
5. Kelly T, Yang W, Chen CS, Reynolds K, He J. Global burden of obesity in 2005 and projections to 2030. *Int J Obes (Lond)*. 2008; 32(9):1431–1437. <https://doi.org/10.1038/ijo.2008.102> PMID: 18607383
6. Vainio H, Kaaks R, Bianchini F. Weight control and physical activity in cancer prevention: international evaluation of the evidence. *Eur J Cancer Prev*. 2002; 11 Suppl 2:S94–100. PMID: 12570341
7. Wolin KY, Carson K, Colditz GA. Obesity and cancer. *Oncologist*. 2010; 15(6):556–565. <https://doi.org/10.1634/theoncologist.2009-0285> PMID: 20507889
8. Horowitz NS, Wright AA. Impact of obesity on chemotherapy management and outcomes in women with gynecologic malignancies. *Gynecol Oncol*. 2015; 138(1):201–206. <https://doi.org/10.1016/j.ygyno.2015.04.002> PMID: 25870918
9. Kichenadasse G, Miners JO, Mangoni AA, Rowland A, Hopkins AM, Soric MJ. Association Between Body Mass Index and Overall Survival With Immune Checkpoint Inhibitor Therapy for Advanced Non-Small Cell Lung Cancer. *JAMA Oncol*. 2020; 6(4):512–518. <https://doi.org/10.1001/jamaoncol.2019.5241> PMID: 31876896

10. Cortellini A, Bersanelli M, Buti S, et al. A multicenter study of body mass index in cancer patients treated with anti-PD-1/PD-L1 immune checkpoint inhibitors: when overweight becomes favorable. *J Immunother Cancer*. 2019;7. <https://doi.org/10.1186/s40425-019-0527-y> PMID: 30813970
11. McQuade JL, Daniel CR, Hess KR, et al. Association of body-mass index and outcomes in patients with metastatic melanoma treated with targeted therapy, immunotherapy, or chemotherapy: a retrospective, multicohort analysis. *Lancet Oncol*. 2018; 19(3):310–322. [https://doi.org/10.1016/S1470-2045\(18\)30078-0](https://doi.org/10.1016/S1470-2045(18)30078-0) PMID: 29449192
12. Kershaw EE, Flier JS. Adipose tissue as an endocrine organ. *J Clin Endocrinol Metab*. 2004; 89(6):2548–2556. <https://doi.org/10.1210/jc.2004-0395> PMID: 15181022
13. Spoto B, Di Betta E, Mattace-Raso F, et al. Pro- and anti-inflammatory cytokine gene expression in subcutaneous and visceral fat in severe obesity. *Nutr Metab Cardiovasc Dis*. 2014; 24(10):1137–1143. <https://doi.org/10.1016/j.numecd.2014.04.017> PMID: 24984824
14. Mauland KK, Eng Ø, Ytre-Hauge S, et al. High visceral fat percentage is associated with poor outcome in endometrial cancer. *Oncotarget*. 2017; 8(62):105184–105195. <https://doi.org/10.18632/oncotarget.21917> PMID: 29285243
15. Antoun S, Bayar A, Ileana E, et al. High subcutaneous adipose tissue predicts the prognosis in metastatic castration-resistant prostate cancer patients in post chemotherapy setting. *Eur J Cancer*. 2015; 51(17):2570–2577. <https://doi.org/10.1016/j.ejca.2015.07.042> PMID: 26278649
16. Ebadi M, Martin L, Ghosh S, et al. Subcutaneous adiposity is an independent predictor of mortality in cancer patients. *British Journal of Cancer*. 2017; 117(1):148–155. <https://doi.org/10.1038/bjc.2017.149> PMID: 28588319
17. Antoun S, Borget I, Lanoy E. Impact of sarcopenia on the prognosis and treatment toxicities in patients diagnosed with cancer. *Curr Opin Support Palliat Care*. 2013; 7(4):383–389. <https://doi.org/10.1097/SPC.0000000000000011> PMID: 24189893
18. Shachar SS, Williams GR, Muss HB, Nishijima TF. Prognostic value of sarcopenia in adults with solid tumours: A meta-analysis and systematic review. *Eur J Cancer*. 2016; 57:58–67. <https://doi.org/10.1016/j.ejca.2015.12.030> PMID: 26882087
19. Sakamoto T, Yagyu T, Uchinaka E, et al. Sarcopenia as a prognostic factor in patients with recurrent pancreatic cancer: a retrospective study. *World Journal of Surgical Oncology*. 2020; 18(1):221. <https://doi.org/10.1186/s12957-020-01981-x> PMID: 32828127
20. Fearon K, Strasser F, Anker SD, et al. Definition and classification of cancer cachexia: an international consensus. *Lancet Oncol*. 2011; 12(5):489–495. [https://doi.org/10.1016/S1470-2045\(10\)70218-7](https://doi.org/10.1016/S1470-2045(10)70218-7) PMID: 21296615
21. Chu MP, Li Y, Ghosh S, et al. Body composition is prognostic and predictive of ipilimumab activity in metastatic melanoma. *J Cachexia Sarcopenia Muscle*. 2020; 11(3):748–755. <https://doi.org/10.1002/jcsm.12538> PMID: 32053287
22. Roch B, Coffy A, Jean-Baptiste S, et al. Cachexia—sarcopenia as a determinant of disease control rate and survival in non-small lung cancer patients receiving immune-checkpoint inhibitors. *Lung Cancer*. 2020; 143:19–26. <https://doi.org/10.1016/j.lungcan.2020.03.003> PMID: 32200137
23. Rounis K, Makrakis D, Tsigkas AP, et al. Cancer cachexia syndrome and clinical outcome in patients with metastatic non-small cell lung cancer treated with PD-1/PD-L1 inhibitors: results from a prospective, observational study. *Translational Lung Cancer Research*. 2021; 10(8). <https://doi.org/10.21037/tlcr-21-460> PMID: 34584855
24. Daly LE, Power DG, O'Reilly Á, et al. The impact of body composition parameters on ipilimumab toxicity and survival in patients with metastatic melanoma. *British Journal of Cancer*. 2017; 116(3):310–317. <https://doi.org/10.1038/bjc.2016.431> PMID: 28072766
25. Planchard D, Popat S, Kerr K, et al. Metastatic non-small cell lung cancer: ESMO Clinical Practice Guidelines for diagnosis, treatment and follow-up. *Ann Oncol*. 2018; 29(Suppl 4):iv192–iv237. <https://doi.org/10.1093/annonc/mdy275> PMID: 30285222
26. Mourtzakis M, Prado CMM, Lieffers JR, Reiman T, McCargar LJ, Baracos VE. A practical and precise approach to quantification of body composition in cancer patients using computed tomography images acquired during routine care. *Appl Physiol Nutr Metab*. 2008; 33(5):997–1006. <https://doi.org/10.1139/H08-075> PMID: 18923576
27. Miller KD, Jones E, Yanovski JA, Shankar R, Feuerstein I, Falloon J. Visceral abdominal-fat accumulation associated with use of indinavir. *Lancet*. 1998; 351(9106):871–875. [https://doi.org/10.1016/S0140-6736\(97\)11518-5](https://doi.org/10.1016/S0140-6736(97)11518-5) PMID: 9525365
28. Mitsiopoulos N, Baumgartner RN, Heymsfield SB, Lyons W, Gallagher D, Ross R. Cadaver validation of skeletal muscle measurement by magnetic resonance imaging and computerized tomography. *J Appl Physiol* (1985). 1998; 85(1):115–122. <https://doi.org/10.1152/jappl.1998.85.1.115> PMID: 9655763

29. Haanen JB a. G, Carbone F, Robert C, et al. Management of toxicities from immunotherapy: ESMO Clinical Practice Guidelines for diagnosis, treatment and follow-up. *Ann Oncol*. 2017; 28(suppl_4): iv119–iv142. <https://doi.org/10.1093/annonc/mdx225> PMID: 28881921
30. Eisenhauer EA, Therasse P, Bogaerts J, et al. New response evaluation criteria in solid tumours: revised RECIST guideline (version 1.1). *Eur J Cancer*. 2009; 45(2):228–247. <https://doi.org/10.1016/j.ejca.2008.10.026> PMID: 19097774
31. Sanchez A, Furberg H, Kuo F, et al. Transcriptomic signatures related to the obesity paradox in patients with clear cell renal cell carcinoma: a cohort study. *Lancet Oncol*. 2020; 21(2):283–293. [https://doi.org/10.1016/S1470-2045\(19\)30797-1](https://doi.org/10.1016/S1470-2045(19)30797-1) PMID: 31870811
32. Martini DJ, Kline MR, Liu Y, et al. Adiposity may predict survival in patients with advanced stage cancer treated with immunotherapy in phase 1 clinical trials. *Cancer*. 2020; 126(3):575–582. <https://doi.org/10.1002/ncr.32576> PMID: 31648379
33. Woodall MJ, Neumann S, Campbell K, Pattison ST, Young SL. The Effects of Obesity on Anti-Cancer Immunity and Cancer Immunotherapy. *Cancers (Basel)*. 2020; 12(5). <https://doi.org/10.3390/cancers12051230> PMID: 32422865
34. Degens JHRJ Dingemans AMC, Willemsen ACH, et al. The prognostic value of weight and body composition changes in patients with non-small-cell lung cancer treated with nivolumab. *Journal of Cachexia, Sarcopenia and Muscle*. 2021; 12(3):657–664. <https://doi.org/10.1002/jcsm.12698> PMID: 33951326
35. Hube F, Lietz U, Igel M, et al. Difference in Leptin mRNA Levels Between Omental and Subcutaneous Abdominal Adipose Tissue From Obese Humans. *Horm Metab Res*. 1996; 28(12):690–693. <https://doi.org/10.1055/s-2007-979879> PMID: 9013743
36. Wang Z, Aguilar EG, Luna JI, et al. Paradoxical effects of obesity on T cell function during tumor progression and PD-1 checkpoint blockade. *Nature Medicine*. 2019; 25(1):141–151. <https://doi.org/10.1038/s41591-018-0221-5> PMID: 30420753
37. Kir S, Spiegelman BM. CACHEXIA & BROWN FAT: A BURNING ISSUE IN CANCER. *Trends Cancer*. 2016; 2(9):461–463. <https://doi.org/10.1016/j.trecan.2016.07.005> PMID: 28459108
38. Wensveen FM, Valentić S, Šestan M, Turk Wensveen T, Polić B. Interactions between adipose tissue and the immune system in health and malnutrition. *Seminars in Immunology*. 2015; 27(5):322–333. <https://doi.org/10.1016/j.smim.2015.10.006> PMID: 26603491
39. Lu J, Zhao J, Meng H, Zhang X. Adipose Tissue-Resident Immune Cells in Obesity and Type 2 Diabetes. *Front Immunol*. 2019; 10. <https://doi.org/10.3389/fimmu.2019.01173> PMID: 31191541
40. Lumeng CN, Bodzin JL, Saltiel AR. Obesity induces a phenotypic switch in adipose tissue macrophage polarization. *J Clin Invest*. 2007; 117(1):175–184. <https://doi.org/10.1172/JCI29881> PMID: 17200717
41. Kratz M, Coats BR, Hisert KB, et al. Metabolic Dysfunction Drives a Mechanistically Distinct Proinflammatory Phenotype in Adipose Tissue Macrophages. *Cell Metabolism*. 2014; 20(4):614–625. <https://doi.org/10.1016/j.cmet.2014.08.010> PMID: 25242226
42. Nishimura S, Manabe I, Nagasaki M, et al. CD8+ effector T cells contribute to macrophage recruitment and adipose tissue inflammation in obesity. *Nat Med*. 2009; 15(8):914–920. <https://doi.org/10.1038/nm.1964> PMID: 19633658
43. Ilan Y, Maron R, Tukpah AM, et al. Induction of regulatory T cells decreases adipose inflammation and alleviates insulin resistance in ob/ob mice. *PNAS*. 2010; 107(21):9765–9770. <https://doi.org/10.1073/pnas.0908771107> PMID: 20445103
44. Nishioka N., Naito T., Notsu A., Mori K., Kodama H., Miyawaki E., et al. (2021). Unfavorable impact of decreased muscle quality on the efficacy of immunotherapy for advanced non-small cell lung cancer. *Cancer Med.*, 10: 247–256. <https://doi.org/10.1002/cam4.3631>. <https://doi.org/10.1002/cam4.3631> PMID: 33300678

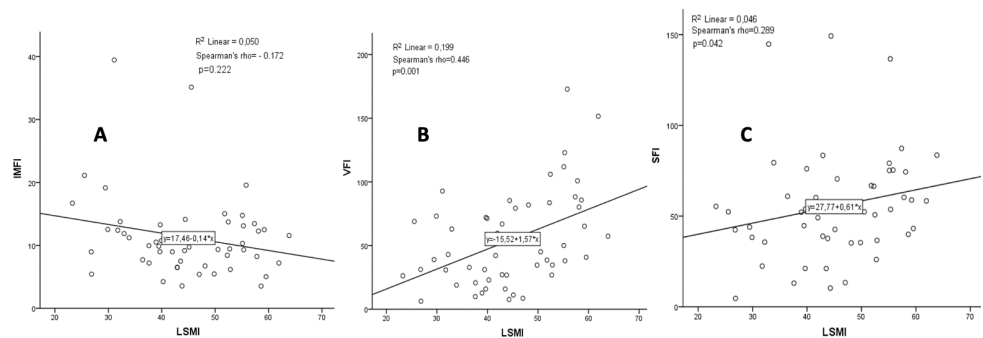
Supplementary data

Figure S1: Scatter-plots demonstrating the correlation between baseline BMI values and A. baseline VFI values, B. baseline SFI values C. baseline LSMI values D. baseline IMFI values.



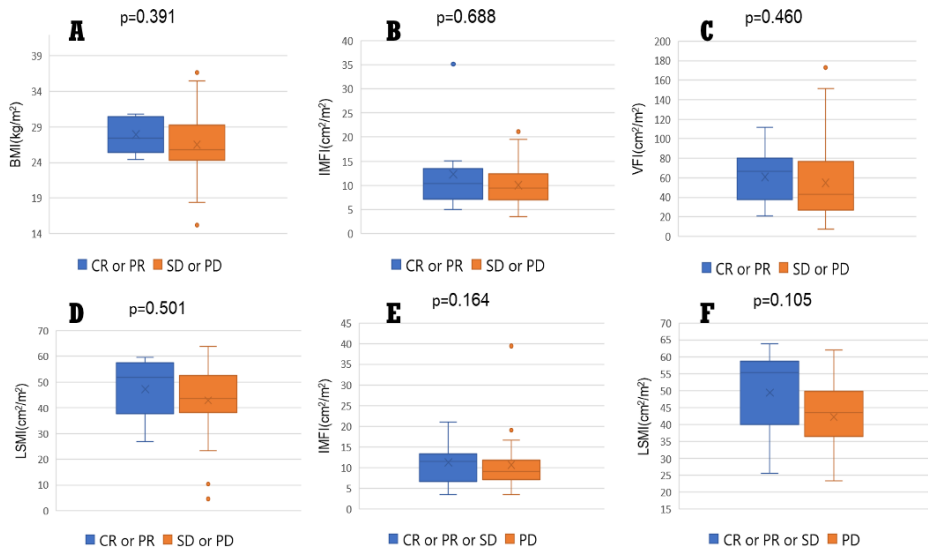
Abbreviations: BMI=Body mass index, LSMI: Lumbar skeletal muscle index (At the level of 3rd lumbar vertebra), IMFI=Intramuscular Fat Index (At the level of 3rd lumbar vertebra), VFI=Visceral Fat Index (At the level of 3rd lumbar vertebra), SFI=Subcutaneous Fat Index (At the level of 3rd lumbar vertebra)

Figure S2: Scatter-plots demonstrating the correlation between baseline LSMI values and A. baseline IMFI values, B. baseline VFI values, C. baseline SFI values.



Abbreviations: LSMI: Lumbar skeletal muscle index (At the level of 3rd lumbar vertebra), IMFI=Intramuscular Fat Index (At the level of 3rd lumbar vertebra), VFI=Visceral Fat Index (At the level of 3rd lumbar vertebra), SFI=Subcutaneous Fat Index (At the level of 3rd lumbar vertebra)

Figure S3: Box-plots demonstrating the differential distributions (Mann Whitney U test) of A. Baseline* BMI values between responders and non-responders B. IMFI values between responders and non-responders C. VFI values between responders and non-responders D. LSMI values between responders and non-responders E. IMFI values in patients who achieved disease control (CR or PR or SD) versus those who experienced PD F. LSMI values of individuals who achieved disease control versus those who had disease progression.



Abbreviations: BMI=Body mass index, LSMI: Lumbar skeletal muscle index (At the level of 3rd lumbar vertebra), IMFI=Intramuscular Fat Index (At the level of 3rd lumbar vertebra), VFI=Visceral Fat Index (At the level of 3rd lumbar vertebra), SFI=Subcutaneous Fat Index (At the level of 3rd lumbar vertebra), CR: Complete response, PR: Partial response, SD: Stable disease, PD: Progressive disease

* **Baseline:** At the beginning of immunotherapy

Table S1: Effect of the studied variables on objective response rate (ORR).

Variable	N=52	CR or PR	SD or PD	P value (chi-square test, 95% CI)
Age				
< 70 years old	31	7	25	0.918
≥ 70 years old	21	5	16	
Gender				
Male	43	10	33	0.947
Female	9	2	7	
Performance status				
0-1	41	10	31	0.664
2	9	2	11	
Histology				
Non-squamous	30	7	23	0.959
Squamous	22	5	17	
Brain metastases				
Yes	10	1	9	0.275
No	42	11	31	
Liver metastases				
Yes	14	3	11	0.864
No	38	9	29	
Bone metastases				
Yes	15	4	11	0.696
No	37	8	29	
PD-L1 status	N=33			
< 1 %	10	2	8	0.708
≥ 1 %	23	6	17	
Baseline albumin levels	N=47			
< 3.5 g/dl	6	0	6	0.202
≥ 3.5 g/dl	41	9	32	
BMI				
< 25 kg/m ²	18	2	16	0.136
≥ 25 kg/m ²	34	10	24	
Baseline LSMI				
< LNL	36	6	30	0.100
≥ LNL	16	6	10	
Baseline IMFI				
Low	26	5	21	0.510
High	26	7	19	

Table S1: Effect of the studied variables on objective response rate (ORR).

Variable	N=52	CR or PR	SD or PD	P value (chi-square test, 95% CI)
Baseline VFI				
Low	26	6	20	1.000
High	26	6	20	
Baseline SFI				
	N=50			
Low	25	3	22	0.088
High	25	8	17	

Abbreviations: BMI=Body mass index; SD=Standard deviation; LSMI=Lumbar skeletal muscle index (At the level of 3rd lumbar vertebra), LNL: Lower normal limit, 55 cm²/m² for males and 39 cm²/m² for females; IMFI=Intramuscular Fat Index (At the level of 3rd lumbar vertebra); VFI=Visceral Fat Index (At the level of 3rd lumbar vertebra); SFI=Subcutaneous Fat Index (At the level of 3rd lumbar vertebra)

Table S2: Log-rank test on the effect of the studied variables on PFS and OS.

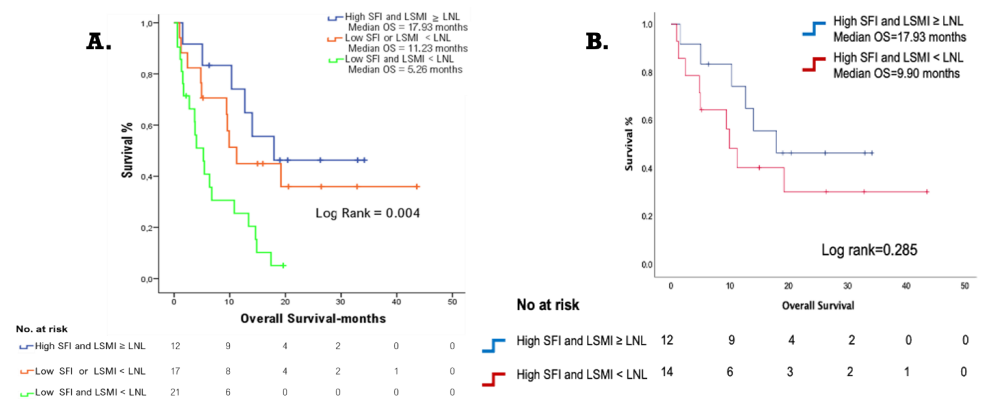
	Median PFS (Months)	p value (log-rank test)	Median OS (Months)	p value (log-rank test)
All patients (n=52)				
Age				
< 70 years old	4.00	0.754	9.43	0.512
≥ 70 years old	7.33		13.37	
Gender				
Male	4.80	0.104	11.23	0.370
Female	1.53		6.77	
Performance Status				
0-1	4.80	0.360	12.70	0.140
2	3.50		5.27	
Histology				
Squamous	5.77	0.222	10.80	0.812
Non-squamous	2.57		9.90	
BMI				
< 25 kg/m²	1.77	0.196	3.77	0.175
25 kg/m² ≤ BMI < 30 kg/m²	6.30		10.30	
BMI ≥ 30 kg/m²	7.33		14.03	
Line of treatment of ICI administration				
1 st line	7.33	0.088	Not reached	0.005
2 nd or later lines	4.67		9.43	

Table S2: Log-rank test on the effect of the studied variables on PFS and OS.

	Median PFS (Months)	p value (log-rank test)	Median OS (Months)	p value (log-rank test)
Brain metastases				
Yes	1.57	0.006	4.80	0.083
No	4.93		12.70	
Bone metastases				
Yes	4.70	0.983	10.80	0.638
No	4.67		10.33	
Liver metastases				
Yes	1.53	0.120	3.77	0.059
No	4.80		12.70	
Baseline albumin levels				
< 3.5 g/dl	1.70	0.011	1.70	0.001
≥ 3.5 g/dl	4.80		11.23	
PD-L1 levels				
< 1%	2.57	0.786	5.27	0.290
≥ 1%	4.67		11.23	
Baseline LSMI				
< LNL	3.00	0.040	6.37	0.009
≥ LNL	7.33		Not reached	
Baseline IMFI				
Low	3.03	0.647	10.80	0.229
High	4.80		12.70	
Baseline VFI				
Low	3.03	0.975	6.37	0.231
High	4.93		11.23	
Baseline SFI				
Low	2.97	0.135	5.43	0.020
High	5.77		14.03	

Abbreviations: BMI=Body mass index, ICI=Immune checkpoint inhibitor, PD-L1=Programmed death ligand-1, LSMI=Lumbar skeletal muscle index (cm²/m²) (At the level of 3rd lumbar vertebra), LNL=Lower normal limits, 55 cm²/m² for males and 39 cm²/m² for females, IMFI=Intramuscular fat index (cm²/m²) (At the level of 3rd lumbar vertebra), Low: Below gender specific median value, VFI=Visceral fat index (cm²/m²) (At the level of 3rd lumbar vertebra), Low: Below gender specific median value, SFI=Subcutaneous fat index (cm²/m²) (At the level of 3rd lumbar vertebra), Low: Below gender specific median value

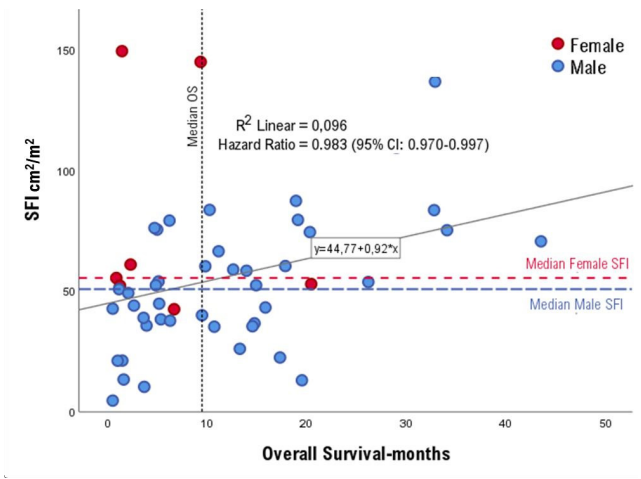
Figure S4: Log-rank test demonstrating the different survival outcomes of A. The patients in our cohort according to the combination of their baseline*¹ SFI and LSMI values B. Between patients with high*² SFI and LSMI \geq LNL*³ and patients with high SFI and LSMI < LNL.



Abbreviations: LSMI=Lumbar skeletal muscle index (cm²/m²) (At the level of 3rd lumbar vertebra), SFI=Subcutaneous fat index (cm²/m²) (At the level of 3rd lumbar vertebra), OS=Overall survival

- *¹ **Baseline:** At the beginning of immunotherapy
- *² **Low:** Below gender specific median value; High: Above gender specific median value
- *³ **LNL:** Lower normal limit, 55 cm²/m² for males and 39 cm²/m² for females

Figure S5: Scatter-plot demonstrating the overall survival values of the patients according to their baseline SFI. Univariate Cox Regression analysis for OS for SFI as continuous variable HR=0.983 (0.970-0.997), p=0.014. Gender was used as a stratification factor.



Abbreviations: SFI=Subcutaneous fat index (cm²/m²) (At the level of 3rd lumbar vertebra), OS=Overall survival

Table S3: Univariate analysis using Cox regression method investigating the hazard ratios of the analyzed categorical covariates on PFS and OS.

COX REGRESSION	PFS		OS	
UNIVARIATE ANALYSIS	HR (95% Confidence Intervals)	p value	HR (95% Confidence Intervals)	p value
Age ≥ 70 years old	0.91 (0.496-1.663)	0.755	0.80 (0.407-1.568)	0.514
Performance status 2	1.39 (0.684-2.823)	0.363	1.76 (0.821-3.773)	0.146
Female gender	1.89 (0.864-4.141)	0.111	1.50 (0.616-3.636)	0.373
Squamous histology	0.69 (0.374-1.262)	0.226	0.92 (0.473-1.798)	0.812
BMI < 25 kg/m ²	1.76 (0.942-3.282)	0.076	1.85 (0.942-3.618)	0.074
Brain metastases	2.71 (1.299-5.667)	0.008	2.02 (0.898-4.529)	0.089
Liver metastases	1.67 (0.868-3.213)	0.125	1.94 (0.962-3.905)	0.064
Bone metastases	0.99 (0.517-1.905)	0.983	1.18 (0.588-2.378)	0.639
PD-L1 < 1%	1.73 (0.474-2.677)	0.787	1.64 (0.652-4.081)	0.295
Baseline LSMI < LLN	2.03 (1.018-4.032)	0.044	2.90 (1.261-6.667)	0.012
Low baseline IMFI	1.15 (0.631-2.096)	0.648	1.50 (0.770-2.931)	0.232
Low baseline VFI	1.03 (0.551-1.848)	0.975	1.50 (0.769-2.919)	0.235
Low baseline SFI	1.59 (0.860-2.925)	0.140	2.20 (1.114-4.333)	0.023

Abbreviations: BMI=Body mass index, PD-L1=Programmed death ligand-1, LSMI=Lumbar skeletal muscle index (cm²/m²), LNL: 55 cm²/m² for males and 39 cm²/m² for females, IMFI=Intramuscular fat index (cm²/m²). Low: Below gender specific median value, VFI=Visceral fat index (cm²/m²). Low: Below gender specific median value, SFI=Subcutaneous fat index (cm²/m²). Low: Below gender specific median value